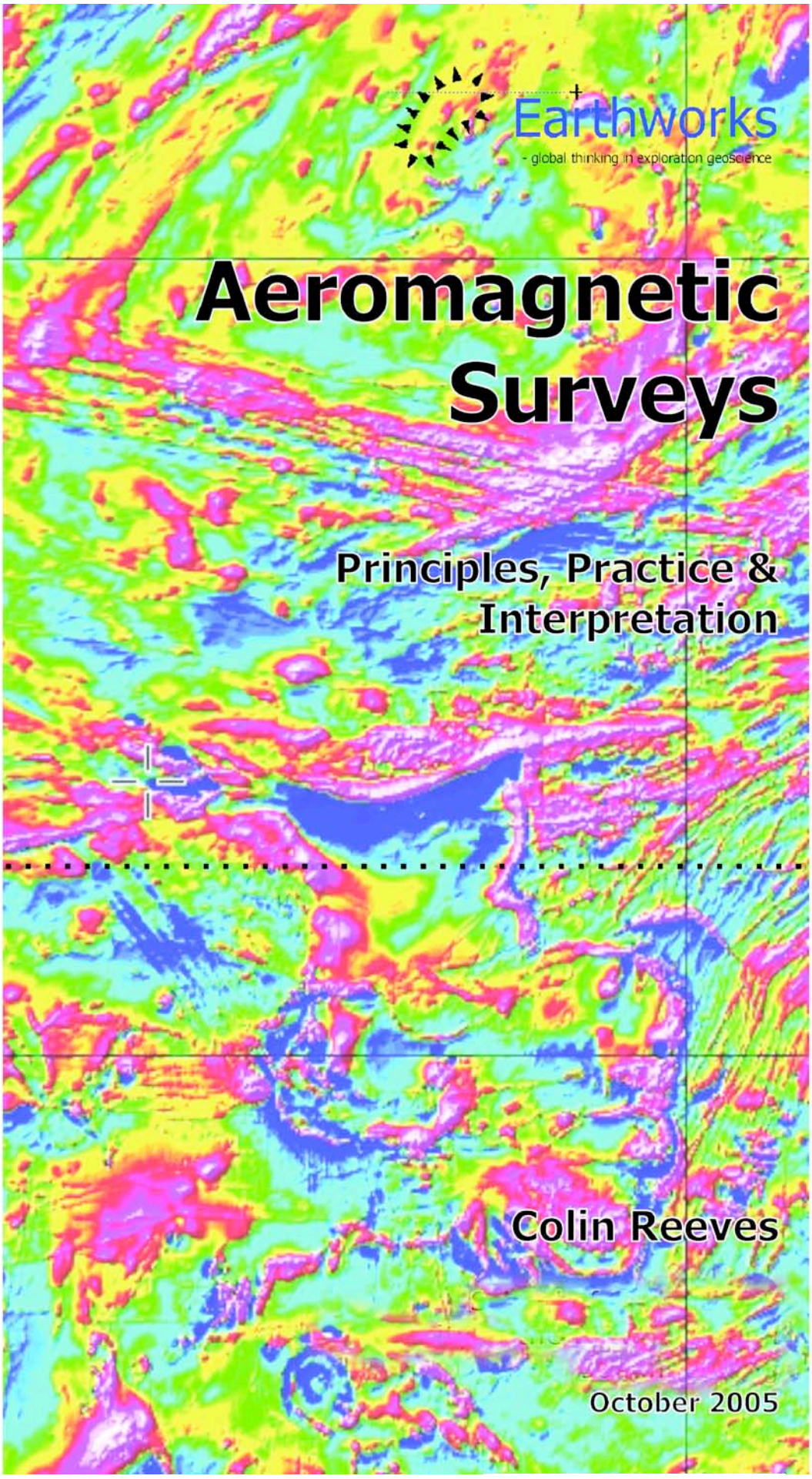

Published by GEOSOFT.

Earthworks
- global thinking in exploration geoscience

Aeromagnetic Surveys

Principles, Practice & Interpretation

Colin Reeves

***Cover:** Aeromagnetic anomalies over parts of South Africa, Botswana and Zimbabwe, courtesy of the African Magnetic Mapping Project.*

Published by GEOSOFT.

Colin Reeves is an independent consultant and an honorary professor at the School of Geosciences, University of the Witwatersrand. He holds degrees from Cambridge, Birmingham and Leeds Universities in the U.K. and has over 35 years' experience in the instigation, execution and interpretation of regional geophysical surveys in Africa, India, Australia and the Americas, spread across the government, commercial and educational sectors. He has been based successively in Botswana, Canada, Australia and the Netherlands where he was professor in Exploration Geophysics at ITC in Delft from 1983 until 2004. His interests include the global-tectonic context of exploration geoscience and national airborne geophysical mapping programmes in Africa and elsewhere. He may be reached at: reeves.earth@planet.nl

Colin Reeves, MA MSc PhD,
Achterom 41A,
2611 PL Delft,
The Netherlands.
reeves.earth@planet.nl
Office/mobile: +31 - 6 11 35 62 72
Residence: +31 - 15 214 6370

FOREWORD

No work, it seems, is ever finished. This is an unfinished work that has a history going back more than 30 years to when I first started interpreting aeromagnetic surveys and found that such interpretation inevitably involved some aspects of educating the users of the interpretation or the readers of the interpretation report in the principles involved in the origin of magnetic anomalies and their relation to geological bodies. Some aspects of it have been written many times in the introductions to professional reports, or in proposals written to try to initiate projects in parts of the world where new aeromagnetic surveys have much to offer.

From 1983 to 2000 I taught exploration geophysics at ITC in Delft and, for a time, the notes evolved further each year and almost kept pace with the growth of the airborne geophysical survey industry and the evolution of new technology. Many former students will be familiar with aspects that have survived the passage of time. Between 1991 and 1993, while I worked for the Bureau of Mineral Resources, Geology and Geophysics (subsequently the Australian Geological Survey Organisation, now Geoscience Australia) I had a chance to update much of the material from current survey practice in that continent that arguably leads the world in airborne geophysical survey technology and this process continued once back in Delft. After about 2000, however, the opportunity to teach aeromagnetics within the annual curriculum at ITC was much reduced. Nevertheless, I was asked to give courses of one or two weeks' duration in such places as India, Angola and Nigeria. So incomplete notes were again pressed into use. But there was never time enough to bring the work to a satisfactorily reproducible conclusion.

I am now involved fully in my own consulting practice and the need for this document is just as apparent as it ever was within almost every project I touch upon. Thanks to a period as a visiting professor in the School of Geosciences at the University of the Witwatersrand in 2005, the opportunity to rework my material into ten chapters of about equal length presented itself and enabled me to discard topics that should now be considered of only historical interest and recast the remainder in a new layout. I endeavoured to bring this to a reproducible format in the closing weeks of 2005, but it still lacks an index and an updated bibliography – and whatever else the reader may still find wanting. I regret that I have never managed to recruit the assistance it would take to turn this into a published work, but even that would age quickly. I am very grateful to all those who, along the way, have contributed in many ways – mostly unwittingly – such as with figures, examples, or simply by letting me know through their questions about prevalent misconceptions that need to be un-taught as hazards along the way to a rational understanding of the subject. Most potential readers, in my experience, prefer to eschew mathematics, so I have tried to make that a policy here as far as is reasonable. What ***is*** needed is an appreciation of the physics and a curiosity about what we can learn about geology through measuring magnetic anomalies from the air.

The first question – why is airborne geophysics so important? – is not addressed here as that is dealt with in a volume that I have written with Sam Bullock under the title *Airborne Exploration* that will be published by Fugro Airborne Surveys in 2006. What would go further than the present volume is a treatise devoted to aeromagnetic interpretation that dealt with the integration of gravity and gamma-ray spectrometry data with geology and that is illustrated with examples from all over the world and from a representative variety of geological terranes. Ideally this would lead into another treatise on the contribution all this can make to understanding the way global geology has evolved over geological time. For the moment, however, there is already enough unfinished business.

Colin Reeves
Delft, 2005 December.

CONTENTS

1.The Earth's magnetic field and its anomalies

2. The magnetic properties of rocks

3. Magnetometers and aircraft installations

4. Sampling theory and survey specifications

5. Data corrections and the flightline database

6. Gridded data: Maps, images and enhancements

7. Processing of grids in the wavenumber domain

8. Quantitative interpretation- the dipping dyke model

9. The dipping dyke extended to other models

10. Qualitative interpretation and the interpretation map

1.

The Earth's magnetic field and its anomalies

1.1 Fundamentals

From the point of view of geomagnetism, the earth may be considered as made up of three parts: core, mantle and crust (Figure 1.1). Convection processes in the liquid part of the iron **core** give rise to a dipolar geomagnetic field that resembles that of a large bar-magnet aligned approximately along the earth's axis of rotation (Figure 1.2). The **mantle** plays little part in the earth's magnetism, while interaction of the (past and present) geomagnetic field with the rocks of the Earth's **crust** produces the magnetic anomalies recorded in detailed (e.g. aeromagnetic) surveys carried out close to the earth's surface.

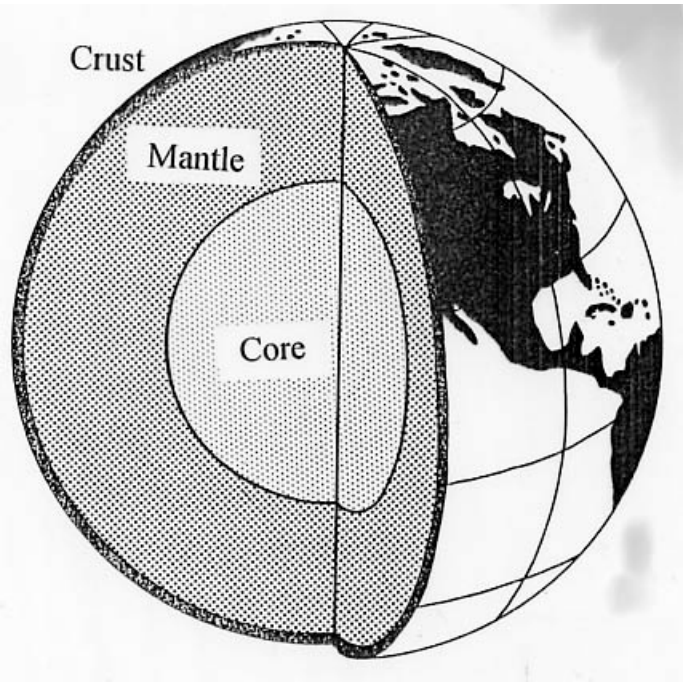

Figure 1.1 *The main divisions of the Earth's volume*

Magnetic field in SI units is defined in terms of the flow of electric current needed in a coil to generate that field. As a consequence, units of measurement are volt-seconds per square metre or Weber/m^2 or **Teslas** (T). Since the magnitude of the earth's magnetic field is only about 5 x 10^{-5} T, a more convenient SI unit of measurement in geophysics is the **nanoTesla** (nT = 10^{-9} T). The geomagnetic field then has a value of about 50 000 nT. Magnetic anomalies as small as about 0.1 nT can be measured in conventional aeromagnetic surveys and may be of geological significance. Commonly recorded magnetic anomalies have amplitudes of tens, hundreds and (less often) thousands of nT. One nT is numerically equivalent to the *gamma* (γ) which is an old (cgs) unit of magnetic field. The gamma still has some common currency but should, strictly speaking, now be replaced by the nT.

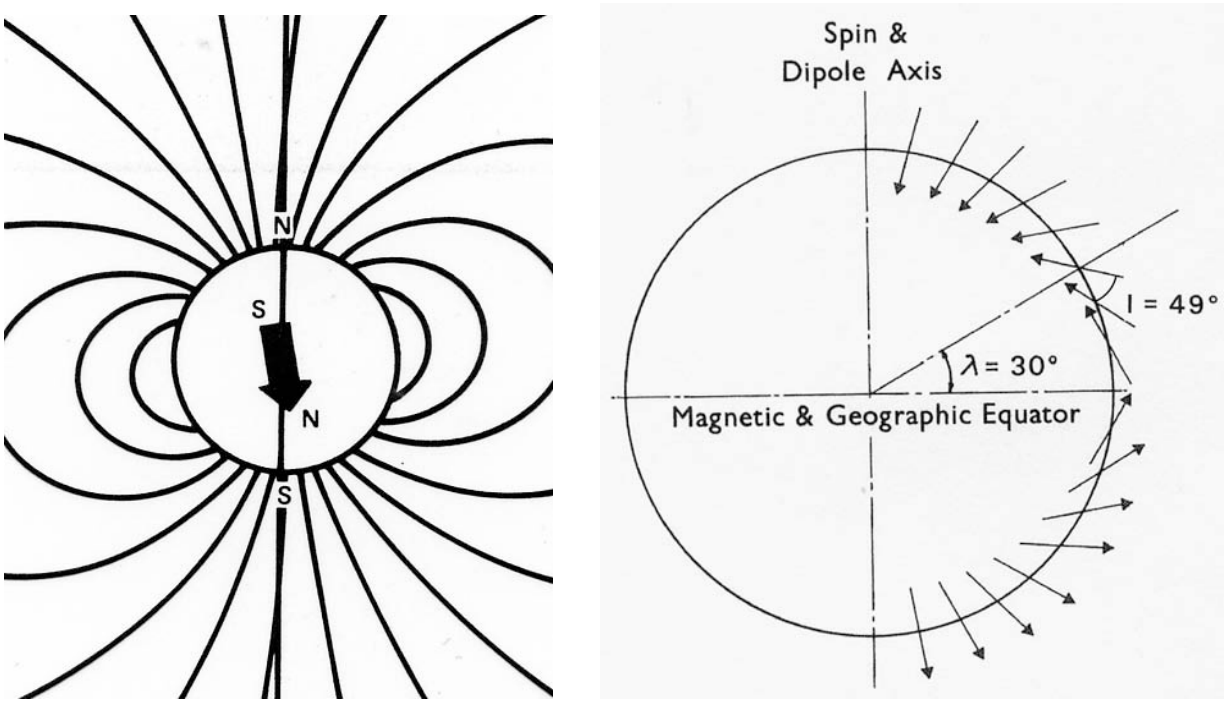

Figure 1.2 *The Earth's dipolar magnetic field and the inclination of the field at varying latitudes*

1.2 The geomagnetic field

The dipolar nature of the geomagnetic field necessitates taking some care in specifying the field's direction. The field is oriented vertically downward at the **north magnetic pole**, is horizontal (and pointing north) at the **magnetic equator** and points vertically upwards at the **south magnetic pole** (Figure 1.2). The magnetic poles have been observed to have moved considerably over historical times and detectable movement occurs even from year to year. However, it is thought that, on average over geological time, the dipole field which best fits the observed geomagnetic field has been coaxial with the geographic poles of rotation. Instantaneously, however - at times such as the present - the virtual magnetic poles may differ from the geographic poles by as much as 10 to 20 degrees.

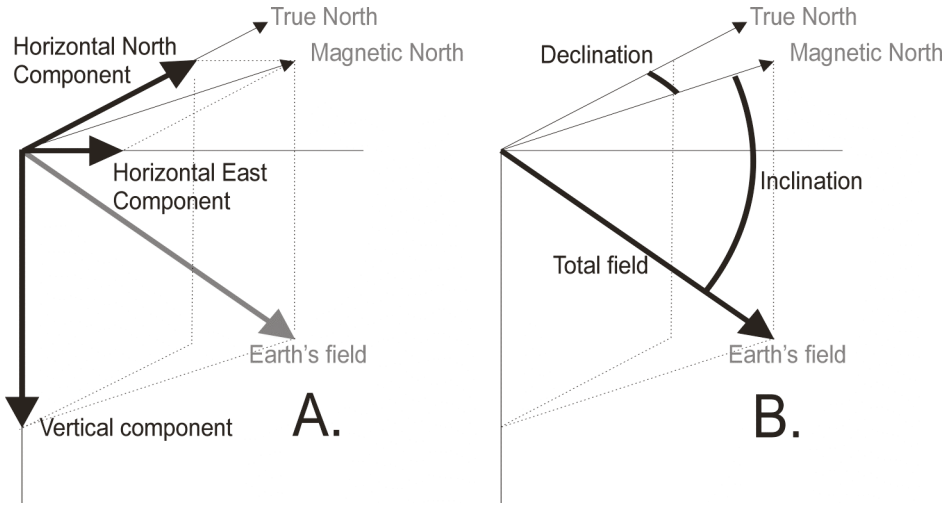

Figure 1.3 *The vector total magnetic field may be defined either as (a) three orthogonal components (horizontal north, horizontal east and vertical) or (b) as the scalar magnitude of the total field, F and two angles, the inclination from the horizontal, I and the declination from true (geographic) north, D.*

The definition of the main geomagnetic field at any point on the earth's surface as a vector quantity requires three scalar values (Figure 1.3), normally expressed *either* as three orthogonal components (vertical, horizontal-north and horizontal-east components) *or* the scalar magnitude of the total field vector and its orientation in dip and azimuth. With the exception of a few specialised surveys (see later), aeromagnetic surveys have always measured only **the scalar magnitude of F**, making the latter system more convenient for present purposes. The angle the total field vector makes above or below the horizontal plane is known as the magnetic **inclination**, **I**, which is conventionally positive north of the magnetic equator and negative to the south of it. ($-90° \leq I \leq +90°$). The angle between the vertical plane containing F and true (geographic) north is known as the magnetic **declination**, **D**, which is reckoned positive to the east and negative to the west. The value of D is commonly displayed on topographic maps to alert the user to the difference between magnetic north, as registered by a compass, and true north. D is less than 15° in most places on the Earth, though it reaches values as large as 180° along lines joining the magnetic and geographic poles. World maps showing observed variation in F, I and D are presented as Figures 1.4, 1.5 and 1.6 respectively.

Simple dipole theory predicts that the magnetic inclination, I, will be related to geographic latitude, ϕ, as follows:

$$\tan I = 2 \tan \phi$$

Hence when, for example, $\phi = 30°$, $I \cong 49°$ (Figure 1.2). Actual measurements of I show some deviations from this simple prediction (Figure 1.5). Similarly, the variations observed in F are not as simple as the dipole theory predicts (Figure 1.4). F varies from less than 22 000 nT in southern Brazil to over 70 000 nT in Antarctica south of New Zealand. It is clear that in the cases of T, I and D there is variation with longitude as well as latitude.

Since mapping of local variations in F attributable to crustal geology is the purpose of aeromagnetic surveys, it is the definition of the 'normal' or global variation in F that must be subtracted from *observed F* to leave the (time invariable) magnetic anomaly that concerns us here. As often in geophysics, the need to define the normal before being able to isolate the ‘anomaly’ is clear. Unlike the simple case of the gravity field, however, the time-variations of the magnetic field are also quite considerable and complex and therefore need to be addressed first.

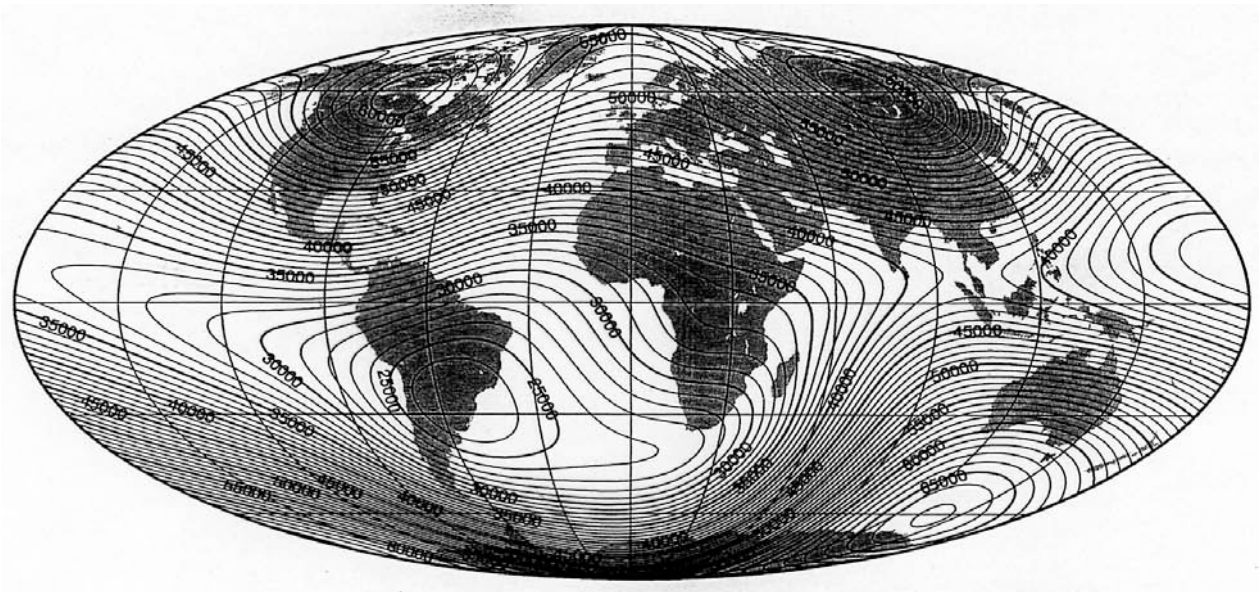

Figure 1.4 *The global variation in F, the scalar magnitude of the total magnetic field, from the International Geomagnetic Reference Field for 1995, given in nanotesla (nT).*

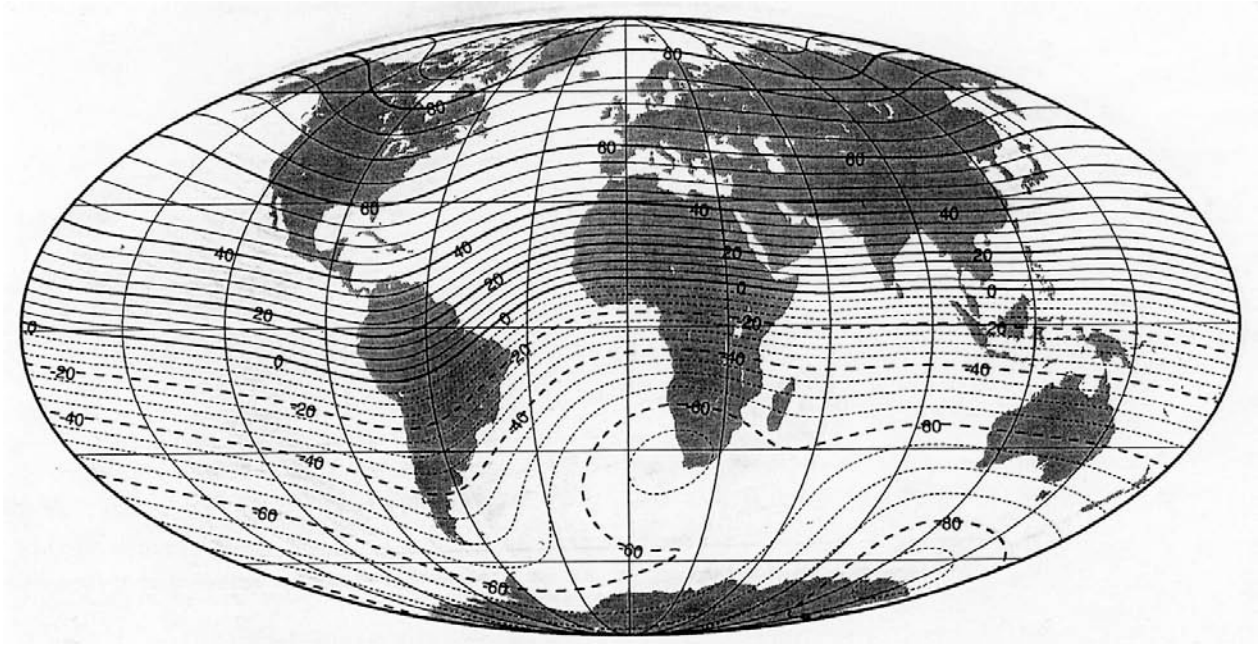

Figure 1.5 *The global variation in I, the inclination of the total magnetic field, from the International Geomagnetic Reference Field for 1995, given in degrees.*

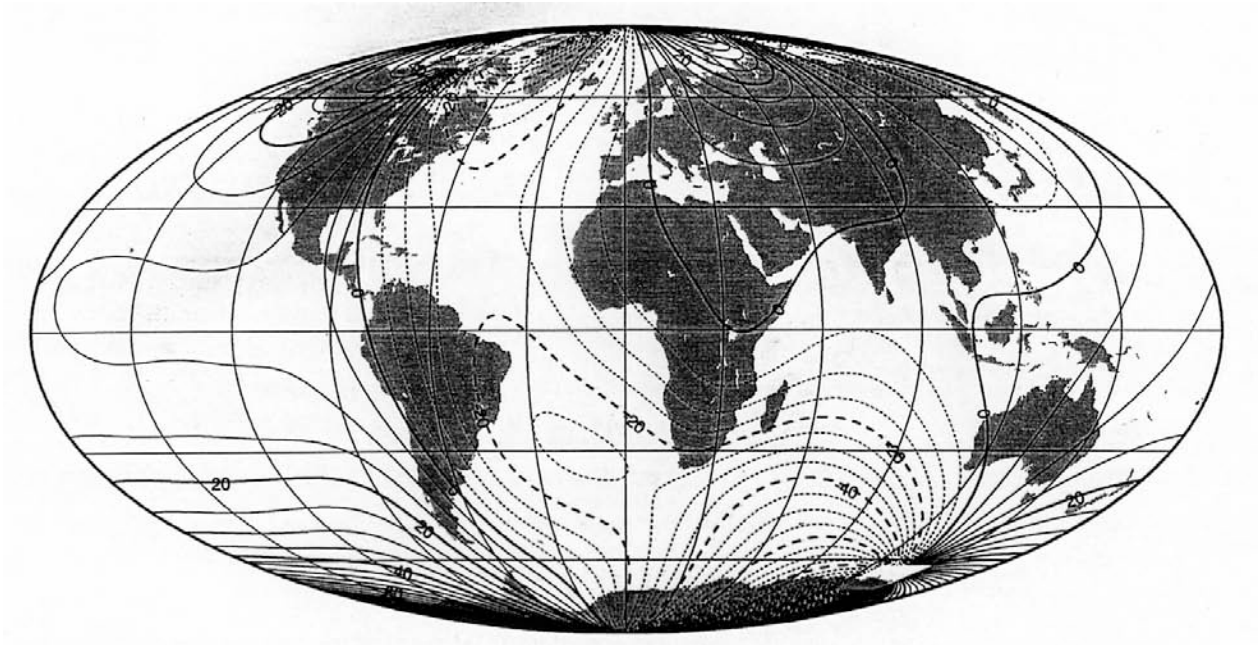

Figure 1.6 *The global variation in D, the declination of the total magnetic field, from the International Geomagnetic Reference Field for 1995, given in degrees.*

The reader is referred to the site http://www.ngdc.noaa.gov/geomagmodels/IGRFWMM.jsp for an interactive calculation of the IGRF field.

1.3 Temporal variations

The variations in F with time over time-scales ranging from seconds to millions of years have a profound effect on how magnetic surveys are carried out, on the subtraction of the main field from the measured field to leave the anomaly, and in the interpretation of the resulting anomalies. These variations are described briefly, starting with variations of short time-span (some of which may be expected occur within the duration of a typical survey) and ending with those of significance over geological time. The record of F from a magnetometer left recording for several weeks is shown in Figure 1.7.

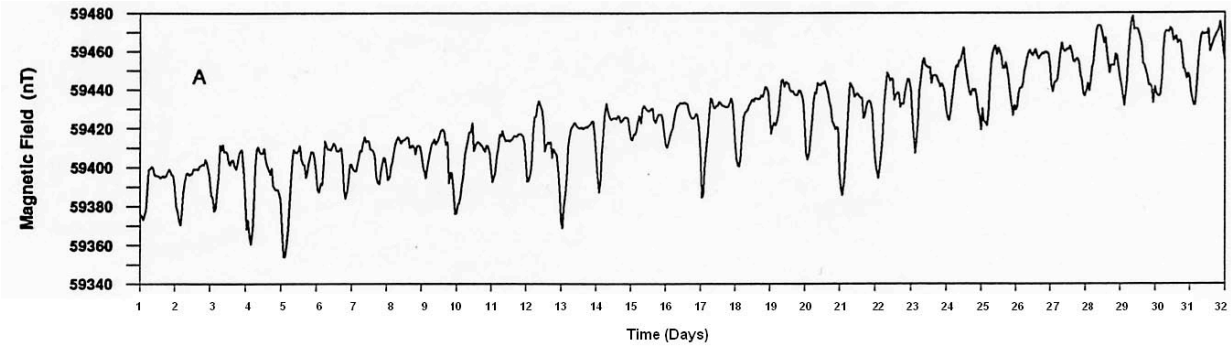

Figure 1.7 *Variations in F at a fixed point recorded over a number of weeks.. Each tick-mark on the time axis is one day.*

(a) Diurnal variations, strictly speaking, follow a daily cycle associated with the rotation of the earth, though common misuse extends the term to any variations in F that are observed over periods comparable with the duration of a day. True diurnal variations arise from the rotation of the earth with respect to the sun. The 'solar wind' of charged particles emanating from the sun, even under normal or 'quiet sun' conditions, tends to distort the outer regions of the earth's magnetic field, as shown in Figure 1.8. The daily rotation of the earth within this sun-referenced distortion leads to ionospheric currents on the 'day' side of the planet and a consequential daily cycle of variation in F that usually has an

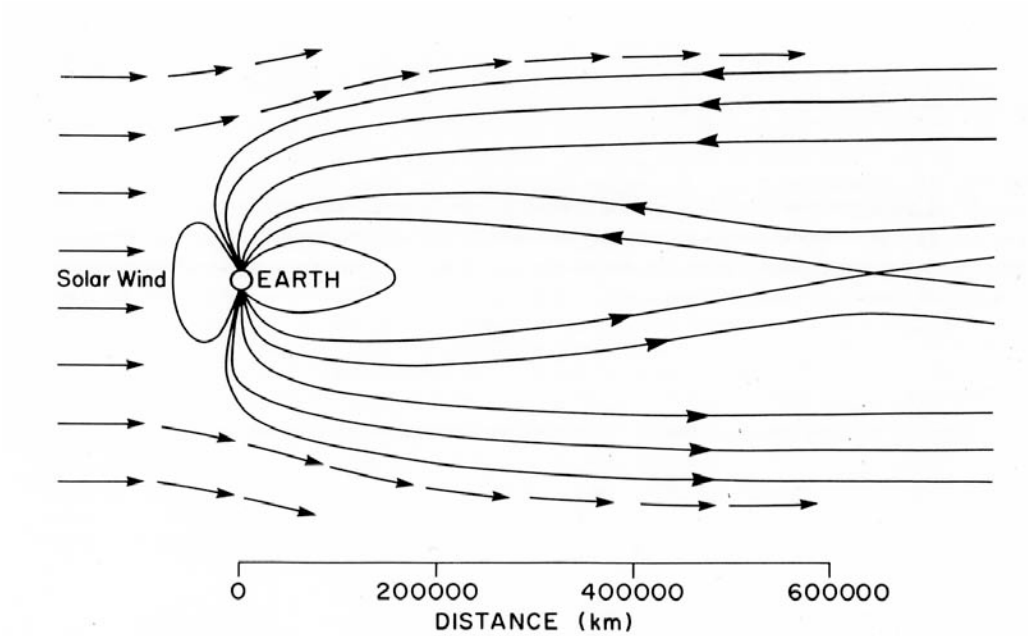

Figure 1.8 *The solar wind distorts the outer reaches of the earth's magnetic field causing current loops in the ionosphere on the day-side of the rotating planet..*

amplitude of less than about 50 nT. The main variation occurs towards local noon when peaks are observed in mid-latitudes and troughs near the magnetic equator (Figure 1.7). The relatively undisturbed night-time period - when highly accurate geomagnetic observations are usually made - are unsuitable for airborne survey operations, so surveys have to be planned so as to allow for corrections to be made for diurnal (and other) variations (see Chapter 2).

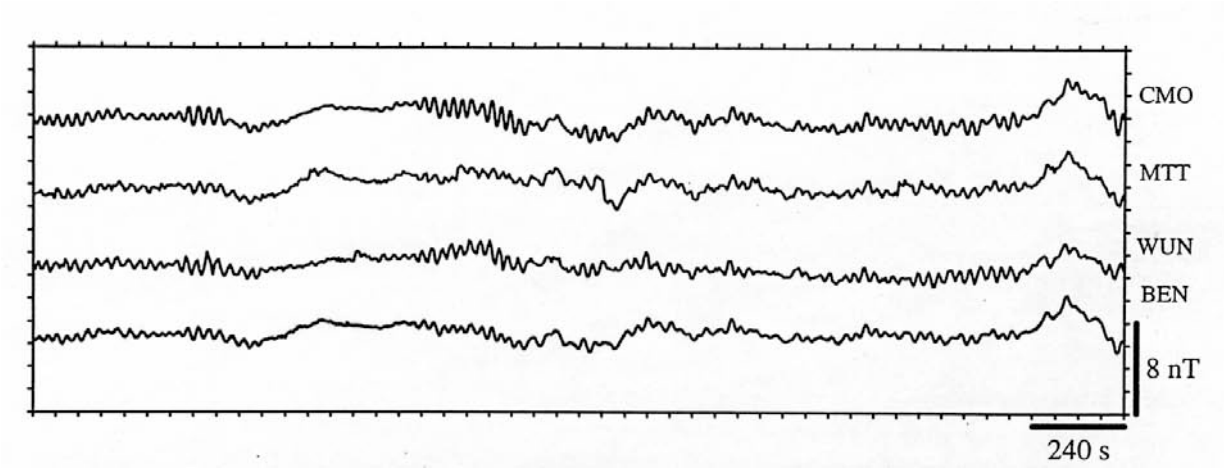

Figure 1.9 *Variations in F recorded at stations a few tens of kilometers apart showing the nature pf micropulsations and their variation from place to place on the Earth's surface.*

(b) Micropulsations occur on a much shorter time scale, commonly over period as short as a few minutes (Figure 1.9). While their amplitudes may be only a few nT, their effect on magnetic records made in an aircraft or at a base station on the ground is significant. Unfortunately, the exact shape of a recorded sequence of micropulsations may change from place to place over a few tens of kilometers (Figure 1.9), so even subtraction of time-variations observed at a fixed location from the anomalies recorded in an aircraft is not without its limitations and effective elimination of such short-term geomagnetic variations is one of the limits presently set to the accuracy with which spatially-related variations in magnetic field may be mapped without distortions attributable to temporal effects.

(c) Magnetic storms are typified by isolated periods of much higher levels of magnetic variation, usually correlated with sunspot activity. Violent variations of several hundred nT may start quite suddenly and continue for periods in excess of 24 hours (Figure 1.10). Their effect is particularly felt in the auroral zones around the earth's magnetic poles.

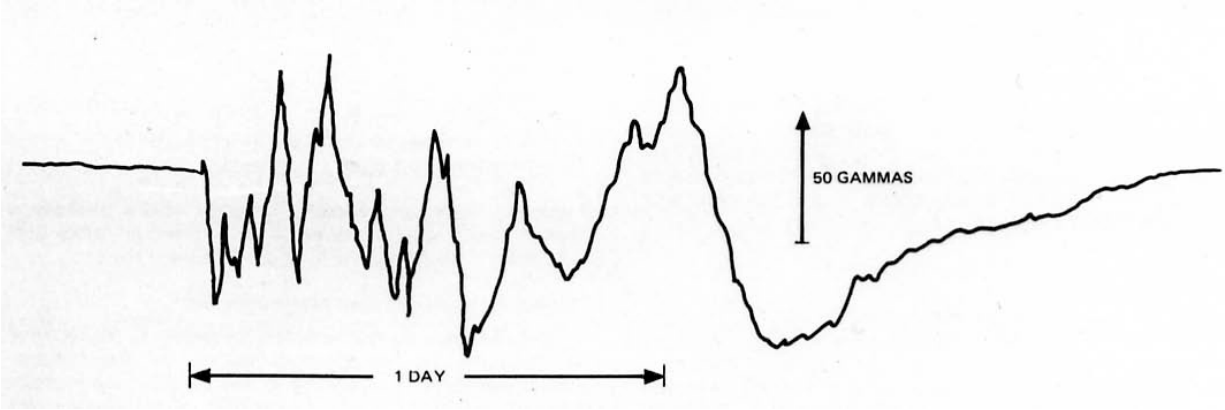

Figure 1.10 *A typical magnetic storm, as observed at a time of high solar activity. The onset of the storm is sudden and violent variations in F may be seen over several tens of hours. Return to 'normal field conditions may take several days.*

Again, the shape of the curve observed in a storm varies from place to place and there is no prospect of acquiring information on spatial variations in F of the quality required in an aeromagnetic survey while a magnetic storm is in progress. In terms of airborne survey practice, therefore, magnetic storms simply add to the periods of enforced inactivity caused by bad weather, equipment failure and other factors beyond the control of the survey crew.

All three of the above factors operate on time-scales that are short in comparison with the time taken to carry out an aeromagnetic survey, which is usually reckoned in weeks or months. They therefore require careful monitoring if good data are to be acquired - from which reliable spatial, time-invariant magnetic anomalies can be reliably mapped (see later).

(d). Secular variation. Variations on a much longer time-scale - hundreds of years - are well documented from historical data and the accurate magnetic observatory records of more recent decades. The main manifestation of secular variation globally is changes in size and position of the departures from a simple dipolar field over years and decades. The effects of these changes at a given locality are predictable with a fair degree of accuracy for periods of five to ten years into the future, but such predictions need to be updated as more recent magnetic observatory and earth satellite recordings become available.

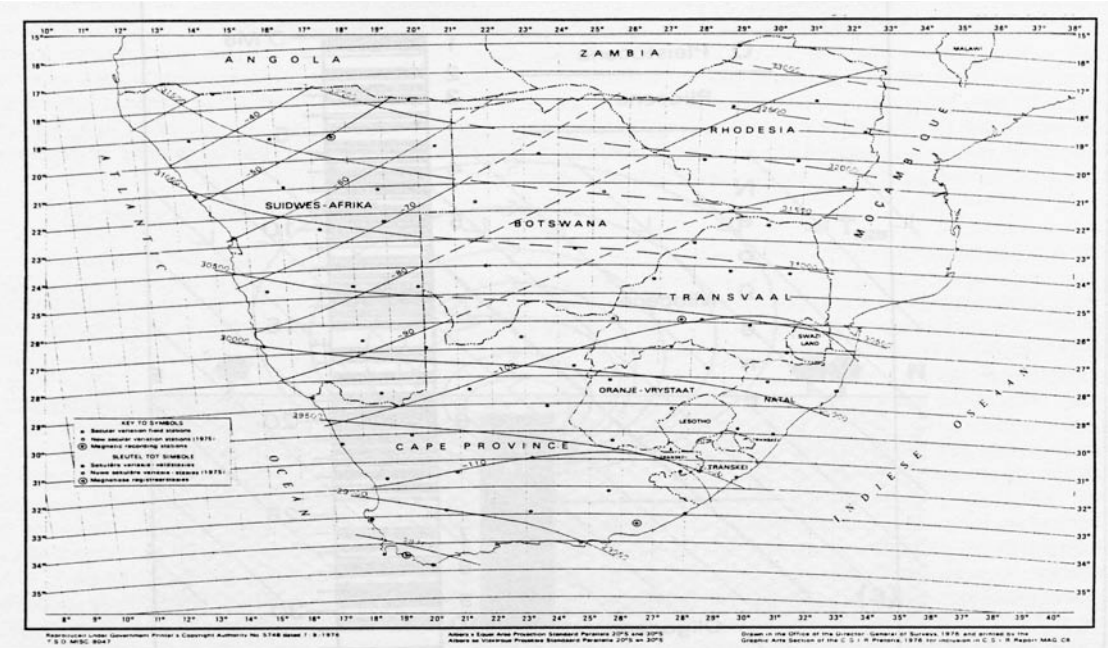

Figure 1.11 *The variations in F from a series of observations at repeat station (dots) in 1970 and 1975. The variations of F with position are shown as heavy lines, while thinner lines show the expected change in F with time in the years ahead.*

From the point of view of magnetic anomaly mapping, secular variations become important when surveys of adjacent or overlapping areas carried out several years apart are to be compared or merged together. Figure 1.11 shows values of F in southern Africa from observations made at 'magnetic repeat stations' (points on the ground visited to re-measure the main elements of the geomagnetic field at five-yearly intervals) for the epoch 1975.0. Thinner contours show the rate of change in F determined from observations made in 1970 and 1965. At a location such as Union's End (24.7 deg S, 20.0 deg E) the value of F at 1975.0 is seen to be about 30550 nT with an annual rate of change of about -

83 nT. On the basis of these values, magnetic values in the vicinity of Union's End at 1990 (for example) would be expected to be about 30550 - (83 x 15) = 29305 nT – a change of 1245 nT change. (Compare with Figure 1.4)

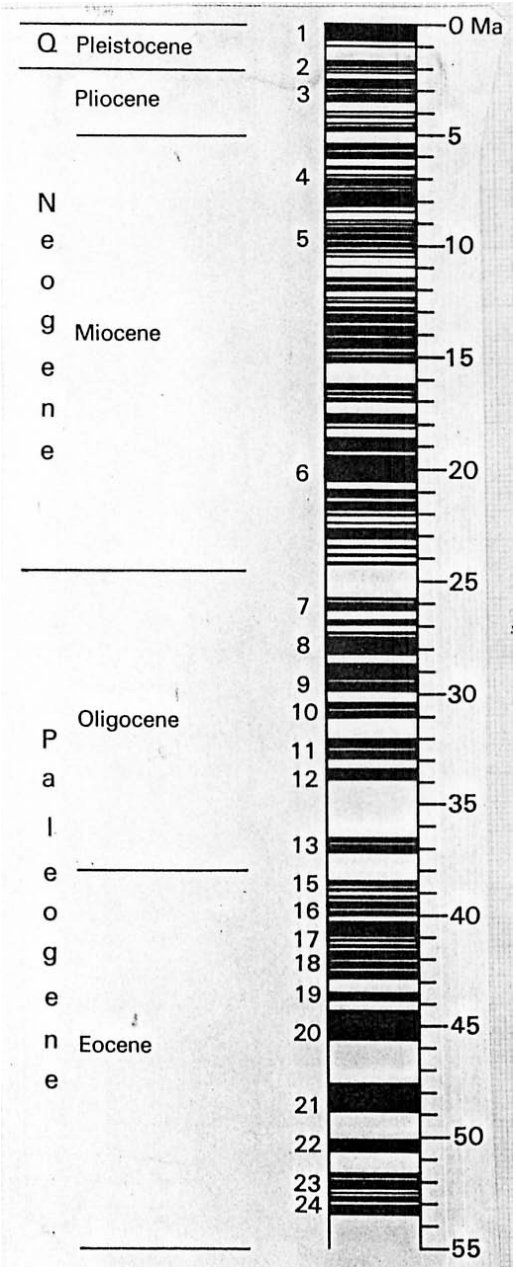

Figure 1.12 *The geomagnetic reversal timescale, vertical axis in millions of years ago (Ma). Periods of 'normal' field direction, as at present, are shaded black, 'reversed' field in white (from Harland et al., 1982).*

As an approach to standardisation of main field removal in aeromagnetic surveying, a mathematical model for the global variation in F is formalised from all available magnetic – and, more recently, satellite - observations worldwide every five years in the **International Geomagnetic Reference Field** (IGRF - see later).

(e) Geomagnetic reversals. Evidence for the direction of the earth's magnetic field in the geological past may be found in the remanent magnetisation of rocks collected from lake-floors, lava flows, sea-floor spreading and other sources. Modern dating techniques allow ages to be attached to the collected rock specimens. Such studies worldwide show that the entire magnetic field of the earth has repeatedly reversed its polarity at irregular intervals of from 10000 years to several million years. The concurrence of all such observations allows a geomagnetic time scale to be determined (Figure 1.12). A consequence of repeated reversals is that, at an arbitrarily chosen moment in the geological past, the earth's magnetic field is just as likely to have been *normal* (i.e. with the polarity of the present-day field) as *reversed.* The reversals themselves take place very quickly in geological terms, perhaps in the space of less than 1000 years, so rocks laid down *during* the reversal process itself are comparatively rare.

The construction of a global magnetic reversal timescale is of fundamental importance in deciphering earth history. Amongst other things, the reversals of the field are recorded in the remanent magnetisation of oceanic crust created as continent separate (Figure 1.13), allowing the age of ocean floor to be dated and the earlier positions of continents to be inferred. Two sequences of anomalies are well-known, one going from the present day back to 'Anomaly 34' at about 84 million years ago (84 Ma), and the M-series that starts at about 118 Ma and goes back to the oldest remaining ocean floor at about 200 Ma. Between these two series there is a long period of normal geomagnetic fields devoid of reversals, known as the Cretaceous Normal

Superchron. Areas of ocean created in this period are devoid of stripes and such regions are sometimes referred to as the 'Cretaceous Quiet Zone'.

For rocks that have acquired a *remanent magnetisation* (see later) in the direction of the ambient geomagnetic field at the time (for example when they cooled through their Curie point temperature) the direction of that remanence may be very different from that of the present-day geomagnetic field. For rocks acquiring remanence in the relatively recent past, the direction of remanence is likely to be approximately either parallel or anti-parallel to the present-day field. Further into the geological past, however, the processes of continental drift will have moved rock localities further and further away from the latitude and longitude for which the magnetic inclination and azimuth recorded in the remanence are typical. Beyond the time taken for a locality to move 90° of geographic latitude through continental drift (about 200 Ma at 5 cm/yr), any direction of remanence is, in theory, possible. This adds considerable complication to the task of interpreting the sources of magnetic anomalies when significant remanent magnetisation is present (see Chapter 2, Section 1).

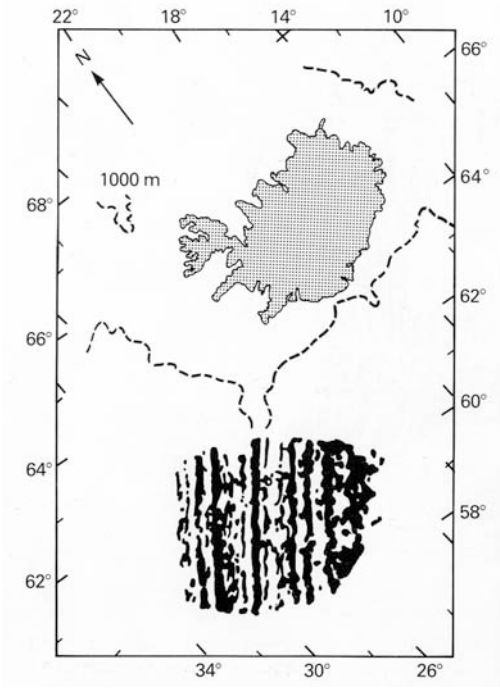

Figure 1.13 *The geomagnetic reversal time scale is recorded symmetrically on either side of the mid-Atlantic Ridge, as shown in this early marine survey of 1966. Positive (normal) anomalies are shown white, reversed anomalies black. (from Heirtzler et al, 1966).*

1.4 The International Geomagnetic Reference Field (IGRF)

It should be clear from the foregoing that aeromagnetic surveys aim to record the variations in F with x and y over a survey area while eliminating all time-based variations. The magnitude of F will fall be between 20 000 and 70 000 nT everywhere on earth and it can be expected to have local variations of several hundred nT (sometimes, but less often, several thousand nT) imposed upon it by the effects of the magnetisation of the crustal geology. The 'anomalies' are usually at least two orders of magnitude smaller than the value of the total field. The IGRF provides the means of subtracting on a rational basis the expected variation in the main field to leave anomalies that may be compared from one survey to another, even when surveys are conducted several decades apart and when, as a consequence, the main field may have been subject to considerable secular variation. Note that, since IGRF removal involves the subtraction of about 99% of the measured value, the IGRF needs to be defined with precision if the remainder is to retain accuracy and credibility.

The IGRF is published by a working group of the International Association of Geomagnetism and Aeronomy (IAGA) on a five-yearly basis. A mathematical model is advanced which best fits all actual observational data from geomagnetic observatories, satellites and other approved sources for a given epoch (Figures 1.4, 1.5 and 1.6). The model is defined by a set of spherical harmonic coefficients to degree and order 13 for (a)

the value of F worldwide at the epoch of the model (e.g. for 1995) and (b) the annual rate of change in these coefficients for the following five years (e.g. 1995-2000). Software is available which permits the use of these coefficients to calculate IGRF values over any chosen survey area. The values currently in use are based on the IGRF 2005 and its tentative extrapolation (prediction) to 2010. Once all relevant actual observations (as opposed to predictions) have become available, it is possible to revise the prediction and announce a definitive reference field. The 9th generation IGRF (revised 2003) is now definitive for the period 1945-2000 and valid for use until 2005. Eventually, a definitive model until 2005 will be adopted with an extrapolation to 2010, and so on. The IGRF coefficients are published by IAGA and can be found at *http://www.iugg.org/IAGA/iaga_pages/pubs_prods/igrf.htm.*

It is normal practice in the reduction of aeromagnetic surveys to remove the appropriate IGRF once all other corrections to the data have been made (see Chapters 4 & 5). Departures of the subtracted IGRF from an eventual definitive IGRF may need to be considered when re-examining older surveys retrospectively. Scarcity of observatories and observations in some parts of the world may limit the accuracy with which the IGRF fits the broad variations in the magnetic field observed in a given survey area, but the new generation of earth-orbiting satellite-borne magnetometers (Oersted, CHAMP) launched since 2000 gives improved coverage of regional features everywhere. From the point of view of exploration geophysics, undoubtedly the greatest advantage of the IGRF is the uniformity it offers in magnetic survey practice since the IGRF is freely available and universally accepted.

Other problems concerned with linking and levelling magnetic anomaly surveys acquired at different times in the process of, for example, making national or continental scale magnetic anomaly compilations will be discussed later (Chapter 6).

1.5 Magnetic anomalies

The scalar magnitude of the magnetic field, F, recorded in an aeromagnetic survey at any given point contains no information on the *direction* of the field. It may, however, be considered as the vector sum of the IGRF (F_{IGRF}) at that point and an anomalous component, ΔF (Figure 1.14(a)). The IGRF component will be oriented in the direction of the earth's main field at that point while the magnetic field due to a local source, ΔF, can, in

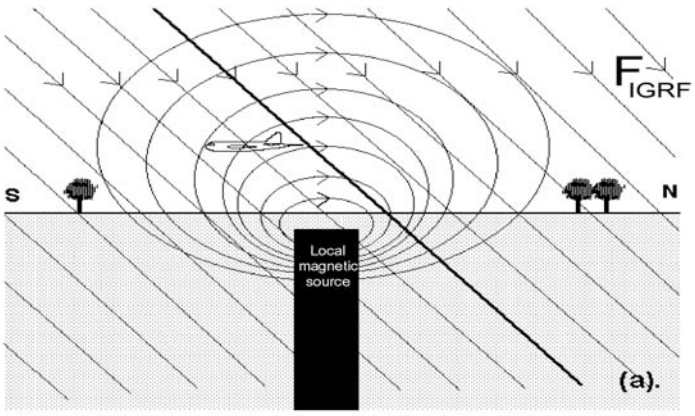

Figure 1.14(a) *At a given location, the airborne magnetometer records the vector sum of the ambient geomagnetic field and the anomalous contribution from (one or more) local sources.*

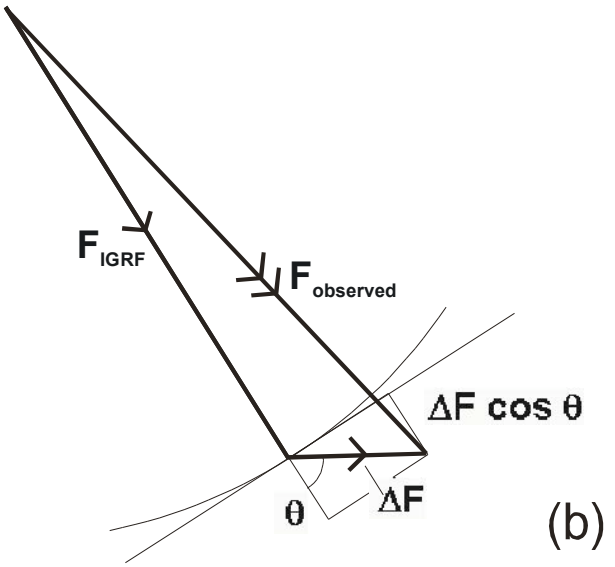

Figure 1.14(b) *$F_{observed}$ minus F_{IGRF} does not differ significantly from the component of ΔF in the direction of F_{IGRF} (= $\Delta F \cos \theta$) as long as $F_{IGRF} >> \Delta F$.*

principle, have any orientation. The two components can certainly be plotted in one plane, however, and F is normally at least two orders of magnitude greater than ΔF (Figure 1.14(b)). As long as this latter condition is (nearly) satisfied, the scalar value ($F_{observed}$ - F_{IGRF}) normally reported in an aeromagnetic survey does not differ significantly from the value of *the component of* ΔF *in the direction of* F_{IGRF}. Hence, total field magnetic anomaly maps record the **components of local anomalies in the direction of the Earth's main field**. When forward-modelling (see Chapter 8) the likely effects of magnetic bodies, the magnitude of this component is calculated for comparison with field observations. (By the same argumentation, in gravity surveys it is the component of the local anomaly in the *vertical* direction that is recorded in a survey and the vertical component of the effect of a model source that is forward-modelled). This will need re-consideration should one of the occasional magnetic anomalies having amplitudes of tens of thousands of nT be encountered in interpretation.

Any traverse of observations across a local magnetic body will normally pass through places where its magnetic field tends to re-enforce the geomagnetic field, as well as places where the local field mostly opposes the geomagnetic field. It follows that even a simple compact magnetic body produces a magnetic anomaly that has both positive and negative parts or 'lobes'. This is a consequence of the physics of the situation and, when it comes to making economical interpretations of magnetic anomalies, it is to be expected that such 'double' anomalies will be commonplace, even though their exact shapes depend on many factors, including the inclination of the present-day earth's field. Figure 1.15 shows a typical example of such an anomaly from nature and, alongside it, the anomaly calculated for a simple, compact, geometrical volume of magnetic rock. The astute reader may already realize that any similarity between the two anomalies indicates that the theoretical body may approximate in depth and dimension to the real rock body causing the natural anomaly. Pursuing this concept is the basis of (quantitative) interpretation of magnetic anomalies that is discussed in later sections.

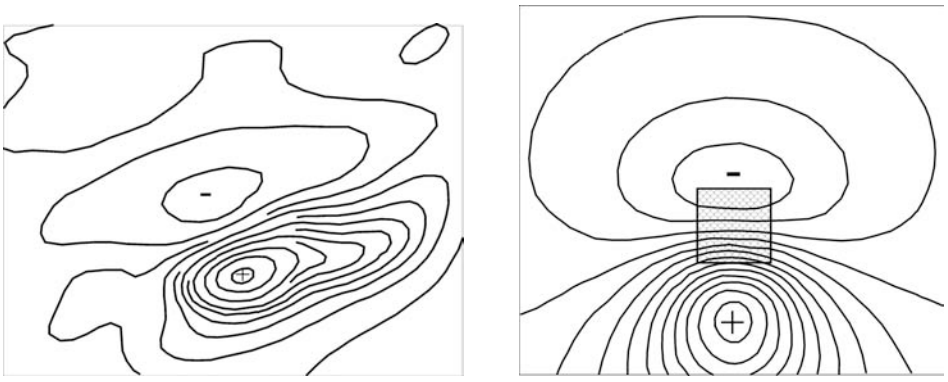

Figure 1.15 *left: A magnetic anomaly from a compact source in nature; right: an anomaly calculated over a simple geometrical body. Both illustrate the typical bi-lobal nature of anomalies in general.*

Further Reading

Breiner, S., 1973. Applications manual for portable magnetometers. GeoMetrics. 58 pp.

Harland, W.B., Cox, A.V., Llewellyn, P.G., Pickton, C.A.G., Smith, A.G. and Walters, R., 1982. A Geological Time Scale. Cambridge University Press. 131 pp. There are many more recent editions, but the clear geomagnetic reversal diagrams have been dropped, along with the authors with the geophysical connections

Kearey, P., and Brooks, M., 2002. An introduction to Geophysical Exploration. Blackwell Science, 262 pp.

McElhinny, M.W., and McFadden, P.L., 2000. Paleomagnetism – continents and oceans. Academic Press, 386 pp.

MacMillan, S., et al., EOS vol 84, No 46, November 2003 list the coefficients for the current IGRF.

2.□ The magnetic properties of rocks

2.1 Induced and remanent magnetisation

When a magnetic material is placed in a magnetic field, the material becomes magnetised and the external magnetising field is reinforced by the magnetic field induced in the material itself. This is known as **induced** magnetisation. When the external field is shut off, the induced magnetisation disappears at once, but some materials retain a permanent or **remanent** magnetisation and its direction will be fixed within the specimen in the direction of the (now disappeared) inducing field. The rocks of the earth's crust are, in general, only weakly magnetic but can exhibit both induced and remanent magnetisation. They inevitably lie within the influence of the geomagnetic field as it is now, and in some cases, they also record indications of how that field was in the past.

Magnetic properties can only exist at temperatures below the Curie point. The Curie point temperature is found to be rather variable within rocks, but is often in the range 550 to 600 deg C. Modern research indicates that this temperature is probably reached by the normal geothermal gradient at depths between 30 and 40 km in the earth, though the so-called 'Curie point isotherm' may occur much closer to the earth's surface in areas of high heat-flow. With these exceptions, it can be expected that all rocks within the earth's crust are capable of having magnetic properties. Since it is also thought that the upper mantle is virtually non-magnetic, the base of the crust may in many cases mark the effective depth limit for magnetic sources. An often-asked question is: Just how deeply can magnetic surveys investigate? The foregoing is an important part of the answer, though further relevant considerations such as the amplitude and wavelength of anomalies originating from buried bodies will be dealt with in a later chapter.

It will also be shown later that magnetic minerals may be created and destroyed during metamorphism and that temperatures reached during metamorphism and, for example, igneous emplacement clearly exceed Curie temperatures. It follows that at least some parts of the metamorphic history of a rock may have had an influence on its magnetic properties. It is fair to say, then, that rock magnetism is a subject of considerable complexity. Only the most important features of direct relevance to interpreting magnetic anomalies will be addressed in this brief summary.

Clearly, all crustal rocks find themselves situated within the geomagnetic field described in Chapter 1. They are therefore likely to display induced magnetisation. The magnitude of the magnetisation they acquire, J_i, is proportional to the strength of the earth's field, F, in their vicinity, where the constant of proportionality, k, is, by definition, the **magnetic susceptibility** of the rock:

$$J_i = k F$$

Strictly speaking, k is the magnetic *volume* susceptibility. (It differs from the mass susceptibility and the molar susceptibility that are not usually encountered in exploration geophysics).

If the magnetic field of the earth could in some way be turned off, the induced magnetisation of all rocks would at once disappear. (The moon, for example, has no significant magnetic field and, therefore, moon rocks *in situ* do not exhibit induced magnetisation). Many rocks also show a natural remanent magnetisation (NRM) that would remain, even if the present-day geomagnetic field ceased to exist. NRM may be acquired by rocks in many ways, but probably the simplest conceptually is in the process of cooling, particularly the cooling of igneous rocks from a molten state. As they cool through the Curie point or 'blocking temperature', a remanent magnetisation in the direction of the ambient geomagnetic field at that time will be acquired. The magnitude and direction of the remanent magnetisation can remain unchanged, regardless of any subsequent changes in the ambient field, as is shown by rocks even billions of years old that still retain their NRM.

The clear distinction between induced and remanent magnetisation is blurred only by *viscous remanent magnetisation* (VRM) that is acquired gradually with time spent in an inducing field and is lost only gradually once that field is removed. For rocks *in situ* - the only rocks of concern for the production of magnetic anomalies - any VRM present can be assumed to be co-directional with (and indistinguishable from) induced magnetisation. VRM can become important, however, when rock specimens are removed for laboratory examination.

For rocks which have cooled through their blocking temperature very recently, the direction of the acquired remanent magnetisation (NRM) will be the direction of the earth's present field. And, since it is not possible to shut off the earth's magnetic field, the remanent magnetisation in these cases will also not, in practice, be distinguishable from the induced magnetisation - as long as the rock remains *in situ*. As a result of the geomagnetic reversals described in Chapter 1.3, however, any point within an igneous intrusion is just as likely to have passed through its blocking temperature at a time when the earth's field was reversed as at a time when it was normal. Thus it should be expected that many rocks showing strong remanent magnetisation will be 'reversely magnetised'. The terms ‘normal’ and ‘reversed’ magnetisation become ambiguous as older rocks - which are likely to have moved their position considerably as a result of continental drift - are considered. In general, the remanent magnetisation recorded in rocks may have almost any direction, determined only by the age of the remanence and the position of the site on the earth’s surface with respect to the (periodically reversing) geomagnetic poles at the time of cooling.

Considered simply, it follows that any rock *in situ* may now be expected to have two magnetisations, one induced and one remanent. The induced component, J_i, will be parallel to the earth's present field, while the remanent component, J_r, may reasonably have any direction. Since they are both vector quantities, they will sum vectorially to give the total magnetisation of the rock *in situ*. The ratio of the scalar magnitudes of these two components is known as the *Koenigsberger ratio*, Q, for the rock:

$$Q = J_r / J_i$$

When a rock specimen is taken into the laboratory, it is possible to measure its magnetic susceptibility and hence determine J_i if the magnitude of the earth's inducing field at the original site is known. It is also possible to measure J_r, and hence the value of Q may be determined. Much more complex rock-magnetic and paleomagnetic studies may also be carried out, which are beyond the scope of this text. But, in general, the interpreter of magnetic anomaly data does not have such results for the large number of rock formations, both exposed and at depth, within the survey area and generalisations based on studies of similar rocks in other areas usually have to be relied upon. Very often, for example, it is necessary to assume that the value of Q is small, i.e. that all significant magnetisation in the rocks is induced and in the direction of the present day Earth's field. When this is clearly not the case, not only the magnitude of total magnetisation, but also its direction must be assumed. This introduces added ambiguity into an interpretation of the source of a magnetic anomaly (see Chapter 8).

Magnetic susceptibility in SI units is a dimensionless ratio having a magnitude much less than 1 for most rocks. Hence a typical susceptibility value may be expressed as (for example)

$$k = 0.0057 \text{ SI.}$$

In the old (but not forgotten) system of electromagnetic units (e.m.u.), the numerical value of magnetic susceptibility for a given specimen is smaller by a factor of 4π than the SI value. Hence:

$$k(\text{SI}) = k(\text{emu}) \times 4\pi$$

$$\text{and } k = 0.0057 \text{ SI} = 0.00045 \text{ e.m.u.}$$

or simply an order of magnitude smaller for many practical purposes.

The *magnetisation* of a rock is perhaps more often referred to. Magnetisation has the same units (nT) as magnetic field, whether it is induced magnetisation, J_i, remanent magnetisation, J_r, or their vector sum. Being a vector quantity, however, the *direction* of magnetisation needs to be specified if the magnetisation is to be unambiguously defined. This is normally done by quoting two angles, one an azimuth, clockwise from geographic north, the other a dip, positive downwards, from the horizontal. This is analogous to the way the earth's field is fully defined at any given point.

2.2 Magnetic domains and minerals

Solid materials in general have magnetic properties that are classified as *diamagnetic*, *paramagnetic*, *ferromagnetic* and *anti-ferromagnetic*. The definition of these terms may be found in a physics text. The first two types of magnetic property have usually been considered as insignificant in magnetic anomaly mapping; rocks having only these properties are often classed simply as 'non-magnetic', since their magnetisation is orders of magnitude less than that of common sources of magnetic anomalies. Ferromagnetic materials, by contrast, contain magnetic 'domains' which magnetise very easily, whereas anti-ferromagnetic materials have domains which cancel each other out to give zero magnetisation. Most magnetic materials of geological significance are imperfectly anti-ferromagnetic, for which class the term **ferrimagnetic** is used (Figure 2.1).

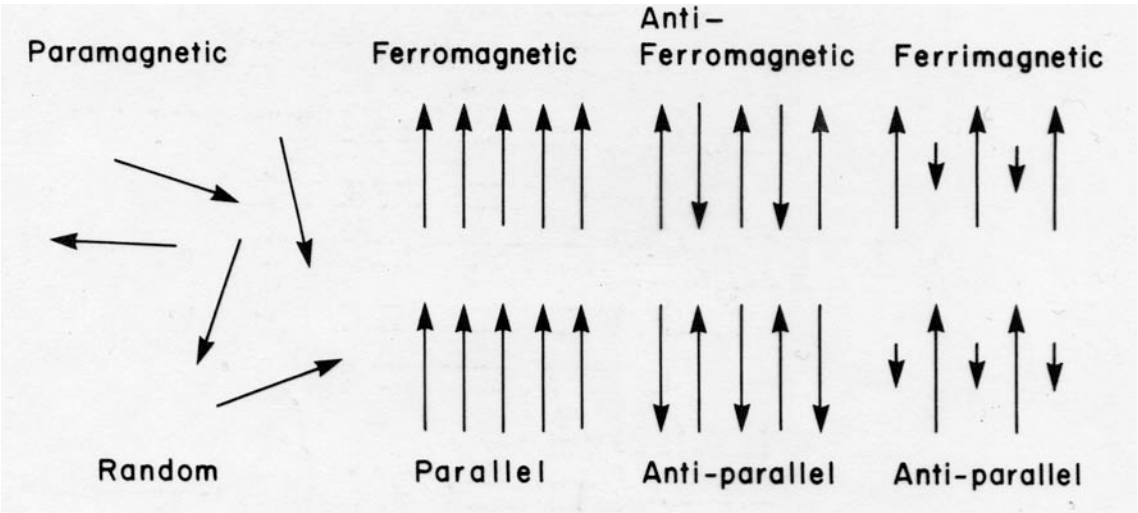

Figure 2.1 *Alignment of magnetic carriers in paramagnetic, ferromagnetic, anti-ferro-magnetic and ferrimagnetic minerals.*

The magnetostatic energy associated with the magnetization of a single mineral grain can be reduced by creating two oppositely magnetized volumes or **domains**. In larger grains, repeated subdivision into more domains is possible until the loss of energy through further subdivision is insufficient to yield the energy necessary for building a new domain wall

(Figure 2.2). It follows that the magnetic properties of any rock are, to some extent, determined by the grain size of the magnetic minerals present. Grains too small to permit subdivision into magnetic domains are known as *single domain grains* and usually carry very 'hard' magnetization, such as may be carried by rocks having a remanent magnetization that is resistant to change (by heating or AC demagnetisation). By contrast, large grains are rather 'soft' in terms of their magnetic characteristics; while they may become strongly magnetized in an inducing field, this magnetization is also easily lost. Mineral grains too small to be observed optically in a thin Chapter can still be of importance in the overall magnetic properties of a rock type.

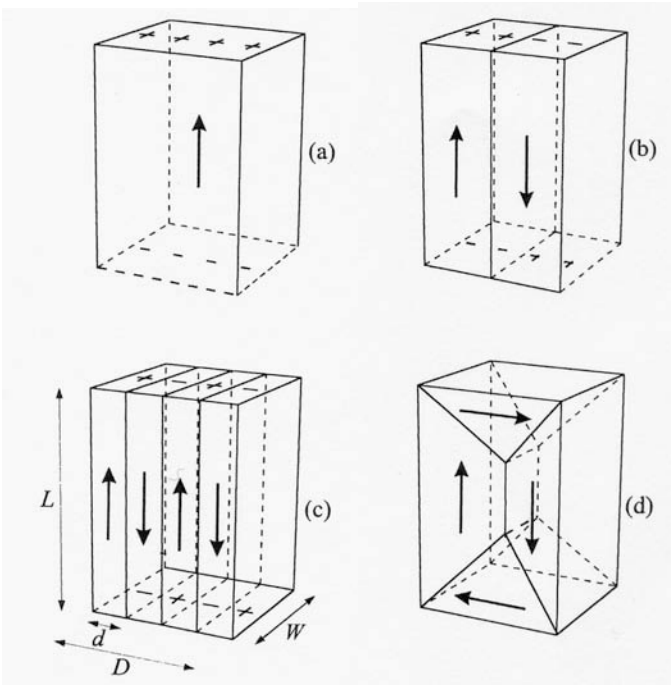

Figure 2.2 *Subdivision of a single mineral grain into a number of magnetic domains (from McElhinny and McFadden, 2000).*

In fact, only a rather small number of minerals display significant magnetic properties. These are the mixed oxides of iron and titanium (Fe and Ti) plus one sulphide mineral, pyrrhotite. In contrast to rock density, where the composition of an entire rock must be taken into account, it follows that the magnetic properties of rocks are determined only by their content of these magnetic 'carriers'. Carriers are usually accessory minerals that bear no simple relationship to the silicate/carbonate mineralogy by which rocks are conventionally classified by the field geologist (Grant, 1985). Ferrimagnetic magnetite accounts for only about 1.5 percent of crustal minerals and is by far the most important magnetic mineral in geophysical mapping (Clark and Emerson, 1991). Pyrrhotite can also be an important source of magnetic anomalies in hard rock areas.

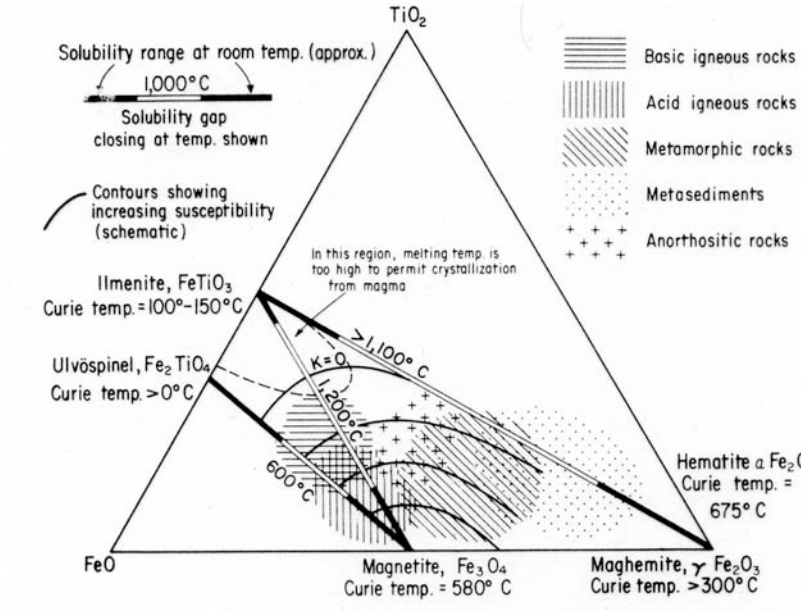

Figure 2.3 Summary of mineralogical and magnetic data pertaining to the Fe-Ti-O system (from Grant, 1985).

The magnetic oxide minerals may all be considered as members of the Fe-Ti-O system as summarised in the ternary diagram of Figure 2.3. Here the relationships between the pure minerals ilmenite, ulvöspinel, magnetite, maghemite and hematite are shown. The compositions of the opaque oxides found in igneous rocks, both acidic and basic, tend to cluster about the

magnetite-ilmenite join, whereas the opaque oxides found in metamorphic rocks cover a much wider field, which lies mostly to the right of this line. Among igneous rocks, those of acidic composition contain oxides having a higher proportion of magnetite to ilmenite than basic rocks, although the total quantity of iron-titanium oxides in acid igneous rocks is usually much less than in basic rocks (Grant 1985).

In comparison to magnetite, the susceptibility of the other Fe-Ti oxides is very small. This is illustrated in Figure 2.4 that lists the magnetic susceptibility of pure magnetite together with that of typical ores that contain high proportions of other magnetic minerals. The susceptibility of most rocks therefore reflects the abundance of 'magnetite' (in the broad sense), the relation between the volume percentage of magnetite, V_m, and magnetic susceptibility, k, may be formulated to a good approximation as:

$$k = 33 \times V_m \times 10^{-3} \text{ SI.}$$

This relationship is illustrated in Figure 2.5, along with that for pyrrhotite which produces a magnetic susceptibility an order of magnitude lower, volume for volume, than magnetite. As shown, grain size can also affect magnetic susceptibility, in that large grains of magnetite and pyrrhotite are relatively more susceptible than small grains. Significant magnetic properties of some rocks have been demonstrated to reside in sub-microscopic magnetite grains which normal petrographic description could totally overlook.

Processes of metamorphism can be shown to radically effect magnetite and hence the magnetic susceptibility of rocks. Serpentinisation, for example, usually creates substantial quantities of magnetite and hence serpentinised ultramafic rocks commonly have high susceptibility (Figure 2.10). However, prograde metamorphism of serpentinised ultramafic rocks causes substitution of Mg and Al into the magnetite, eventually shifting the composition into the paramagnetic field at granulite grade. Retrograde metamorphism of such rock can

Mineral/ore	susceptibility (SI)
pure magnetite	15
magnetite ore	0.07 - 14
ilmenite ore	0.3 - 4
pyrrhotite	0.001 - 0.1
hematite ore	0.0004 - 0.01
pyrite	0.0001 - 0.00

Figure 2.4 *Magnetic (volume) susceptibility ranges of the main magnetic minerals as ores.*

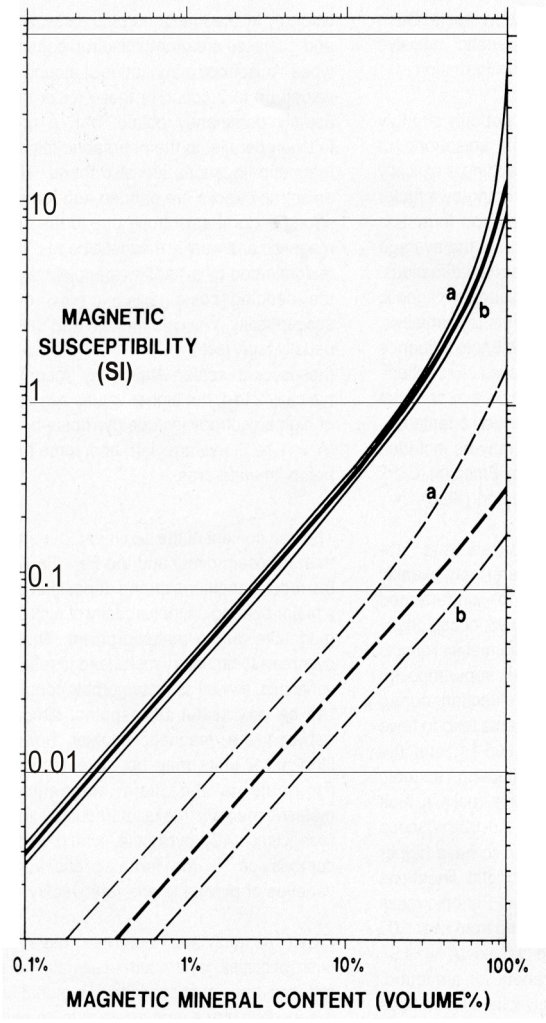

Figure 2.5 *Magnetic susceptibility of rocks as a function of magnetic mineral type and content. Solid lines: Magnetite; thick line = average trend, a = coarse-grained (>500 mm), well crystallised magnetite, b = finer grained (<20 mm) poorly crystallised, stressed, impure magnetite. Broken lines: Pyrrhotite; thick line = monoclinic pyrrhotite-bearing rocks, average trend; a = coarser grained (>500 mm), well crystallised pyrrhotite; b = finer grained (<20 mm) pyrrhotite (after Clark and Emerson 1991).*

produce a magnetic rock again. Other factors include whether pressure, temperature and composition conditions favour crystallisation of magnetite or ilmenite in the solidification of an igneous rock and hence, for example, the production of S-type or I-type granites. The iron content of a sediment and the ambient redox conditions during deposition and diagenesis can be shown to influence the capacity of a rock to develop secondary magnetite during metamorphism.

Oxidation in fracture zones during the weathering process commonly leads to the destruction of magnetite which often allows such zones to be picked out on magnetic anomaly maps as narrow zones with markedly less magnetic variation than in the surrounding rock. A further consideration is that the original distribution of magnetite in a sedimentary rock may be largely unchanged when that rock undergoes metamorphism, in which case a 'paleolithology' may be preserved - and detected by magnetic surveying. This is a good example of how magnetic surveys can call attention to features of geological significance that are not immediately evident to the field geologist but which can be verified in the field upon closer investigation.

In the case of remanent magnetisation, the most important carriers appear to be members of the hematite-ilmenite solid solution series. Titanohematites containing between 50 mole% and 80 mole% ilmenite are strongly magnetic and efficient carriers of remanence. Pure magnetite has to be exceedingly fine-grained to retain a remanent magnetisation, though magnetite contaminated with small amounts of ulvöspinel or ilmenite can acquire significant remanence.

Pyrrhotite can be the main magnetic mineral in many metasedimetary rocks, particularly in areas of metallic mineralisation, so its position of secondary importance in geophysical mapping should not be underestimated. Monoclinic pyrrhotite (Fe_7S_8) is ferrimagnetic, in contrast to the more iron-rich varieties which are only paramagnetic.

It may be clear already that the magnetic properties of magnetite and its related minerals - and pyrrhotite - in rocks is a complex topic, a better understanding of which is germane to effective interpretation of magnetic survey data. This is the role of 'magnetic petrology' which aims to formally demonstrate the creative use of ground-truth through integration of petrological and rock magnetic studies in order to enhance our ability to develop realistic geologic models as an end product of aeromagnetic surveys. Significant results from a variety of studies in magnetic petrology were presented by Wasilewski and Hood (1991).

2.3 General observations on the magnetic properties of rocks

Figure 2.6, from the informed and comprehensive review by Clark and Emerson (1991), shows typical ranges for the magnetic susceptibilities encountered in a variety of common rock types. Wide ranges of values are found even within one type of rock, and the total range encountered covers many orders of magnitude, from virtually non-magnetic rocks, to values exceeding k = 1. This may be contrasted with the relatively narrow range of density values encountered for the same types of rock. The same cautions concerning the prediction of rock types from their anomalies are therefore even more important in the case of magnetic properties; there is clearly a great deal of overlap between the likely magnetic susceptibility of quite dissimilar rock types.

It is by no means simple to distil simple guidelines from the vast literature on the magnetic properties of rocks. However, the interpreter of aeromagnetic surveys should not be discouraged and, in so far as generalisations are possible, the following statements may be made by way of encouragement - without detailing the many exceptions.

(a) ***Sedimentary rocks*** are usually non-magnetic. This is the basis for many applications of aeromagnetic surveying in that the interpretation of survey data assumes that magnetic sources must lie below the base of the sedimentary sequence. This allows rapid identification of hidden sedimentary basins in petroleum exploration. The thickness of the sedimentary sequence may be mapped by systematically determining the depths of the magnetic sources (the 'magnetic basement') over the survey area. Exceptions that may cause difficulties with this assumption are certain sedimentary iron deposits, volcanic or pyroclastic sequences concealed within a sedimentary sequence and dykes and sills emplaced into the sediments.

(b) ***Metamorphic rocks*** probably make up the largest part of the earth's crust and have a wide range of magnetic susceptibilities. These often combine, in practice, to give complex patterns of magnetic anomalies over areas of exposed metamorphic terrain. Itabiritic rocks tend to produce the largest anomalies, followed by metabasic bodies, whereas felsic areas of granitic/gneissic terrain often show a plethora of low amplitude anomalies imposed on a relatively smooth background field.

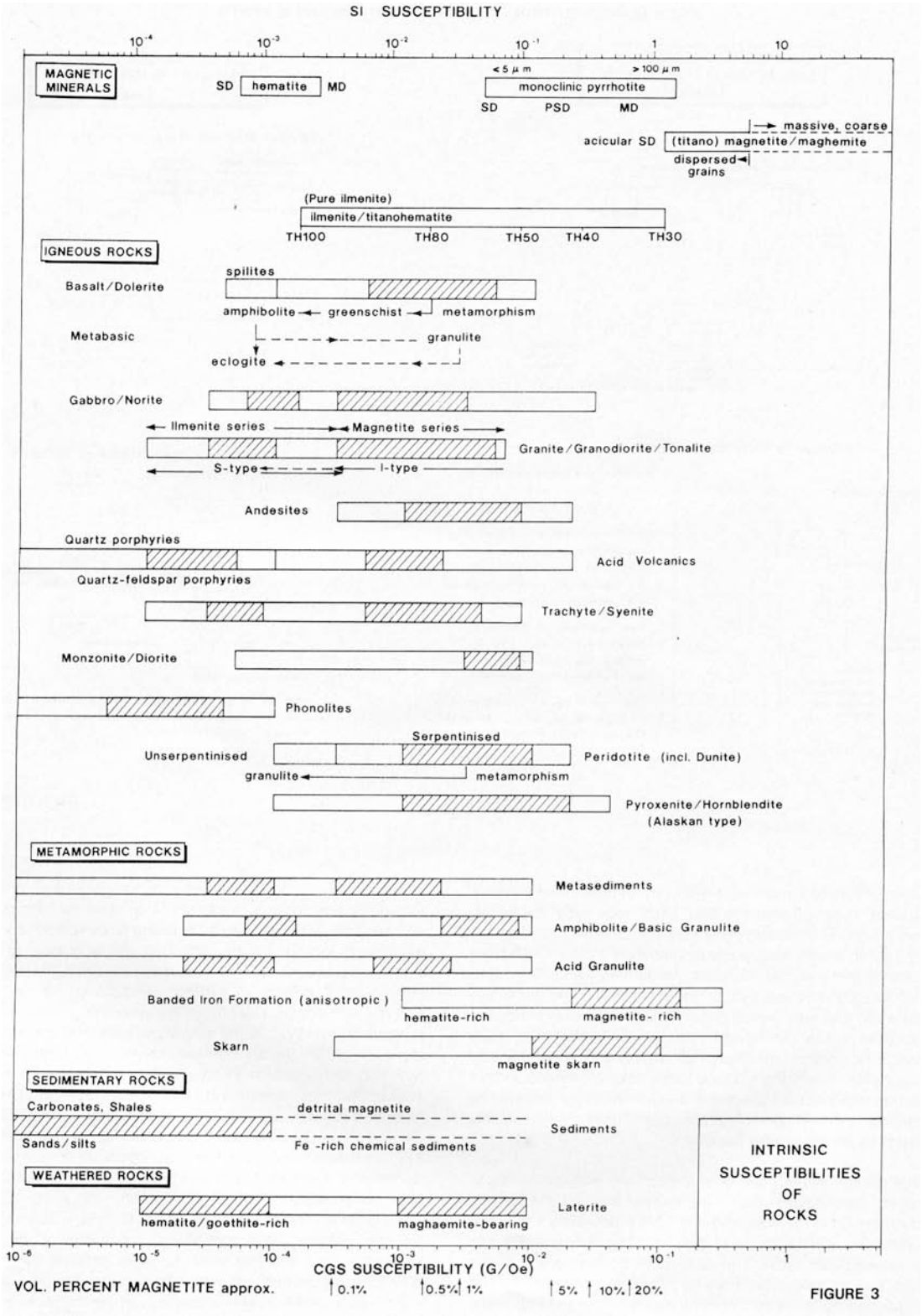

Figure 2.6 *Susceptibility ranges of common rock types (from Clark and Emerson 1991).*

(c) ***Igneous and plutonic rocks***. Igneous rocks also show a wide range of magnetic properties. Homogeneous granitic plutons can be weakly magnetic - often conspicuously featureless in comparison with the magnetic signature of their surrounding rocks - but this is by no means universal. In relatively recent years, two distinct categories of granitoids have been recognised: the magnetite-series (ferrimagnetic) and the ilmentite-series (paramagnetic). This classification has important petrogenetic and metallogenic

implications and gives a new role to magnetic mapping of granites, both in airborne surveys and in the use of susceptibility meters on granite outcrops. Mafic plutons and lopoliths may be highly magnetic, but examples are also recorded where they are virtually non-magnetic. They generally have low Q values as a result of coarse grain size. Remanent magnetisation can equally be very high where pyrrhotite is present.

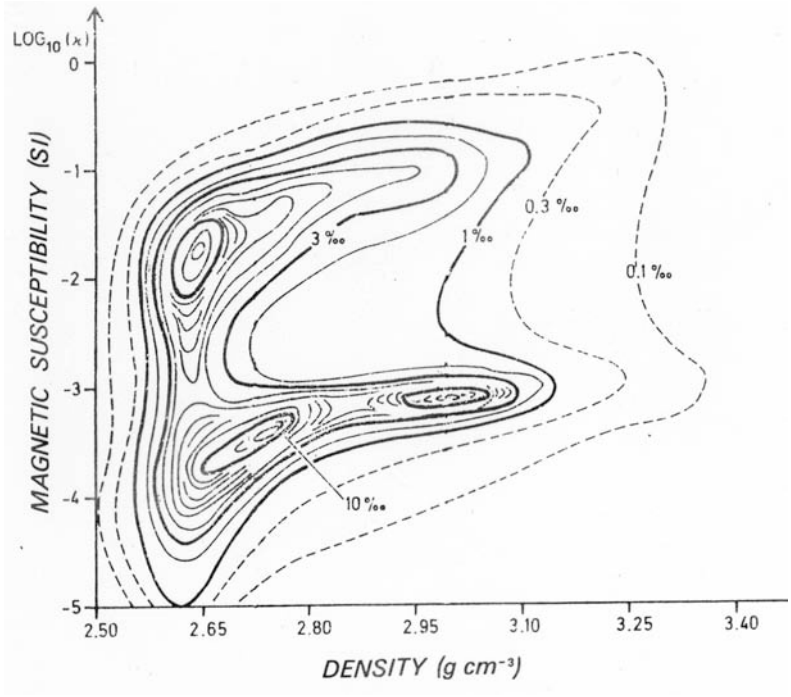

Figure 2.7 *Frequency distribution of 30 000 Precambrian rock samples from northern Scandinavia tested for density and magnetic susceptibility (after Henkel 1991).*

(d) ***Hypabyssal rocks***. Dykes and sills of a mafic composition often have a strong, remanent magnetisation due to rapid cooling. On aeromagnetic maps they often produce the clearest anomalies which cut discordantly across all older rocks in the terrain. Dykes and dyke swarms may often be traced for hundreds of kilometres on aeromagnetic maps - which are arguably the most effective means of mapping their spatial geometry (Reeves 1985, for example). Some dyke materials have been shown to be intrinsically non-magnetic, but strong magnetic anomalies can still arise from the contact auriole of the encasing baked country rock. An enigmatic feature of dyke anomalies is the consistent shape of their anomaly along strike lengths of hundreds of kilometres, often showing a consistent direction of remanent magnetisation. Carbonatitic complexes often produce pronounced magnetic anomalies.

(e) ***Banded iron formations/itabirites***. Banded iron formations can be so highly magnetic that they can be unequivocally identified on aeromagnetic maps. Anomalies recorded in central Brazil, for example, exceed 50000 nT, in an area where the earth's total field is only 23000 nT. Less magnetic examples may be confused with mafic or ultramafic complexes.

(f) ***Ore bodies*****.** Certain ore bodies can be significantly magnetic, even though the magnetic carriers are entirely amongst the gangue minerals. In such a case the association with magnetic minerals may be used as a path-finder for the ore through magnetic survey. In general, however, the direct detection of magnetic ores is only to be expected in the most detailed aeromagnetic surveys since magnetic ore bodies form such a very small part of the rocks to be expected in a survey area.

In an important and pioneering study of the magnetic properties of rocks, almost 30 000 specimens were collected from northern Norway, Sweden and Finland and measured for density, magnetic susceptibility and NRM (Henkel, 1991). Figure 2.7 shows the frequency distribution of magnetic susceptibility against density for the Precambrian rocks of this area. It is seen here that whereas density varies continuously between 2.55 and 3.10 t/m^3, the distribution of magnetic susceptibilities is distinctly bimodal. The cluster with the lower

susceptibility is essentially paramagnetic ('non-magnetic'), peaking at k = 2 x 10^{-4} SI, whereas the higher cluster peaks at about k =10^{-2} SI and is ferrimagnetic. The bimodal distribution appears to be somewhat independent of major rock lithology and so gives rise to a typically banded and complex pattern of magnetic anomalies over the Fenno-Scandian shield. This may be an important factor in the success of magnetic surveys in tracing structure in metamorphic areas generally, but does not encourage the identification of specific anomalies with lithological units.

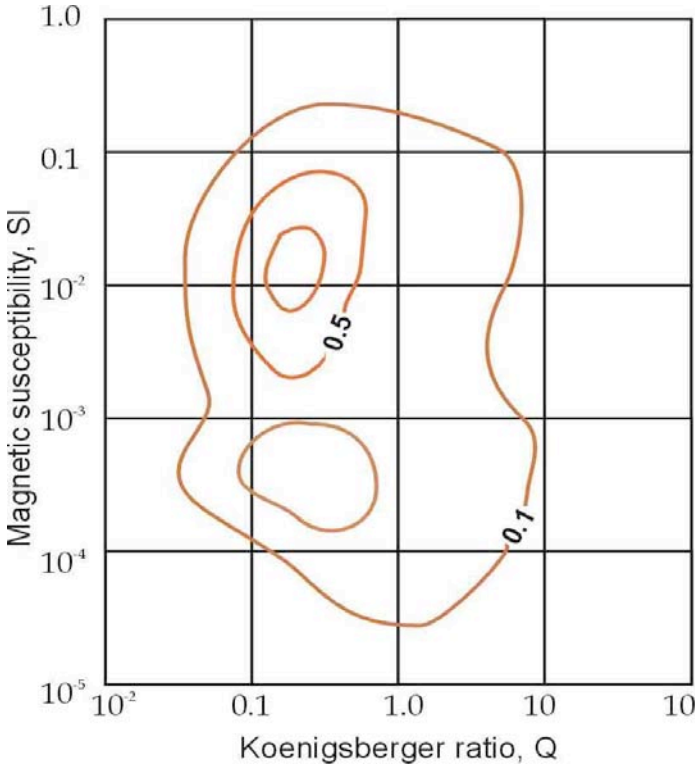

Figure 2.8 *Frequency distribution of 30 000 Precambrian rock samples from northern Scandinavia: Koenigsberger ratio versus magnetic susceptibility (after Henkel 1991).*

It should be noted from Figure 2.7 that, as basicity (and therefore density) increases within both clusters, there is a slight tendency for magnetic susceptibility also to increase. However, many felsic rocks are just as magnetic as the average for mafic rocks - and some very mafic rocks in the lower susceptibility cluster are effectively non-magnetic.

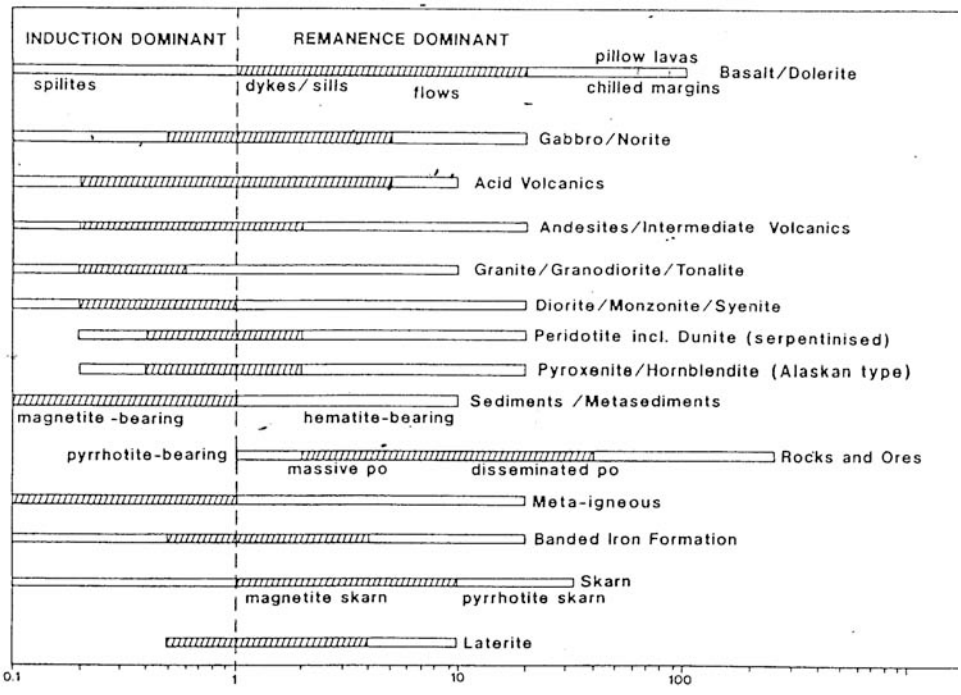

Figure 2.9 *Ranges of Koenigsberger ratio for a selection of common rock types (from Clark and Emerson 1991). The hashed bands indicate the more commonly occurring ranges, covering ~75% of the Q ratio values.*

Figure 2.8 shows the relationship between magnetic susceptibility and Koenigsberger ratio, Q determined in the same study. The simplifying assumption, often forced upon the aeromagnetic interpreter, that magnetisation is entirely induced (and therefore in the direction of the present-day field) gains some support from this study where the average Q for the Scandinavian rocks is only 0.2. Figure 2.9 shows the ranges of Q value determined for a range of rocks where, once again, a wide range of values is exhibited.

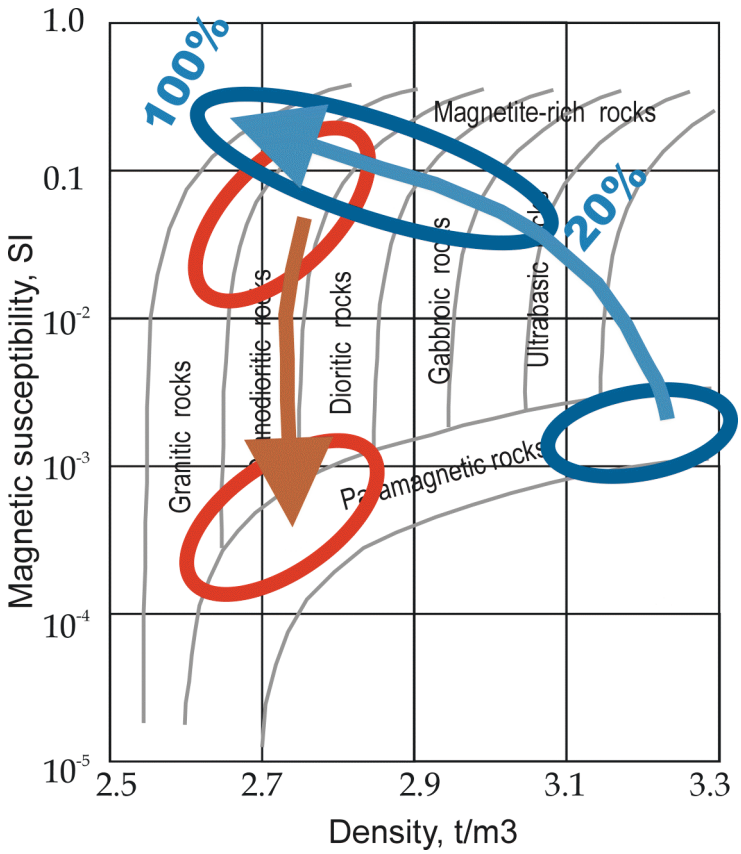

Figure 2.10 *Some effects of metamorphism on rock magnetism. In blue, the serpetinisation of olivine (blue) turns an ultramafic but non-magnetic rock into a highly magnetic one. In red, the oxidation of magnetite to maghemite reduces magnetic susceptibility by two orders of magnitude.*

The possible effects of metamorphism on the magnetic properties of some rocks are illustrated in Figure 2.10. The form of the figure is the same as Figure 2.7 and attempts to divide igneous and metamorphic rocks according to their density and susceptibility. Two processes are illustrated. First, the serpentinisation of olivine turns an essentially non-magnetic but ultramafic rock into a very strongly magnetic one; serpentinites are among the most magnetic rock types commonly encountered. Second, the destruction of magnetite through oxidation to maghemite can convert a rather highly magnetic rock into a much less magnetic one.

2.4 Methods of measuring magnetic properties

(a) In the laboratory and at outcrops. A 'susceptibility meter' may be used on hand-specimens or drill-cores to measure magnetic susceptibility (Clark and Emerson, 1991). This apparatus may also be used in the field to make measurements on specimens *in situ* at outcrops. Owing to the wide variations in magnetic properties over short distances, even within one rock unit, such measurements tend to be of limited quantitative value unless extremely large numbers of measurements are made in a systematic way.

(b) In a drillhole. Susceptibility logging and magnetometer profiling are both possible within a drillhole and may provide useful information on the magnetic parameters of the rocks penetrated by the hole.

(c) From aeromagnetic survey interpretation. The results of aeromagnetic surveys may be 'inverted' in several ways to provide quantitative estimates of magnetic susceptibilities, both in terms of 'pseudo-susceptibility maps' of exposed metamorphic and igneous terrain, and in terms of the susceptibility or magnetisation of a specific magnetic body below the ground surface (see Chapter 9).

(d) Paleomagnetic and rock magnetic measurements. The role of paleomagnetic observations has been important in the unravelling of earth history. Methods depend on the collection of oriented specimens - often short cores drilled on outcrops with a portable drill. Studies concentrate on the direction as well as the magnitude of the NRM. Progressive removal of the NRM by either AC demagnetisation or by heating to progressively higher temperatures (thermal demagnetisation) can serve to investigate the metamorphic history of the rock and the direction of the geomagnetic field at various stages of this history. Components encountered may vary from a soft, viscous component (VRM) oriented in the direction of the present day field, to a 'hard' component acquired at the time of cooling which can only be destroyed as the Curie point is passed. Under favourable circumstances other paleo-pole directions may be preserved from intermediate metamorphic episodes. Accurate radiometric dating of the same specimens vastly increases the value of such observations to understanding the geologic history of the site.

The reader is referred to McElhinny and McFadden (2000) for further information on these methods, though it must be stressed that, in general there is an imbalance between the tremendous effort and expenditure invested in mapping geophysical anomalies and the comparatively modest investment in trying to measure the rock properties that give rise to geophysical anomalies. A notable exception is the work of Korhonen *et al.* (2003).

2.5 The approach of the interpreter

In geophysical interpretation, it is seldom possible to interpret rock type directly from anomalies. With the large range of magnetisations found amongst rocks, this is doubly difficult for magnetic anomalies. This is not to say that the potential for deriving geological information from aeromagnetic anomalies is limited. On the contrary, given that magnetic anomalies map only the distribution of minor minerals, their power to map geology – particularly hidden geology – is substantial. This arises in large part from the magnetic *contrasts* (as opposed to absolute magnetisation values) that often exist between one rock unit and its neighbour(s) as a consequence of the bi-modal distributuon shown in Figure 2.7. Further information comes from observing the shape (in plan view) of individual anomalies and the texture of the anomaly patterns as a whole. This will be discussed further in later Chapters. Within the context of magnetic properties of rocks, however, it is necessary to conclude this Chapter with a few remarks about how to handle the complexities of rock magnetism from the standpoint of someone attempting to carry out interpretation of magnetic anomalies from a typical airborne survey.

While there are some exceptions, in most cases any given survey area will most probably be almost totally devoid of precise rock magnetic measurements; very often survey areas will be almost totally devoid of outcrop, as this is frequently the motivation for using aeromagnetic reconnaissance in the first place. The interpreter then has to rely largely on experience when trying to understand the geological message in the anomaly patterns. What has been said in the foregoing Chapters about rock magnetism is a brief summary of such experience. A second and more area-specific line of approach is to search for potential source rocks for the more prominent of the anomalies revealed by the survey. A

minimum requirement for this is to have the aeromagnetic survey (contours or images) at the same scale and projection as the local geological map and then to search for possible correlations between anomalies and outcropping rock types. A short-list of five to ten rock-types probably associated with the more well-defined magnetic anomalies will provide a useful starting point. It is often also the case that identifying rock-types that have *little or no* representation (or, at best, an area of low relief) in the anomaly map can be equally as useful. By such techniques, the interpreter strives to use the anomaly pattern as a means of extrapolating from the 'known' (or 'mapped') geology into the 'unknown'. Rigour, curiosity and hours of endeavour can pay dividends in understanding that are optimally encapsulated in an 'interpretation map'. An appropriate degree of caution or scepticism about the accuracy of the pre-existing geological map is important in this process. Access to reliable outcrop information is a bonus as poor exposure often drives the mapping geologist to be more or less imaginative in interpolation between what has been seen in the field. The value of the aeromagnetic survey is its ability to improve on the field mapping, so little is gained if the geological map is followed religiously as given information in geophysical interpretation, even where the map area is devoid of ground control from outcrop.

Further reading

Clark, D.A., and Emerson, D.W., 1991. Notes on rock magnetisation in applied geophysical studies. Exploration Geophysics vol 22, No.4, pp 547-555.

Grant, F.S., 1985. Aeromagnetics, geology and ore environments, I. Magnetite in igneous, sedimentary and metamorphic rocks: an overview. Geoexploration volm 23, pp 303-333.

Henkel, H., 1991. Petrophysical properties (density and magnetization) of rocks from the northern part of the Baltic Shield. Tectonophysics, vol 192, pp 1-19.

Korhonen, J.V., Aaro, S., All, T., Nevanlinna, H., Skilbrei, J.R., Säävuori, H., Vaher, R., Zhdanova, L., and Koistinen, T., 2002. Magnetic anomaly map of the Fennoscandian shield, scale 1:2 000 000

McElhinny, M.W., and McFadden, P.L., 2000. Paleomagnetism – continents and oceans. Academic Press, 386 pp.

Reeves, C.V., 1985. The Kalahari Desert, central southern Africa – a case history of regional gravity and magnetic exploration. *In* Hinze, W.J. (ed), The utility of gravity and magnetic surveys, Society of Exploration Geophysicists, special volume, pp 144-156.

Wasilewski, P., and Hood, P.J., 1991. Special issue: Magnetic anomalies, land and sea. Tectonophysics, vol 192, Nos. 1/2.

3.

Magnetometers and aircraft installations

3.1 A brief history of airborne magnetometers

There is a long history of magnetometers designed and constructed on mechanical principles to measure the direction of the Earth's magnetic field, either in vertical or horizontal planes (dip-needles, compasses). The development of magnetometers effective in exploration, i.e. usable for making large numbers of readings over a given area of interest in a reasonably short space of time, however, dates only from the invention of the electronic magnetometer during the second world war. The first such magnetometer, known as the ***flux-gate***, was designed to detect submarines from over-flying aircraft and the sensor measured only the scalar magnitude of the total geomagnetic field. This design concept avoided all the complications associated with precise orientation of the sensor that was difficult and time-consuming to achieve and immediately enabled the instrument to be carried by a moving vehicle such as an aircraft. This allowed a very rapid rate of progress over a survey area. (It was to be fifty years before the same capability was achieved for effective gravimetric surveys where orientation of the sensor is much more critical). Three fluxgates mounted orthogonally were employed. Two were linked to servo motors each driven by non-zero output from the associated fluxgate, so ensuring that the third fluxgate was aligned with the geomagnetic field. The advent of this new technology, followed by the availability in peace-time of personnel trained in airborne operations during the war, produced a business opportunity that set airborne geophysical surveying into motion in the exploration industry (Reford and Sumner, 1964).

The technology was progressively refined with time and the capabilities of the initial electronic equipment, rudimentary by today's standards, developed all the while. In the late 1950s the ***proton precession magnetometer*** made its appearance and, despite on-going refinement of the flux-gate instrument, eventually replaced it in routine survey operations.

Optical pumping magnetometers first came into airborne service in the early 1960s but they did not seriously replace earlier types of magnetometer until the late 1980s when expiry of the original patent led to their more general application. Helium, rubidium, cesium and potassium types have all been used. Cesium vapour magnetometers are now used extensively in the airborne survey industry on account of their high sensitivity and rapid reading capability. Readings accurate to much less than one part per million of the total field may be made ten times per second. This degree of

sophistication is unnecessary in ground-based surveys where magnetic anomalies tend to be higher in amplitude and much more affected by ‘noise’ due to geological sources in the surface and overburden layers. For ground surveys, then, proton-type magnetometers are quite adequate and much less costly than optically-pumped systems.

Both on the ground and in the air, magnetic gradiometers have gained in popularity in recent years. These systems will be described briefly at the end of this Chapter since this refinement is not critical to the broader understanding of airborne magnetometer systems as a whole.

3.2 Principles of airborne magnetometers

(a). Optical absorption magnetometer

The physical principle on which the optical absorption magnetometer is based is known as Larmor precession. In the presence of an external magnetic field, the orbital motion of a charged particle - such as an electron in its orbit around an atomic nucleus - precesses (i.e. wobbles in the fashion of a spinning top) about the direction of the magnetic field. The angular frequency of this precession is directly proportional to the magnitude of the magnetic field. A constant of proportionality - the Larmor frequency - is peculiar to each element. The so-called alkali metals which occupy the first group of the periodic table and therefore have a single electron in the outermost orbit are most suitable for the exploitation of this effect.

Consider atoms in which two closely similar electron energy levels (A1 and A2) exist along with a much higher energy level (B). The existence of closely-spaced levels A1 and A2 is attributable to the Zeeman effect in which a single energy level is split in the presence of a magnetic field to which the magnetic moment of the electron may be either parallel (A1) or anti-parallel (A2). Suitable illumination of the alkali-metal vapor atoms in a closed glass cell - for example with circularly polarised light from an emission spectrum of the same element which interacts only with electrons in the A1 level - will selectively excite electrons from the A1 level to the B level. From here they will spontaneously fall back to the A1 and A2 levels with equal likelihood. However, while they will be re-excited from the A1 level, they will remain undisturbed in the A2 level where they will consequently accumulate. This process is known as 'optical pumping'. Once level A1 is free of electrons there will be no further absorption of light, the cell is transparent and strong light output is registered by a photocell.

An electromagnetic field - of the correct Larmor frequency for the ambient magnetic field - when applied to the cell will disturb electrons from the A2 level and return them to the A1 level. This causes the cell to become opaque and the optical pumping to restart. The correct frequency is determined by adjusting it until minimum light transmission by the cell is recorded. Electronic circuitry is used to track this applied frequency and keep it tuned to variations in the magnitude of the ambient magnetic field. In the case of Cesium, the Larmor frequency is 3.498 Hz per nT giving an applied frequency of 174.9 kHz for an ambient field of 50 000 nT. Accurate monitoring of the applied frequency can achieve almost instantaneous values for the absolute magnitude of the ambient magnetic field at the cell with a sensitivity of about 0.01 nT.

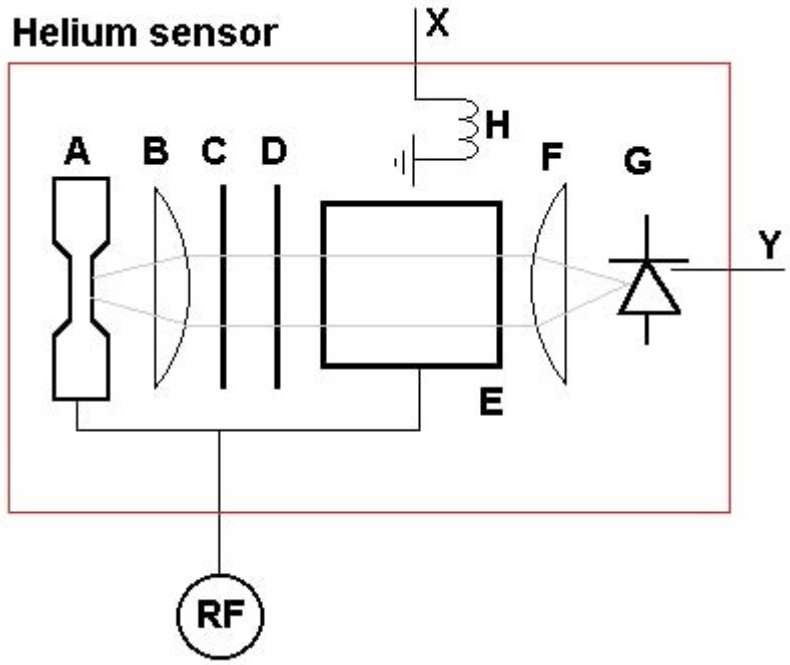

Figure 3.1 *Schematic block diagram of the sensing element of a Helium magnetometer. A = helium lamp, B = lens, C = filter, D = circular polarizer, E = helium absorption cell, F = lens, G = photo-detector, H = coil of radio-frequency oscillator tracking the Larmor frequency for maximum darkening of cell, RF1 = Radio-frequency power oscillator (16 MHz) maintaining the ionised state of helium by strong plasma discharge in the region of the lamp and weak plasma discharge in the absorption cell. External electronic circuitry for control and measurement is connected at X and Y. (Courtesy of EG&G Geometrics).*

Instruments exploiting this principle are often referred to as 'alkali-vapor magnetometers'. Early magnetometers of this type employed rubidium vapor, but cesium vapor has become more popular and a potassium vapor instrument has been proven in practice in recent years. Larmor precession is also shown by the gas helium and cesium-vapor, potassium-vapor and helium magnetometers are all presently available commercially. The principle was first exploited in the 1960's, but usage was restricted by patents. The most important of these did not expire until 1987 which accounts for the comparatively recent growth in application of optical absorption instrumentation in airborne geophysics.

Practical problems with cesium vapor magnetometers include the eight discrete spin-states for ^{133}Cs which give rise to not one but eight closely-spaced spectral lines. The relative importance of these varies with the angle made between the optical axis of the instrument and the magnetic field direction, giving rise to variations in the absolute magnetic field value. This has been reduced to less than 1 nT in the so-called split-beam instrument in which the light beam is split, circularly polarised in opposite directions, and passed through two halves of the cell before recombination. A second problem is posed by the 'dead-zones' which form a solid angle of about 30 degrees about the optical axis. If the magnetic field direction falls within this orientation, the magnetometer will not work. This calls for some care with orientation of the sensor with regard to the direction of flight of the aircraft (along control lines as well as regular flight lines) and the magnetic inclination of the geomagnetic field. More sophisticated electronics have significantly reduced this problem to a heading effect of no more than

0.1 nT and instrumental noise below 0.001 nT in current production models (Hood 1991).

Helium has a Larmor frequency of 28.02468 Hz/nT or about eight times higher than cesium. This permits a significantly higher sampling rate and the production instrument has a proven noise level in operation of less than 0.005 nT. Absolute measurements of the magnetic field to this accuracy at intervals of 1/10th of a second (or about 7 metres at normal aircraft speeds) exceeds any likely requirements for along-line sample interval. Equatorial dead-zones of 30 degrees cause no problems in high magnetic latitudes if the optical axis is vertical. The sensor itself occupies a very small volume and can be mounted conveniently in the end of a stinger or in an aircraft wing-tip. It is shown schematically in Figure 3.1. Similar performance is claimed for the potassium vapor instrument, so all three instrument types meet basic requirements for current magnetic surveys and appear to offer reliable performance in routine survey production.

(b). Proton precession magnetometer

The proton free-precession magnetometer exploits another (but related) area of nuclear physics, namely the tendency of a free proton (H+) to align its magnetic moment with an ambient magnetic field and precess about that field direction when disturbed. A quantity (usually about half a litre) of a liquid rich in protons - such as water or alcohol - in a sensor bottle is subjected to a strong applied magnetic field by way of passing a current through a coil wound round the bottle. Turning off that current causes the protons to search for the direction of the only remaining magnetic field - that of the earth - and to precess around it. The frequency of precession is given by

$$f = g_p T / 2\pi m_o$$

where g_p is the 'gyromagnetic ratio of the proton' which is known to be 2.67520×10^{-8} T^{-1} s^{-1}. T is the magnetic total field and m_o is the magnetic permeability of free space.

In the simplest instrument, a signal-detector detects the precession frequency by counting the number of cycles, N, in a timed interval, t.

$$f = N/t = g_p T / 2\pi m_o$$

If t is chosen such that $1/t = g_p T / 2\pi m_o$ then N = T and the number of cycles counted is numerically equal to the measured field in nT. Since T is about 50 000 and f about 2 kHz, a counting time of 25 seconds would be required.. This is inconveniently slow, even if the precession signal were still detectable after such a long time period. An early sophistication was to compare the signal to a high frequency oscillator which locks onto a multiple of the precession frequency giving an accuracy of one part in 50 000 with a counting period of less than 1 second.

Note that there is no need to orient the sensor other than to make sure that the field of the coil and that of the earth are not nearly coincident. For airborne installations it is sufficient for the sensor axis to be horizontal at high magnetic inclinations and vertical at low inclinations. A mounting transverse to the axis of the aircraft may be preferable in middle latitudes. Note also, as with the optical pumping instrument, the readings are

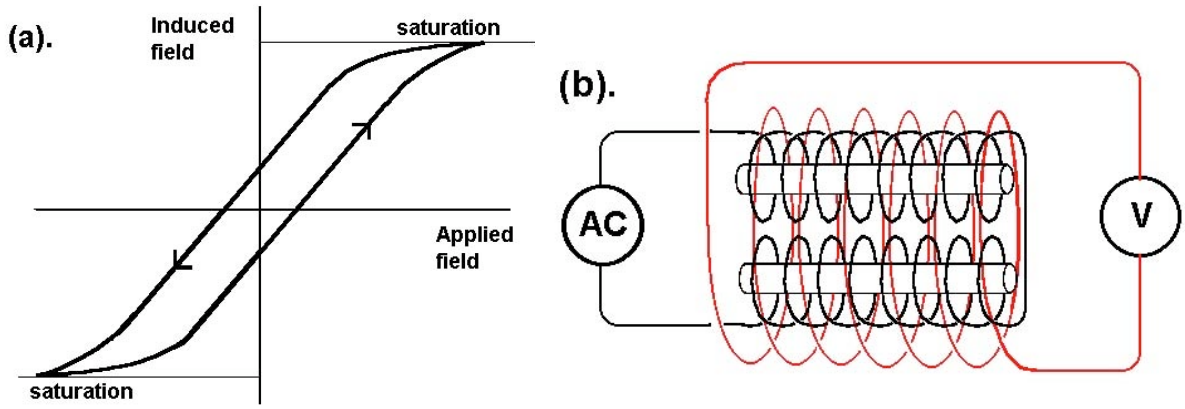

Figure 3.2 *(a) Hysteresis loop showing the relationship between the applied (AC) magnetic field and the field induced in a susceptible material when saturation is reached during each cycle. (b) Schematic diagram of the sensor of fluxgate magnetometer.*

absolute, avoiding any need for calibration. The sensor's function is intolerant of high magnetic gradients, but that is seldom a problem in the air.

Proton precession instruments have been used widely and are still the preferred instrument for ground magnetic surveys where they are relatively inexpensive and offer more than adequate accuracy and sampling speed. Readings can, however, only be made discretely (rather than continuously) since it takes a finite time to polarise the protons and then observe the precession. The additional accuracy desirable in an airborne installation can only be achieved at the expense of longer sampling times. Nevertheless, instruments with one nT sensitivity and half-second sampling were still in use in airborne surveys into the 1990s, particularly perhaps in helicopter installations where slow speed and low ground clearance tend to give large anomalies and adequate time for an individual measurement.

(c). Flux-gate magnetometer

The sensor element of the flux-gate magnetometer consists of two identical rods of a material with high magnetic permeability. If one such rod is wound with a coil through which an alternating current (about 1000 Hz) is passed, the field induced in the core will be driven to saturation during each half-cycle and a plot of induced field against applied field will describe a hysteresis loop (Figure 3.2a). If the second rod is placed alongside the first, wound in the opposite direction but given the same alternating current, its induced field will always be exactly equal in magnitude and opposite in direction to that in the first rod. The sum of the induced magnetic fields, detected by a secondary coil wound around both the primary cores (Figure 3.2b), is always zero.

However, when an external magnetic field - such as the earth's - is present, the external field will assist the saturation of one core while opposing that of the other during each half cycle. As a result, the combined effect of the induction of both cores is non-zero twice each cycle, i.e. pulses of magnetic field appear each half-cycle as the current flow passes through zero. These pulses may be detected by a suitable amplifier connected to the secondary winding. A third coil (not shown), co-axial with the second, carries a

current which is adjusted by way of the amplifier output to null-out the earth's field exactly and so reduce the observed pulses to zero. The magnitude of the current in the third or compensating coil necessary to maintain this condition may then be used, with suitable calibration, to assess continuously the magnitude of the external field component along the axis of the system.

In addition to the need for calibration, the instrument is somewhat temperature sensitive and has to be carefully oriented so that its axis is in the direction of the total magnetic field vector. In early airborne systems, this was achieved by mounting two further flux-gate elements such that all three were mutually perpendicular. The two subsidiary fluxgates were each linked to a servo-motor feed-back system which adjusted the orientation of the entire system so that the second and third flux-gates always registered a field of zero, thus ensuring that the first flux-gate is precisely aligned to the earth's field. These features all presented some difficulties for airborne survey operations and the practical advantages of sensors without moving parts should be obvious.

With appropriate sophistication over the period of 30 years or more over which flux-gate instruments performed airborne service, sensitivities of 0.1 nT were eventually achieved. A continuous signal could be recorded on moving chart-paper giving very clearly defined anomalies in the pre-digital era. The relative convenience of other magnetometer types made the flux-gate instrument more-or-less obsolete for airborne applications about the same time as digital acquisition technology was first introduced in the early 1970's.

3.3 Aircraft installations and magnetic compensation

(a) Birds and stingers

It is clear that great pains must be taken to eliminate spurious magnetic signals that may be expected to arise in an aeromagnetic survey from the aircraft itself. Standard tests must also be defined to measure the success with which this has been achieved for any given survey aircraft and magnetometer system. When monitoring a survey carried out by a contractor it is essential to ensure that these tests are performed before the acquisition of survey data commences, at the end of the survey to check that nothing has changed, periodically during survey operation if that extends over a number of months and whenever a major modification - such as an engine change - is carried out to the aircraft.

The airframes of modern aircraft are primarily constructed from aluminium alloys which are non-magnetic; the main potential magnetic sources are the engines. As a first approach, then, magnetometer sensors have always been mounted as far away as possible from the aircraft engines. The earliest magnetometer configurations simply involved placing the sensor in a 'bird' which was towed behind and below the aircraft to reduce the magnetic effect by simply increasing the distance as much as possible. This is still often the preferred arrangement for helicopter installations (Figure 3.3) for which a great advantage is usually the ability to mount and de-mount equipment quickly in an available aircraft at the survey locality. Apart from being an inelegant arrangement for fixed-wing aircraft, bird operation has potential dangers and additional sources of noise and error are evident through manoeuvering of the bird itself during flight.

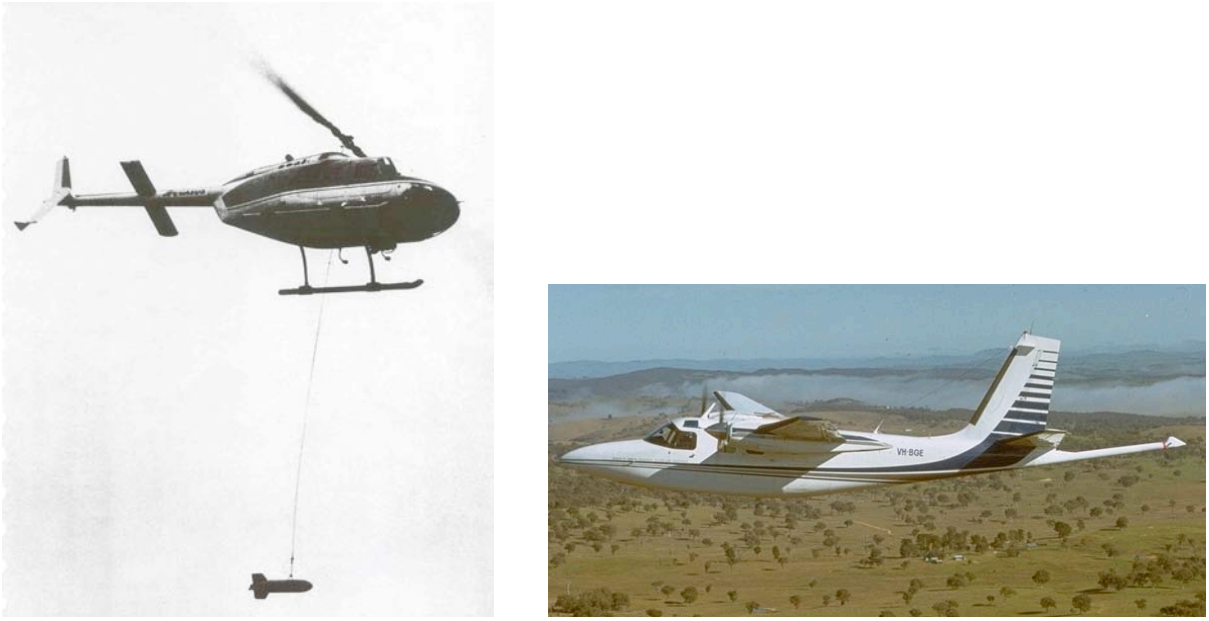

Figure 3.3 *Left, a magnetometer slung below a helicopter as a 'bird' installation and, right, a magnetometer in a 'stinger' behind a fixed-wing aircraft.*

A rigid extension of the airframe - usually to the aft in the form known as a 'stinger' (Figure 3.3) - solves many of these problems but necessitates closer attention to the sources of magnetic effects on board the aircraft. There are principally three sources:

(a). Permanent magnetisation of the aircraft which will be unchanging unless engines are changed or magnetic objects (such as toolboxes) are brought on board.

(b). Magnetisation induced in engine (or other) components by the earth's magnetic field. The magnitude and direction of the magnetisation will be dependent on the relative orientation of the aircraft and the geomagnetic field and so will change with survey location (different magnetic inclinations), direction of flight and even with small adjustments to flight direction in three dimensions during normal manoeuvre along a single flight line.

(c). Magnetic fields set up by electrical circuits within the aircraft and any eddy currents induced - according to Biot-Savart's Law (see ttp://webphysics.davidson.edu/physlet_resources/bu_semester2/c14_biotsavart.htm) - in the airframe as a result of the motion of the conductive airframe through the earth's magnetic field .

For many years these effects were dealt with sequentially. The permanent magnetic field of the aircraft at the magnetometer sensor was compensated ('backed-off') by passing appropriate DC currents through each of three orthogonal coils in the vicinity of the sensor. The induced component was offset by mounting pieces of highly-permeable material close to the sensor in a position (found by trial-and-error) such that their magnetic effect was always equal and opposite to that of the engines. The eddy-current effects were similarly mimicked but in opposite sign by coils of wire placed close to the sensor. Since the success of all these measures could only be fully proved in flight (see later in this Chapter) and most of them could only be adjusted on the ground, the compensation of an aircraft was a tedious and time-consuming business which had to

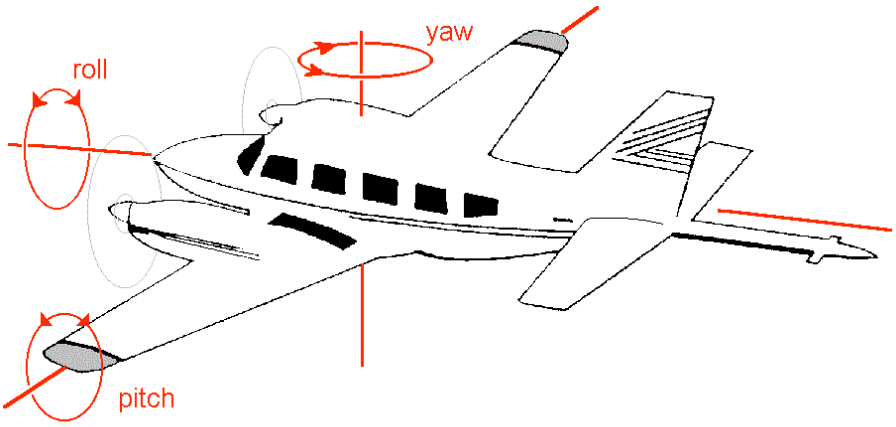

Figure 3.4 *Pitch, roll and yaw manoeuvres of an aircraft about three orthogonal axes: (a) transverse horizontal, (b) longitudinal horizontal and (c) vertical respectively.*

be often repeated to ensure ongoing system integrity. In more recent times, active magnetic compensators have been developed to address these problems 'on-line' during survey flight.

(b). Active magnetic compensation

The principle of the active magnetic compensator is that the magnetic effects of different heading directions and aircraft manoeuvres are first measured during a calibration flight in the absence of magnetic anomalies and then subtracted in real-time during survey operation as magnetic anomalies are recorded. During calibration and survey operation the attitude of the aircraft with respect to the geomagnetic field is continuously monitored using three orthogonal flux-gate sensors. During survey operation, the recorded aircraft attitude is used to apply an appropriate correction to each reading of the magnetometer. The following sequence of procedures is carried out before a survey commences.

In the vicinity of the survey area, an area of known low magnetic anomaly relief is chosen and the survey aircraft flown to high altitude over it. At an altitude of, say, three to four thousand metres it can be assumed that any variations due to the local geology will be vanishingly small and, consequently, the effect of the geomagnetic field will not change significantly with x,y position (within a suitably confined area) and any magnetic variations recorded can be safely attributed to effects of heading and manoeuvre. The aircraft then flies around the four sides of a square oriented either north-east-south-west or parallel and perpendicular to the chosen flight-line direction of the survey, should that differ from north-south or east-west. With the compensator in 'calibration' mode, along one side of the square the aircraft executes manoeuvres of ±10 degrees in roll, ±5 degrees in pitch and ±5 degrees in yaw, each within a period of a few seconds (Figure 3.4). This exercise is then repeated on each of the other three sides of the square in turn. The results are stored in the memory of the compensator and applied automatically when the instrument is in 'survey' mode. For example, a value is now known by the compensator for the magnetic effect of a 3 degree roll to starboard when the aircraft is heading west and is recalled and applied as a correction whenever that attitude is encountered in flight. The results of the recorded magnetometer output

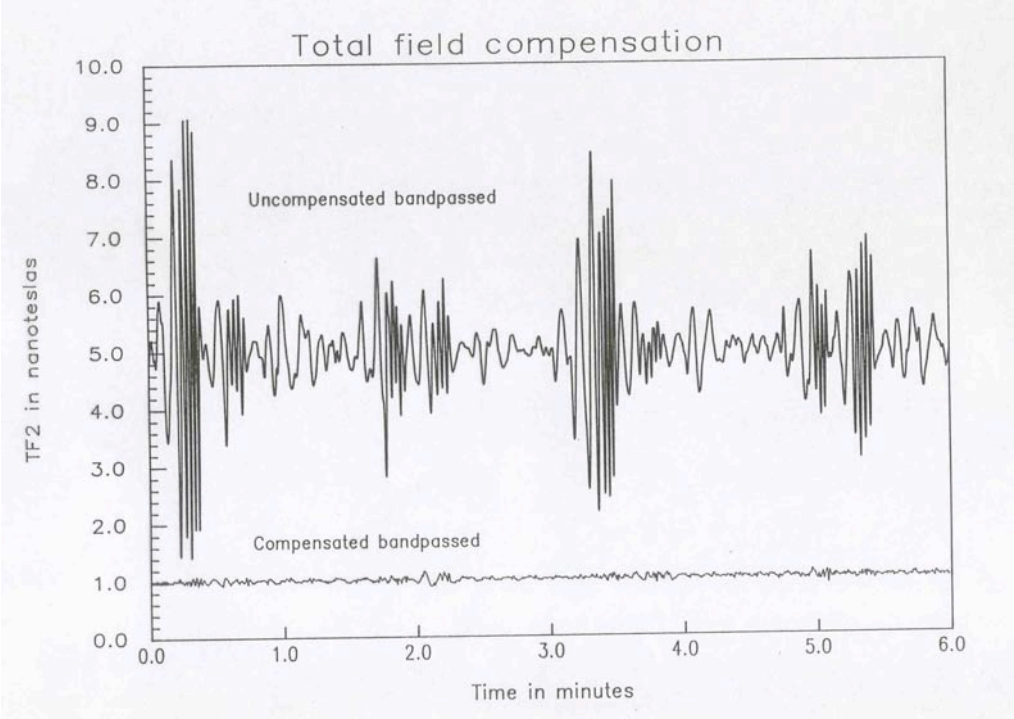

Figure 3.5 *Top trace: magnetometer output recorded during the execution of pitch, roll and yaw manoeuvres. Bottom trace: the same output after application of the automatic compensation. The noise level is reduced to a small fraction of 1 nT.*

before and after application of automatic compensation are shown in Figure 3.5. It is necessary to assume that the compensation remains unchanged after the compensation flight. Since this assumption could be doubted, the compensation is checked periodically during the flying of a single survey and repeated in its entirety when surveying commences at a new locality with a different magnetic field direction.

The achievement of suitable compensation is the responsibility of a survey contractor or other organisation carrying out a survey. The survey client - or a technical consultant - needs to have the quality of the compensation demonstrated and this is usually a requirement in airborne survey contracts. The following tests are carried out periodically to demonstrate the success of compensation.

3.4 Performance testing

(a). The 'clover-leaf' test.

The 'clover-leaf' test is designed to demonstrate that the aircraft and system have no significant 'heading effect', i.e. that the same magnetic field value will be recorded at a given location in x,y, regardless of the direction in which the location is overflown (once corrections for temporal variations of the magnetic field have been applied). A visible point on the ground in an area of few magnetic anomalies is chosen and overflown at survey altitude in, say, a northerly direction. The aircraft then turns and flies over the same point again in an easterly direction, then in a southerly direction, a westerly direction and finally in a northerly direction again to check for any diurnal variation since the first overflight. Figure 3.6 demonstrates the resulting flight-pattern that gives rise to the name of the test.

(c). The 'figure-of-merit' test

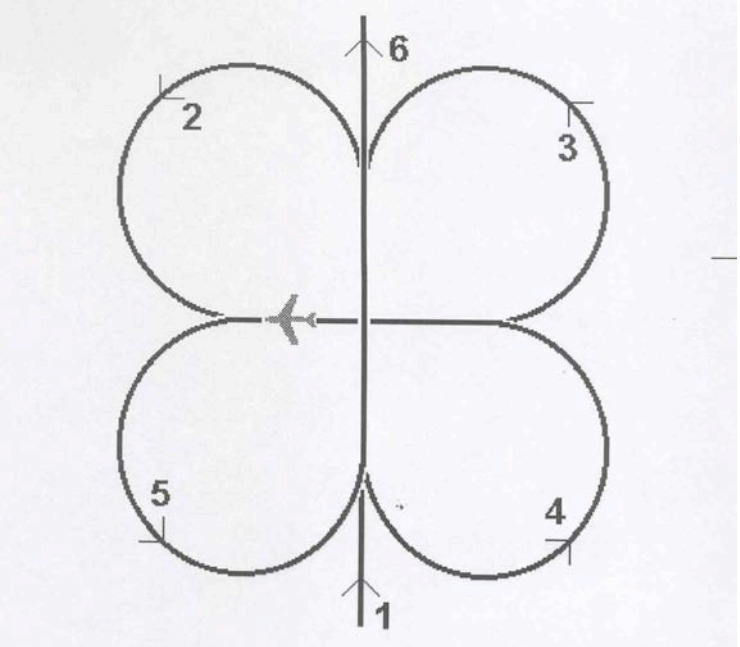

Figure 3.6 *Flight path in plan for a typical 'clover leaf' test.*

A 'figure of merit' for a system is obtained by carrying out the roll, pitch and yaw movements described in Chapter 3.3 (b) while flying at high altitude (2000-3000 m above terrain) in each of the four cardinal compass directions with the compensator (where fitted) in survey mode and adding the peak-to-peak amplitude of the magnetic signal obtained for each manoeuvre, i.e. the difference between the magnetometer reading when rolled 10 degrees to port and when rolled 10 degrees to starboard when heading north, is added to the equivalent number for the ±5 degree pitch and the ±5 degree yaw and in turn added to the three nT values obtained for these three manoeuvres on each of the other three cardinal directions, making 12 terms in all.

In the 1970s, a figure of merit of 12 nT was typical for regional surveys employing a proton magnetometer with sensitivity of 1 nT. With improved compensation, this was reduced to 4 nT for a 0.25 nT noise level. Current optical-pumping magnetometer systems with the currently standard automatic compensation equipment routinely achieve figures-of-merit of a fraction of 1 nT.

(d.) Lag test

The differing positions of magnetometer (or other) sensor and positioning equipment within the aircraft and possible electronic delays in recording one or both values are checked by overflying a magnetic object such as a bridge twice, the second time in the direction opposite to the first. The displacement between the two anomalies relative to the source is twice the shift that must be applied to bring magnetic and positional information into registration. A lag of 0.1 to 0.2 seconds - equivalent to about 10 metres on the ground - is not uncommon.

Since survey lines are often flown alternately in opposite direction (i.e. after completion of flying one line east-to-west, the aircraft turns around and flies the next line west-to-east), failure to correct adequately for lag can result in values being shifted systematically east on lines flown east-west and west on lines flown west-east. This is one possible cause of the so-called 'herringbone' effect sometimes seen on contour maps of surveys which have not been reduced correctly. However, in modern surveys such effects are more often due to incomplete levelling of the flight lines (see Chapter 5).

(e). Noise level monitoring

Noise experienced while recording a magnetometer profile can be divided into discontinuous and continuous noise. The former causes spikes to appear on the profile which may be attributed to a plethora of sources, internal and external to the aircraft. These include lightning, DC trains and trams, powerlines, radio transmission, electrical switching, and so forth. Such effects usually demand manual elimination - or non-linear filtering - during data reduction. The continuous effects will be largely eliminated by the compensation system in a modern installation, but there will be detectable residuals which still set the limit to the sensitivity of the system.

The noise level is conventionally monitored in flight by calculating in real-time the 'fourth difference' of successive readings of the magnetometer. This is the numerical equivalent of the fourth derivative of the recorded profile and may be calculated readily from the relationship:

$$\text{4th difference} = (T_{-2} - 4T_{-1} + 6T_0 - 4T_{+1} + T_{+2}) / 16$$

where T_{-2}, T_{-1}, T_0, T_{+1} and T_{+2} are five consecutive readings centred on the current reading, T_0. When plotted continuously during flight the width of the fourth difference trace is characteristic of the noise level being encountered. Spikes, DC level shifts and other extraneous effects are also readily apparent to the survey operator in an on-line presentation of the fourth-difference.

In practice it is found empirically that the noise level is linearly dependent on the figure of merit such that

$$\text{Noise level} = \text{FOM}/15$$

or slightly less than the average of the figure-of-merit manoeuvre signals (Teskey et al 1991).

3.5 Navigation and position fixing systems

Navigation and position-fixing systems have to fulfill three functions in the execution of airborne surveys:

a). To assist the pilot in flying as closely as possible to the prescribed flight-path along each survey line;

b). To enable accurate recovery of the path actually flown in this attempt, and

c). To enable the observed anomalies to be plotted on a map and recovered, where necessary, on the ground, preferably in relation to visible topographic features.

Achieving these seemingly simple objectives has been one of the most tedious, time-consuming and labour-intensive parts of airborne survey operations throughout most of the history of airborne geophysics and the inadequacies of the various methods employed have been a major factor in limiting the ultimate quality of the data gathered. All 'surveys' presuppose the collection of data and the relation of those data to their x,y

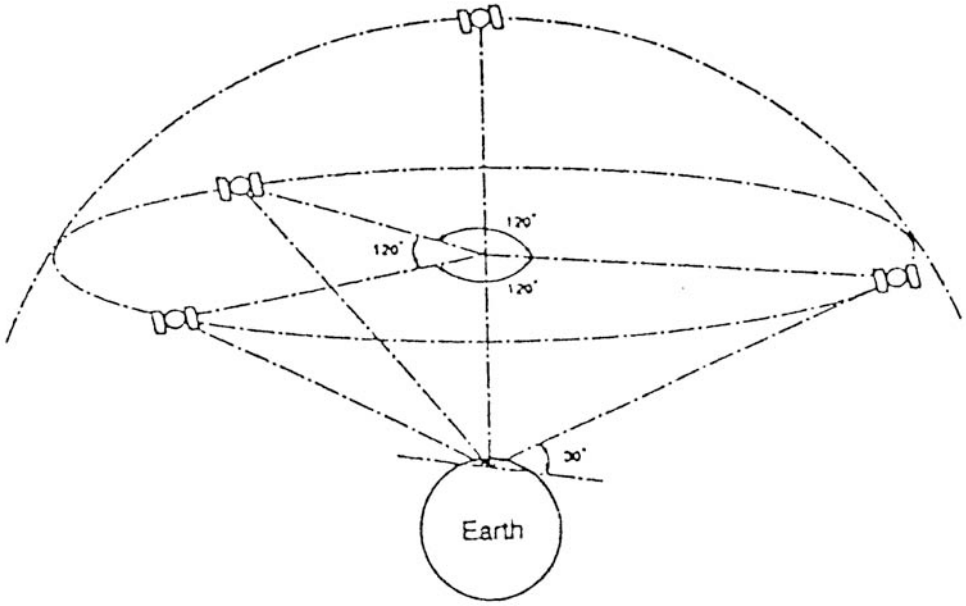

Figure 3.7 *Global positioning systems (GPS) depend on the accurate 'ranging' of four satellites positioned favourably with respect to the survey area.*

coordinates. Where the survey is carried out from a moving vehicle, the simultaneous capture of accurate x and y values assumes an importance no less than that of the geophysical parameters beings surveyed. (In the case of airborne surveys, the capture of a vertical position parameter is also a concern – see later).

Perhaps the single most important technical development in airborne survey practice occurred in the early 1990s with the advent of global positioning systems (GPS). GPS relies on the simultaneous reception of signals from a number of earth-orbiting satellites from which a geo-centric position for the survey vehicle can be derived in real time (Figure 3.7). The positioning of sufficient dedicated first-generation GPS satellites to enable such a system to be fully operational at all places on the earth's surface at all times signaled the start of the GPS era. The universality of the system allows GPS receivers to be mass produced and therefore available to potential users at a cost that is modest compared to alternative methods of positioning with comparable accuracy. Since the accuracy achievable very simply with GPS has matched or exceeded that possible with earlier, more complicated and more costly positioning systems, GPS quickly became adopted as the principle method of navigation and position fixing used by almost all operators in airborne geophysical surveys. GPS will therefore be described first, with subsequent reference to systems used in the past which are, in some cases, still of ancillary importance, and of real interest to those who have to deal with airborne data acquired during the pre-GPS era where accurate position-fixing is often a limit to data quality.

(a). Global positioning system (GPS).

The US Department of Defense's NAVSTAR system comprises a constellation of 24 satellites, of which 21 are in use, the remainder on stand-by. Each satellite transmits coded signals at two microwave frequencies known as L1 and L2 (1575.42 MHz and 1227.6 MHz respectively) that enable the receiver to calculate the satellite's precise

position at the time of transmission and the distance from the satellite to the receiver. The L1 band was originally available for civilian use and provides an accuracy better than 100 m for 95 percent of readings. Greater accuracy is achievable using the precise (or P) code which is transmitted on both the L1 and L2 bands.

The principle of positioning using the NAVSTAR satellites is no different from that used in other forms of positional surveying. The distance from a known point (in this case a satellite) to the receiver is calculated by 'ranging', i.e. calculating the distance from satellite to aircraft by measuring the time taken for the signal to travel and knowing the velocity of propagation (Figure 3.7). To do this requires both transmitter and receiver to have carefully synchronized clocks - a microsecond error between the clocks is equivalent to 300 m in range. All satellites have clocks which can be considered perfectly synchronized with each other, while the error in synchronization of the receiver clock is treated as one of the unknowns. Range (or 'pseudo-range', since the receiver clock-time is uncertain) is measured by comparing the time-shift between identical step-coded signals generated by the satellite and by the receiver. This can be achieved with an accuracy of about 1 per cent of the pulse period (which is 1 millisecond for the civilian code) equivalent to ± 3 metres at the speed of light. Information on the satellite orbit - included in the transmitted signals - allows its instantaneous position to be calculated for the time of the pulse transmission. Simultaneous ranging of four satellites gives four pseudo-ranges that can be resolved for the four unknowns - the x, y and z coordinates of the receiver and the error in the receiver clock-time. This is done automatically in the receiver.

The satellites are placed in orbits such that at least six of them are always visible from any point on the earth. Monitoring of satellites from accurately positioned ground stations allows precise details of their orbits to be updated and the latest ephemeris details are up-loaded periodically from the ground stations to each satellite for onward transmission to the receivers. The accuracy of a fix, however, depends on the geometrical arrangement of the four satellites used and is best when they define the apexes of a tetrahedron with the largest possible volume. Readings made instantaneously with a single receiver in an aircraft have proved accurate to ± 20 m in x and y. As a result of the geometrical configuration, height information is subject to errors about three times greater than this.

Some of the sources of error can be eliminated or reduced by operating in a so-called 'differential mode' (DGPS). In this mode, a second receiver is operated at a fixed point on the ground and is observed to display minor variations in the x and y values obtained for this fixed point. These variations are attributable to various causes (such as the ionosphere) but may be assumed to be equally applicable to the mobile receiver in the aircraft, if it is ensured that both receivers are using the same four satellites. The output of the mobile receiver can then be corrected for the variations observed at the fixed receiver. This was originally achieved in post-processing of the data but now more usually by transmitting fixed-station x,y information by UHF radio to the aircraft in real time. Single station GPS accuracy (± 20 m) is already adequate to enable a pilot to follow a desired flight-path with accuracy adequate for most surveys; differential mode can be demonstrated to achieve accuracy of ± 5 m which is adequate for almost all airborne survey purposes.

A bonus is that the accurate GPS time signal can be used as a time-base for all airborne data recording, as well as for the precise synchronization of a ground magnetometer

base station with the airborne system. GPS aboard the aircraft offers additional benefits for the pilot, such as the capability to display the direction and distance to the start of a pre-programmed flight line and, while on line, the off-track error (left or right) and the distance to the next way-point or line end. A sequence of consecutive line start-points and end-points may be pre-programmed for a single flight or 'sortie'.

A single disadvantage may be noted, and that is that such accurate x,y information can only be used in following up anomalies on the ground using similar (but hand-held) GPS equipment. While this is becoming increasingly popular, a purely GPS position-fixing system lacks any opportunity (except via maps, which are far from accurate in many parts of the world) to relate geophysical anomalies to features identifiable on the terrain.

(b). Flight-path recovery in the pre-GPS era

In the many years of survey operation before the advent of GPS, problems surrounding position-fixing occupied a large part of the effort of survey execution. This was particularly true in remote areas of the world where maps of high quality were unavailable. In these cases, the advent of satellite imagery in the 1970s provided a new type of base map that offered advantages. A downward-looking camera in the survey aircraft, exposing one frame of 35 mm film every few seconds, recorded the ground locations that were actually flown over, while the pilot had a strip of maps, aerial photographs or satellite images from which to steer the aircraft along each desired flight-line. Such systems evolved from the earliest airborne geophysical surveys, perhaps with the addition of some more modern electronic support until the advent of GPS. Electronic support systems included the Doppler navigator, inertial navigation and range-range radar, depending on survey location and the need for precision. A summary of these techniques, written at a time when such techniques were about to reach the end of their useful lives, is given by Bullock and Barritt (1989). One survivor of the earlier era is the advantage of having pictures from a downward-looking camera. These days, where such a camera is used, it is invariably a digital video camera and its use is mostly for identifying man-made metallic objects such as barns, power-lines, railways, etc that can be associated with local magnetic anomalies (often referred to as 'culture') when the acquired data is first being inspected for data quality. With the advent of digital data acquisition on board the aircraft in the 1970s, the flight-path recovery information was the last item to remain in the analogue world and at the end of the time-consuming and labour-intensive flight-path recovery operation, the flight-path map was digitized to give the x,y positions of the aircraft that could be matched with the digitally recorded data by way of a system of ***fiducial numbers*** that was common to both analogue and digital data sets. These days, fiducial numbers are derived from the GPS clocks.

It should be noted that geophysical readings are always made on a time basis and that the distance covered in unit time will vary, not only on account of any variations in the air-speed of the aircraft, but also on account of any wind which will cause air-speed to differ systematically from ground-speed.

3.6 Altimeters and digital elevation models (DEM)

The purpose of flight-altitude measurements as part of an airborne geophysical survey is twofold: first, to give the necessary data for post-flight survey altitude verification, and second, to give a possibility to make flight-altitude corrections for the primary geophysical data. Such corrections can significantly improve the accuracy and usefulness of primary data.

The standard instrument for the measurement of survey altitude has been the radar altimeter. In addition, a barometric altimeter is part of standard avionics in any aircraft. In recent years two new alternatives have emerged: a laser altimeter, and the utilization of the GPS navigation signal for a full 3D flight path recovery. (An essential part of any altimeter system in low-altitude surveying is an automatic warning/alarm-signalling system for crew safety).

(a) Radar altimeter

The two-way distance from the aircraft to the ground and back is measured based on the known velocity of electromagnetic waves in vacuum (air) and on the recording of the small but finite time difference δt that will elapse between the transmission and the reception of the ground-reflected EM signal. It is technically advantageous to convert the measurement of δt into a proportional difference δf in a frequency-modulated sweep signal. The carrier-wave frequency is typically about 4300 MHz, the modulation sweep 100 MHz, and the modulation rate 100 cycles per second. When a certain frequency f1 is transmitted to the ground from the transmitter antenna, this signal will be recovered at the receiver antenna after a time difference of δt. Meanwhile, the transmitter signal frequency has increased into value of f2 because of the modulation. This direct reference signal is compared with the ground-reflected signal f1, and the difference δf can be accurately determined. The value of δf can be calibrated to give a direct display of ground clearance.

The advantages of the radar altimeter are its good accuracy and compact size. An accuracy of ± 2 per cent or ± 1 meter is routinely achieved with modern radar altimeters. This is sufficient in most airborne surveys.

In special airborne surveys like sea-ice thickness or bathymetric measurements, the accuracy of a radar altimeter may not be sufficient. If the accuracy goal is in the decimeter range, then a laser altimeter is a solution.

(b) Barometric altimeter

This type of altimeter is very seldom relied upon as a single device for measuring flight altitude. It operates on the precise measurement of atmospheric pressure differences between a known reference level (e.g. the base airfield), and survey altitudes. The pressure difference can be calibrated into relative values of altitude differences.

$$h_b - h_a = k\, T \log (p_a / p_b)$$

where h_a is the altitude of the lower point, h_b the altitude of the higher point, p_a and p_b are the air pressures at the lower and upper points respectively, k is a constant and T the temperature (Biddle, undated).

The main drawback of the barometric altimeter is its inadequate long-term accuracy, about ± 10 meters in favorable conditions, although a good short-term precision can be achieved with quality instrumentation.

(c) GPS altimetry

The GPS navigation signal can be solved for all three spatial co-ordinate values of the on-board receiver, including the geocentric distance of the aircraft, i.e. its distance from the centre of the earth. At least four satellite signals must be continuously available, the satellite geometry must be good, and a stationary reference receiver must be utilized for real-time or post-flight signal processing. If good-quality radar altimeter data is also recorded on board the survey aircraft, the combination of the two data sources makes it possible to subtract the altimeter height from the geocentric distance to calculate the topographic elevation of the ground surface along the survey lines. The example in Figure 3.8 shows that an accuracy of ±2 m in topographic elevation data with this technique is attainable in practice. Such a digital elevation model (DEM) of the survey area may be a very useful survey product, in addition to the geophysical survey results. The model can be calibrated and bench-marked against points of known height on the ground surface and gives a uniformity of coverage that cannot be achieved by digitizing published contour maps, even in the well-mapped areas where such maps are available.

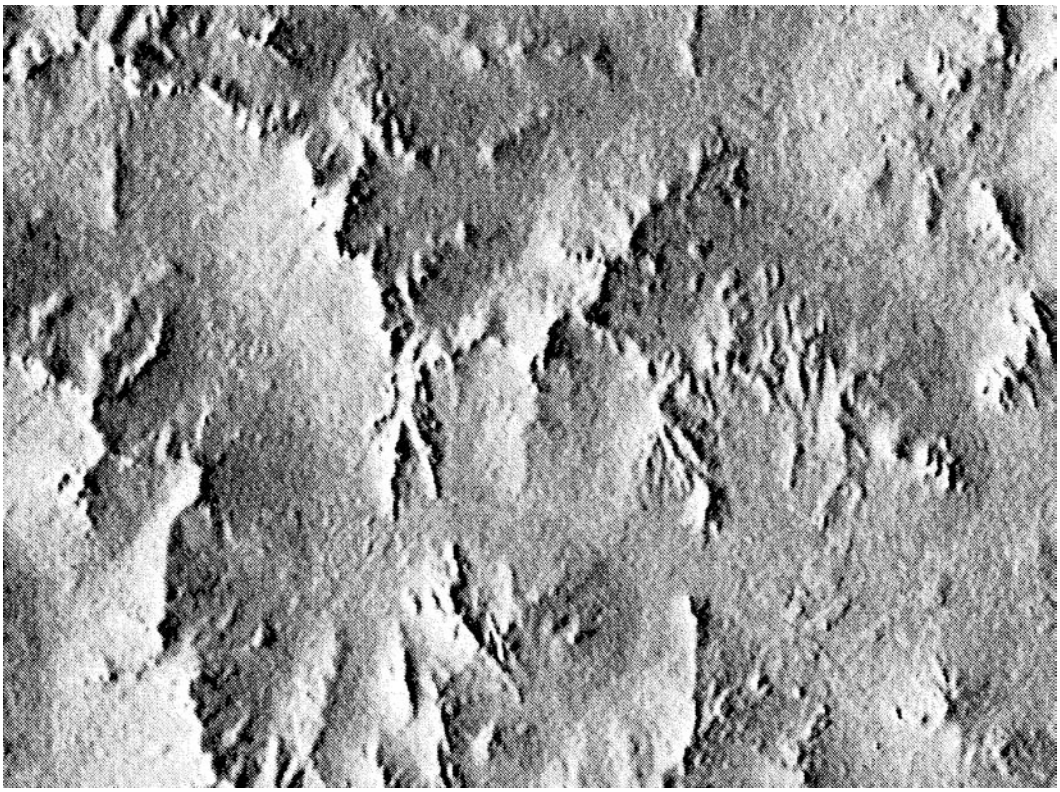

Figure 3.8 *Processing together the output of the radar altimeter and GPS-based height information can produce a detailed digital elevation model of the survey area with an accuracy of ±2 m. The example here shows drainage patterns in an area of Western Australia (courtesy of Geoscience Australia).*

3.7 Recording systems, production rates

It should be clear from the foregoing that an airborne survey aircraft must carry a wealth of sophisticated equipment in addition to the geophysical sensors selected for a particular survey – which, with the exception of the magnetometer have so far not been mentioned. The nerve centre is invariably a computer system. The computer has a screen that serves to inform the operator of current system functionality, and a keyboard that enables the operator to input instructions or respond to requests from the system. The computer runs a dedicated data acquisition software package that requires a minimum of human interaction under normal circumstances. Some systems are now in use where the equipment operation can be carried out by the pilot as the only person on board - with consequent saving of weight which can be translated into longer aircraft endurance through extra fuel capacity.

The main concern of the operator should be that all systems are functioning correctly, that all necessary calibrations have been carried out prior to, during or after each flight, and that the data are being correctly stored during flight. A typical set-up from the past is illustrated schematically in Figure 3.9.

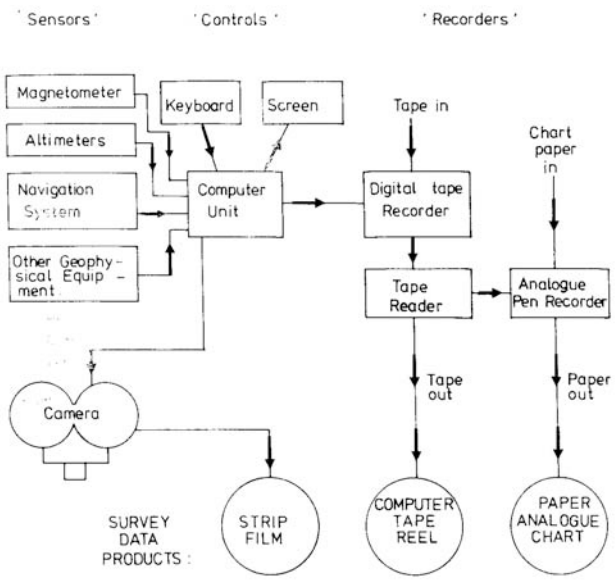

Figure 3.9 *Schematic diagram of a (very old) airborne data acquisition system.*

Average survey production rates with fixed-wing aircraft are typically in the range of 100 to 200 flying hours per month, depending on survey area and specifications. The efficiency (ratio of productive survey-line mileage divided by total mileage flown) is typically from 50 to 70 per cent depending largely on the ferry time necessary to travel from the operational base airfield to the first survey line on each given flight or sortie. Each flight will be designed to utilize the aircraft endurance and other factors (weather conditions and hours of daylight, for example) to acquire as many full survey lines as possible. A fixed-wing aircraft carrying out aeromagnetic (and gamma-ray spectrometer) survey for geological reconnaissance typically acquires 20 000 line km of useful data per month, though this may increase considerably under favourable circumstances.

3.8 Magnetic gradiometer systems

Certain advantages can be claimed for recording the gradient or first derivative of the total field rather than just the total field itself. (Care should be taken to avoid confusion between the vertical *gradient* magnetic anomaly and the vertical *component* anomaly recorded by some early ground magnetometers). The gradient - or rate of change of total field value with position - may be measured either in the vertical direction or in a specified horizontal direction, typically transverse to the flight direction of the aircraft or parallel to it. The main advantages are (virtual) freedom from diurnal variations in the measured difference and better resolution of closely-spaced and near-surface magnetic sources through suppression of the 'regional' component from deeper-seated sources which, in theory, approaches zero. This is illustrated in Figure 3.10 which compares the resolution of the total field anomaly over two closely-spaced bodies with that of the first vertical derivative.

Most successful attempts at this approach have, in fact, measured not the gradient directly but the *difference* between total field readings made simultaneously by two sensors separated by a known vertical or horizontal distance. It can be shown that the difference, $\delta T/\delta h$, and the true derivative, dT/dh, are closely similar as long as the separation δh between the two sensors is a small fraction of the distance between sensors and source. It follows that such surveys in fact record not one but two values for the total field from which the gradient is calculated by subtraction, in effect making the gradient determination a supplement to (rather than a replacement of) the total field

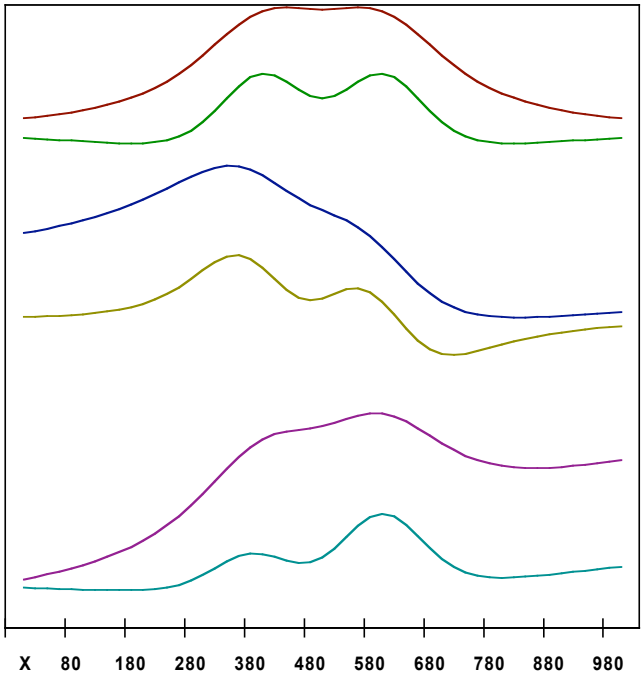

Figure 3.10 *Comparison between the total field and vertical gradient magnetic anomalies over two parallel vertical dykes separated by an amount equal to their individual widths (a) for a vertical inducing field (b) for a magnetic inclination of -70 degrees and (c) as (b) but in the presence of a regional gradient. The separate identity of the two dykes is clearer in the vertical gradient anomaly; the presence of two separate sources may have escaped recognition in the total field anomaly alone.*

reading. The fact that the 'traditional' total field data is still gathered allows compatibility with earlier surveys and those in adjacent areas.

The method is not without its limitations, however. Theory shows that, as a result of the narrower anomalies for a given body, gradient measurements require a closer sample interval (see Chapter 4) to satisfy the requirements of adequate sampling - about one-third of the source-sensor distance as opposed to one half for the total field. This results in the need for more closely-spaced lines if the detail recorded on profiles is to be fully represented in contour maps and images. Since the difference between the two instrument readings is usually quite small, the dynamic range of gradiometer systems is limited by the accuracy with which each of the two magnetometers can function; a true difference of 1 nT is less than the noise level if each sensor can record to only 1 nT accuracy. Anomalies of a few hundredths of nT/m are significant in practical magnetic gradiometry.

Early gradiometer systems approached this problem by using large separations, for example, by having one sensor in a stinger installation and the second in a bird on a cable perhaps 40 m below. The dynamic-range limitations mentioned above would be evident in a system where fluxgate or proton precession sensors were employed, even with such large separations. A further source of error would be variations in the position of the bird relative to the stinger.

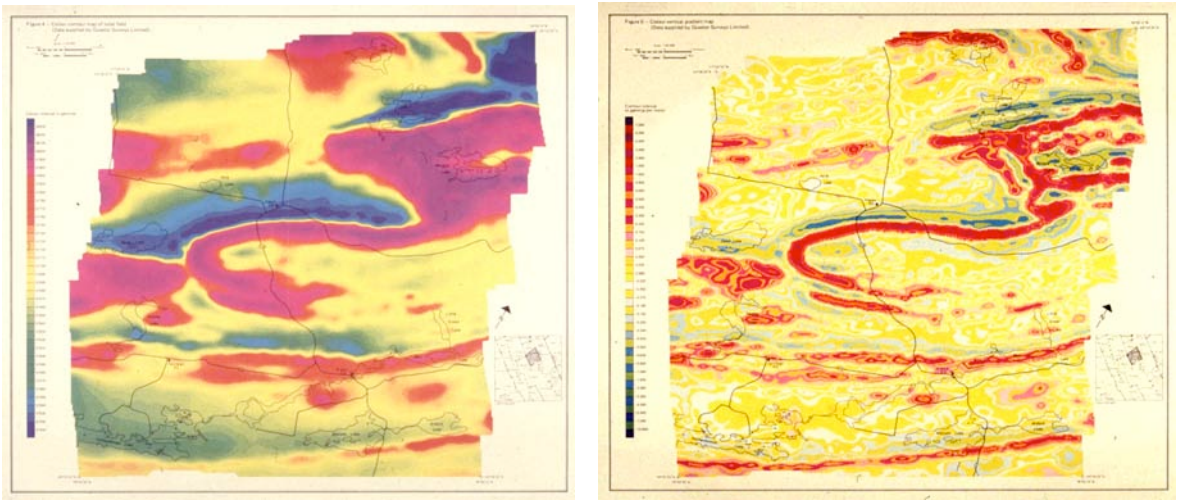

Figure 3.11 *Aeromagnetic total field anomaly map (left) and measured vertical gradient anomaly map (right). Note that, through suppression of the longer wavelength anomalies, the anomalies on the vertical gradient map follow the traces of the (near) outcropping geological formations very closely. (courtesy of the Geological survey of Canada).*

The advent of optical pumping magnetometers led to more successful systems with small separations in rigid stinger mountings, of which that developed by the Geological Survey of Canada was an early example (Hood and Teskey 1989). One of the clear advantages shown for this system is in geological mapping of hard-rock terrane, typical in mineral exploration, where the patterns of vertical gradient anomalies follow the outlines of geological units much more closely - and are thus more attractive to the interpreter - than the total field contours where magnetic sources of all depths - including those located far below the ground surface - may largely determine the appearance of the data in map form (Figure 3.11).

The gradient along-track can, of course, be determined from successive readings of a single magnetometer, and this approach may be employed to calculate the horizontal derivative from any magnetic profile. An across-track gradient can be measured by placing a magnetometer sensor in each wing-tip of an aircraft and subtracting the readings to give an instantaneous difference across-track. Combining along-track and across-track gradient values allows computation of the azimuth of the magnetic gradient. This information can then be used in the gridding and contouring process to help constrain the interpolation of magnetic values between adjacent flight lines (Chapter 6).

Despite these evident advantages, magnetic gradiometer surveys have so far grown in popularity only slowly in the 1990s and 2000s. One of the reasons may be that, with the advent of more detailed, lower altitude surveys with more sensitive instruments (and GPS), the geological detail visible in total-field surveys is already much improved. Calculation (rather than observation) of a vertical or horizontal gradient (Chapters 6 and 7) is just one of a multitude of enhancement techniques employed successfully to maximise the expression of geological information at the data processing stage. In the fullness of time, even these techniques may be improved further (at very little extra cost) by running a second or third magnetometer sensor routinely during data gathering. Where the concern is primarily with keeping costs down, it can also be shown that a

slight increase in line-spacing can be tolerated without loss of geological detail if a horizontal gradiometer system is employed at the wider line spacing.

4. Sampling theory and survey specifications

4.1 Continuous potential fields and discontinuous geology

Potential fields such as gravity, magnetic and electrical fields are continuous in space, devoid of abrupt changes and discontinuities. They are said to be *Laplacian*. Their assured smoothness assists in the task of planning surveys because we are assured that there is a limit to just how much change can occur between one obervation point and the next. In mapping magnetic anomalies, however, the intention is to trace the geology across an area, even where it may not be well-exposed. In Section 2 it was shown that lithological boundaries in geology are often associated with boundaries in magnetic properties and may therefore be found in the field and defined within millimetres in a suitably situated outcrop. Tracing such boundaries from their aeromagnetic expression to the ground therefore involves a process that starts with the continuous Laplacian field that is measured in the aircraft and locating the associated physical discontinuity in the geology. Stated briefly, this is the work of aeromagnetic interpretation and its representation in the form of a map that represents the discontinuous geology over the survey area. We shall see later various methods of visualising and processing aeromagnetic data that assist in reaching this objective. However, we should already be interested in planning surveys such that all the necessary criteria for sampling the potential field are met so that we do not end up trying to interpret a data-set that simply misses some of the information we require about the anomaly field of interest. This is what is meant by adequate sampling.

In all but a few very specialised surveys, airborne magnetometry has always set out to measure ***only*** the scalar magnitude of the total magnetic field. As shown in Figure 1.14, this is the vector sum of the field attributable to the earth's core (and approximated by the IGRF) and the sum of all local effects due to the magnetisation of crustal rocks. To achieve this ambition with useful precision and sensitivity requires attention to a number of fundamental issues. The previous section dealt with the need to have suitable measuring equipment (magnetometer plus ancilliary equipment) and the elimination of unwanted effects of the survey platform (aircraft) itself. In this section we introduce some aspects of sampling theory and their consequences for designing surveys such that no significant anomalies are missed and that the required resolution of geological detail is achieved. An idealised situation in aeromagnetic surveying is shown in Figure 4.1.

4.2 Source-sensor separation and anomaly "wavelength"

One of the most important parameters in designing and interpreting aeromagnetic surveys is the vertical distance between the magnetic source and the magnetometer sensor (Figure 4.1). This is called the source-sensor separation, S. Since any cover formations that may be present are probably non-magnetic, S includes not only the air space between the ground surface and the aircraft (or ***terrain clearance***) but also the depth of burial of the igneous and metamorphic rocks giving rise to the anomalies (the ***magnetic basement***). It should be clear that, when depths are estimates from magnetic anomalies, the result obtained is S and estimates of depths of burial – the most important parameter for exploratory drilling, for example – require the terrain clearance of the aircraft to be taken into account.

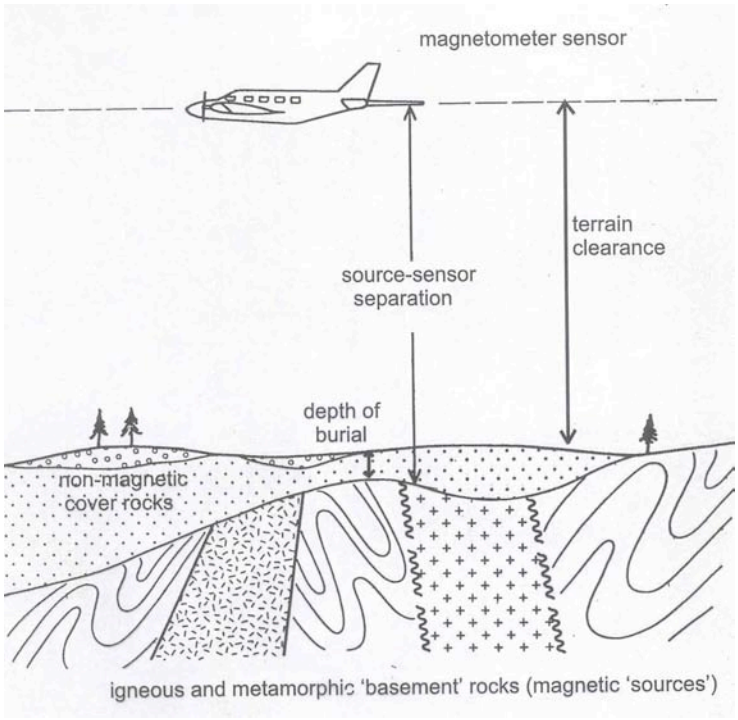

Figure 4.1 *A typical section for an aeromagnetic survey where the igneous and metamorphic rocks that make up the so-called magnetic basement are at least partly hidden by non-magnegtic overburden. The diagram also defines the terms source-sensor-separation, terrain clearance and depth of burial of the magnetic basement.*

Given that theoretical anomalies that may be expected over given geometrical bodies follow simple mathematical formulae (Section 8), it is an easy matter to ***forward model*** anomalies using simple computer software and so derive anomaly curves for a variety of circumstances. In Figure 4.2(a) the effect on the expected anomaly of taking a simple dyke-like body and steadily increasing S is seen. The most obvious effect is that, as the body becomes more deeply buried, the amplitude of its anomaly decreases markedly. This might be expected intuitively. However, from Section 2, it should be remembered that rock bodies can have a wide range of magnetisations due to magnetic susceptibility ranges that span many orders of magnitude. It follows that the amplitude of an anomaly is not a very useful parameter in estimating the depth of the source – a high amplitude anomaly is achieveable both by a rather weakly magnetic shallow body or by a highly magnetic one buried at considerable depth, not to mention many intermediate possibilities. This is the *principle of equivalence* familiar in many areas of geophysics. We can imagine that, in a theoretical model, we can compensate for the loss in anomaly amplitude with depth of burial by increasing the magnetic susceptibility of the body. In Figure 4.2(b) the curves of Figure 4.2(a) have been normalised in this way and it becomes clear that, as S increases the horizontal dimension of the anomaly increases proportionally. The term "wavelength" may be used to describe this horizontal dimension, but in reality the magnetic anomaly over any body is comprised of contributions from many different wavelengths. What is

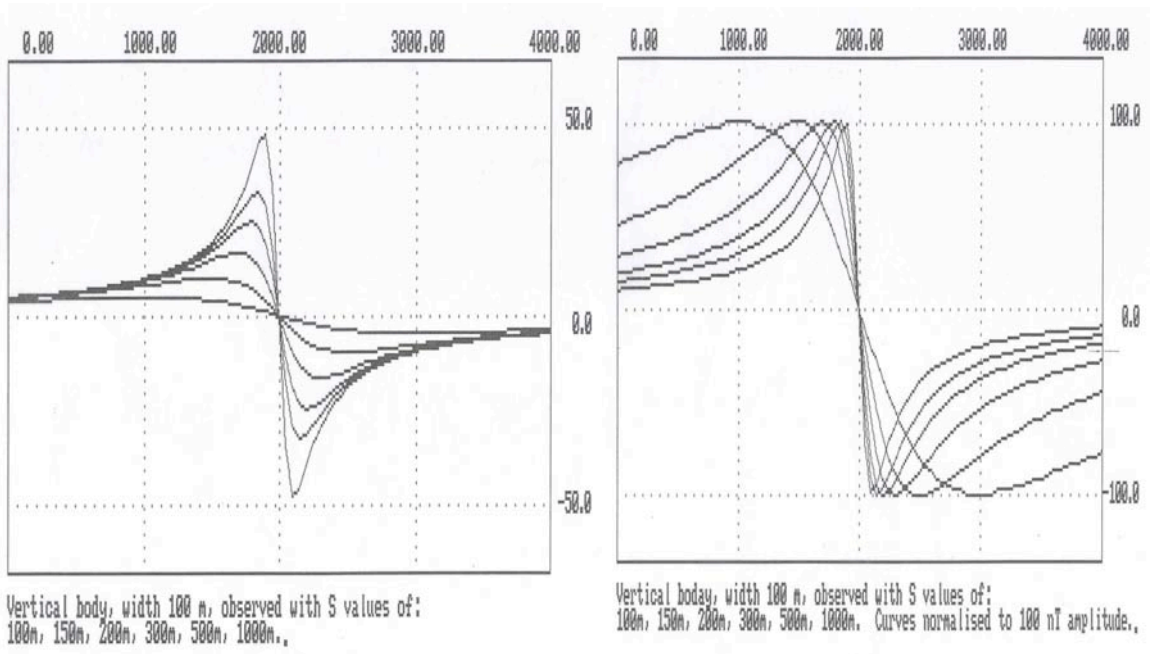

Figure 4.2 *The 'wavelength'of magnetic anomalies in relation to the source-sensor separation, S. For explanation, see text.*

perhaps more useful is to think of a window in the profile within which most of the 'interesting parts' of the anomaly fall. Mathematically, the anomaly tends asymptotically to zero beyond the limits of the window, so these faraway parts of any anomaly are predicatably monotonous. In practice these remoter parts are seldom observed on account of other geological bodies in the vicintity of the first one producing their own magnetic anomalies and interfering to some extent with each other. For practical purposes, over a reasonably compact source body, the window within which most of the interesting parts of the anomaly fall has a dimension of approximately 4 to 5 times S. (It follows that the linear dimensions of anomalies are always larger than those of the source body – see, for example, Figure 1.15.) The deepest source in Figure 4.2(b) (1000 m) still shows most of its interesting features within a window only 4000 m in width.

4.3 Anomaly detection and definition

In planning any survey, an early consideration would be to position the flight-lines such that no significant anomalies escape detection. At the same time, the detector (magnetometer) must be placed very close to the source (to secure resolution of closely spaced geological sources – see later in this Section) and moved physically along each scan line or 'flight line' in turn by flying the aircraft up and down along parallel lines in a pre-arranged flight plan. It should already be clear that the most important parameters in such a scheme are (a) the closeness of the apparatus to the source (or terrain clearance) that is safe or desirable and (b) the spacing between adjacent lines that is necessary to build a coherent picture without omitting significant features.

The operational costs of airborne geophysical surveys in any area are, to a good first approximation, proportional to the total distance that needs to be covered in flying along every scan line or flight line. For a given survey area, it follows that the cost is inversely

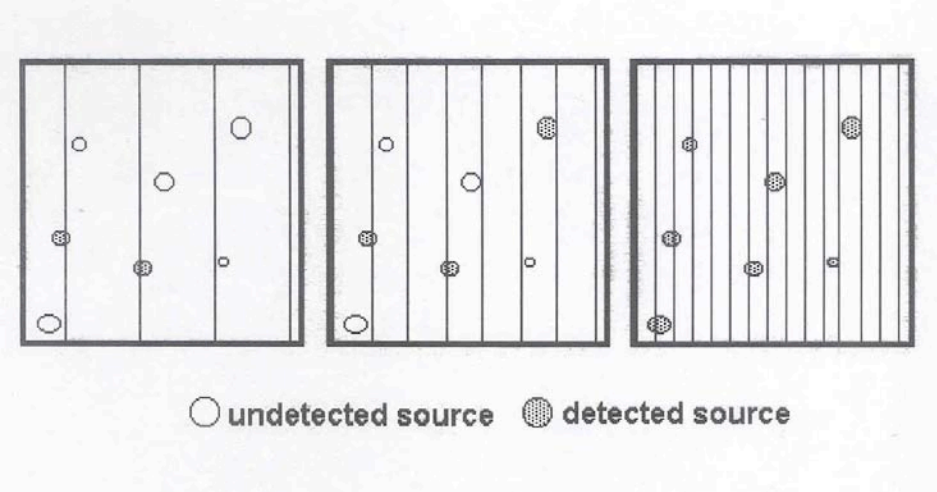

Figure 4.3 *As flight-line separation decreases, the number of anomalies that escape detection also decreases. All anomalies are detected once the line-spacing is no more than about 4-5 times S.*

proportional to the line spacing; a small line-spacing leads to a large number of lines and a high cost while a wide line-spacing leads to a relatively small number of lines and a low cost. The cost is therefore related to the resolution required, through the line-spacing necessary to ensure detection of all relevant anomalies. Figure 4.3 shows the effect of decreasing line spacing on the detection of a fixed number of sources in a given area. The horizontal dimension of the anomaly over a given compact source increases with flying height - the source becomes a larger 'target' (in area) as terrain clearance increases. At the same time, however, the amplitude of the anomaly will decrease with increasing survey altitude - leading eventually to its disappearance into the noise envelope of the recording system (see later in this section). Perhaps more serious is that the horizontal dimension of the anomalies over all other compact sources will also increase with altitude such that the amount of overlap between them will increase and the resolution of geological detail will become badly compromised. There is clearly little future in geophysically mapping the finer details of geology at the altitudes of earth-orbiting satellites, or even at the altitudes used for conventional aerial photography or civil aviation! Resolution of closely-spaced anomalies is best served when source-sensor separation is at a minimum.

Where sources outcrop (s = t, Figure 4.1), the limit to resolution is set by considerations of the safety of aircraft flying at low altitude. Conventional fixed-wing survey aircraft in terrain free of significant topography are routinely operated at terrain clearances of 100 m, 60 m and even 30 m in some countries. This figure can be reduced further, where resolution demands, by slinging the sensor in a bird below a helicopter, or by carrying out surveys on the ground. Ground surveys with magnetometer sensors less than a metre above ground with line spacing measured in decimeters have been carried out for archeological investigations of limited areas, for example. The principle is the same.

Attention must be paid, however, to taking sufficient readings along each flight line such that the anomalies fully defined. Note that whereas the line-spacing criteria discussed above ensure that all anomalies are *detected*, intepretation of profile information further requires that – along flight lines, at least – they are fully *defined* in shape. The criteria for definition are therefore more exacting than for detection.

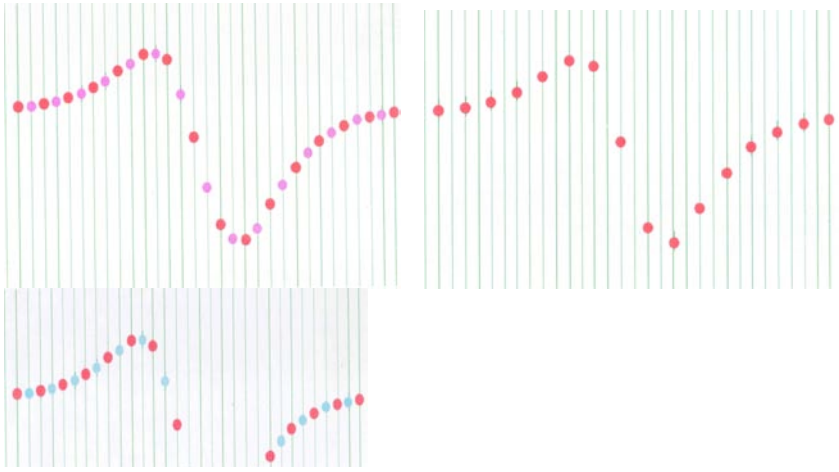

It is very often necessary in geophysical data processing to ***interpolate*** values between points on a profile. This process is sometimes known as ***splining*** and a number of mathematical functions are commonly used to ***spline*** a smooth curve between readings. An example of such an application would be to interpolate between unevenly-spaced field readings to give values at a regular sampling interval so that digital filtering could be applied (see Section 6). The ability to spline between values can be used to build a test for just how often along-profile the airborne magnetometer should take observations, as illustrated in Figure 4.4. Imagine a typical magnetic anomaly sampled at a number of points along its length. When is the number of sample points sufficient to fully define the anomaly? One criterion is as follows. We take a profile of equally-spaced values and discard every seond reading. We replace the discarded readings by values splined between the remaining readings. We then compare the splined values with the original (discarded) ones. When they agree within a certain threshold, then it is clear that the remaining points (those not discarded) are already sufficient to define the anomaly – since the discarded values can be replaced mathematically without loss of information.

Experiments carried out on the above basis using theoretical anomalies as the starting point have been used to show that a sampling interval of 0.5S is sufficient to define anomalies in profile. Even a sampling interval of 1.0S – if it cannot be avoided – does not lead to serious loss of information since the transition from acceptable to unacceptable is a gradual one.

In practical terms, a survey flown at 80 m above terrain with outcropping magnetic sources (S = t = 80 m) will be fairly complete with a line spacing of 320 m, and perhaps even 400 m spacing will not show serious deterioration in detecting sources. The sample spacing along lines, however, needs to be no greater than about 40 m (S/2) to fully define them along each profile. A typical speed for an aeromagnetic survey aircraft is 250 km per hour or about 70 m per second. Clearly a magnetometer reading only once per second is insufficient to meet our sampling criterion. Fortunately, in practice, this restriction has long since disappeared (and in the days of one-second magnetometer sampling, the terrain clearance was usually greater, 120 or 150 m) and modern magnetometers measure 10 times per second (equivalent to 7 m on the ground) or even more frequently.

It follows, of course, that observations are made at much closer spacing along lines than is the value of the line spacing, i.e. closely spaced values along widely-spaced lines. We will return to this situation in Section 6 when we will need to discuss gridding of

airborne profile data. Suffice it for the moment to say that it is a common problem with line-based data. Since adjacent and parallel profiles tend to resemble each other when flown across geological strike, economies in survey operation used to be made by flying across-strike and increasing the line spacing beyond what might now be considered wise. The more modern trend for higher resolution surveys has thankfully reversed this trend and with lines no more than 400 m apart and sampling every 7 metres along profile the direction of the lines is less critical. In many areas the size of whole geological map sheets (say, scale 1:250 000) the geological strike is not, in any case, consistent over such large areas. When surveys are flown as a patchwork of map sheets over time, to cover an entire country, for example, it is often more important to opt for a consistent flight direction, usually north-south or east-west to assist in stitching adjacent survey together once they are all complete.

4.4 Resolution of geological detail

Where magnetic sources are buried under significant thicknesses of non-magnetic rocks, such as the sediments of a basin covering the igneous and metamorphic rocks below, resolution of anomalies arising from the basement is limited by our inability to fly lower than a safe ground clearance. In this case, the source-sensor distance will be no less than the sediment thickness and the line-spacing could be several times this value without loss of detail in basement anomalies. (Recently, interest has increased in the detection of weak anomalies arising from the sedimentary section itself in such surveys over sedimentary basins. In this case, low terrain clearance and line spacing no more than about twice that permitted for outcropping sources may be appropriate).

It is understandable that these guidelines have often been transgressed in the interests of covering a larger area within a fixed budget, and often this can be done without compromising the quality of the survey too seriously. In each case, the objective of the survey needs to be kept clearly in mind; a small loss scientific rigour may be a small price to pay for a greater area of coverage within a given budget. Similarly, the law of diminishing returns may apply - halving the line spacing certainly doubles the cost and may only provide a small percentage more of useful information, depending on the objective of the survey. In a practical setting, cost (next to safety) cannot be denied a leading place in the planning of a successful survey. However, one of the major developments in recent years has been in the presentation of geophysical data as images that are physically attractive to the user (Section 6). There is no doubt that close line-spacing affords the extra resolution that adds welcome crispness to such images.

Figures 4.5 serves to illustrate the extremes of detail (and the lack of it) that might be encountered in aeromagnetic surveys in different geological settings. In Figure 4.5(a) the magnetic basement (Archean granites and gneisses) outcrops in the central area and a very complex pattern of anomalies is evident. Further north, the contour lines become rather more widely spaced and it is known from drilling that non-magnetic cover rocks attain a thickness of several hundred metres here. The wavelength of the anomalies increases accordingly. A line spacing of 400 m was used in this survey and it is certain that anything less would have missed detail in the most crowded areas of the map. Figure 4.5(b), by contrast, shows a very small number of contour lines, even when it is realised that the contour interval (10 nT) is five times more frequent than in Figure 4.5(a) (50 nT). In this case the survey was flown over the sea (non-magnetic!) and below no more than about 100 m of sea-water sedimentary rocks are known to exist to a

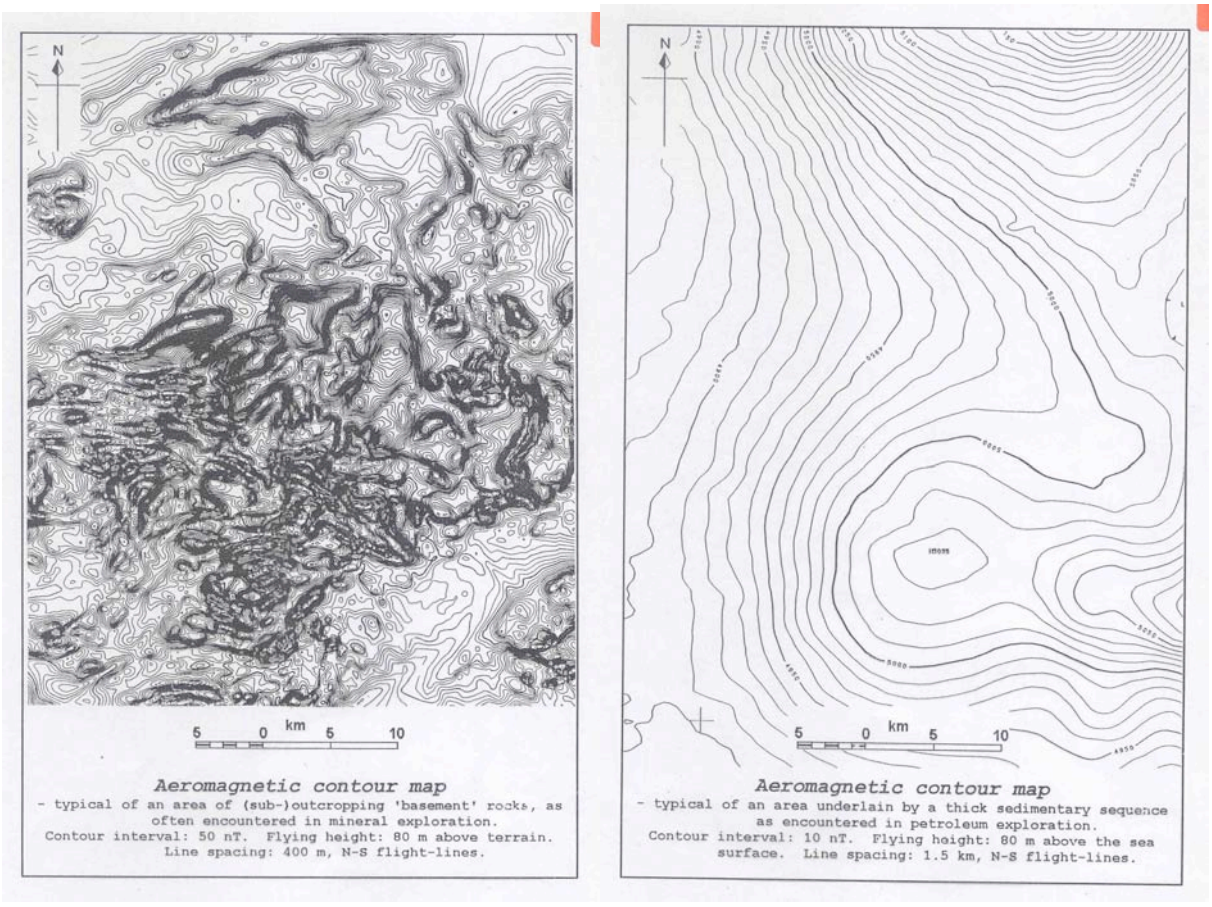

(a) *(b)*

Figure 4.5 *Aeromagnegtic anomaly contours over two quite dissimilar areas of geology, outcropping Archean basement in (a) and a thick offshore sedimentary basin in (b). Courtesy of Geoscience Australia.*

depth of perhaps 10 km or more. The magnetic anomalies must arise from igneous and metamorphic rocks below the sediments and, as a result of their enormous depth of burial, give low amplitude anomalies with a wavelength of several tens of kilometres. There is one shallow-seated anomaly evident in the NW quadrant of the contour map. This is due to the presence of an offshore drilling platform which happened to lie close to one of the flight lines of the survey. It also indicates that this is an example of an aeromagnetic survey over an area that may be promising for oil exploration. By contrast, any economic interest in the area of Figure 4.5(a) would almost certainly be for solid minerals.

The necessity of flying with low terrain clearance when mapping areas of near-surface magnetic basement is illustrated in Figure 4.6. Here, theoretical magnetic profiles have been calculated for various flying heights over an idealised piece of geology in which magnetic units of width 50 m or 100 m alternate with non-magnetic units of similar widths. Observing the resulting profiles shows that a profile only resolves identifiable peaks for separate units when the terrain clearance is less than the size of the feature of interest. At 100 m terrain clearance, the larger units are resolved, while the smaller gaps only become evident at less than 50 m terrain clearance. The general lesson to be learnt from this is that probably most anomalies seen as single features at survey altitude will be the result of several (or many) closely spaced magnetic units within the rock itself and a ground magnetometer traverse over outcropping rocks can be expected

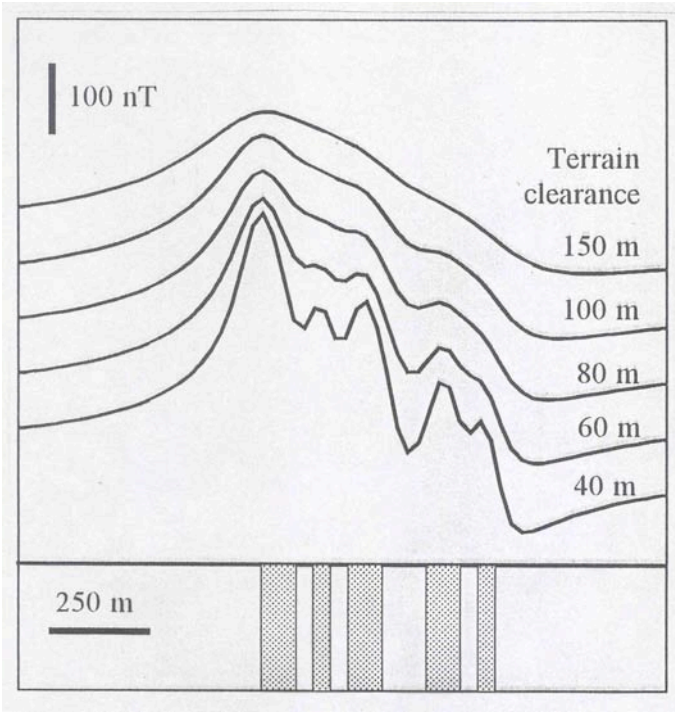

Figure 4.6 *The effect of terrain clearance on the resolution of geological detail.*

to look much more complex than what is seen from the air. With a ground magnetometer with a sensor about 2 m above the ground, details and structures on the scale of a few metres will be resolvable, necessitating great care with choosing a sampling interval for the ground magnetometer that is fine enough to make good use of this resolution.

4.5 Survey specifications and the survey contract

Having considered the flight-line spacing and the survey altitude, a number of other survey specifications need to be addressed. All specifications will, in practice, be set out in a document that will be used as the basis on which contractors can bid to deliver the required survey at a competitive price. The specifications serve to define the minimum acceptable level of performance for which payment will be made by the client.

(a) Survey outline

The first specification will usually be the definition of the survey area itself. This needs to be defined in detail not only for legal reasons but also very often to allow a new survey to be related accurately to pre-existing surveys to which it may eventually be linked at the data processing stage. A sketch map with all survey boundaries defined in geographic (or other) coordinates will be necessary. The extension of lines beyond the survey boundary to the extent necessary to allow confident interpolation of results at least to the boundary itself (in other words, ensuring no deterioration in quality within the boundary) should be included.

(b). Survey altitude

Survey altitude will be defined as the required mean terrain clearance. In the past some surveys were flown at constant barometric altitude, though this is now seldom the case. In either event, a tolerance will be stated. The tolerance is the amount by which actual flying may deviate from the nominal terrain clearance value without the results becoming unacceptable. Where data become unacceptable, lines will be required to be re-flown, usually at the contractor's expense. A recent development is the possibility to fly the survey on a pre-determined ‘loose drape’. The ability of any aircraft to climb is limited, and failure to clear topographic features is fatal. This limits the extent to which constant terrain clearance (a close drape) can be maintained with safety where there is significant topography or isolated hills. To avoid adajacent lines being flown at noticeably different

heights in the vicinity of topography (which tends to show up as streaking on final data compilations), a less-stringent drape can be defined such that the terrain clearance varies steadily and within the climbing capabilities of the aircaft. Inevitably, some areas in the vicinity of topography are flown at greater terrain clearance with some lack of resolution, but this is generally considered preferable to ugly streaking that cannot be removed completely in later processing.

(c) Line spacing

Similarly, the chosen line-spacing will be defined and a tolerance stated such that no two adjacent lines will exceed in separation, say, 1.5 times the nominal separation over a distance considered to be significant (perhaps ten times the line spacing). Exceeding this tolerance could lead to a gap in the survey coverage across which it would be impossible to interpolate with confidence, even if no significant anomalies were actually missed. Thanks to GPS assistance to the pilot, such deviations are now largely a thing of the past and regular flight patterns such as illustrated in Figure 4.7 are routine,

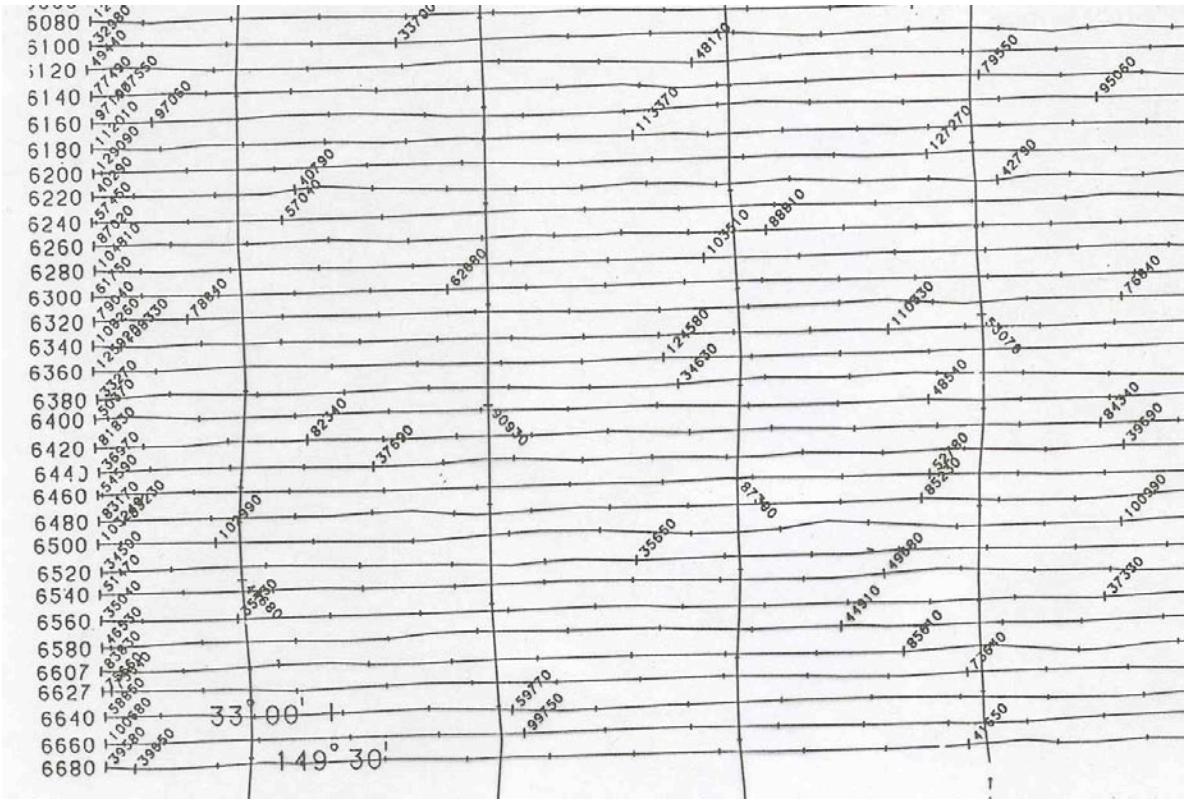

Figure 4.7 *A fragment of a flight path map with flight lines at 400 m spacing and tie lines at 4000 m, illustrating the regular flight pattern achievable with modern position-fixing equipment.*

bringing their own subtle bonus to data quality and anomaly resolution.

(d) Line direction.

Selection of the direction in which the survey area is scanned by the flight-lines can cause much discussion, mainly on account of the possibly conflicting advantages of one direction over another. To minimize the risk of loosing small anomalies between flight-

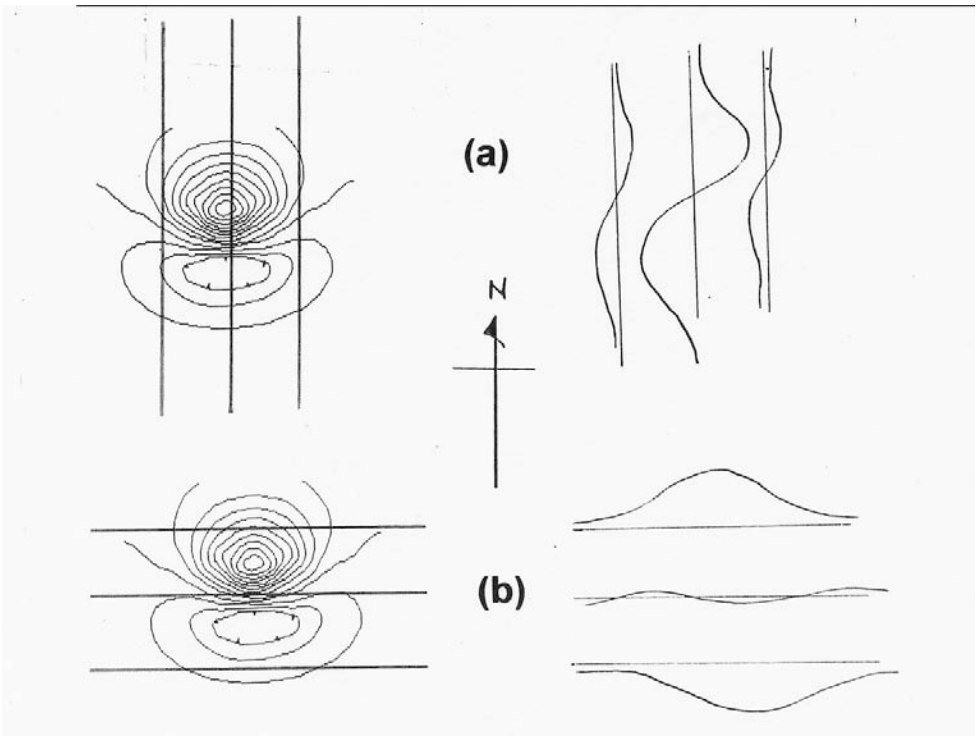

Figure 4.8 *The advantage of flying flight lines in a north-south direction over anomalies at lower magnetic inclinations where even the anomalies over circular bodies tend nto be extended east-west and the principal profile is certainy north-south.*

lines, it is obviously wise to orient lines normal to any predominant geological strike direction in the survey area. The short wavelength (across strike) features will then be sampled fully on each flight line, while the longer wavelength (along strike) features will still, hopefully, be adequately sampled by the wider spacing afforded by the flight lines. The geological strike could be complex, however, as in metamorphic terranes that have undergone several phases of folding and faulting. Injection of dykes at a later phase may follow a strike direction that is very different from the strike of the country rock and may not, then, be well recorded by a survey direction which suits the host-rock geology.

In low magnetic latitudes, it can be shown that the dipolar nature of compact magnetic sources leads to anomaly patterns that are more extended in an E-W direction and therefore better defined by N-S flight lines; N-S profiles give a more complete definition of profiles over local anomalies than could be achieved by E-W profiles, each one of which might only cross the positive or the negative part of the anomaly (Figure 4.8). Where magnetic inclination is low and the geology strikes N-S, there is already an obvious conflict between the two possible directions.

Many countries have adopted a systematic approach to magnetic anomaly mapping on a sheet-by-sheet basis. To build up such a coverage from individual surveys logically requires that flight lines are flown parallel to one or other of the sheet boundaries - usually N-S or E-W - choosing the direction that is most nearly normal to the principal geological strike in each sheet area.

When flight lines are spaced closely together, the scope for sampling the anomalies only poorly is quite small and the choice of line direction is far from critical. The issue only

becomes of real importance where line-spacing is wide. Poor sampling across line is then inevitable but sound choice of line direction could minimize its effect.

(e) Control line (or tie-line) spacing.

The need to run a small number of lines normal (usually) to the flight-line direction arises from the need to provide some additional control on temporal variations in the earth's magnetic field and will be addressed in Section 5. Usually a control line spacing no more than ten times the flight line spacing is chosen; in other words about 10 percent of all flying is devoted to tie-lines. This is determined by a number of factors that are far from simple in theory and ultimately relate to the extent to which we can be confident in smoothly interpolating between the control values provided by the intersections of lines and tie-lines when applying corrections to values recorded on the flight lines. This confidence decreases with time spent flying between intersections and the time taken should probably not exceed about five minutes' flying-time or about 20 km distance. Thus, in a survey with widely-spaced survey lines, such as is sometimes encountered in petroleum exploration, the ratio of 10:1 between the line and tieline spacings could reduce to 5:1 or even 2:1.

(f) Sampling interval.

Modern magnetometers are capable of sampling ten times per second, equivalent to a ground spacing of about 7 metres per sample. This more than satisfies any theoretical requirement for discretely sampling continuous anomalies so that they may be faithfully reconstructed by interpolation (Section 4.3).

Gamma-ray spectrometers can do no better (on account of counting statistics for a manageable crystal volume) than one sample per second, or 60-70 metres on the ground. Less critical parameters (such as temperature and barometric pressure) might be adequately sampled less often - say every 10 seconds.

4.6 The noise envelope

Finally, the limit to the data quality is ultimately set by the random noise which is inevitably recorded along with the desired signal. Noise can have a variety of sources which are related to the dynamic range of the instrumentation (or the precision with which readings can be made) and interference from spurious effects in the equipment and the aircraft. Micropulsations are one natural source of such unwanted interference. Since magnetic sources of geological interest are just as likely to give rise to weak anomalies as strong ones (all rocks are potentially interesting, but the magnetisation of rocks is known to span several orders of magnitude) the noise level achieved in recording is the ultimate limit to the useful detail that can be revealed by a magnetic survey Figure 4.9 illustrates how anomalies will escape detection once their amplitude is comparible with the noise envelope.. Consequently, minimising the noise level in order to lower the detection limit for subtle anomalies is a constant source of attention in developing and adjusting instrumentation. Present day magnetic surveys routinely operate from fixed-wing aircraft with a 'noise envelope' of no more than 0.1 nT.

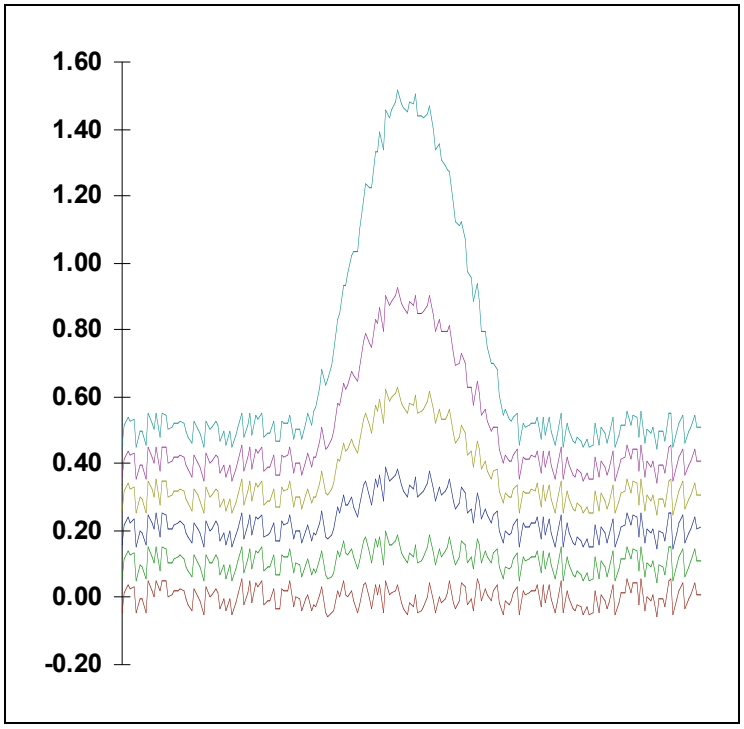

Figure 4.9 *The limit of detectability of low-amplitude anomalies is set by the noise envelope. Anomalies of amplitude 1.0 nT, 0.5 nT, 0.3 nT, 0.15 nT and 0.05 nT are progressively subsumed into the 0.01 nT noise envelope.*

The noise envelope may be defined as the difference between an individual reading and the *average* of a given number of adjacent readings symmetrically disposed either side of the test reading. Where the number of readings averaged is large, magnetic variations due to genuine anomalies begin to interfere; where the number is too small, statistical variation is not eliminated. An optimum number of readings over which to average can therefore be determined by experiment and used as the window over which 'smoothing' could be applied to raw data to reduce noise without damaging anomalies we seek to record accurately. A specified noise envelope sets the target that must be met in eliminating aircraft effects and temporal variations in the execution of a survey.

4.7 Survey costs

Naturally, when any survey strategy is first mooted, one of the most important considerations is cost. Bringing specially equipped aircraft from distant locations, local operating costs and infrastructure, reliability of fuel supplies, weather conditions, civil aviations requirements, the size of the survey, demand elsewhere in the world, all influence the final cost per line-kilometre, so it is notoriously difficult to make hard and fast statements about the cost of airborne magnetic surveys. Many combined airborne magnetic and gamma-ray spectrometer surveys were executed at well under US$10 per line-kilometre in many parts of Australia in the 1990s, but fierce commercial competition brought contractors into financial difficulties. While this ensures low prices, it does not ultimately serve the interests of the client if a survey has to be abadonned before completion for financial reasons.

5.

Data corrections and the flightline database

5.1 Quality control

Many activities and problems surrounding the actual execution of an aeromagnetic survey are of a practical and logistic nature (such as getting the necessary permits and securing supplies of fuel) and need not concern us here, except to emphasise again the importance of the skills and experience of the small number of airborne survey contractors that routinely take these problems in their stride. Further practicalities surround the potential disruptions caused by poor weather or too much magnetic disturbance, all of which detract from the optimum rate of progress that might be expected. At the start particularly, delays may be experienced while all the equipment on board the aircraft – that may have travelled from a far part of the world where conditions, including magnetic inclination may have been quite different – is adjusted and calibrated to conform to the terms of the new contract. Usually the client appoints a consultant or technical authority to ensure that all these criteria are met before time is invested in data acquisition that may fall outside of specification. Getting things right is normally also in the interests of the contractor since repetition of unsatisfactory survey lines will detract from the overall efficiency of the operation and add to its costs. Some of the tests that need to be carried out and recorded were discussed in the previous section.

Once production is established, however, data starts to accumulate according to a pre-defined plan so that coverage is built up systematically and the operation base is perhaps moved progressively through the survey area to minimise the amount of time wasted on ferrying the aircraft from airport to flight-line each day. The contractor checks the quality of the data each day and, in consultation with the technical authority, it is certified that at least minimum standards are achieved. The operations continue until the technical authority certifies to the client that all the necessary data have been acquired to a sufficiently high standard, that the final compilation is possible with the data available and that the aircraft may therefore be de-mobilised to another project.

Amongst the tasks that are important at this stage is the inspection of individual profiles for spurious anomalies that may be due, for example, to isolated single erratic readings or to short-wavelength anomalies due to man-made metallic objects such a buildings, pipelines or railway tracks. Such ‘cultural’ effects can often be

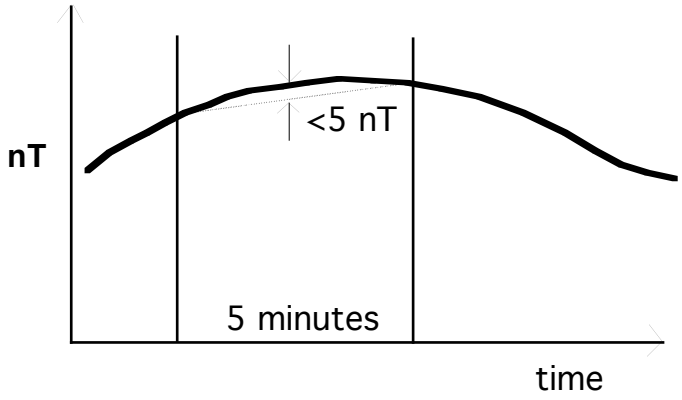

Figure 5.1 *To remain within acceptable limits during survey operation, the diurnal variation in the magnetic field, recorded at a base station, should not differ by more than a defined amount (e.g. 5 nT) from a straight line drawn between any two points five minutes apart in time.*

identified on the video of the flight and the offending readings may be deleted and replaced by splined-in values. As will be shown in Section 6, some of the most exacting tests of data quality involve displaying the data as images. Any level-shifts between adjacent flight lines can show up very clearly and so adjustments may be made appropriately. In effect, this involves going immediately to a type of final product for the survey on a provisional basis. Fortunately, the computer power necessary to do this already in the field office is provided by conventional (laptop) computers. However, in the cause of a logical description of the procedures, it is first necessary to describe some earlier stages of the data reduction procedures systematically.

5.2 Elimination of temporal variations

Of the time variations mentioned in Section 1.3, micropulsations, magnetic storms and diurnal variations occur over periods of time that are short compared with the time taken to carry out a typical aeromagnetic survey. The three measures normally taken to eliminate these - base-station subtraction, tie-line levelling and micro-levelling - are described below.

The limit set to achievable accuracy by the noise level of modern magnetometer systems is about two parts per million of the scalar magnitude of the field being measured and four orders of magnitude less than the amplitude of large anomalies in that field. An almost intractable problem in data reduction is posed by fully eliminating time variations in the magnetic field to this accuracy. It is not practicable to make all the measurements that are necessary to eliminate all ambiguity and the skilled processor engaged in the reduction of data is, as a consequence, ultimately required to make some adjustments which can be justified only on the basis that they make the resulting maps and images 'look better' - i.e. value judgments, rather than unequivocal scientific observations.

(a). Base station subtraction.

It is a relatively straightforward matter to run a recording base station magnetometer at a location on the ground while the aircraft is flying and subtract the time-synchronised magnetic variations at the fixed base from the profiles recorded in the air to give a residual where the temporal dependency has been eliminated and is only a function of space. Unfortunately, this assumes that the geomagnetic variations recorded at the base station are fully representative of such variations over the whole survey area. In fact, it can be shown that such variations are only imperfectly time-synchronous over distances of 50 km or so and individual features - such as micropulsations - can change phase and amplitude significantly within distances of this order. These effects are exacerbated during magnetic storms when flying operations are, in any case, suspended.

The restriction of survey flying to times of low geomagnetic activity is usually defined in a survey contract by the so-called 'diurnal tolerance'. Since most of the processes employed later in the removal of temporal variations assume that geomagnetic variations approach linearity over periods of several minutes, it is necessary to specify an allowable departure from linearity on a recording ground magnetometer (base station) trace. A definition often employed is that non-linearity should not exceed 5 nT over any five-minute period. This is assessed by drawing any 'five minute chord' and measuring the greatest difference in nT between this and the observed magnetic field (Figure 5.1) Some authorities claim that this is unnecessarily stringent, particularly in high magnetic inclinations where storms are more frequent, and leads to needless expensive hours of aircraft idleness.

Before subtraction is carried out, great care must be taken to ensure that airborne profiles are not corrupted by any magnetic interference (such as the effect of passing vehicles) recorded only at the base station. Furthermore, the ground profile should be suitably smooth (or be smoothed) to ensure that subtraction of the ground values does not amount to an addition of noise to the airborne profile. Ideally, a ground magnetometer no less precise and accurate than that employed in the aircraft should be used. However, in general, subtraction of base-station readings immediately reduces errors due to temporal variations in an airborne profile to levels less than about 10 nT.

For surveys in areas of high magnetic relief, it has been argued that base-station subtraction alone gives adequate removal of temporal variations. In most cases, however, it seems likely the following procedures will further improve the data quality.

(b). Levelling at line intersections.

Aeromagnetic surveys have always been planned with a network of flight-lines and 'tie-lines' or 'control-lines' to provide a method of eliminating temporal variations from the observed anomalies (Figure 4.7). The principle is that, once heading effects of the aircraft have been eliminated and since the magnetic (anomaly) field we strive to record is essentially time-invariant, any ***difference*** observed in the recorded value between two overflights of the same point (i.e. at any intersection in the flight-path)

must be attributable to temporal variations, even though neither of the two values is itself necessarily correct.

The mis-ties at all intersections may then be examined and adjusted systematically in an attempt to reduce them to an amplitude below the noise envelope. For example, DC level shifts can be applied to lines or tie-lines where all mis-ties are systematically too high or too low. If the line with the largest mis-tie average is adjusted first and all the mis-ties are then recalculated, the process can be repeated on the line or tie-line which *then* has the highest average mis-tie, and so on.

In practice, the diurnal variation ***within*** a single line is often considerable - simple level-shifts are insufficient and a low-order polynomial has to be determined from the mis-tie values and applied to the data from each flight. The scheme employed by the Geoscience Australia to carry out this operation is as follows.

A tie-line, Line A (Figure 5.2), central to the survey area (preferably passing through areas of low magnetic relief - see later - and flown in a period of low geomagnetic activity) is selected as a reference standard for the survey area. A second tie-line, Line B, is referenced to the first by observing the differences in mis-ties against time in all the regular flight-lines which cross both Line A and Line B. A low order polynomial fitted to these differences is used as the basis of adjusting Line B to Line

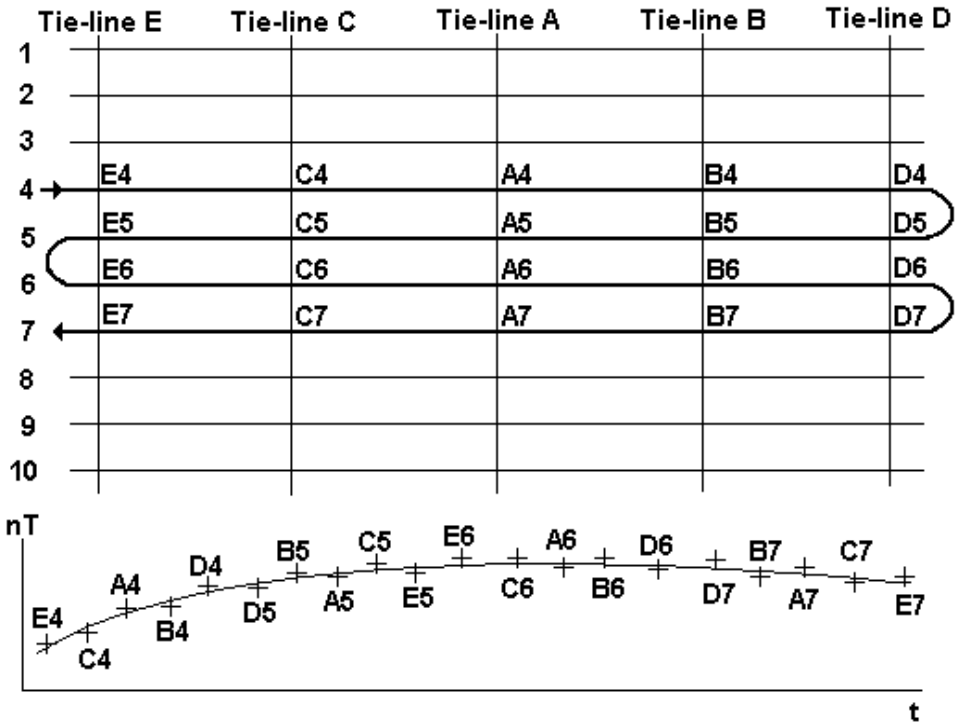

Figure 5.2 *Illustration of the procedure for control-line levelling described in the text.*

A. The process is repeated for Line C, which lies on the opposite side of Line A from Line B, and so on until all the tie-lines have been levelled together. These adjusted tie-lines are used as the framework upon which all the flight-line data are then 'hung' in the following manner.

For each flight of regular survey lines, the differences at intersections between observed magnetic values and the adjusted values for the ties are then examined in time order. A low-order time-based polynomial fitted to the differences is taken as the temporal variation which is then subtracted from all the observations made during the flight. In fact, if base station subtraction has already been carried out, the variations are the *difference* in temporal variation between that recorded at the base station and that recorded in the air.

It is assumed that temporal variations are a smooth function of time, i.e. that the time taken to fly from one intersection to the next is short compared to the period of any time variations. This is clearly more likely to be true on tie-lines where intersections are encountered more frequently than on flight lines. It is also assumed that intersection points are accurately located in x,y on both flights; mis-location will lead to the unjustified comparison of readings with a different 'geological signal'. To reduce this problem, points are weighted during polynomial fitting with lower weights being assigned to observations made in areas of high magnetic gradients. Rogue points lying outside a few standard deviations of the fitted polynomial line may be rejected completely from the analysis (at the discretion of the data processor) to avoid unjustified distortion of the data in the correction process.

(c) Microlevelling

Creating a grid and imaging the result (Section 6) usually reveals that the levelled profile data is still less than satisfactory in that some line-related noise remains evident. This effect has been described as 'corrugations' and the standard procedure for its removal as 'decorrugation' or 'micro-levelling'. Note here that making a grid and imaging the data is now often used as part of the quality-control process in a survey (Section 5.1) and that use of this technique - even in the field on a day-to-day basis as new data is acquired - is becoming quite commonplace.

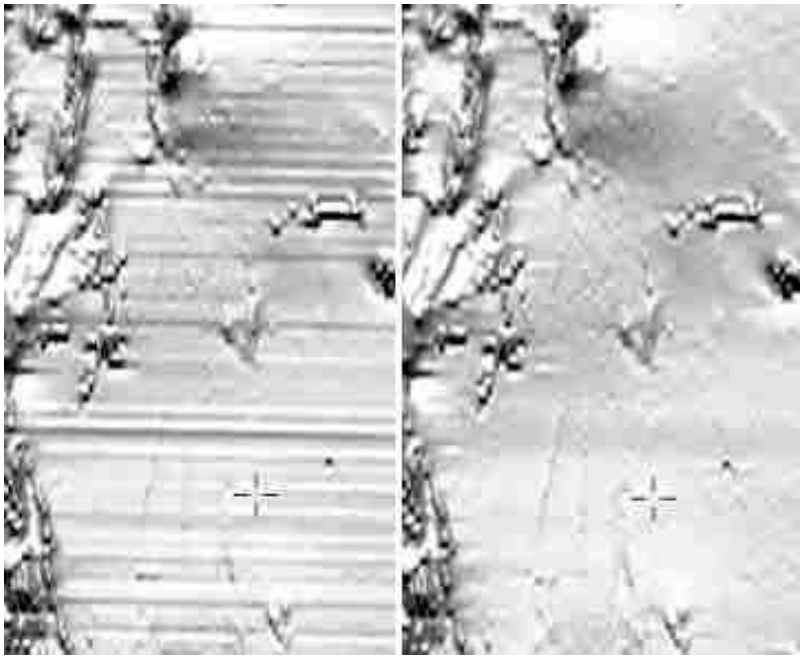

Figure 5.3 *(a) magnetic image of data prior to micro-levelling and (b) the same data after micro-levelling, showing distinct visual improvement.*

The micro-levelling procedure used to remove line-related noise has become standard in recent years and was described by Minty (1992). It has no basis in the physics of geomagnetism and can, with equal justification, be applied to other line-based data such as gamma-ray spectrometry. It is essentially a filtering process that seeks to

identify and remove features whose wavelength in the across-line direction is equal to twice the line spacing and in the along-line direction to the spacing between tie-lines. The need for micro-levelling arises, at least in part, from the imperfections in the polynomials applied to 'hang' the flight line data on the tie-lines - and imperfections in the difference values used to calculate those polynomials. The result is that the long-wavelength component is slightly out of register with neighbouring lines and individual lines of data therefore show up, particularly, for example, when calculating shaded relief effects (Section 6) in directions near normal to the flight line direction (Figure 5.3). Micro-levelling is applied to gridded data and the adjustments made to improve the grid are then fed back as a correction to the original profile data so that, when next gridded, line-related noise should not be evident.

Adjustments made in micro-levelling should be confined to a few nT; micro-levelling should not be used to cover up errors attributable to poor application of conventional levelling procedures. The assumption in micro-levelling is that the near-DC component of each profile resembles that of its neighbour, i.e. that the 'regional' field varies only smoothly from line to line across the whole survey area. The broad warp of this variation is controlled by the tie-lines. The danger is that genuine geological features can also follow flight lines and micro-levelling could remove these. In practice a threshold is used to limit removal to low amplitude features that are more likely to be related to problems of imperfect levelling than to geology.

Older aeromagnetic data sets can often be 'improved' by micro-levelling. However, the justification for this is often limited to improved cosmetic appearance; line-related noise in older data is just as likely to be due to poor navigation as to imperfect removal of temporal variations and the danger of removing genuine geological features in the cause of making the data 'look better' is very real.

(d) Summary

It may be useful to summarise the possible errors that may reside in the magnetic profile data as a result of the uncertainties in the process of removal of temporal variations:

- temporal variations recorded on the ground and subtracted from the airborne data may differ from the temporal variations experienced by the airborne magnetometer.

- the assumptions made in the tie-line levelling process may be flawed and lead to long-wavelength distortion of the anomaly field.

- the process of micro-levelling is essentially arbitrary.

Some numbers derived from the data reduction of an aeromagnetic survey of an area 120 km by 160 km in South Australia (in 1993) may help clarify the magnitude of these corrections. Base station subtraction changed the magnetic value recorded on lines by an average of about 35 nT with this value changing by, on average, about 3 nT over the time taken to fly a line. Tie line levelling then changed values by an average (without regard to sign) of 1.7 nT with an average range of 3.1 nT (maximum

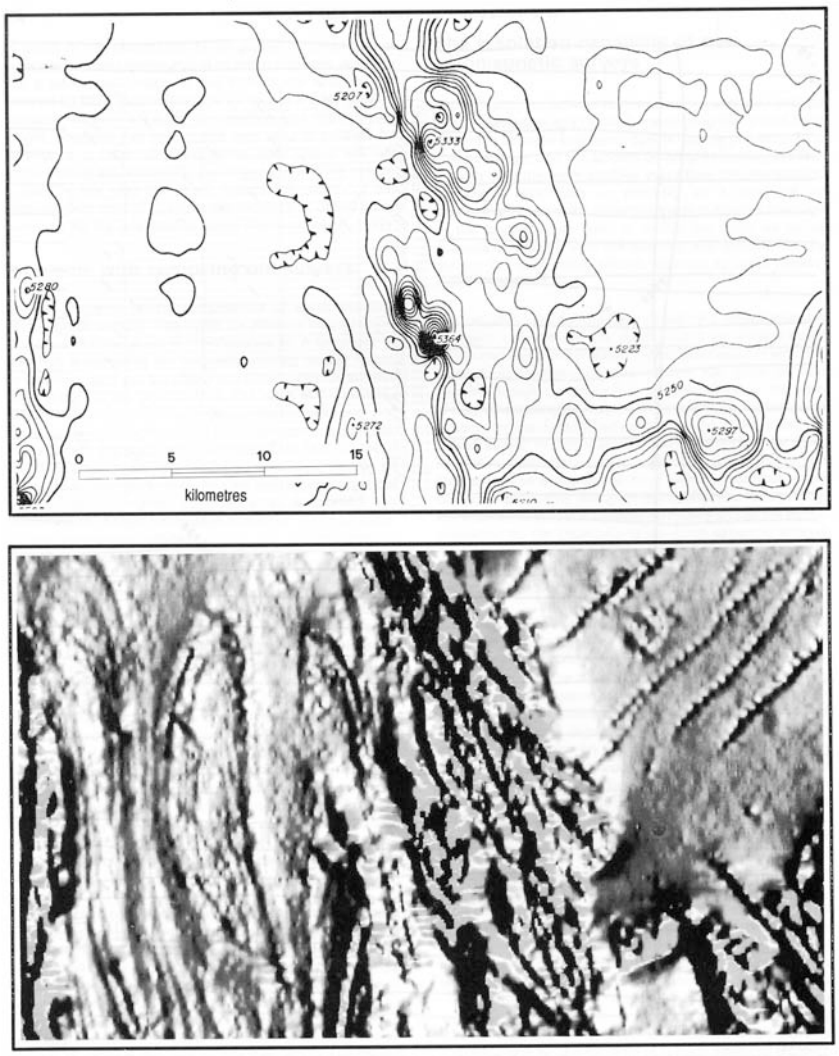

Figure 5.4 *Above: Aeromagnetic contour map, typical of the quality achievable in the early 1970s. Below: Grey scale shaded-relief image of a survey carried out to more modern specifications in 1991. Superior instrumentation, survey specifications and imaging methods reveal many features in the geology not evident in the earlier survey (from Reeves, 1992).*

to minimum) over the length of a line. Microlevelling adjusted 70% of data points by amounts less than 1.0 nT and 23% of data points by less than 0.1 nT. While the adjustments made in micro-levelling may appear small, it should be noted that about three-quarters of the data points were adjusted by an amount exceeding the nominal noise envelope of the data (0.1 nT).

The nature of the imperfections in the assumptions made lead to an error in the data set which will have both systematic and random elements. The error is of limited importance for interpreting the geology within a single survey area, but has consequences when, for example, surveys of adjacent areas flown and reduced as separate projects are compared. With older data especially, the magnitude of these errors is difficult to assess, particularly for surveys which predate the introduction of some of the processes described above and particularly where the processing sequence is less than perfectly documented. As a consequence, magnetic anomalies of long wavelength - i.e. comparable with or longer than the dimension of a typical survey area - say 150 km by 150 km - are even now only poorly determined in conventional aeromagnetic surveys. To improve on this situation would require elaborate investment in more rigorous survey practice. Since anomalous features of long wavelength are, generally speaking, of least interest from the standpoint of mapping geology or assessing resource potential, this would be hard to justify in practical terms.

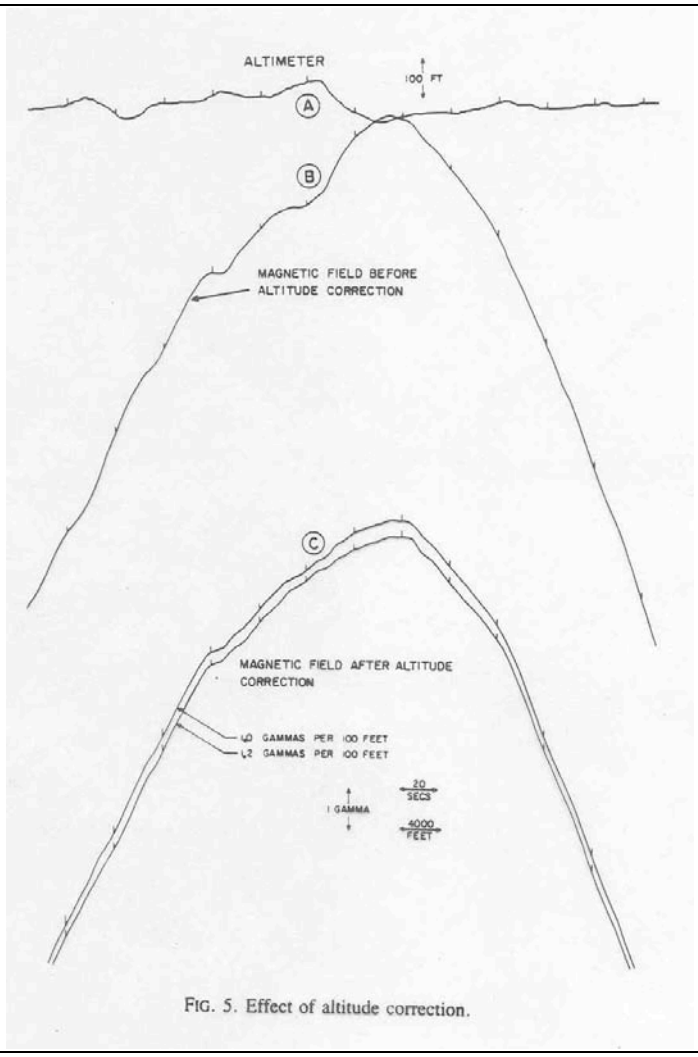

Figure 5.5 *Application of altitude corrections to profile data acquired in a constant barometric altitude survey (from Reford 1980).*

The located profile data in a modern survey should be limited in its accuracy only by the uncertainties discussed above and relative errors over short distances in recent data are probably already much less than 1 nT. Figure 5.4, which compares contour presentation of survey data acquired in 1973 with image presentation of a new survey of the same area carried out in 1991, shows that genuine anomalies of geological origin with amplitude 1 nT or less are easily revealed in the more recent survey.

It will never be possible to take an instant 'snapshot' of the magnetic anomalies over a whole survey area. While deployment of additional ground base stations across a survey area might provide better control of diurnal variations, it would add operational costs and difficulties which would tend to counter the welcome trend towards lower survey costs. Nevertheless, on-going refinements in the processing of magnetic profile data can be expected.

5.3 Other corrections and the final profile data.

(a) Height correction

Most often it is not considered necessary to correct the readings of an airborne magnetometer for height, though there is certainly a 'free-air' gradient of the magnetic field at any given locality. The magnitude of this gradient is usually about 0.04 nT/m which approaches the limit of detectability even for a sensitive airborne vertical gradiometer system. However, high-sensitivity total field surveys flown with less than perfect control on the altitude of the aircraft - particularly where flown over areas of low magnetic relief such as are typical over thick sedimentary successions - are sometimes seen to have variations of fractional nT amplitude in the magnetometer channel sympathetic with variations in the altimeter reading. The

magnetic variations can be reduced or eliminated, often by determining a suitable free-air gradient empirically by applying corrections for a range of gradients on a trial-and-error basis, as illustrated in Figure 5.5.

Where height corrections are applied, this should be the first phase of data processing since the implemented corrections will influence the subsequent removal of temporal variations and the micro-levelling of the data. Height correction would be beneficial to a precise scheme of tie-line levelling; a difference between measured and nominal (specified) height of only 3 m would be sufficient to produce a difference in T equal to the 0.1 nT noise envelope on the profile of an optical pumping magnetometer and height differences of several tens of metres will not be uncommon in practice. Application of height corrections would ensure that comparisons of T values made at line-intersections were more valid, though variations of T with h as a result of local anomalies (as opposed to the free-air gradient) would still not be taken into account.

(b) Removal of IGRF

Once coefficients are available for the IGRF at the epoch of the survey (Section 1.4), it is possible to calculate a value for the IGRF at every point where an airborne magnetometer reading is made in a survey and subtract that value from the observed value to give the 'anomaly' defined (in Figure 1.14) as the departure of the observed field from the global model. The global model field over a typical survey area is, in effect, a very low order surface which may even be well-approximated by a linear gradient. There are no significant consequences for the accuracy of processing if this gradient is removed at the beginning or at the end of the data reduction sequence.

Of more importance is the fact that the *absolute* value of the observed field is usually only poorly determined, even though most modern magnetometers record absolute values. After base-station subtraction, the quoted value is simply the *difference* between the airborne magnetometer reading and the magnetometer reading at an arbitrary point on the ground. The exact relationship between the total field at the ground station and the IGRF at that point is usually still not determined.

In theory, the base station values could be compared with magnetometer records at a permanent magnetic observatory from which an accurate absolute value could be derived for the crustal anomaly at the base station and hence the for the airborne values. This is seldom done; the nearest magnetic observatory is often thousands of kilometres from the survey area, adding cost and complexity to survey operations. In Canada, a small number of airborne magnetometer calibration points has been set up at conspicuous cross-roads in areas of low magnetic gradient (Teskey et al, 1991). These points may be overflown in cardinal compass directions with an airborne magnetometer system. The ground points have been carefully linked to nearby magnetic observatories, enabling the value recorded by the airborne magnetometer at the moment of overflight to be related directly to absolute observatory values of T.

Often, particularly in the past, the corrected values of T resulting from an airborne survey are added to an arbitrary constant value such as 5000 or 10000. This removes possible confusion consequent upon contouring negative values but has little other merit. Sometimes the arbitrary constant is an estimate of the total field value in the survey area, leaving magnetic values on final maps looking very similar to true total field values except that the horizontal gradient attributable to the IGRF will have been removed. The importance to the user of all these procedures being fully documented by an analyst reducing a survey should be obvious. From the user's point of view, there is clearly a need for caution when reading the absolute values of magnetic field recorded in survey output (map or digital). The need to apply level-shifts and warps to final survey data when attempting to join grids of surveys of adjacent areas 'seamlessly' (Section 6) is a consequence of (a) the lack of rigour in determining absolute values in normal survey practice, (b) the poor control over long wavelength geomagnetic variations which results from large distances between aircraft and ground station and (c) the arbitrary nature of some data-reduction practices applied to remove temporal variations.

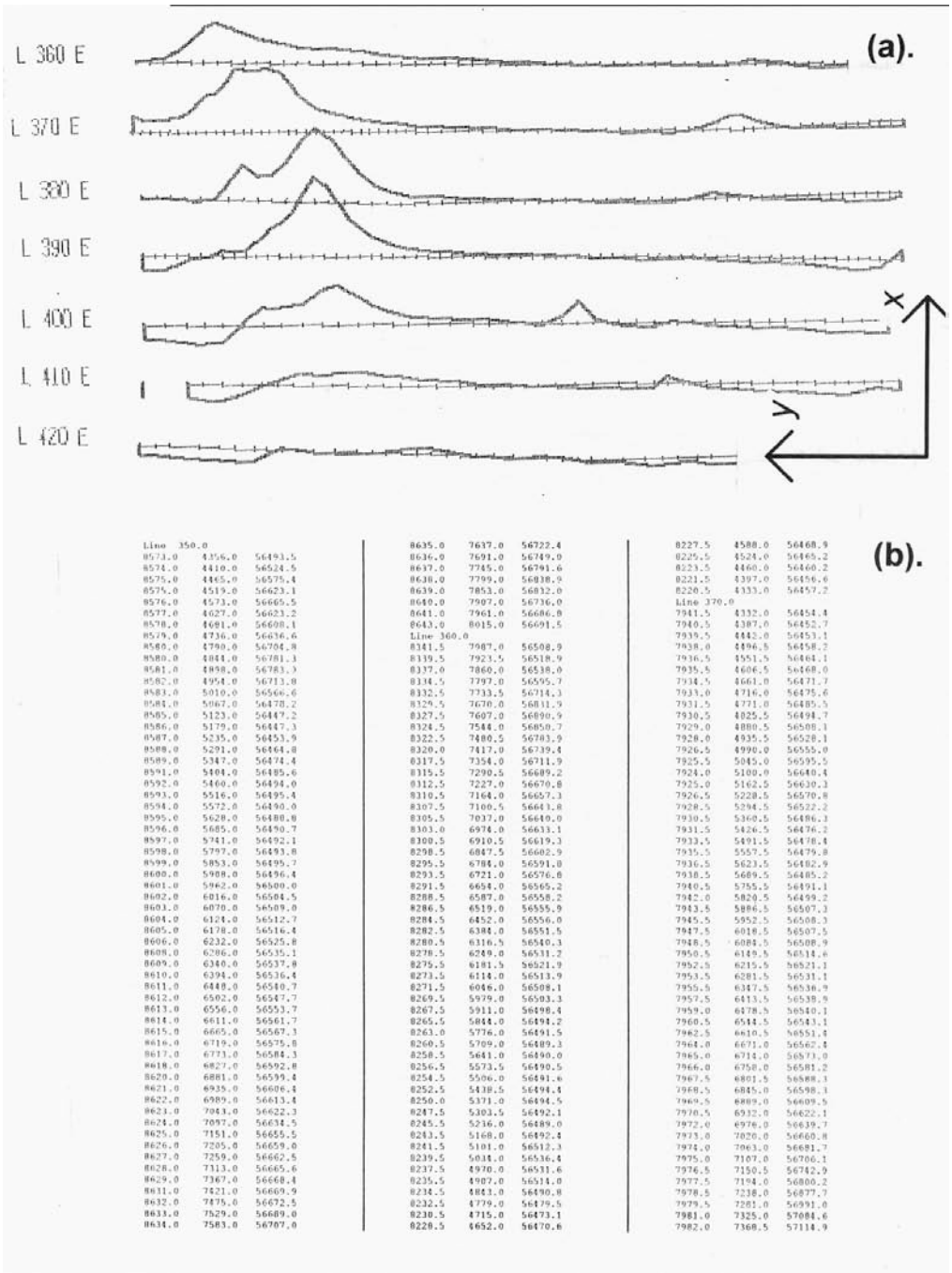

Figure 5.6 *Example of magnetic profile data: (a) in profile presentation and (b) as a listing of x, y and T values.*

(c) Final profile data.

An example of a small section of the final profile data resulting from a modern aeromagnetic survey is shown in Figure 5.6 in digital and profile format. Data of this type is the starting point for the preparation of contour maps and images and the interpretation of individual anomalies from the original profile data to be discussed in Sections 6 to 10. The levelled profile data or XYZ file (in practice, the final database of the survey with all the necessary corrections made) is the culmination of the data

acquisition and compilation process and the start of procedures to visualise and interpret the results. It is convenient to think of this product as the end of the responsibility of the (single) survey contractor and the beginning of the activities of all the many users who will try to extract new geological or exploration data from the survey.

5.4 Digitising of old contour maps

A great deal of airborne survey data, particularly aeromagnetic surveys, from the earlier years (before about 1972) before full digital survey acquisition was established, are now available only as contour maps printed on paper. The methods of data presentation and visualisation to be described in the sections ahead can be of value in the examination of old data, so it is appropriate to end this Section with a mention of the possibility of digitising older surveys so that these digital techniques may be applied. There is also a great deal of merit in the compilations that have been made of data, old and new, to give regional coverages of magnetic anomaly patterns over areas as large as whole continents. Much of this work included the recovery and digitising of data from the pre-digital era.

The analogue chart records from the aircraft in these early years can sometimes also be located and represent the most original form of the data from early surveys but, once digitised, their compilation still requires a great deal of other effort, including, for example, digitising the flight path and registration of profile data with it. It is often the case that some information necessary for such a compilation is missing, even when it is attempted. In other cases, badly created or badly stored digital data tapes from the early days of digital data (1970s and 1980s) may be so time-consuming to acquire and/or decode that digitising paper contour maps is the most efficient way to start a digital data-processing scheme on older data. Usually, a scanned-image of the map is acquired and viewed on the computer screen after registration to geographic coordinates. In view of the foregoing comments about real data being acquired only the flight lines of a survey, it is optimal if the map shows the original flight-path and that contour intersections with the flight-path are recorded systematically. Current software allows a scanned image of the map to be displayed on a computer screen and the cursor is made to follow the flight line and capture the x and y value for each contour intersection. Only the z value (total field anomaly) at each x,y location then has then to be entered and recorded in an output file. This file is then exactly similar to the XYZ file emerging from the compilation of a new digitally acquired survey, except that the quantity (and quality) of the data is much reduced. While the data of the old survey is reproduced as closely as possible in such a scheme, it should be clear that anomalies smaller in amplitude than the contour interval will be missed and the resolution will be compromised. The dynamic range of old data is set by this, rather than the sensitivity of the original magnetometer. Such shortcomings have proved small, however, in comparison to the advantages to be gained through using digital presentation and processing techniques to reveal geological features that were not evident in the original contour maps that had remained, in many cases, a single static output product for many years.

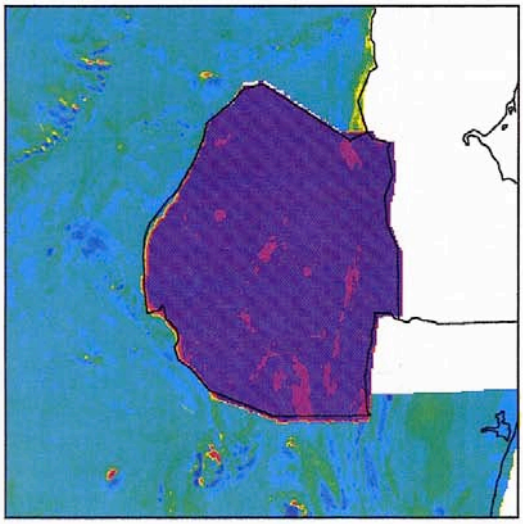

FIGURE 5A Aeromagnetic surveys for South Africa and Swaziland linked without correction. Note the areas of overlap in the west, exact butt join in the south and small gaps in the north. A large DC shift masks any other mismatch

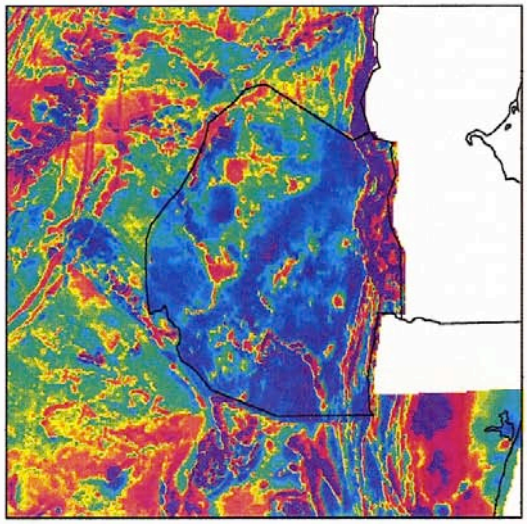

FIGURE 5B Aeromagnetic surveys for South Africa and Swaziland linked with the best DC shift calculated at the northern end of the join. Note that although the surveys match well in the north, there is an increasing mismatch towards the south. Geologic features can be traced across the survey boundaries, but actual magnetic field values are discontinuous

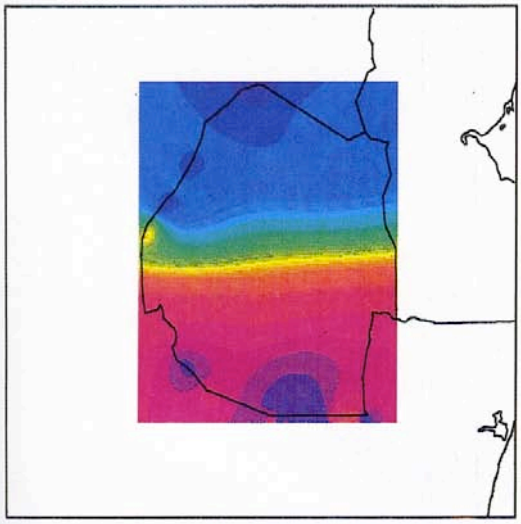

FIGURE 5C Empirically-derived correction grid to apply to the Swaziland data. The relatively high frequency corrections lie around the survey boundaries, whereas the interior of the correction grid is as smooth as possible

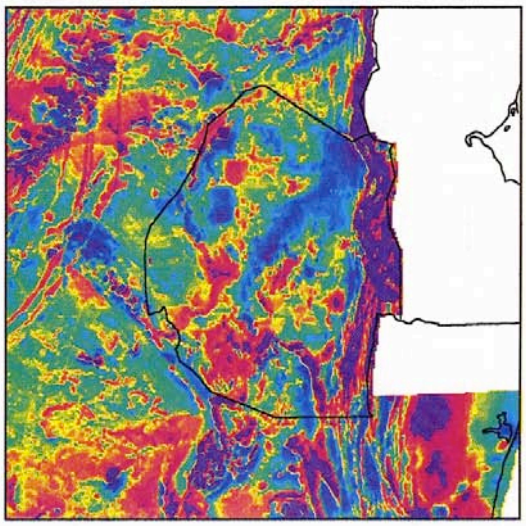

FIGURE 5D Aeromagnetic surveys for South Africa and Swaziland linked after the application of an empirically-derived correction grid based on mismatch at the survey boundaries. The survey boundaries are now almost invisible and geologic features crossing the boundary are clear and delineated by continuous magnetic anomaly values

Figure 5.7 *Linking and levelling of a grid to match surrounding data – see captions for explanation.*

Digitising should obviously not introduce any new errors or loss of quality in the data. This should always be verified by comparing the output contours from computer processing with the original hand-drawn contours from which they were derived. Differences should be scarcely perceptible. Preferably the effects of any imperfect interpolation of data values between flight lines in the original (hand) contouring should also be minimised. Where flight lines are not shown on the paper maps, it is

necessary to draw imaginary flight lines perpendicular to the geological strike and record X,Y,Z for each contour intersection.

5.5 Linking and levelling of grids

The widespread use of aeromagnetic surveying over more than 50 years has resulted in the coverage becoming complete in many parts of the worlds over large areas – in the case of Australia, for example, over the entire continent (see Section 7.4). With individual surveys of various vintages, however, the quality of the data is often uneven and some of the limitations to normal survey practice outlined above inevitably mean that adjacent – or even overlapping – surveys do not immediately come into agreement in terms of their background levels when surveys are patchworked together to give a continuous coverage.

There are many possible causes and often more than one of them may apply. As explained in Section 5.2, there is always some doubt about the perfect removal of short-term temporal variations, but in recent surveys this is unlikely to amount to level

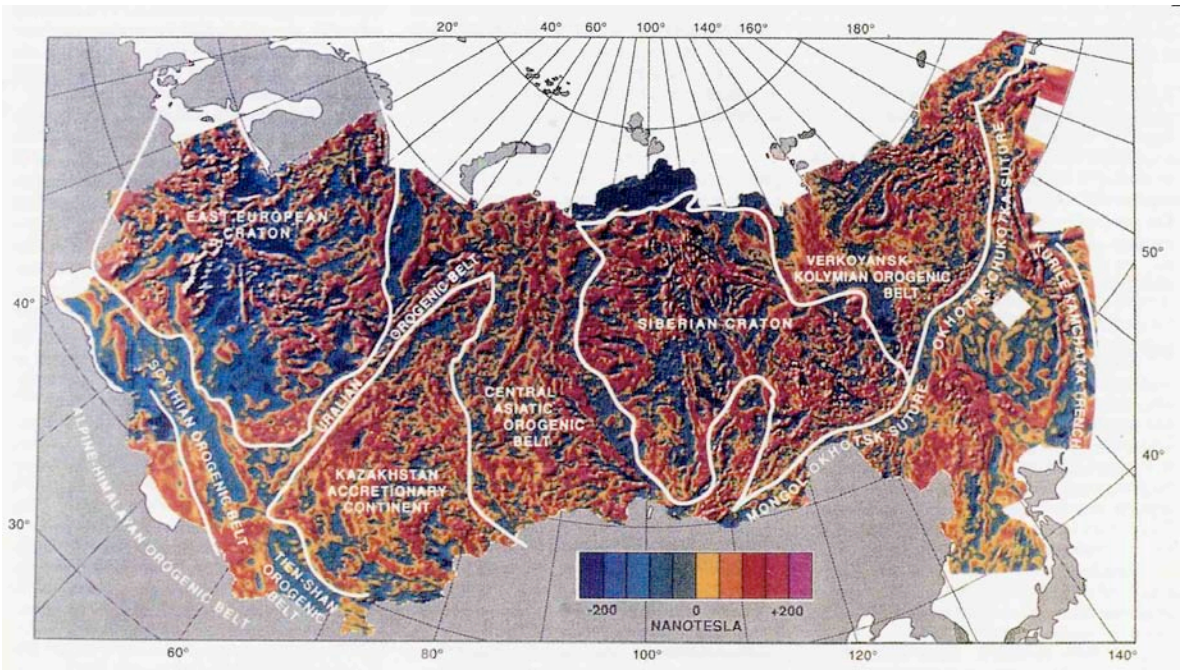

Figure 5.8 *Systematic aeromagnetic anomaly mapping of Russia has revealed some of the major tectonic divisions of Eurasia (from Zonenshain et al, 1992).*

errors of more than a few nT. A second cause might be secular variation in the geomagnetic field, though this should also give only minimal differences between surveys, provided that a regional (IGRF) field appropriate to the date of the survey is removed from each survey in turn prior to their compilation together. In some cases it will be found that an inappropriate regional will have been subtracted during initial processing. Now, many years later, a better model may be used - provided the incorrect field originally subtracted is known and can first be added back. Remember that the pattern of anomalies is virtually time-invariant so all long-term time variations should be eliminated by subtraction of the *correct* model field for the time of the survey.

Other - and often more serious! - causes arise from the application of an incorrect or arbitrary reference field from surveys. Sometimes, for example, in early surveys, an algebraically defined planar or sloping surface was subtracted from data values without reference to any geomagnetic field model. This can be repaired if what was removed is still known and can be added back in. In other cases, an arbitrary constant will have been added to the processed data to bring all 'anomaly' values near to the absolute value of the geomagnetic field in the survey area. In yet others, an arbitrary constant will have been added, typically to make all anomaly values positive to avoid problems with contouring negative numbers with early computer algorithms.

With increasing data processing sophistication in newer surveys, these problems come under better control, but there is still a persistent need to make the best use of old data where new surveys cannot be afforded in the foreseeable future. One of the most thorough-going attempts to define magnetic anomalies against an absolute framework has been made in Australia where a continent-wide array of recording magnetometers was deployed and a number of circuits of low-level aeromagnetic traverses flown simultaneously in order to produce a national network along which absolute anomalies were available after subtraction of the best available diurnal and secular variations from the recording ground-based magnetometers and permanent magnetic observatories (Tarlowski *et al.*, 1996).

In principle, without such control, it is necessary to link adjacent surveys together somewhat arbitrarily by examining values along a line of overlap and adjusting one survey by adding a low-order polynomial surface to bring it into agreement with values in the adjacent survey. These adjustments can be tapered off across the width of a survey, or over a ceratin distance from the margin (see Figure 5.7). Clearly, one survey has to be taken as a standard against which the other is adjusted. Without long wavelength control, these arbitrary local warps themselves can accumulate into an unsubstantiated regional variation when many surveys are stitched together over a large area. In terms of what has been discussed earlier in this section, the conclusion is that the methodology of airborne magnetic survey acquisition does not support the acquisition of (low amplitude) anomaly variations where the wavelength is greater than the dimensions of individual surveys, i.e. probably no more than 200 or 300 km. This is an area of ongoing research.

Computer processes have been developed to ‘link and level’ adjacent surveys to produce data compilations without the unsightly level-shifts that would otherwise appear along survey boundaries. The main objective is to adjust one or both overlapping surveys by applying level-shifts and warps until the near-DC components of both grids come into agreement.

The retrieval and compilation of pre-existing surveys for many of the continents has necessitated the adoption of procedures of this type in order to display attractively the magnetic anomaly signature of the geology and tectonics of large areas of the earth’s crust. While it is fair to say that the extraction of new geological information from compilations of this sort is still in its early phases, it is already clear that many aspects of the evolution of the continental crust over billions of years of geological time will be well-served by careful attention to magnetic anomaly data of this sort.

Figure 5.8 shows the magnetic anomalies over the land area of Russia with some indication of the main tectonic provinces revealed by this admirable survey effort superimposed. There is quite some effort still required to complete a magnetic anomaly map of the world – oceans and continents – but there is no doubt that such an item would be a worthwhile contribution to understanding of global geology (Reeves *et al.* 1997). This is discussed further in Section 7.4.

*** *** ***

6.

Gridded data: Maps, images and enhancements

6.1 Visualisation

With this section we leave behind everything to do with data acquisition and compilation and begin with the processes of presenting and enhancing the resulting data and interpreting its geological information content. What has gone before, however, is essential in understanding the theoretical basis of the data being examined and being aware of the potential limitations to what can be done with it on account of the physical parameters of the acquisition and processing procedures.

Digital data files – in particular the database of XYZ data resulting from a survey – are the starting point for this second part of the journey. The interpreter requires this vast quantity of numerical data to be presented in a format that can be appreciated by human perception. This means going from digital data in computer-storage media to maps and images that can be seen, examined and discussed with others.

The present section introduces the main methods by which aeromagnetic data may be visualised for the convenience of the user and outlines some of the possibilities for enhancing the data through digital filtering in the space domain. The particular physical properties of Laplacian fields allows a large number of other useful processes to be applied to aeromagnetic data by way of the Fourier transformation to the spatial-frequency or wavenumber domain and this is discussed in Section 7. These may all be seen as different methods of ***visualisation*** of the data.

The extraction of geological information from a survey is also known as ***interpretation*** and usually has both ***qualitative*** and ***quantitative*** aspects. While both play important parts, it is easier to introduce the quantitative aspects first in Sections 8 and 9 before concluding with an introduction to the more qualitative aspects of intepretation and the integration of aeromagnetic data with other types of geo-information in the concluding section, Section 10. The passage of work through these several phases is common for many types of geophysical investigation and not confined only to aeromagnetic data. The phases are summarised in Figure 6.1. Very often the conclusion of the interpretation report is that certain features are sufficiently interesting to justify the initiation of a follow-up programme. In this case, the cycle restarts with the planning of suitable follow-up surveys, either on the ground or in the air.

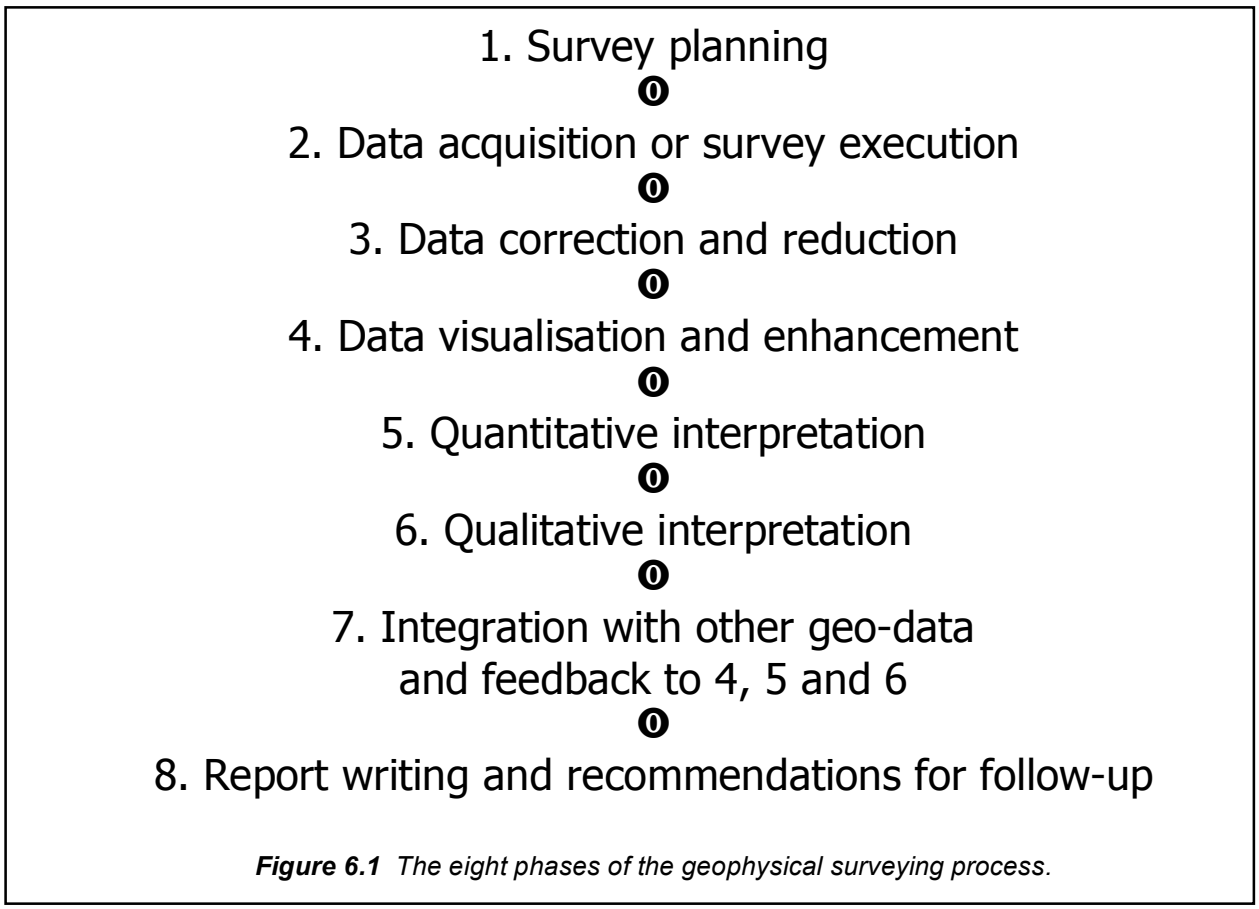

Figure 6.1 *The eight phases of the geophysical surveying process.*

6.2 Profiles and Profile maps

Section 4 dealt with some of the consequences of having closely-spaced but discrete sample points along survey lines. In general, provided that the rules of along-line sampling given in Section 4.3 are not violated, along-line data has an adequate number - if not a surplus - of sample points. Between lines or across the flight direction, this is seldom the case since fully adequate across-line sampling (i.e. very close line-spacing) leads to a large increase in survey costs. Even the most detailed surveys are usually flown at a spacing no closer than 100 or 200 m, when fully adequate sampling would require this to be reduced to about 50 m (for a survey at 100 m terrain clearance) with a two- or four-fold increase in acquisition cost. The law of diminishing returns militates against such extravangance.

Once again, then, we face the reality that we have less data points than we would wish and we are forced to make *estimates* of values in areas where we have not actually made measurements (i.e. between flight lines) if we are to reproduce our surveys as continuous fields on two-dimensional maps. On the positive side, we can at least expect that the Laplacian field we are measuring will vary smoothly between discrete observation points; in potential field surveys, certainly, there are no abrupt discontinuities to be found.

One straightforward but little-used approach is to avoid this problem by showing the results acquired along each flight line as profiles plotted against the geographical position of the flight-lines themselves. This is illustrated in Figure 6.2 and is commonly know as the profile map. Normally the Z value is plotted at a distance to the west of a

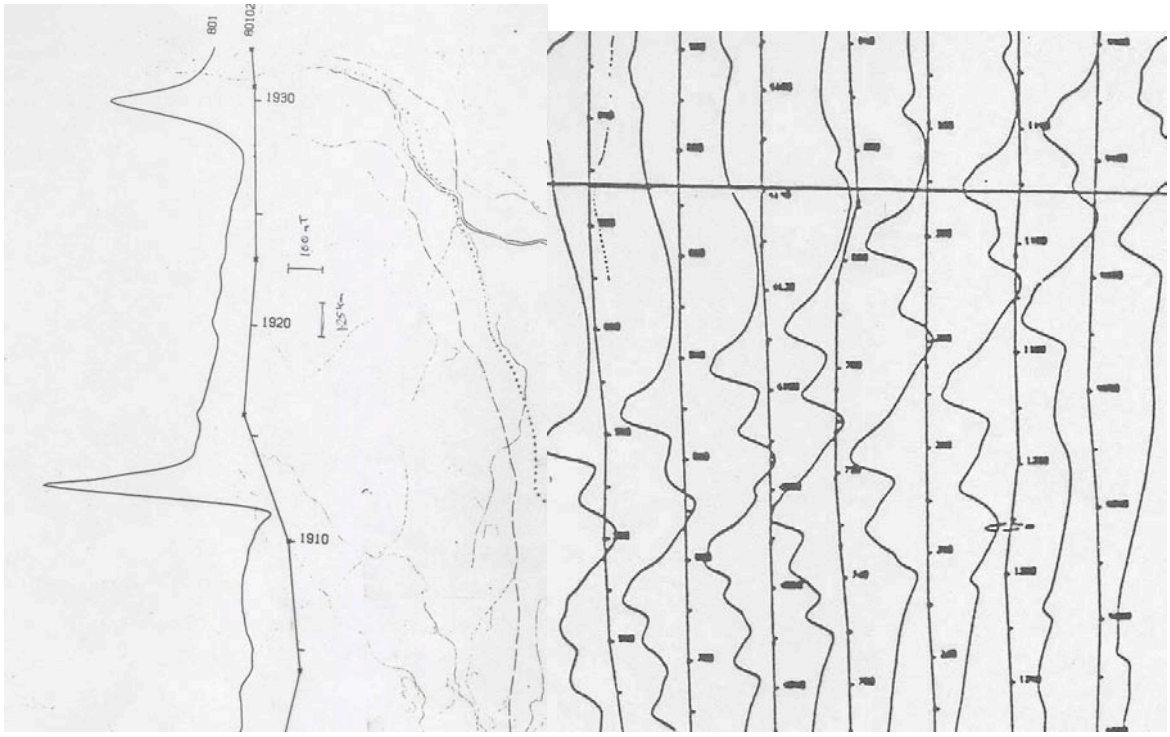

(a) (b)

Figure 6.2 *(a) A single magnetic profile plotted against the corresponding flight path map showing two well-defined anomalies. (b) A small area of a profile map showing profiles plotted against flightlines and illustrating the continuity of anomalies from lineto line that is often evident in such maps.*

N-S profile, proportional to the magnitude of Z, in this case the magnetic anomaly. Careful choice of *vertical scale* (i.e. measurement units per cm) and *base level* (i.e. the field value for zero displacement from the observation track) is necessary for clarity of presentation. The profile map has the merit of being a faithful representation of all the data recorded and has some particular advantages in helping the human eye to follow anomalies from one line to the next where their shapes share a certain similarity, particularly where features are striking more or less normal to flight-lines and where the spacing between profile lines is so large that interpolation of Z values between adjacent profile lines becomes uncertain. Furthermore, they do not suffer from any *aliasing* which can occur when profile data is re-sampled for contouring (see Section 6.4). On the other hand, features of longer wavelength are not easily recognised on a profile map presentation.

The profile map is certainly one very useful form of visualisation. We shall see in this section that there are many others. It can even be argued that 'beauty is in the eye of the beholder' and different interpreters will each have their own preferences as to which type of data presentation has the most value or is the most appealing to the eye.

In all cases, however, each original observation point has at least three digital attributes:

(1). a grid or geographical easting value (x);
(2). a grid or geographical northing value (y) and
(3). a geophysical field value (z).

Note that there is usually more than one Z value for a given survey - altimeter readings, time and other values are usually stored against each x,y position, even when only one geophysical parameter is recorded.

6.3 Contouring by hand.

Hand-contouring is time-consuming and demands a great deal of skill and care and, in airborne surveys, was replaced gradually by computer-based methods in the 1970s. In the earlier years, the skill - and sometimes the imagination! - of the draftsman was used to interpolate between the flight-lines and so estimate magnetic anomaly values where they had not been measured. While this had some merit in allowing rational human input and a guarantee that the results were aesthetically pleasing, the method was prone to ambiguity - and the certainty that two draftsmen working on the same data set would *not* come up with exactly the same result. It is as well - even today - to indicate the location of the flight lines on any map presentation. These lines show where the contoured values can be given the greatest credibility; everywhere else on the map, values are obtained by interpolation, in other words by estimating what the results *might have been* had more observations been made. Once again, the need for adequate sampling in the field should be noted; the better the orginal sample distribution, the less the ambiguity in contouring.

Good quality contouring should observe most of the following features:

1). There are no sharp corners; contours are as smooth as the data will allow.

2). Contour lines are spaced parallel to each other and as far apart as possible consistent with the restrictions of the data; 'bunching' of contours in areas without observations implies high gradients that have not been measured.

3). Contours need *not* be perpendicular to traverses; strike directions are independent of the survey lines.

4). Economical *lengths* of contours are drawn;

5). 'Saddle points' require particular care;

6) Single-point anomalies should be questioned or omitted.

Hand contouring requires a great deal of skill and patience with both pencil and eraser. The result may be enhanced by hand colouring (shading, crayoning) of the intervals between contour lines - red for high areas, blue for lows, spectral colours between. This may be useful to help reveal the anomalies and the 'topography' of the anomalous field.

Hand contouring (with or without colouring) is often adequate for small data sets with only one Z value. If many Z values are involved, or if there is a large number of data points, it can become tedious. For large data sets, or for repeated Z values, computer contouring is now almost universally used. Advantages are:

1) Repeatable results (not dependent on interpolative skills of the draftsman).

2) Allows subsequent digital data processing of the map information and hence the production of a variety of maps from which the interpreter may choose the most appropriate.

3). Options to select various parameters in the contouring process and to attempt – even by trial-and-error, if necessary – various options for optimising the results.

6.4 Computer contouring.

Computer contouring follows a totally different path from hand contouring. All contour-drawing algorithms are basically very simple: they require Z values to be on a square *grid* or *raster*. Each square in that grid - i.e. a square having four data values, one in each corner - is then examined in turn. Along each of the four sides of the square, the intersection of contour lines is calculated by (usually) linear interpolation between the corner values (Figure 6.3). These intersection points are then joined by straight lines. Each line is, of course, continuous with the same value in the neighbouring square, so

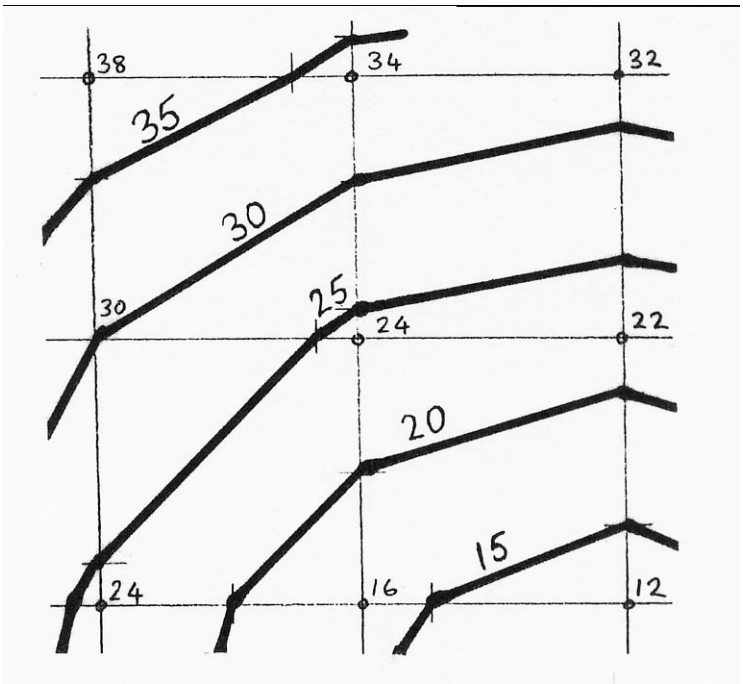

Figure 6.3 *An illustration of the interpolation of contour line intersections between grid nodes in the construction of a contour map using a typical computer algorithm.*

each contour line gets made up of simple straight-line segments crossing each square of the grid. Despite the angles in the lines at each grid side, contours look smooth to the eye as long as the straight line sections are short, compared with the thickness of the line. In practice, as long as the size of the grid cell is no larger than about 2.5 mm (1/10 inch), the contours appear smooth.

The key to successful computer contouring is the use of the profile point data as the basis for *interpolating* values onto a square grid with cells that will appear no bigger than 2.5 mm on the plotted map. To calculate the physical size of the cell (in metres on the ground) then requires only knowledge of the final plotted map scale required. For example: a scale of 1:1 000 000 indicates a cell-size of no more than 2500 m; for scale 1:50 000 the cell-size is 125 m and for 1:10 000, 25 m.

Note that this requirement already demands the creation of a large number of grid point values. A map 50 cm x 50 cm requires 200 points x 200 points (= 40 000 points) which have to be obtained by interpolation between the field values. This is regardless of map scale or the number of original observation points; it is only dependent on the physical size of the desired map.

Computer contouring can then be considered logically in three stages:

1) **Gridding**: Observational data are interpolated onto a grid;
2) **Contouring**: Gridded data are contoured to produce a 'plot file';
3) **Plotting**: The plot file is used to drive the physical plotting device.

The 'plot file' is simply a list of pen movements (lower pen, move pen, lift pen, etc) which may need to be interpreted differently by different plotting devices (screens, printers, plotters…). For computational efficiency, most plotting programs are now device-independent. In modern hardware systems only a device-specific *driver* need be installed to activate a particular type of peripheral plotter. Most printing devices working on A4 or A3 paper can be used to produce contour maps of high quality and larger maps can be produced on plotters that will work with paper up to a metre in width and produce plots of A0 size. Almost all these devices now work by managing a very fine array of dots on the printed page (whether in black-on-white or in colour). This emulates the production of images on a computer screen, the main difference being that large maps can only be viewed piecewise on a screen by panning and zooming since the number of dots or picture elements on the physical screen is far less than that required for displaying large maps at full resolution.

Similarly, the process of calculating intersections of contour lines with grid sides (Stage 2) is rather mechanical and can be carried out routinely by a computer algorithm. The main types of sophistication necessary are the abilities to use contour lines of various thicknesses for different contour line intervals (e.g. thin 10 nT, medium 50 nT, thick 250 nT), progressive deletion of contour lines in areas of high gradient, choice of interval between labels, even choice of lettering style on the contour labels an so on. As a result of the large demand for contouring programs to handle data of many types, the fruits of an enormous investment in software creation of this sort can be enjoyed at little cost and implemented on a personal computer (PC or laptop). There are still particular advantages to be found in using software designed specifically for geophysical applications, however.

Gridding, the start of the process - and hence the limit to what may be achieved in subsequent stages with the gridded results - is somewhat more involved conceptually and needs further consideration under the next sub-heading.

(a) Bi-directional gridding.

The choice of gridding method to be employed to create successfully the grid of values needed for the first stage of contouring depends in large part on the distribution of the data points in the data to be processed. In the case of airborne surveys we are invariably dealing with more-or-less parallel traverses of closely spaced observations.

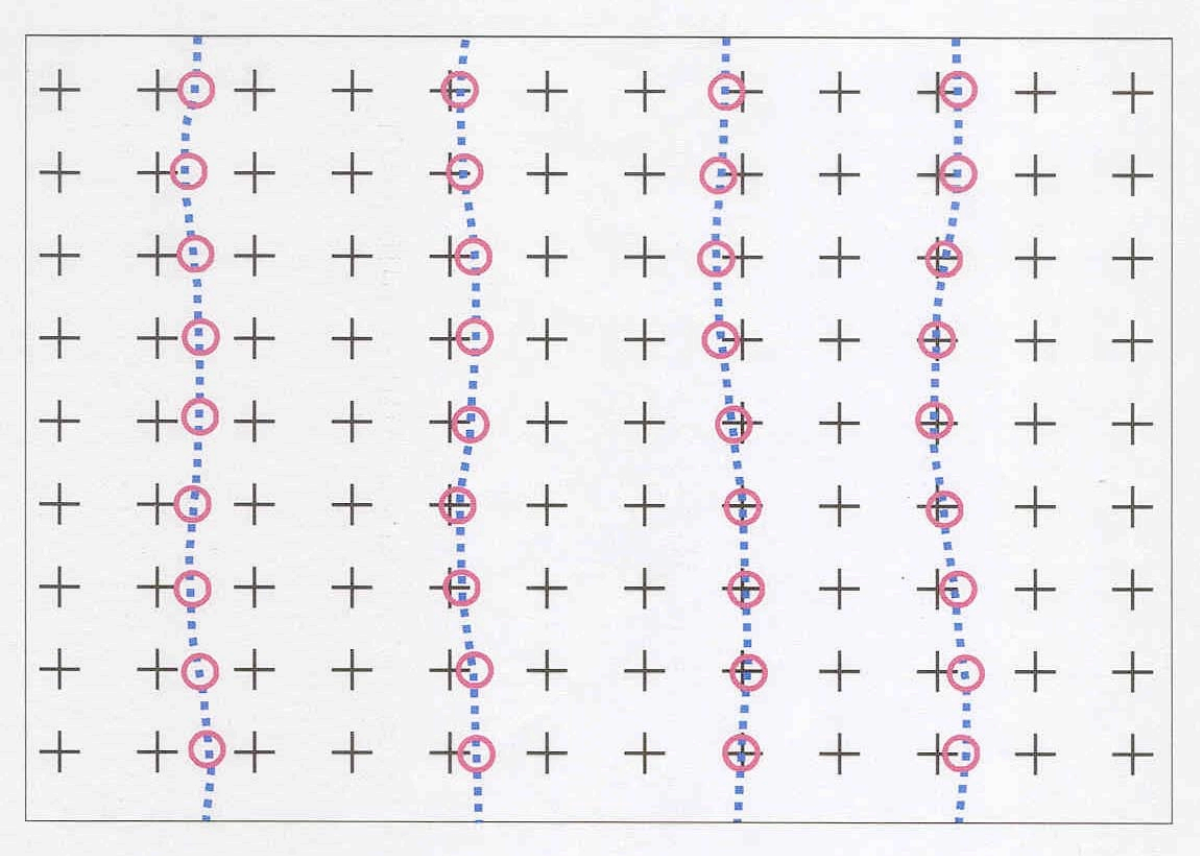

Figure 6.4 *The principle of bi-directional gridding, first interpolating between closely-spaced values along-line to derive a value at each grid row (circle) and then interpolating (splining) across-line to derive values at each grid node (cross).*

Here so called *bi-directional gridding* is often quite suitable and, being conceptually fairly simple, this is a good starting point.

The original data are provided in an XYZ file such as that shown in Figure 5.6. The program functions in two stages (Figure 6.4):

• Stage 1 - interpolation **along** flight-lines to give a z-value at each intersection of each flight line with a row of grid nodes.

• Stage 2 - interpolation **across** flight-lines (i.e. along each grid row) to give values at each grid node.

Choice of several means of interpolation, such as linear, Akima or cubic splining is often available at each stage. The optimum type of interpolation often differs between the two stages. For example, linear interpolation is often sufficient *along* flight lines where there are usually more samples in the original data than are required in the grid. *Across* lines, meanwhile, cubic or Akima splining usually performs better since the flight-line spacing is often wider than would be wished for adequate sampling of the anomalies and this type of interpolation often performs better where data points are rather widely spaced.

The importance of the risks of aliasing in this process should be clear. Consider the sampling interval along line, across line and in the final grid (Figure 6.4). The original along-line sampling interval will usually (by design) be more than is strictly necessary to record all the wavelengths present in the anomalies recorded at flight altitude. Reducing

the sampling to the grid spacing, i.e. increasing the size of the sampling interval, introduces the risk of aliasing which should be countered by first passing the down-line data through an anti-alias filter to remove short wavelengths (high wavenumbers) that could appear as longer wavelengths (lower wavenumbers) in the re-sampled data. All such filter parameters used should, of course, be carefully recorded. Across-line, on the other hand, the grid interval is less than the line spacing. The danger here is that the interpolation procedure will introduce spurious anomalies by inappropriate interpolation procedures; anomalies centred *between* flight lines are undesirable. Note, by the way, that a grid size equal to about one quarter to one fifth of the line spacing is quite typical and is normally a dimension adequate to reconstruct anomalies from outcropping sources reliably from the gridded data, i.e. ideally no more than about one half the terrain clearance.

The grid orientation *need not* be parallel and perpendicular to the original line direction. Because of the dangers of undersampling, the across-line splining is best done in the direction of the longest wavelength anomalies which is usually the geological strike direction. To benefit from this, some gridding algorithms allow the creation of a grid rotated with respect to the flight-lines. This will usually facilitate greater continuity of geological features between flight-lines on the gridded map, as illustrated in Figure 6.5.

Other possible methods of interpolation between scattered data points include:

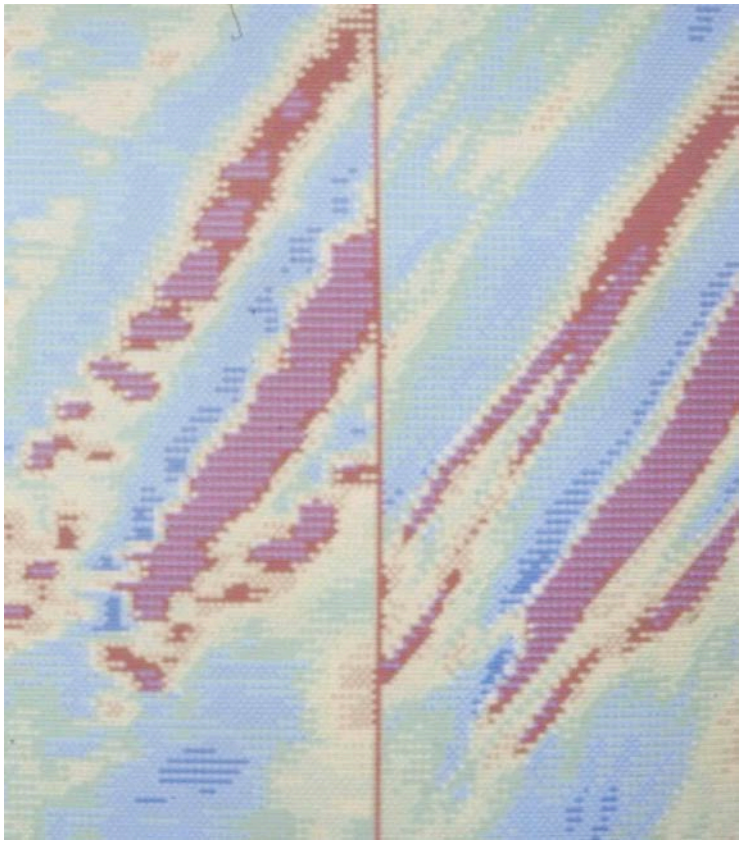

(a) (b)

Figure 6.5 *(a) A grid generated on an east-west orientation. (b) The same data gridded parallel and perpendicular to the NE-SW strike direction of the geology giving better continuity of features.*

(b). the method of least curvature (Briggs, 1974) used to grid randomly distributed data.

(c). 2D surface fitting, e.g. a cubic spline in two directions, minimum curvature, etc.

(d). Kriging - determine the statistically most probable value at each grid-node from the surrounding real data values.

(e) TIN gridding – A TIN is make up of irregularly distributed non-overlapping triangles. This method is often used to produce a representation of a geogaphic surface.

The more exhaustive the treatment of the data, the more accurate the resulting grid should be, but the more intensive in computer usage. Even simple algorithms such

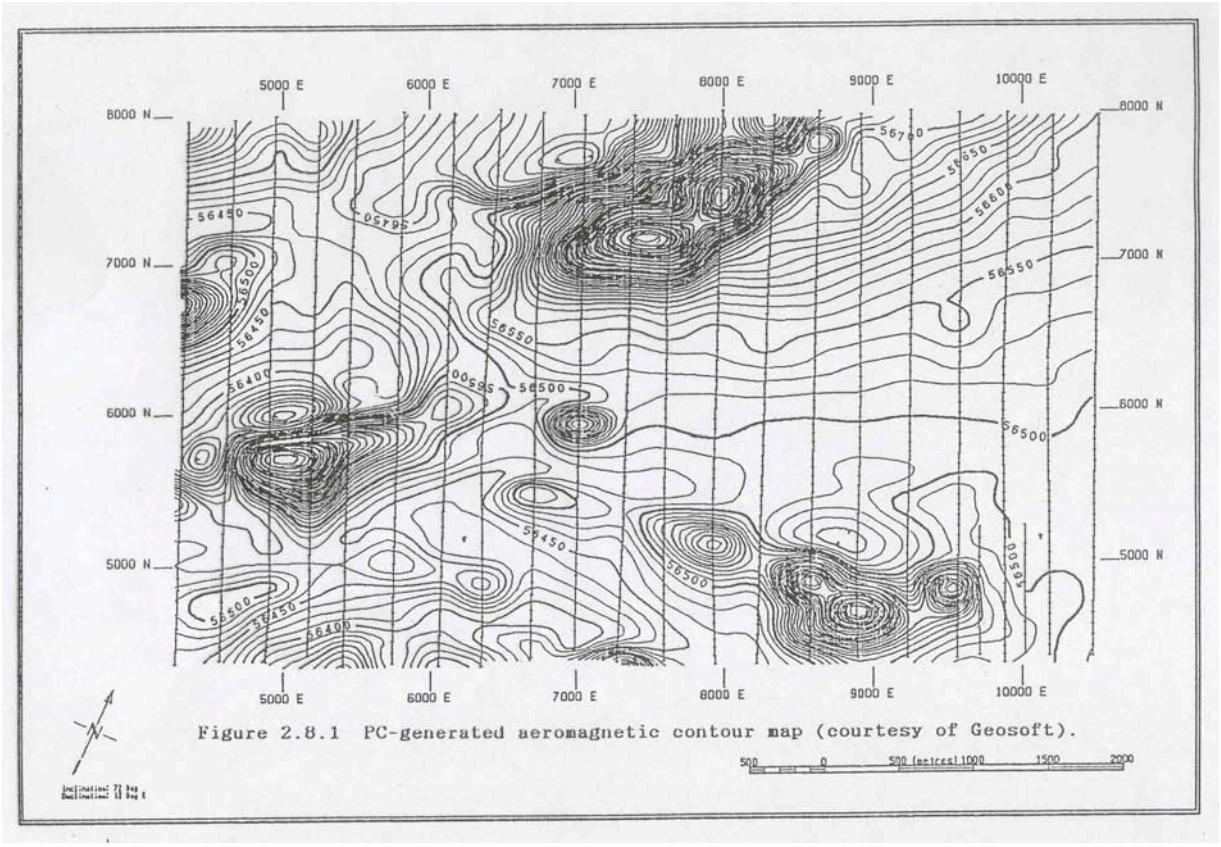

Figure 6.6 *An example of a computer-generated contour map using early PC software and hardware (original size A4).*

as bi-directional gridding often give adequate results in a very short time and are certainly sufficient for early examination of data sets. More elaborate treatment may be justified where maps of high quality, e.g. for publication, are to be generated. An example of the quality of contour map product easily achievable with early PC equipment and commercially available software is shown in Figure 6.6.

6.5 Alternative map presentations - Images.

Once a reliable grid has been created, several types of visual presentation are available, of which contouring is only perhaps the most traditional - and once familiar. Most of the alternative methods rely on using the grid or raster directly by displaying each grid value as a picture element or *pixel*, either on a screen display or on a paper copy. The only immediate consequence of using a pixel or image presentation is that, usually, a smaller grid-cell size needs to be used in grid creation; the 2.5 mm grid cell size recommended for the contour map is too coarse for pixel display. While this means gridding with more pixel values (halving the sample interval increases the number of cells in the grid by *four*), the power of even modest PCs and laptops is now adequate to deal with such data quantities without difficulty. A pixel or raster map measuring 50 cm x 50 cm would require 250 000 grid values at 1 mm resolution, about 6 times more than for the contour map of the same area. Existing gridding algorithms are quite adequate - only the required grid cell size need be changed.

The pixel or raster map display has now been quite familiar in presentations of satellite imagery for several decades and the type of technology developed in this field during the 1970s and early 1980s was adapted and adopted in the display of geophysical data very soon afterwards. The main types of display that have found popularity in aeromagnetic surveys are illustrated in Figure 6.7 and described below.

(a) Grey-scale raster map

In this presentation, each cell of the grid is ascribed a grey pixel, the brightness of which depends on the magnetic value at that grid point. The highest values might be white, the lowest black, (or vice versa) with often a total range of 256 grey levels, equivalent to the dynamic range of the 8-bit computer *word*. An example is shown in Figure 6.7(b). To distribute the range of Z values optimally over the available grey levels often requires the use of some type of *contrast stretching* (see, e.g., Drury, 1987). For example, all the pixels in the image may be divided equally among the available grey levels, defining, then, the boundary between grey levels at an arbitrary set of 'contour' intervals.

Subtle variations in grey-tone over long ranges are not detected by the human eye, but local contrasts *are* easily seen. For this reason, short-wavelength anomalies tend to stand out and there is an enhancement of anomalies attributable to near-surface geological features. At certain magnetic inclinations, the negative lobe of an anomaly which flanks a positive (or vice versa) often gives an optical '3D' effect, as through the magnetic anomaly field were an undulating white surface, illuminated from the side of anomalies that appear bright. (It should also be noted that human vision is easily deceived by these effects and the interpreter should take care to make sure that what he *thinks* he sees is actually what the data is trying to say, particularly since the choice of black or white for the 'high' values is often different for different image makers!)

(b) Shaded relief raster maps

Since we are trying to visualise data, and we have seen already that there are certain endemic properties of human eyesight that can be exploited to give more persuasive visualisations, we would do well to think of capitalising on these advantages. The shaded relief map is perhaps the most widely accepted of these..

The human eye can easily be deceived into seeing the magnetic variations as though they were physical topography. Even a simple positive anomaly which appears white (or black) in grey-scale can be made to appear to the eye as a hill by calculating the first horizontal derivative in the direction of a supposed illumination. A positive slope (i.e. a slope facing towards the 'sun' and given a light shade) then appears brighter than a negative slope (i.e. a slope facing away from the 'sun' and shaded dark). Let it be clear from the outset that we are using variations in the *intensity of illumination scattered from a white surface* to create this effect; shadows are not involved, though some have, confusingly, called their images 'shadowgrams'. This process can easily be carried out on a grid using a small filter operator (Section 6.7). The same data seen in Figure 6.7(a) is re-displayed in this way in Figure 6.7(c). Choice of azimuth and elevation of the illumination source can be made to highlight the desired features and suppress others. Some software allows the imaginary sun to be moved around the sky interactively and

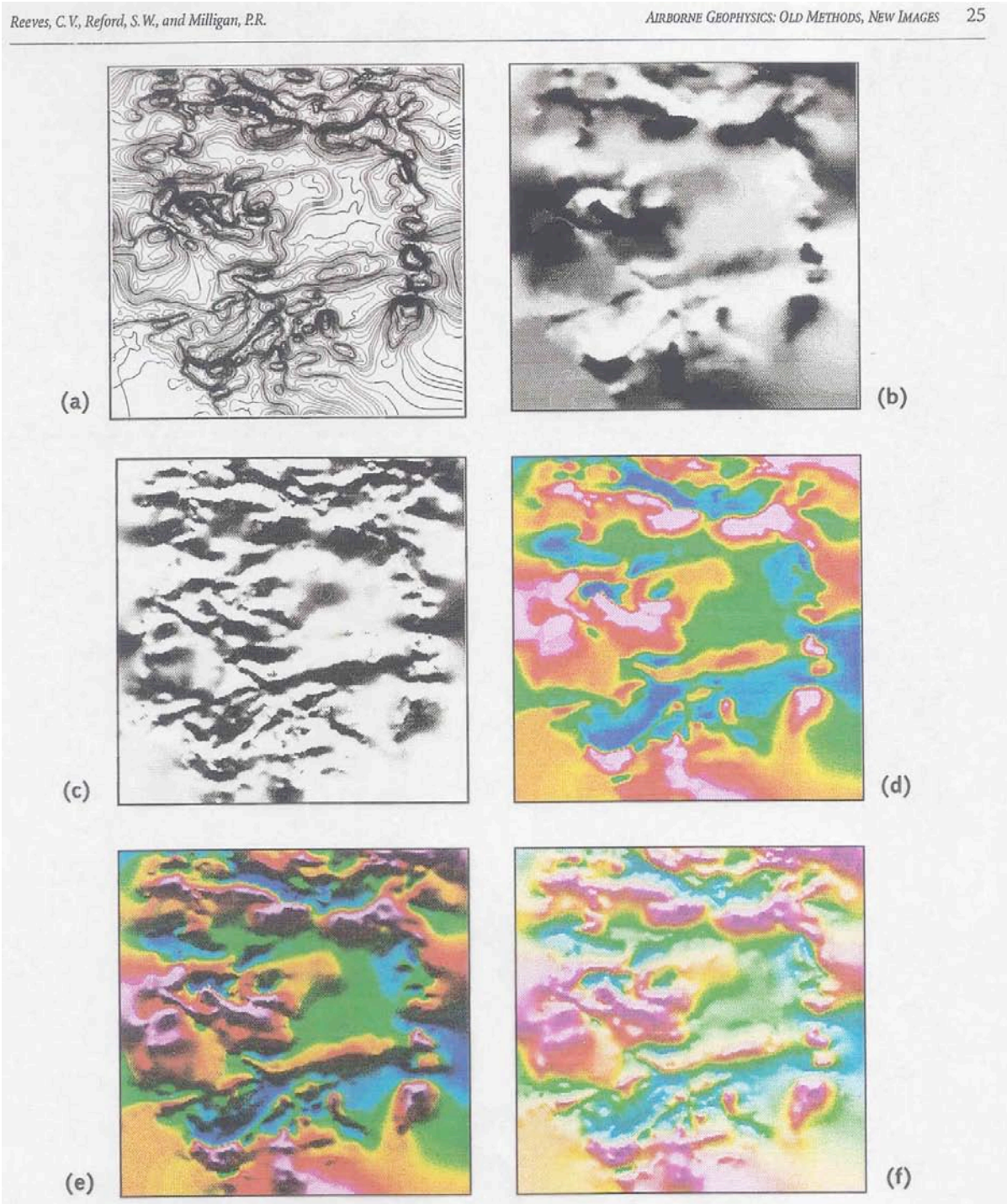

Figure 10: *The stages in the development of an optimum presentation of magnetic anomaly data as an image, as explained in the text. (a) Contour map; (b) grey-scale image (black = high, white = low); (c) shaded relief image with northerly illumination; (d) colour raster image (red = high; blue = low); (e) combined shaded relief and colour raster image (i.e., c + d); (f) shaded relief image using the HSV colour model.*

Figure 6.7 *The main types of image display of aeromagnetic data described in the text (from Reeves, Reford and Milligan, 1997).*

the interpreter can then recongise features that appear only at certain sun-angles that might otherwise be missed.

(c) Colour Raster Maps

Perhaps more popular in recent years is the colour raster map which, in effect, simulates the hand colouring of intervals between contour lines with a range of colours from the natural spectrum: red (high) through orange, yellow, green and blue (low). For each grid value, an appropriate colour shade is chosen (most probably again after some judicious contrast stretching across the available colour range) depending on its magnetic value, and plotted on the computer colour screen or on a paper map using an appropriate colour table.

Colour raster maps (a) look attractive to the eye, catching the attention of many new potential data users and (b) reveal at once the difference between 'highs' and 'lows' which may not be immediately obvious on a contour map. However, they do tend psychologically to emphasise long wavelength and high amplitude magnetic features which may not be the most closely related to the near-surface geology. The data of Figures 6.7(b) and (c) are presented in this format in Figure 6.7(d).

(d) Combined colour raster and shaded relief maps

Since the shaded relief style of presentation described in (b) above tends to emphasise the short wavelength features; it tends to be complementary to the colour raster which tends to emphasise the long wavelength features. In fact, the two styles may be combined by overprinting the grey of the shaded relief onto the colour map. One advantage is to reveal magnetic features that are of low amplitude and so become 'lost' within one colour level on the colour map. (For example, see Paterson & Reeves, 1985, Figures 8 and 12). This is illustrated in Figure 6.7(e).

Better than simply overprinting the grey scale onto the colour - which makes the whole image (on average) darker - is to modulate the colour intensity with the value of the horizontal derivative so that colours appear paler (less saturated) on bright slopes and 'blacker' on dark slopes. In effect, this involves a conversion from the three-dimensional Cartesian coordinate space of the red-green-blue additive colour system of screen displays (or the subtractive magenta-yellow-cyan colour system on paper) to a cylindrical coordinate space of hue, saturation and value (HSV, Figure 6.8) which is more attuned to human visual perception. (Milligan et al, 1992). In the HSV model, *hue* refers to the repetitive colour sequence of the natural colour wheel (red-yellow-green-cyan-blue-magenta-red), *value* is the intensity of the colour and *saturation* is the lack of white.

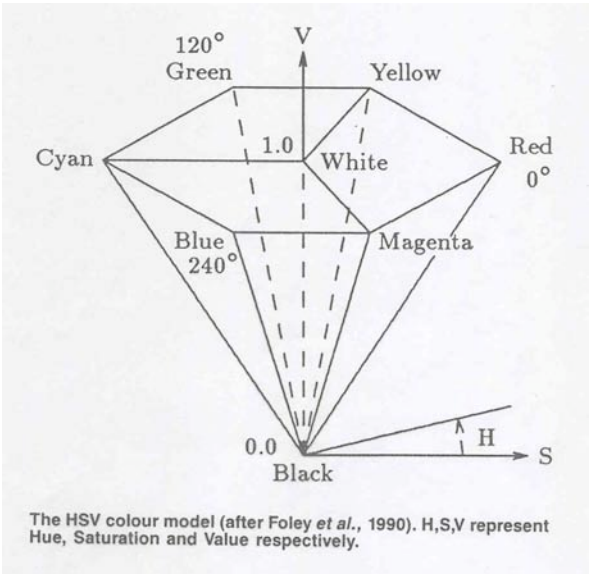

Figure 6.8 *The HSV colour model.*

Hue is measured around the vertical axis from 0 to 360°, saturation varies from 0 at the vertical axis radiating out to 1 on the surfaces of the hex-cone and value varies from black (0) through shades of grey

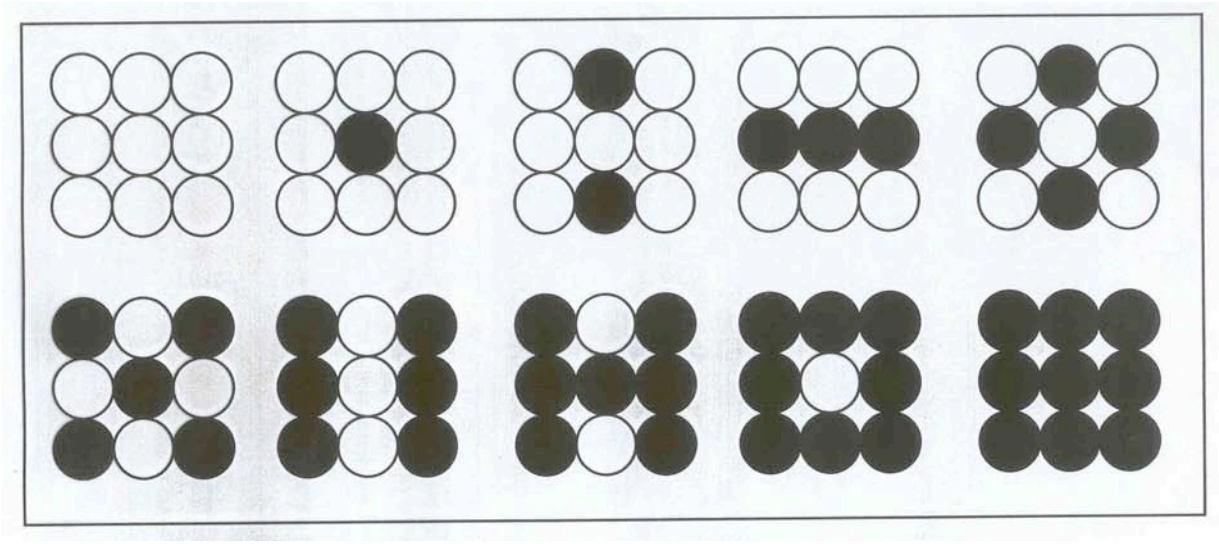

Figure 6.9 *A pixel made up of of a 3 x 3 dot pattern may be used to create ten grey levels.*

along the central axis to white (1) at the top. Thus, for a colour of constant hue and saturation, if its value is decreased it darkens towards black, and for a colour of constant hue and value, if its saturation is increased it becomes whiter. In normal perception of landscapes, the hue remains constant, while areas in direct sunlight are undersaturated and appear 'washed out'. At the same time, areas in relative shadow are low in value with less reflected light. To achieve this on a geophysical image, negative values of the horizontal gradient are used to decrease the colour value towards black and positive values of the gradient are used to reduce saturation towards the axis. Images prepared in this way look very bright and pleasing to the eye (e.g. Figure 6.7(f)).

While a large number of other map presentation types can be envisaged, the above list contains most of the most popular types at the time of writing. While this part of the art of geophysical data processing has undergone rapid development in recent years, styles approaching the optimum now appear to be established and it is largely a matter of choice from the user community as to which presentations become the most popular. Fashions, maybe, will change. As long as images are viewed only on a screen, users may, in any case, change quickly from one presentation to another according to need. When data have to be committed to paper and published, for example as a national map, then choices of presentation style will be far more critical.

6.6 Dithering patterns

While a photographic process may allow a very large number of different levels of grey to be portrayed, many printing processes on paper and computer screen allow only "1-bit logic" per dot position - in other words a dot may be only 'on' (black or white) of 'off' (white or black). Typical of this are the laser printers used with many PCs. The user will be aware that the quality achievable with such devices is defined by the number of 'dots-per-inch' set by the manufacturer. If we allocate each dot position to a value in our geophysical grid, then we can show only two levels at each dot position - black (= dot) or white (= no dot). The number of grey levels can be increased by grouping the fundamental dots into pixels each made up of a number of dots, e.g. nine dots arranged

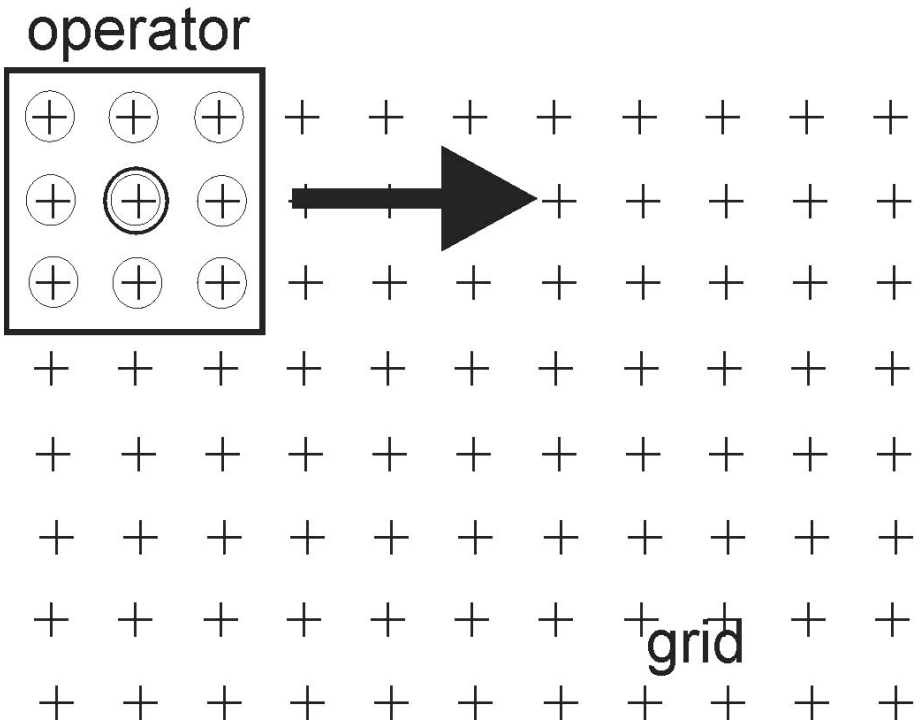

Figure 6.10 *The principle of convolution in the 2D space domain. An operator is moved sequentially by columns and rows over a grid stopping at each grid node in turn. At each stop, each of the grid values within the small circles is multiplied by the corresponding value in the operator to calculate a value that is assigned to a new grid at the position of the larger circle.*

in a 3 x 3 pixel. This allows the simulation of ten grey levels for the pixel by increasing the number of black dots within the pixel from 0 to 9 (Figure 6.9).

Assembling a number of similar pixels to cover a certain area produces a "dither pattern" over that area that simulates a grey level. Increasing the size of the pixel (e.g. to 4 dots by 4 dots) gives more grey levels (17) but reduces the resolution as the pixels themselves become larger and more visible. Pixels bigger than about 1 mm square are considered unattractive, requiring that the original dot raster must possess at least 4 dots per mm (for an acceptable 4x4 pixel) or about 100 dots per inch. Computer printers with resolutions of 300-1800 dots per inch are now commonplace and have become very popular for geophysical map-making applications and rival traditional photogprahic products for image quality. The principle has been very successfully applied to colour printers and plotters, making full colour maps at a chosen scale on normal paper available from a relatively inexpensive peripheral device. Here the number of magenta, yellow or cyan dots plotted within each pixel determines the colour that appears at that location. This approach also solves most of the problems of displaying aeromagnetic data as contours at such small scales as 1:1 000 000 where line thicknesses are too cumbersome and labelling is illegible. Other refinements to the dithering process, such as the avoidance of a dark colour dot being overprinted on a bright one (making the overall image less vivid) and the use of white spaces (unfilled pixels) to achieve pastel colours can only be mentioned here in passing. Since geophysicists are not alone in needing this type of presentation for their work, a vast amount of technical expertise is available quite outside the scope of these notes.

6.7 Digital filtering of gridded data in the space domain

So far we have demonstrated the principal methods of *visualisation* of digital data as maps and images on the screen and in hard copy. In doing so we have also introduced at least two methods of *enhancement*, namely contrast stretching and horizontal derivative calculation. One of the great advantages of working with equally-spaced data points (or with profile data interpolated to an equal spacing) is the ability to apply ***digital filters*** that may be ***convolved*** with the data grid and so effect various types of digital *data processing.* As with profile data, gridded data may also be processed by convolution with space-domain filters (Figure 6.10). In the case of gridded data, the filter operators themselves must also be two-dimensional arrays of values which are scanned along every row of data. While centred over each data point in turn, a calculation is performed in which all the data points covered by the operator are involved and a new value is written to the corresponding position of the output grid. It can perhaps be appreciated already that the number of arithmetic operations is quite high but this is quite feasible for PC applications even over data sets typical of airborne geophysical surveys. Some of the most familiar examples are given under the following headings.

(a) Smoothing.

The two-dimensional equivalent of the 3-point smoothing operator is a 3 x 3 array of filter values, each having a weight of 1/9. The effect of such a filter is to average the value at a given grid node together with the values at its eight nearest neighbours to give a new value at the centre point (Figure 6.11). The operator is moved row-by-row over the whole grid to produce a new grid of smoothed values. If necessary, the operator may be used repeatedly (i.e. applied again to the output grid of the first operation) for further smoothing.

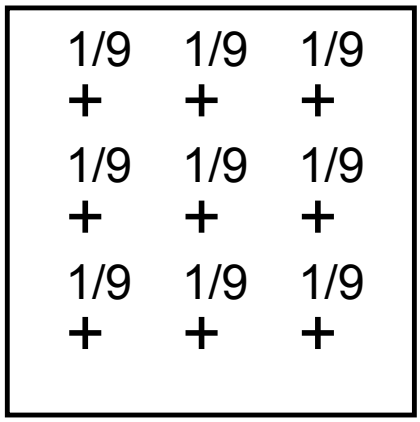

Figure 6.11 *9-point two-dimensional smoothing operator.*

(b) First horizontal derivative.

On a profile, the first horizontal derivative may be calculated only in the forward (or in the reverse) direction along the profile itself. With gridded data, the derivative may be computed in any azimuth from 0 to 360°. The first horizontal derivative in the *south-to-north* (y-) direction df/dy (= A) may be estimated by the output of a filter operator such as that shown in Figure 6.12(a). Note that it is convenient, in order to avoid calculating

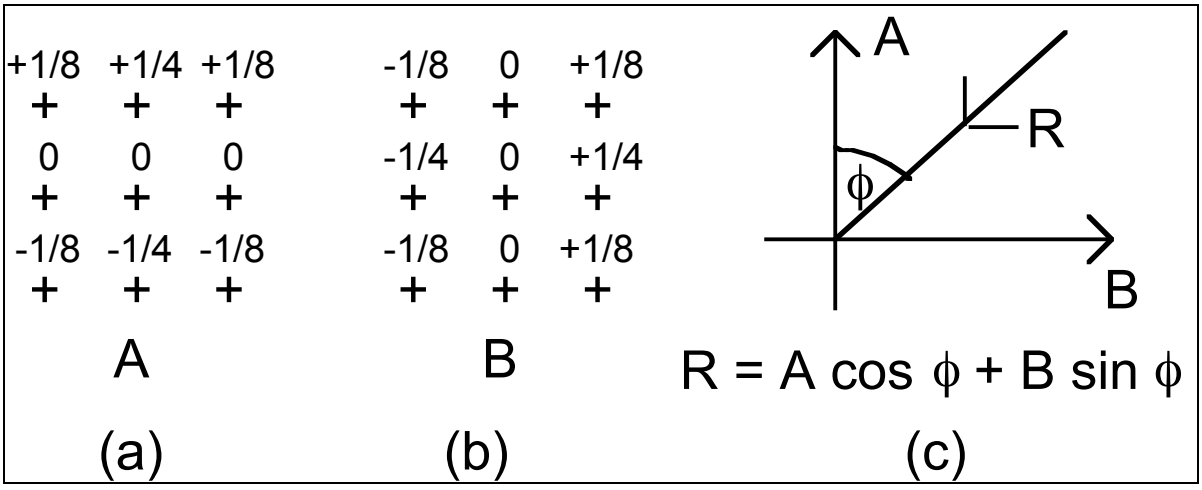

Figure 6.12 *First horizontal derivative filtering on gridded data.*

values at points other than grid nodes, to calculate the gradient over *two* grid spacings; the operator has zero weights in the middle east-west row. The distance between the samples being two grid units is taken into account by taking only *one half* of the actual values in the top and bottom rows (1/8 + 1/4 + 1/8 = 1/2). Note also that, instead of calculating the gradient using just one N-S column of three data points, the result is averaged over three such columns, but the centre column is given as much weight as the sum of the two outside columns. The numerical values obtained should be rationalised by division of the result by the physical dimension of the grid cell (metres) to give the result in (e.g.) nT/m.

Similarly, in the west-to-east (x-) direction df/dx (= B) may be estimated using the operator shown in Figure 6.12(b) which has similar properties to the above.

Operators A or B give the derivatives in the y- and x-directions respectively. The first horizontal derivative in any other azimuth direction may be calculated as (A cos ϕ + B sin ϕ) with appropriate regard to the sign of the cosines and sines as ϕ goes from 0 to 360° (Figure 6.12(c)).

This result is similar to that obtained by using an artificial illumination process to produce a shaded relief image or 'hill shading' from any desired angle.

(c) Second vertical derivative.

For some applications, the second vertical derivative has the advantage of being non-directional. If we use the Laplacian potential field property that the sum of the second derivatives in the three orthogonal directions equals zero, then the sum of the estimates of the north-south and east-west second *horizontal* derivatives will equal (-1) x (the second *vertical* derivative). By analogy with the second horizontal derivative operator for profile data, an estimate of d^2f/dx^2 is given by the operator in Figure 6.13(a) and for d^2f/dy^2 by that in Figure 6.13(b). Their (negative) sum is shown in Figure 6.13(c). An equally valid estimate can be made using the NW, NE, SE and SW corners of the square (the second-nearest neighbours), provided that allowance is made for the square of the greater length of the diagonals ($(\sqrt{2})^2$ instead of 1^2) as shown in Figure 6.13(d). The two estimates may then be averaged by combining the two operators as one, as

shown in Figure 6.13(e) and the result expressed as (e.g.) nT/m^2 by division of the result by the square of the true size of the grid unit.

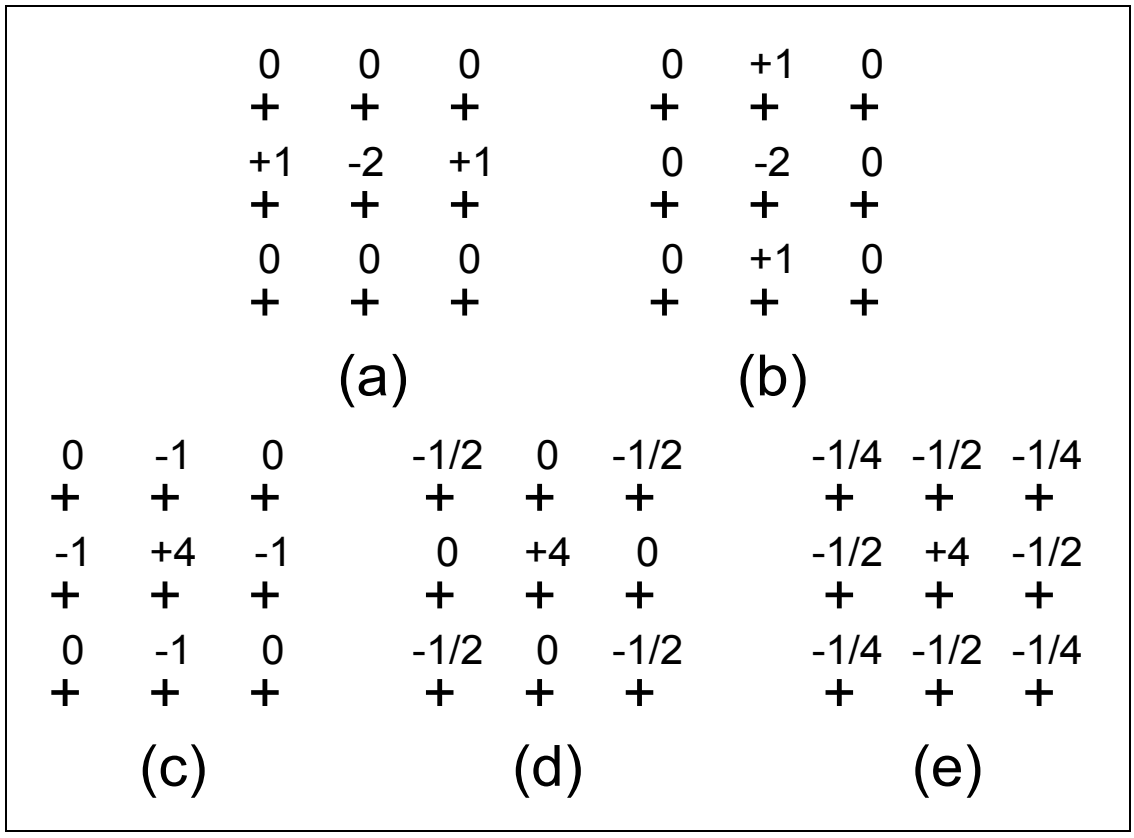

Figure 6.13 *Second vertical derivative operators for gridded data as explained in the text.*

Note the similarity between this approach and the ideas put forward in pre-digital days of computing second vertical derivatives from contour maps (e.g. Rosenbach, 1955) by comparing the central value with the average of values on a surrounding circle of given radius to estimate the second vertical derivative at the central point. In the case shown in Figure 6.13(e), the four points on a circle of radius a (= the grid spacing) is given the same weight as the four points lying on the circle or radius √2a, given the correction for the square of the larger radius of the second circle. All other circles are weighted as zero.

(d) Directional filtering.

In some cases, it may be desirable to suppress (i.e smooth) short wavelength variations in one direction but not in the direction at right angles. With airborne surveys, this can become necessary when flight lines have been poorly levelled together. This may be done by using a Hanning (‘elliptical') filter which has a long dimension across-track (i.e.

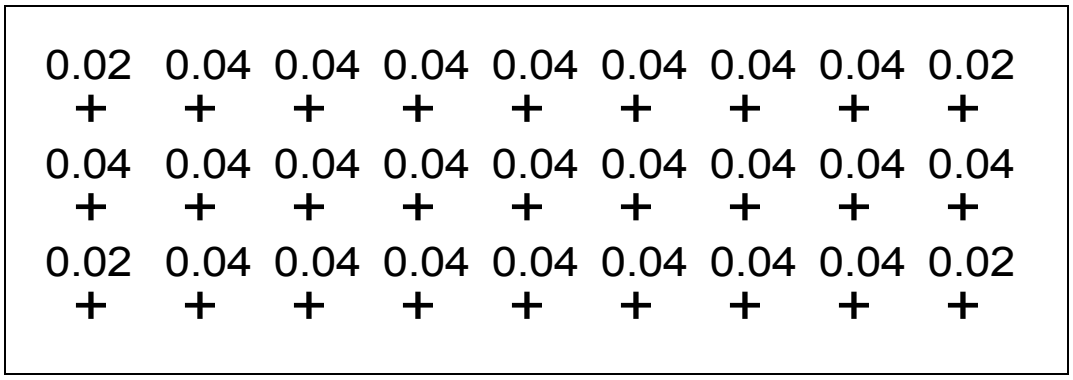

Figure 6.14 *A directional filtering operator*

averaging the values on several adjacent flight lines) but only a short dimension along track (to minimise smoothing of individual anomalies). Such a filter is illustrated in Figure 6.14 where it is seen that the smoothing criterion is satisfied by all values adding to 1.0. The fact that poor levelling tends to lead to values on alternate flight lines being either too high or too low makes the unfiltered anomaly field appear *corrugated* or to show a *herringbone* effect. The filtering process is then known as *de-corrugation* and can be quite successful, provided there is not too much real information (signal) across track having a wavelength less than about five flight line spacings. The effect is similar described in Section 5.2 for microlevelling but the method is less sophisticated.

Many other possible filters may be designed in the space domain, but usually the most useful ones are those with an output that approximates to a physically meaningful quantity. Depending on the results obtained – and experience will show that some filters are unsatisfactory in some cases when, for example, the noise becomes enhanced so as to dominate over the signal – each of the output grids may be imaged or visualised using any of the methods described earlier in this section. This gives gives rise to an almost limitless number of possible maps from any one dataset. In practice, however, the user should be critical as to how many of these maps are essentially different and can make a useful contribution to the intepretation process.

In the next section we shall see that an even greater range of potentially useful enhancements can be achieved by using processes in the wavenumber domain.

*** *** ***

7.

Processing of Grids in the Wavenumber Domain

7.1 More visualisation options – the wavenumber domain

Figure 7.1 illustrates graphically the routes by which digital gridded data may be brought to the human eye, either directly from the grid, via the space-domain filtering processes described in Section 6 and via processing in the wavenumber domain – sometimes called the spatial-frequency or Fourier domain. It is this third option that is described in this section.

Any function in the space domain may be represented fully in the wavenumber domain as spectra of wavenumber and phase. These spectra show the power or energy content of the data plotted against the different wavelengths present in the anomaly field. Elements with low wavenumber, near-DC components, appear in the early part of the spectrum (Wavenumber is the inverse of wavelength, so features of near-infinite wavelength have wavenumbers approaching zero). At higher wavenumbers, energy of shorter wavelengths is represented, eventually reaching regions that are below the Nyquist frequency imposed by the gird cell size or the orginal sampling pattern in the survey.

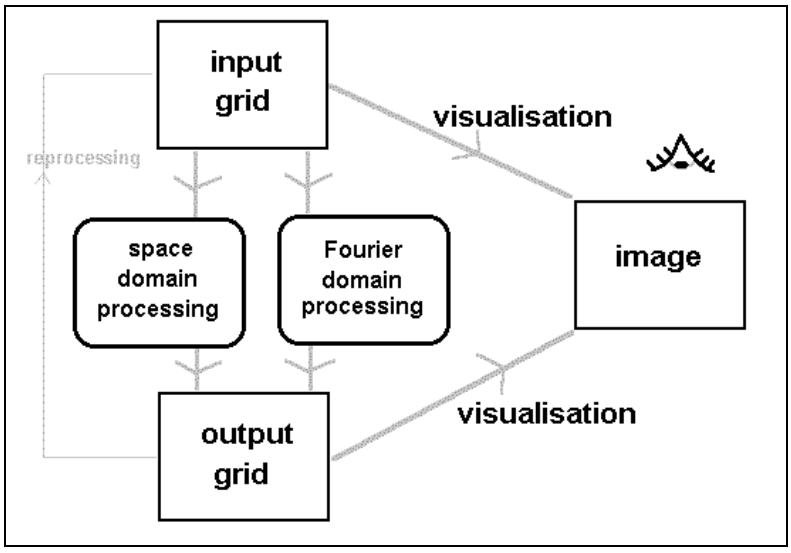

Figure 9.1 *The routes to images, either directly from the original grid or via digital processing in either space-domain or the Fourier domain, more correctly known as the wavenumber or spatial frequency domain.*

The link between the space domain and the wavenumber domain is the ***Fourier transform***. Forward transformation takes us from the space domain to the wavenumber domain and reverse transformation from the wavenumber domain back to the space domain, without loss of information. Fast Fourier transformation (FFT) routines are available as computer software packages, but why would we want to make use of them?

In Section 6.7 some of the many filtering processes possible in the space domain were introduced. It was also seen that, as the filter operators become more complex, the method becomes cumbersome. It was also mentioned that output grids are most useful when they approximate to physically meaningful functions, such as with the gradient of the field and shaded relief images. In the wavenumber domain, many physically meaningful functions can be calculated analytically. It is also the case that the laborious process of convolution is equivalent to simple multiplication in the wavenumber domain. It is therefore quite efficient to pay the penalty of making the forward and reverse FFT operations to secure the advantages of a wide range of easy processes in the wavenumber domain (Figure 7.2). The process breaks down into these three stages (Bhattacharyya, 1965):

•1. Transformation of the grid to two-dimensional spectra in the wavenumber domain;
•2. Multiplication of the spectrum with a wavenumber domain filter and
•3. Reverse transformation of the filtered spectrum back to the space domain

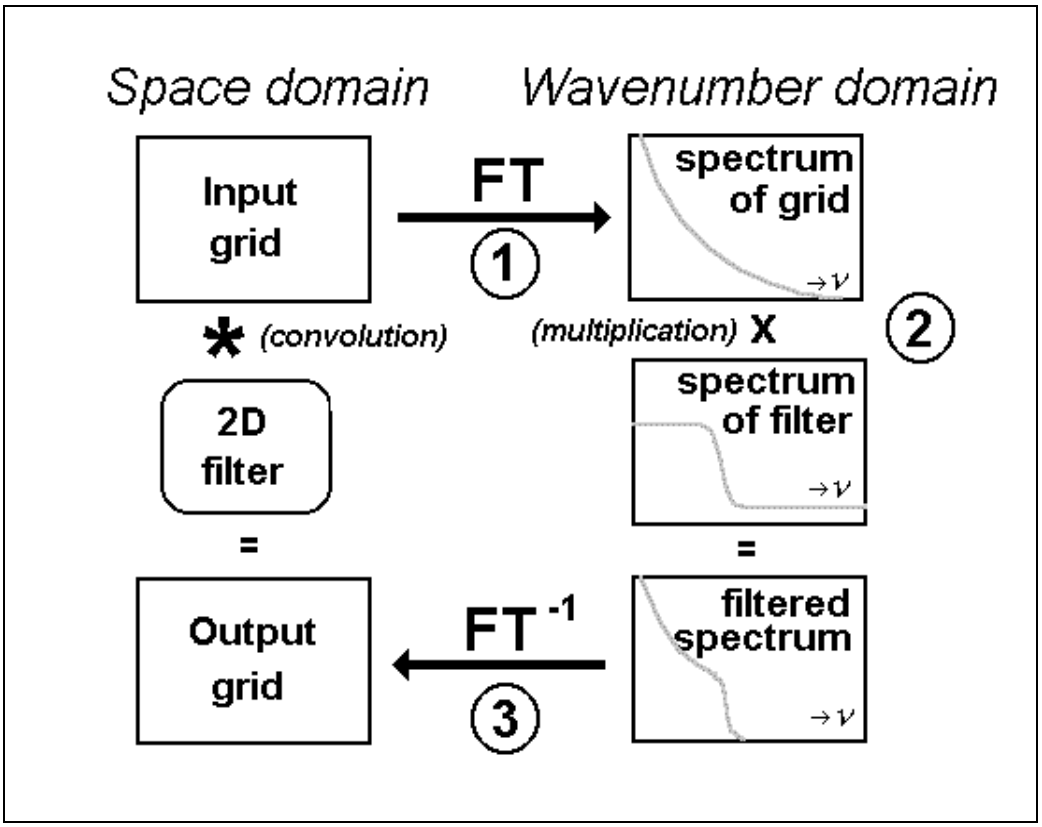

Figure 7.2 *A three stage process using multiplication in the wavenumber domain can be more efficient than convolution in the space domain.*

As a further advantage, calculation of the 2D spectrum of a given data set allows decisions to be made based on examination of the spectra and making decisions based on what is seen there, for example whether or not the wavelengths we wish to separate are sufficiently different to allow hope of real success. In a logical approach, then, systematic processing begins after stage 1 with *spectral analysis*. Ideally, the spectrum is plotted as a contour or raster map of power values in the u,v plane (u = wavenumber in the x direction, v = wavenumber in the y direction). However, for ease of presentation, the two-dimensional power spectrum is often produced as a radially-averaged plot of energy against wavenumber.

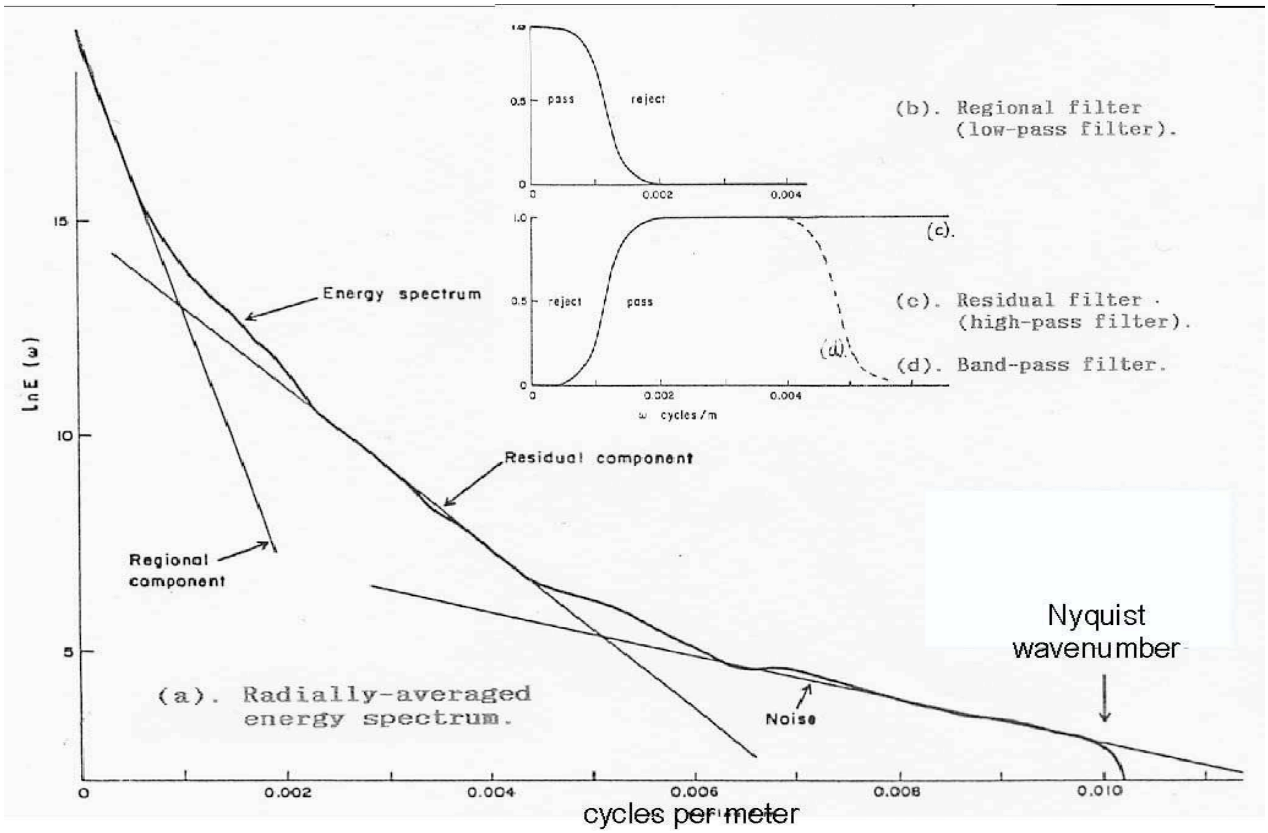

Figure 7.3 *The energy spectrum in the wavenumber domain, spectral analysis and the design of filters for regional-residual separation.*

7.2 Spectral analysis

A typical plot of a radially-averaged power spectrum is shown in Figure 7.3. Note the use of a natural logarithmic scale on the power (= amplitude squared) axis. In general it is found that potential field anomalies analysed in this way display something approaching a natural power-law spectrum such that much energy comes from large, deep sources (at low wavenumbers) and relatively little (orders of magnitude less) from small, shallow ones (high wavenumbers) with an approximately exponential decay with wavenumber. Beyond the Nyquist wavenumber the spectrum is meaningless (any energy originally here will be aliased or folded-back into lower wavenumbers), but usually noise predominates at wavenumbers approaching the Nyquist wavenumber if a sound sampling regime was established for the survey.

(a). Regional-residual separation

It was shown by Spector and Grant (1970) that when a statistical population of magnetic or gravity sources exists at around a specific source depth, then the expression of those sources on a plot of the natural logarithm of energy against wavenumber is a straight line having a slope of $-4\pi h$. It follows that where a spectrum shows a number of straight-line branches, statistical populations of sources exist at a number of depths. In Figure 7.3(a)

three such branches can be recognised and the spectrum divided into parts labelled *regional component*, *residual component* and *noise*.

To separate the regional field, a regional (or *low pass*) filter could be multiplied point-by-point with the spectrum (Figure 7.3(b)) where low wavenumbers are passed, high wavenumbers rejected, with an approximately Gaussian *roll-off* between them to minimise *ringing* (also known as Gibb's phenomena) when the output is reverse-transformed to the space domain.

The complement of the low-pass regional filter is the *high pass* or *residual* filter (Figure 7.3(c)). The residual grid may be obtained either by applying such a filter in the wavenumber domain, or by subtracting the regional field from the original data grid.

In practical cases, the residual filter would usually be designed to roll-off again at wavenumbers corresponding to noise so that noise could be eliminated simultaneously. The filter then becomes a *band-pass* filter (Figure 7.3(d)), retaining only information from a range of wavenumbers considered important for the study of the residual anomalies at hand. In general, the better the separation between straight-line branches of the radially-averaged power spectrum, the more successful the eventual separation into regional and residual components is likely to be. However, this separation is never perfect since sources at any depth tend to contribute to *all* smaller wavenumbers in the spectrum to a greater or lesser extent. An example of successful separation of a residual component is given in Figure 7.4.

7.3 Other processes in the wavenumber domain

Since the aim of map processing is principally to aid the interpretation of the field data, we are at liberty to use any type of process which meets this criterion; mathematical rigour in the perfect separation of wavenumbers is not a pre-requisite. However, it should clear that only those derived (processed) maps to which some physical meaning can be ascribed are useful in practice. In addition to regional-residual separation described above, the following wavenumber domain processes fall into this category and are therefore used most commonly. Some examples of output are given in Figure 7.5.

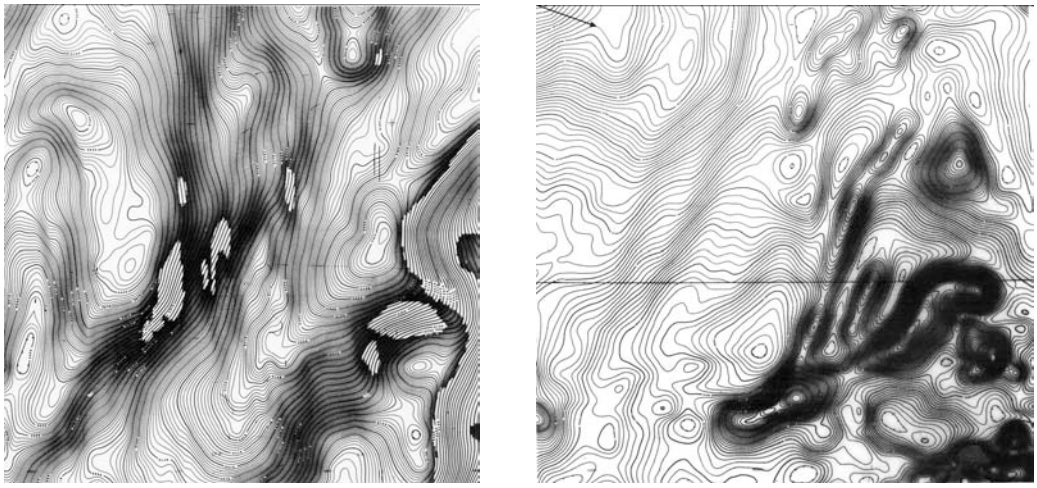

Figure 7.4 Regional-residual separation. (a) original anomaly field; (b) residual component.

(a). Vertical derivatives

Computation of the first vertical derivative in an aeromagnetic survey is equivalent to observing the vertical gradient directly with a magnetic gradiometer and has the same advantages, namely enhancing shallow sources, suppressing deeper ones, and giving a better resolution of closely-spaced sources (Section 3.8). An example is given in Figure 7.5(c). Second, third and higher order vertical derivatives may also be computed to pursue this effect further, but usually the noise in the data becomes more prominent than the signal at above the second vertical derivative. The equation of the wavenumber domain filter to produce *nth derivative* is:

$$F(\omega) = \omega^n$$

Horizontal derivatives may also be calculated, noting that a direction (azimuth) need to be chosen, giving another element of choice for optimum presentation. Alternatively, the *maximum* horizontal gradient at each grid point can be displayed, regardless of direction.

(b). Upward and Downward Continuation

A potential field measured on a given observation plane at a constant height can be recalculated as though the observations were made on a different plane, either higher (upward continuation) or lower (downward continuation). The equation of the wavenumber domain filter to produce *upward* continuation is simply:

$$F(\omega) = e^{-h\omega}$$

where is h is the continuation height. This function decays steadily with increasing wavenumber, attenuating the higher wavenumbers more severely, thus producing a map in which the more regional features predominate.

The equation of the wavenumber domain filter to produce *downward* continuation is

$$F(\omega) = e^{h\omega}$$

This is a curve which is zero at zero wavenumber and increases exponentially at higher wavenumbers, thus emphasising the effect of shallow sources - and noise! Noise removal is thus an essential first step before downward continuation, and continuation depths should not exceed real source depths. Some careful experimentation is usually necessary to obtain acceptable results. (Example: Figure 7.5(d)).

(c) Directional filtering

The foregoing filters are completely expressed in their radially averaged representation since they are radially symmetric about the origin of a two-dimensional plot of wavenumbers in the x and y directions (the u,v plane). Directional filters are used to selectively remove anomalies or noise (e.g. corrugation) in a certain strike direction and their 2D response has a notch which reduces to zero amplitude at a certain range of wavenumbers and of a certain azimuth. A filter with a zero notch in the direction of the flight lines might serve as another way of moving line-related noise such as poor levelling. (Example: Figure 7.5(f))

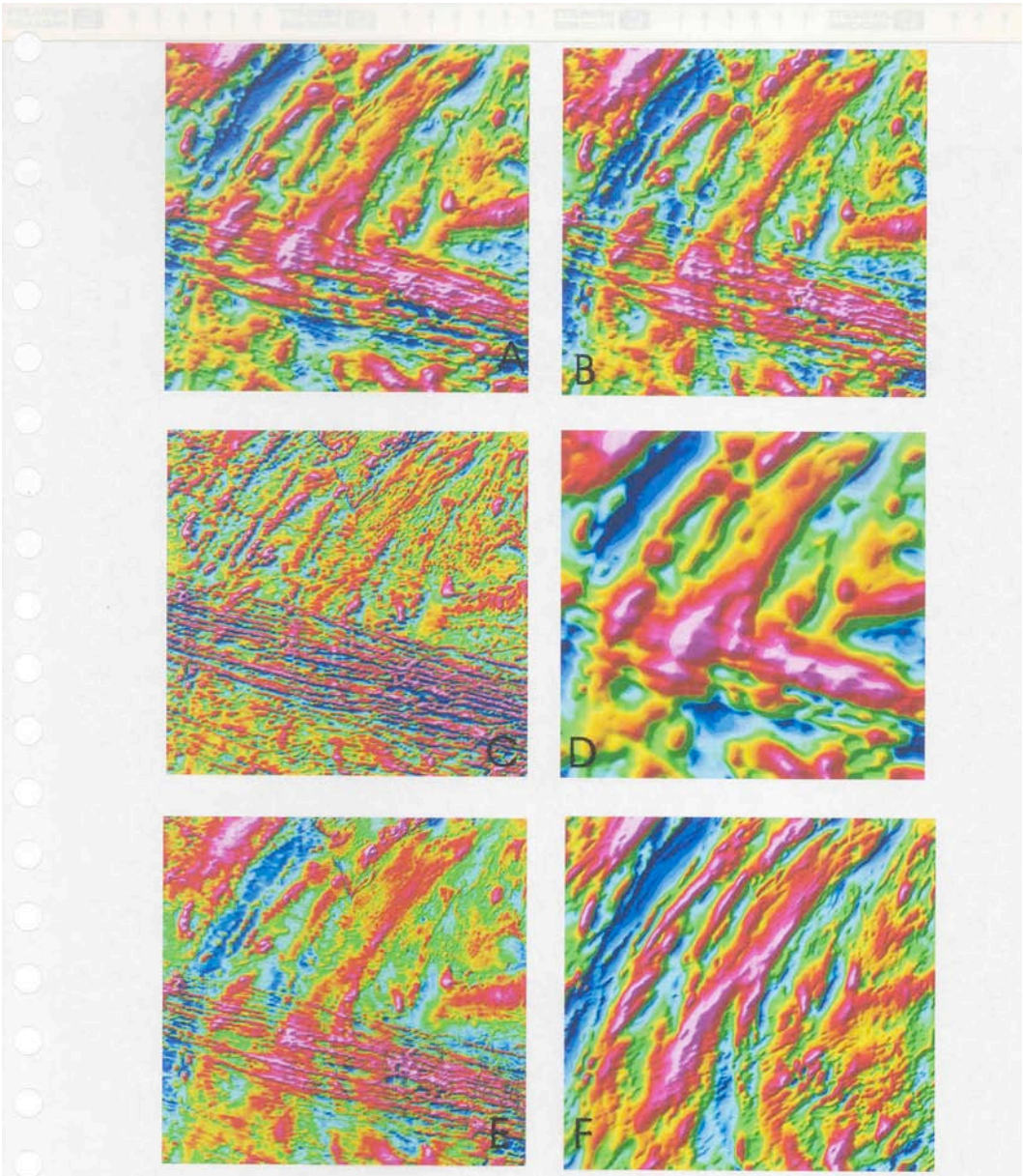

Figure 5.4
Examples of data processing in the Fourier domain. A: Original data including parts of Botswana and Zimbabwe. B: Reduction to pole. C: First vertical derivative. D: Upward continued by 4000 m. E: Susceptibility map. F: Directional filtering. The area consists of Precambrian rocks hidden by cover of Kalahari sand and intruded by pre-Kalahari dykes in a swarm trending N110degE. The magnetic inclination is minus 55 deg (southern hemisphere). The arcuate NE-NW to N-S trend of the Precambrian geology is clear when the dyke trend is removed by directional filtering (F). Data courtesy of AMMP.

(d) Reduction to the pole

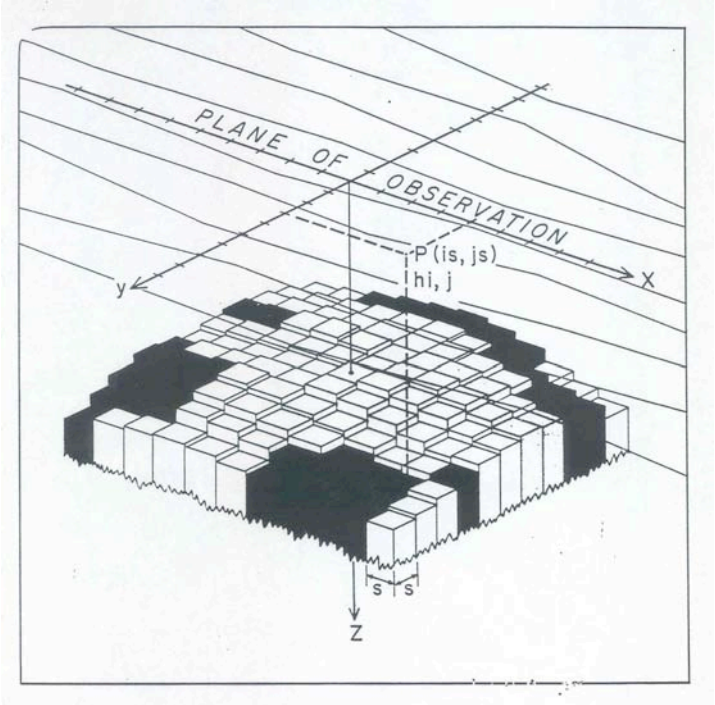

Figure 7.6 *Susceptibility mapping sets out to determine the equivalent susceptibility of each vertical prism of dimension equal to the original data grid. Unlike in this illustration, it is usually assumed that the top of each grid cell is at the same level; it is seldom possible to model magnetic anomalies by topography on the basement surface using reasonable magnetic susceptibility contrasts (from Grant, 1973).*

By implementation of filters on both the amplitude and phase spectra of the original grid, the shapes of magnetic anomalies may be simplified so that they appear like the positive anomalies located directly above the source expected for inducely magnetised bodies at the magnetic poles (I = ±90°). This will fail partially where remanent magnetisation is present and theoretical difficulties are encountered when trying to reduce-to-the-pole a grid of observations at very low magnetic inclinations (see Section 9). Nevertheless, where it can be successfully carried out, reduction-to-the-pole maps can make the task of delineating magnetic sources considerably more straightforward. Note that this approach is confined to magnetic anomalies; gravity anomalies d not suffer at low latitudes since the gravity field is vertical everywhere. (Example: Figure 7.5(b)).

(e) Susceptibility Mapping

Potentially a very powerful method for converting the continuously varying magnetic anomaly field into a function more closely representing the discontinuous geology of the source rocks is susceptibility mapping (Grant, 1973). The subsurface is assumed to be made up of a large number of square-topped vertical prisms, one per cell of the original data grid, extending to infinite depth (Figure 7.6). The magnetic susceptibility of each of these prisms is calculated such that the combined magnetic effect of all prisms is the originally observed magnetic anomaly field. In practice, this type of inverse modelling is achieved in three steps carried out in the wavenumber domain:

1. Reduction to the pole;
2. Downward continuation to the level of the top surface of all the prisms;
3. Correction of the spectrum for the effect of the spectrum of the anomaly due to a prism (Bhattacharyya, 1966).

Only information on susceptibility should then be left in the spectrum. Prior removal of the IGRF or a similar trend surface is a pre-requisite. The method is powerful in areas of steeply dipping geology such as is typical of Precambrian terrane. (Example: Figure 7.5(e)).

Note that the method assumes only induced magnetisation and that only positive magnetic susceptibilities are physically meaningful. The fact that areas of negative susceptibility

often appear in susceptibility maps is an indication that the 'only induced magnetisation' assumption is breaking down – or that there are bodies present that are not perfectly vertical.

[For gravity data, a similar procedure - without the need for pole reduction - may be carried out to produce a pseudo-density map. Theory demands that the depth of both the top *and the bottom* of the prisms is supplied by the user in this case. Curiously, for agreement of the results of most such studies in Precambrian areas with observed surface rock densities, the bases of the prisms need to be set at a depth of 6-7 km (e.g., Gupta and Grant, 198?). Whether or not this indicates true density homogeniety at greater crustal depths is an interesting speculation.]

It should be noted, finally, that the output of all these wavenumber domain processes, after reverse transformation to the space domain, is a new grid in the space domain. As with original grids and grids processed in the space domain, the output grid can, in principle, be displayed using any of the many visualisation techniques - contour maps, raster maps in colour or grey-scale, etc., on screen or on paper - described in Section 6 (see Figure 7.1). The range of possibilities is clearly very large, while substantial differences between maps of seemingly quite different processing sequences can be quite minor. While it is good to prepare a small number of carefully produced maps and images that will serve the purposes of the interpretation process – and perhaps to help convince others of the geological detail contained in the survey data – the effective interpreter needs to make a judicious choice of output forms. Bringing the interpretation process to a finite and manageable conclusion is often *not* well-served by the availability of too many - even attractive - map or image products.

7.4 Continental and global magnetic anomaly maps

While images of data arising from any one individual survey can be made to appear very attractive using the above methods, a particular problem arises when data from more than one survey covers the area of interest. This has been of particular importance in recent years as it has become widely realised that the coverage of many regions by existing surveys nears completion, but to view the results in a regional sense necessitates the simultaneous display of data from *all* these surveys. While, as we have seen, a colour or shaded relief image may offer the most effective way of displaying data covering a large area, image-style presentation accentuates a particular problem at the boundaries of individual surveys, namely that there is usually a 'step' in the background level of the results from one survey to another. This linking and levelling problem was discussed in Section 5.5.

These difficulties notwithstanding, major progress has been made in the 1990s and more recently in compiling magnetic anomaly images of whole continents. The first was published for North America (without Mexico) in 1997. One of the more satisfactory results appeared for Australia with several editions appearing in the early 1990s (Figure 7.7). This consists of over 10 million line-km of data acquired over almost 50 years in the airborne geophysical programmes of the national geoscience authority (BMR, later AGSO and now Geoscience Australia). The image is composed of data from almost 1000 separate surveys. The work undertaken to display the as yet incomplete coverage for Africa is described by Barritt (1993).

Recent years have also seen great strides in the acquisition of reliable magnetic anomaly patterns from earth-orbiting satellites. Arguably the most successful of these is the CHAMP satellite designed and operated by German teams. It is orbiting at an elevation of 450 km, but this will reduce with time to 350 km. Clearly, such altitude does not permit the resolution of geological features on the scale of individual map sheets, but it does give the first reliable and repeatable picture of magnetic anomalies over the whole of the earth's

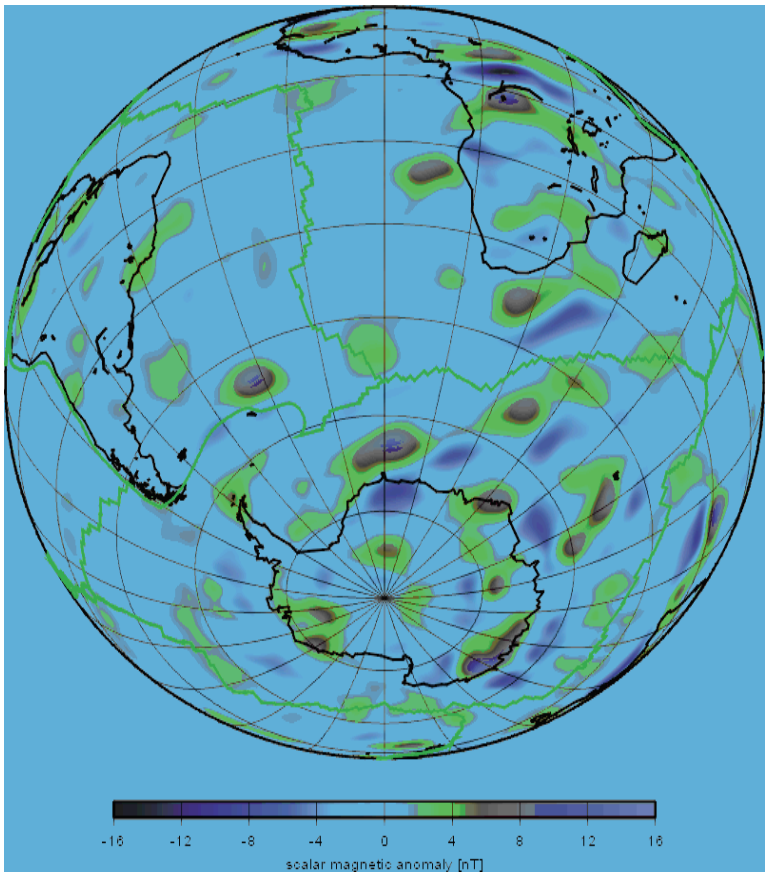

Figure 7.8 CHAMP lithospheric magnetic anomaly map, 2004 (courtesy of GFZ Potsdam)

surface. Figure 7.8 shows an image of southern Africa and the adjacent oceans. Anomalies are no more than a few tens of nT in amplitude and the interpretation of many of them is not readily ascribed to known geological features, but it is certain that a new glimpse of the structures within the earth has been obtained and they provide a challenge for future research.

* * * * *

8 Quantitative Interpretation - the Dipping Dyke Model

8.1 Principles for potential field interpretation

(a). Objective - qualitative or quantitative?

The objective of interpretation is to use the observations made in a survey:

• to improve the description of the configuration of rocks in the ground that give rise to the anomalies (e.g. geological mapping of poorly exposed or unexposed areas);

• to set limits to the depth, size, areal extent, etc of each body causing an anomaly.

In defining interpretation in this way, it is already implied that interpretation has both ***qualitative*** and ***quantitative*** aspects. Ultimately they become inseparable when an interpretation is carried out thoroughly.

Qualitative interpretation involves the description of the survey results and the explanation of the major features revealed by a survey in terms of the types of likely geological formations and structures that give rise to the evident anomalies. Typically, some geological information is available from outcrop evidence within the survey area (or nearby) and very often the role of the geophysical data is to extend this geological knowledge into areas where there is no outcrop information (i.e. extrapolation from the known to the unknown) or to extend mapped units into the depth dimension (i.e. to help add the third dimension to the mapped geology).

Quantitative interpretation involves making numerical estimates of the depth and dimensions of the sources of anomalies and this often takes the form of modelling of sources which could, in theory, replicate the anomalies recorded in the survey. In other words, conceptual models of the subsurface are created and their anomalies calculated in order to see whether the earth-model is consistent with what has been observed, i.e. given a model that is a suitable physical approximation to the unknown geology, the **theoretical** anomaly of the model is calculated (*forward modelling*) and compared with the **observed** anomaly. The model parameters are then adjusted in order to obtain a better agreement between observed and calculated anomalies.

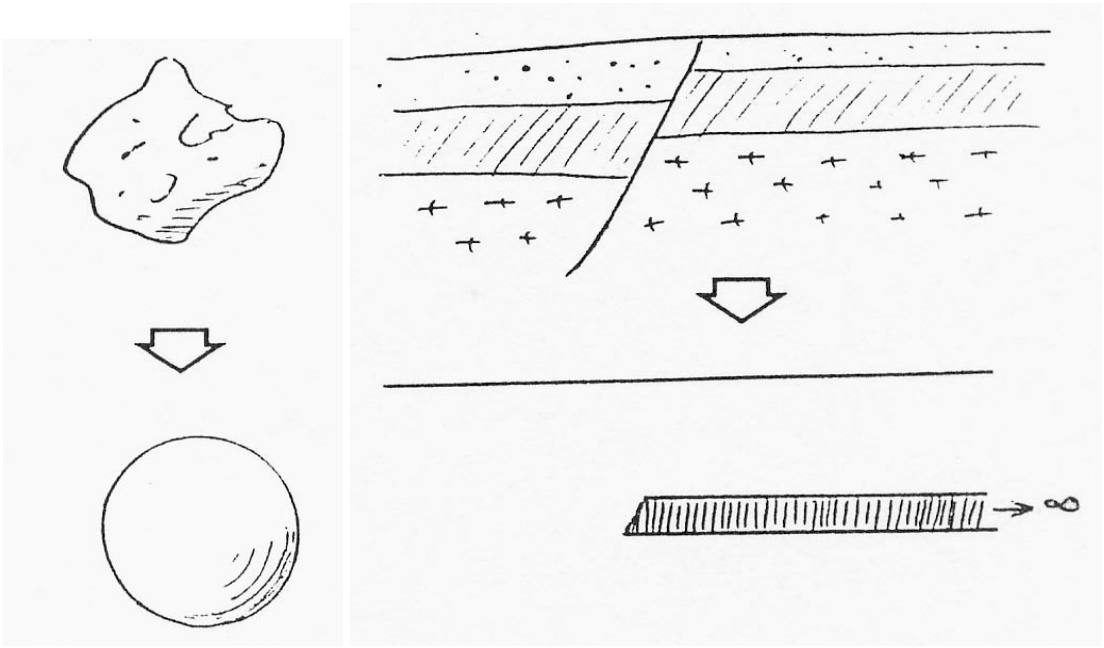

Figure 8.1 *Complex geological bodies are reduced to simple models, the anomalies of which may be readily calculated*

(b) The principle of non-uniqueness

To uniquely define a three-dimensional subsurface model from a two-dimensional set of survey data is impossible. The solution is *underdetermined*; there is an infinite number of possible physical models that could theoretically account for a given anomaly. However, this does *not* mean that the interpretation exercise is pointless or endless. Nor does it mean that all solutions are valid. Even where no unique solution is possible, mathematical limits may be set to (e.g.) the depth and dimensions of possible sources. In practice, what is known about the geology - and what it is geologically reasonable to speculate about the unknown - usually provides sufficient limitations for only a very small number of conceptually different solutions to be considered useful.

(c). Economy of hypothesis - simplification of sources in modelling.

Geological bodies and structures are often very complex in nature and, as a first approximation in geophysical modelling, it is usual that a simplification is made of the source. This is also consistent with the principle of economy of hypothesis that requires that a minimum number of arbitrary assumptions are made. In other words, a more complex model is only invented when a simple model is found to be inadequate to explain all the available (geophysical and other) data.

Examples of simplified models include: (a) a sphere as an approximation to a compact ore body, (b) a horizontal slab, of semi-infinite extent, the edge of which represents a fault (Figure 8.1).

Furthermore, at least in the initial phases of source modelling, it is very common on to employ a 2D model, i.e. a model that is invariable along strike, and therefore completely

defined by one cross-section. Although this is clearly not perfectly true in nature, it is very often the case that errors due to the fact that the real source is of finite strike length are much less than those due to other causes. Often, extension of the effort to modelling fully in three dimensions often cannot be substantiated by the quality of the survey data, though obviously this should be attempted where it is justifiable.

Models that are of finite extent in all three dimensions are known as ***3D models***, of which the sphere is the simplest. In many practical cases, the confinement of the model in all three dimensions often adds computational complexity - and additional postulation! - for little gain in accuracy or credibility. For this reason, simple approximations are often used to take into account the effect of non-infinite strike lengths. Such models are known as 2½D models.

(d). Removal of regional, establishment of base level.

All anomalies occur as local variations imposed upon (a) other local variations, (b) regional variations and (c) noise. Put another way, potential field data usually has energy in the profile or grid data from a large range of wavenumbers. All possible precautions should be taken to establish a reasonable regional field or base level for each anomaly. In the field, for example, an isolated profile should be extended to a reasonable distance from the source so that the interpreter has chance to estimate the asymptotic level of the anomaly.

The regional may be defined as the value of the field which would exist if there were no local disturbance due to the source we are trying to interpret. The regional is actually unknown and may become quite subjective. It can be treated as an additional variable in an interpretation, but reasonable limits may be set from common sense provided by human intervention.

8.2 Some specific considerations for magnetic surveys

In view of the dipolar nature of magnetic sources, individual anomalies are often quite complex and, on account of the erratic magnetic properties of many rock types, simplifying assumptions such as uniformity of magnetisation tend to be of only limited validity. A result of this is that calculated anomalies often cannot be made to fit observed anomalies as well as with their counterparts in gravity, for example, when subjected to ***quantitative*** interpretation.

However, ***qualitatively***, magnetic data sets usually express considerably more detail and so much more use can be made of techniques in qualitative interpretation. Quantitative considerations are addressed first here since a thorough appreciation of the theoretical characteristics of magnetic anomalies is essential for an interpreter who wishes to undertake systematic interpretation. Comprehensive interpretation will normally include both quantitative and qualitative elements.

Attention is drawn to the fact that some specific factors need be considered when anticipating the expected shapes of magnetic anomalies:

(a). *The inclination of the earth's magnetic field* at the survey locality;

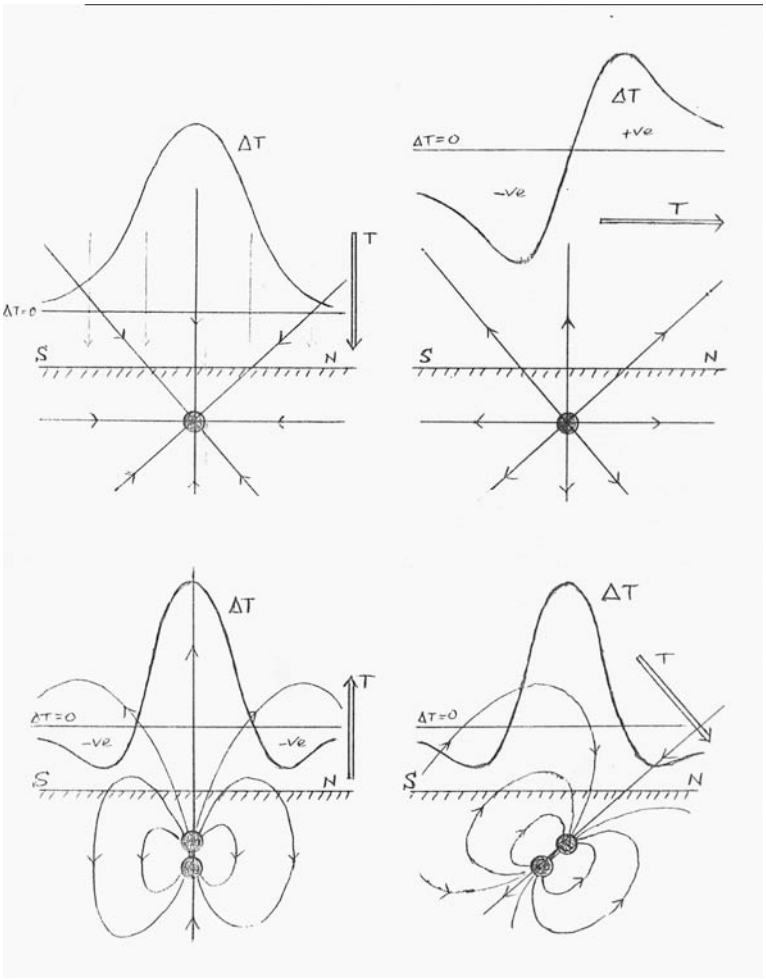

Figure 8.2 *Magnetic anomalies over permanent magnetic monopoles and dipoles.*

(b). *The strike direction of 2D bodies* with respect to magnetic north. (This quantity can be obtained from knowledge of the magnetic *declination* at the locality, together with the strike direction with respect to true north which can usually be estimated from the magnetic anomaly map);

(c). *The strength of the magnetic total field.* Inclination, declination and total field strength may be found for a survey area from local or global (IGRF) charts of magnetic parameters at the start of an interpretation exercise. Strictly speaking, charts applicable to the survey area at the time of the survey should be used, though secular variations will not often be found to have effects significant to magnetic anomaly modelling over periods less than 10 years or so. As a starting point, it is often helpful to calculate a number of anomalies for typical geological bodies under these magnetic field conditions as an aid to recognition of real anomalies in the map area under interpretation.

(d). The possibility of there being *induced magnetisation, remanent magnetisation or both;* both are vector quantities and they will add vectorially.

For simplicity, *only* total magnetic field anomalies are discussed, i.e. the component of the anomalous magnetic field in the direction of the earth's main field at the anomaly location (see Pedersen et al, 1990). The following discussion needs extension before application to *vertical component* anomalies or *vertical gradient* anomalies.

Figure 8.2 demonstrates the origin of magnetic anomalies over magnetic monopoles and dipoles. It is very useful to be able to sketch anomalies in this way from first principles. Note that in all cases the shape of the anomaly depends on the direction of the earth's field and, in the case of the dipole, the disposition of the dipole.

In general, even the simplest of source models produces anomalies that have both positive and negative parts (or ‘lobes') from a single source with a single physical

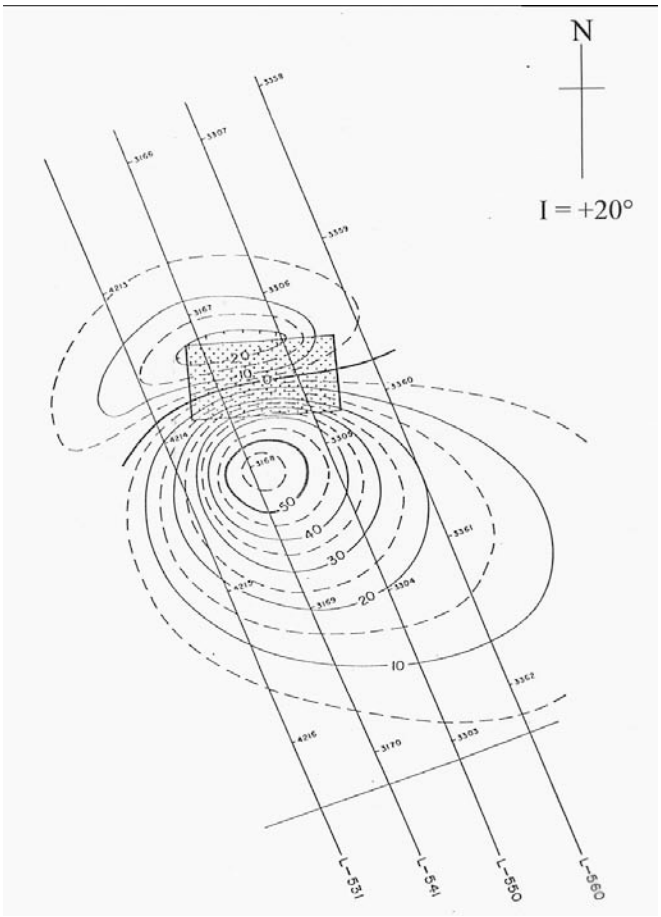

Figure 8.3 *Typically, a magnetic anomaly over a single compact source has both positive and negative parts or 'lobes'.*

property contrast with respect to its host rock. Figure 8.3 shows a typical example confirming this from nature.

8.3 Graphical interpretation methods; slope-length depth estimators

Often one of the most useful pieces of information to be obtained from aeromagnetic data is the *depth* of the magnetic source (or rock body). Since the source is usually located in the so-called 'magnetic basement' (i.e. the igneous and metamorphic rocks lying below the - assumed non-magnetic - sediments), this depth is also an estimate of the thickness of the overlying sediments. This is an important piece of information in the early phases of petroleum exploration. Sufficient depth estimates from a large number of magnetic sources allow the depth of the basement to be contoured and this is then a rough isopach map of the sediments.

For this reason, several methods have evolved in the early days of magnetic interpretation simply to estimate the depth of sources from their anomalies without reference to any specific source models. Two simple manual methods are described, together with the most sophisticated method which was developed before computer-based techniques became commonplace. The 'wavelength' (see Section 4.2) of anomalies is primarily related to their depth of burial; shallow bodies give sharp, short wavelength anomalies, deep bodies give broad anomalies. The amplitude of the anomalies, on the other hand, is directly related to the strength of magnetisation of the source.

(a). The 'straight-slope' method

The tangent is drawn to the steepest gradient of an individual magnetic anomaly on a section of profile (see Figure 8.4). The horizontal distance, S_s, over which the tangent line is coincident with the anomaly profile is measured. A depth estimate is then obtained by multiplying S by a factor which usually falls in the range 1.2 to 1.6. For a vertical dyke-like body with various α values of width to depth-of-burial (α = w/h) the factor values are tabulated in Figure 8.5 for various effective magnetic inclinations. (The table repeats symmetrically for effective inclinations from 45° to 0°). For an approximation which disregards the geometry of the source, it may be said that:

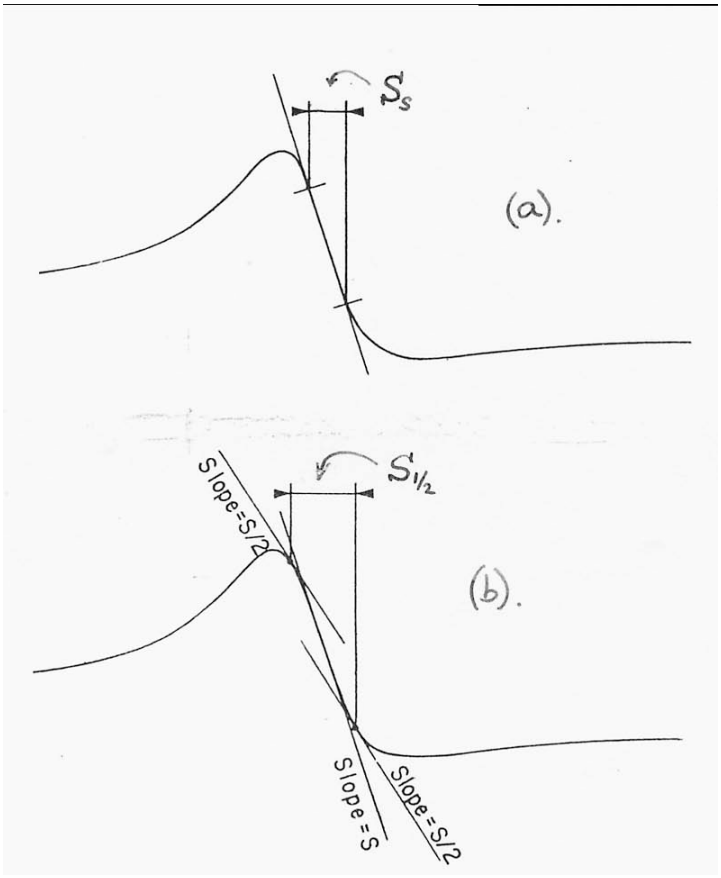

Figure 8.4 *(a) Length of 'straight slope' of inflexion tangent; (b) length between tangents at 'half-slope'.*

$$h = 1.4\ S_s \pm 20\%$$

The straight-slope method gives ambiguity (not least) on account of the indistinct points where tangent and curve start to diverge.

(b) Peter's 'Half-Slope' method

Here the same tangent is drawn as in the straight-slope method but ambiguity is reduced by drawing two more tangents at *half* the slope of the first (Figure 8.4). Now the horizontal distance between these two new points of tangency is measured, $S_{½}$. The depth estimate is then:

$$h = 0.63\ S_{½}$$

in the case where h = 2 w. Note that $S_{½} \approx 2.2\ S_s$

In present-day interpretation practice, these methods can only be considered as 'rough-and-ready' first indications of depth, but they are still useful for the geophysicist to have in mind when first confronted with an aeromagnetic map of a new area, or with an anomaly on a field profile.

(c). Inflexion Tangent Intersection (ITI) method.

It may be argued that the above methods make only limited use of the full anomaly as recorded, and that other tangents and essential distances could also be taken into account in an interpretation. This approach was followed to its logical conclusion by Naudy (1970).

Naudy's method involves the comparison of certain (a) horizontal and (b) vertical distances measured from the observed profile and defining the shape of a field anomaly with the same parameters calculated for a range of theoretical models. Theoretical models used include the dyke, the contact or fault and the horizontal thin sheet, and a pair of nomograms is presented for each of a number of geometrical configurations in each case.

The horizontal and vertical parameters are determined by drawing tangents to the field curve at its inflexion points (Figure 8.6). In the example, the measured horizontal parameters are Hl, H2, H3 and H4 (in metres) and the measured vertical parameters are V1 and V2 in nanoteslas. These values are plotted on logarithmic graph paper of a suitable scale and then compared with the theoretical values shown on the sets of

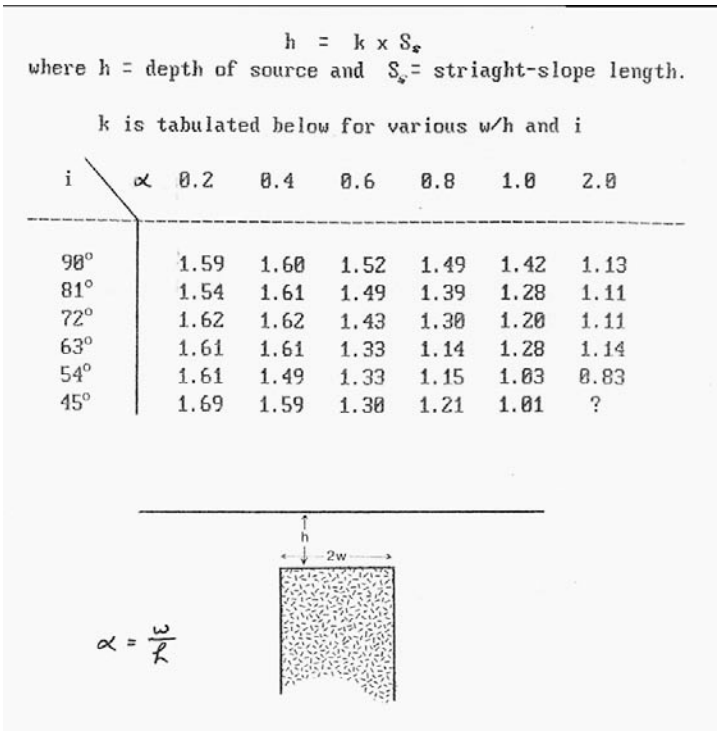

Figure 8.5 *Values for the factor by which the straight-slope length should be multiplied to give depth values for various dyke widths and magnetic inclinations.*

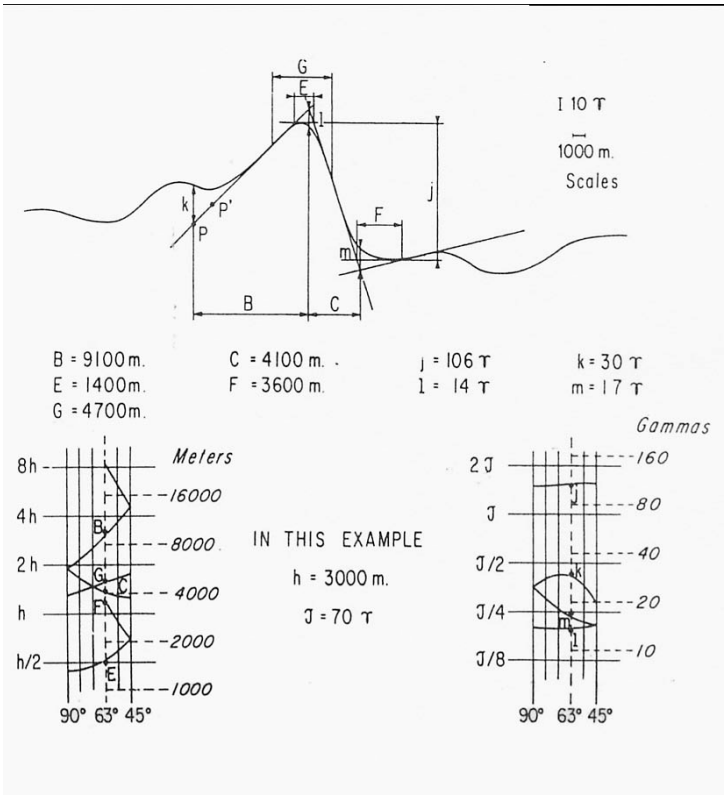

Figure 8.6 *A worked example of the Inflexion Tangent Intersection (ITI) method of interpretation (from Naudy, 1970). 1γ=1 nT*

nomograms. For each of the three geometrical models, a range of values of α (= w/h) for the dyke and η (= H/h) for the fault is represented by the nomograms, and for each value of α (or η) a nomogram is given for both the horizontal and the vertical parameters. Within each nomogram, magnetic inclination varies from 90° to 45°; the nomograms repeat symmetrically beyond this range. The best fit of the parameters measured from the field curve to the nomograms is then sought for both the horizontal and vertical parameters. It may be necessary to re-interpret the field curve using, for example, a different zero line, to obtain a coincident match for both parameters on the same model and inclination.

Once a satisfactory fit is obtained, the following information may be recorded:

1). the model chosen and its α or η value.

2). the depth to the top of the body in metres.

3). the apparent magnetisation contrast of the body with its surroundings in nT.

4). the apparent inclination, which is a function of the dip and strike of the body, and of the direction and intensity of its induced and remanent magnetisation.

Generally it is assumed that the magnetisation is induced. Remanent magnetisation can only be recognised with any certainty from aeromagnetic data in the case of bodies that are strongly magnetised in a direction quite different from the present-day field direction (see Section 8.6).

8.4 The flat-topped dipping dyke model.

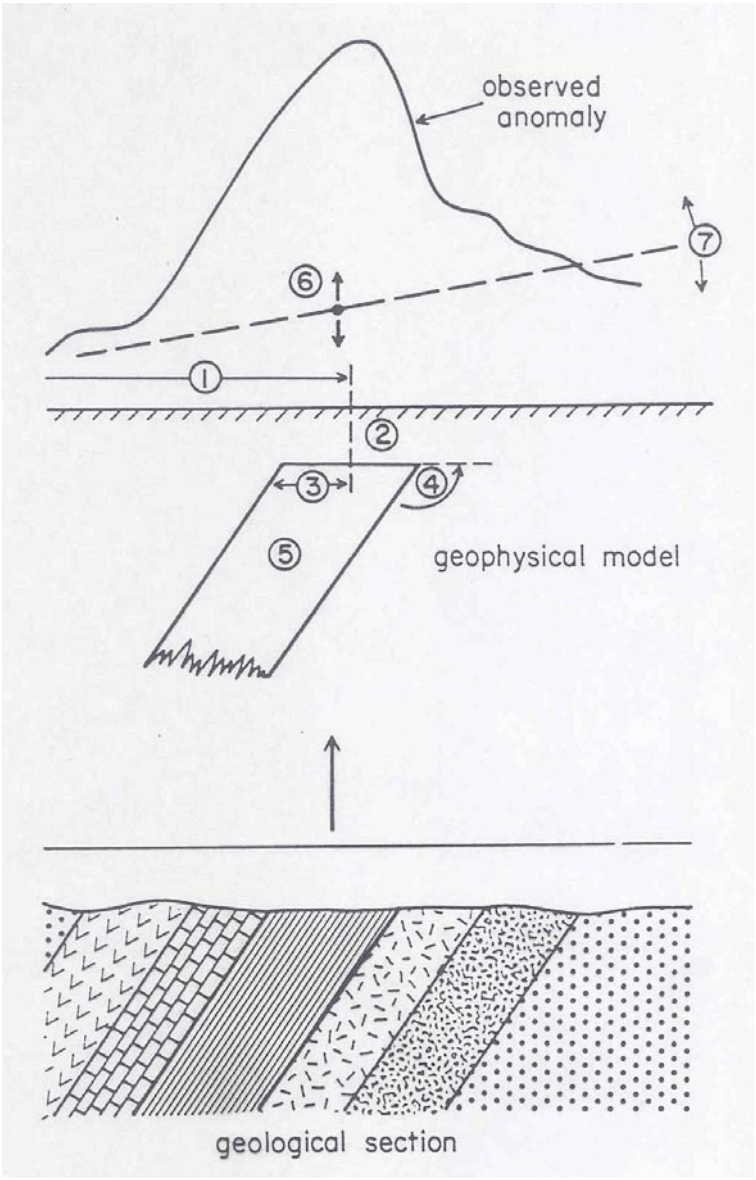

Figure 8.7 *The seven parameters that define the flat-topped dipping dyke model: 1. position of centre; 2. depth of burial; 3. half-width of top; 4. dip from traverse direction, 5. magnetic susceptibility, 6. base level; 7. base slope.*

It can be seen from the foregoing that an accurate interpretation of magnetic anomalies cannot be made without making some assumptions about the geometry of the source body. By far the most useful geometrical model for source bodies in practice is the 'dipping dyke', a uniformly magnetized two-dimensional (2D) body with parallel dipping sides extending to infinite depth and with a horizontal top surface (Figure 8.7). This is the physical analogue not only of a dyke in the geological sense (i.e. a thin-intrusive body emplaced along a fissure), but also of a relatively magnetic unit in a sequence of metasedimentary rocks which has been folded and then eroded down to a certain level. The model can also be extended to larger intrusions and, by removing one side to infinity, to the modelling of dipping faults and contacts. It can also be shown that errors of only limited significance are introduced when this model is applied to the interpretation of magnetic profiles over bodies whose strike length is in reality far from infinite (see Section 9.4).

The magnetisation of such a dyke, whether from induction in the present earth's field or from a remanent magnetisation, produces sheets of magnetic poles (N or S) on each of the top and the two side surfaces of the dyke. The mathematical formulation of the dyke anomaly (Figure 8.8) with induced magnetisation has the equation:

$$\delta T = (\text{amplitude factor}) [\theta \sin(2I-d) + \ln(R2/R1) \cos(2I-d)]$$

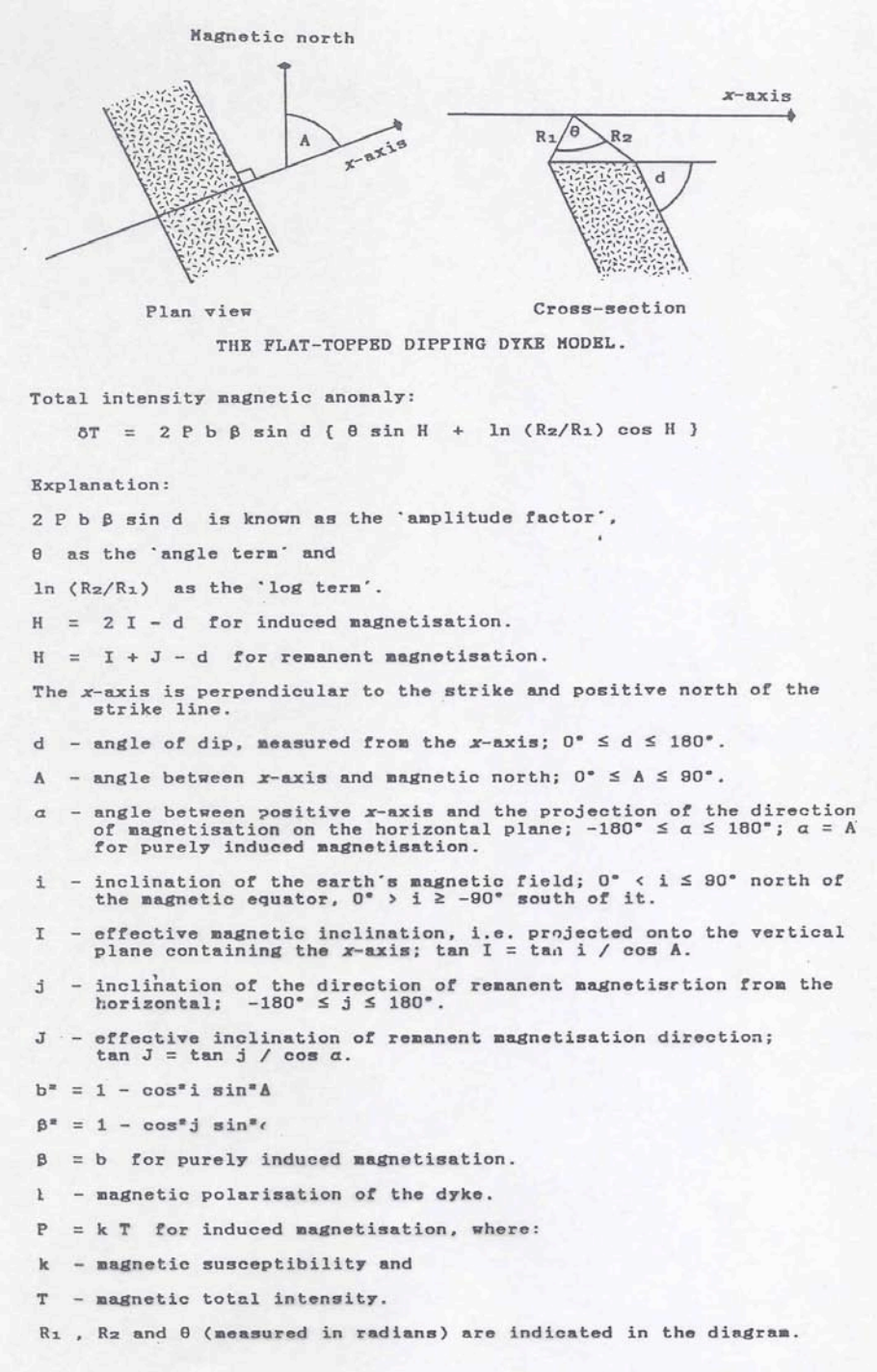

Figure 8.8 *Formulation of the flat-topped dipping dyke anomaly (from Reeves, 1989, after Reford and Sumner, 1964).*

Along a profile over a given dyke at a given locality, the amplitude factor and (2I-d) both remain constant; only θ and ln(R2/R1) change along the profile. By inspection (see Figure 8.9) θ (known as the ***angle term***) traces a symmetrical curve centred above the middle of the body's top surface, while ln(R2/R1) (known as the ***log term***) traces an antisymmetrical curve centred at the same point. The relative proportions of these two curves that are added together in any given field profile is determined by the value of H (= 2I-d) and its sine and cosine.

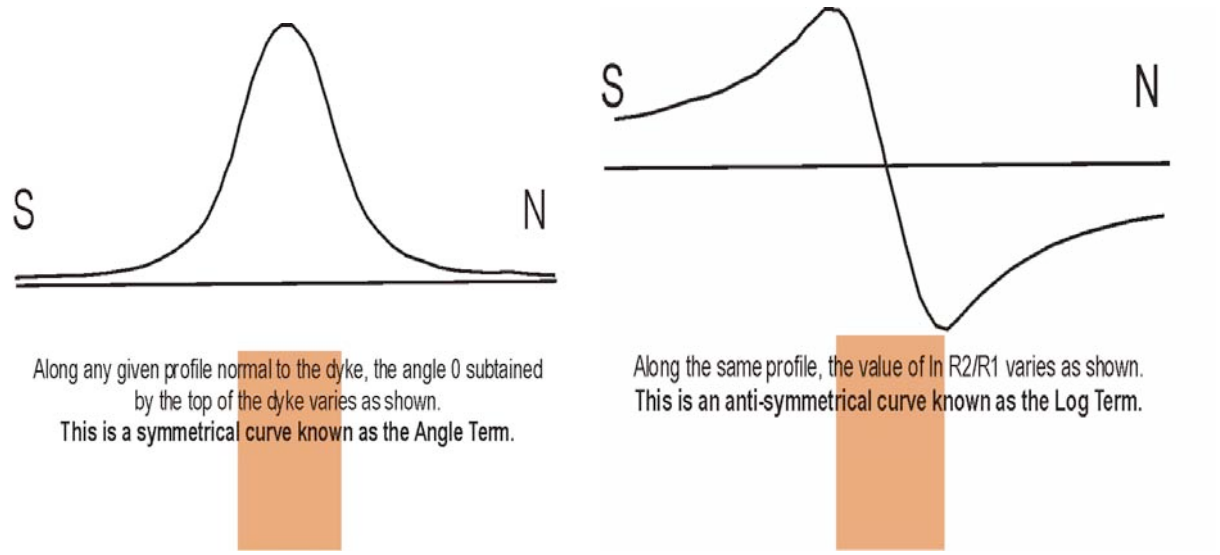

(a) (b)

Figure 8.9 *(a) Angle term and (b) log term of the dyke anomaly*

Now, d is the dip of the dyke, measured from the north horizontal (vertical = 90°) and I' is the *effective* inclination of the earth's magnetic field - in the plane at right-angles to the strike direction. To keep things simple, dykes striking at right-angles to the inducing field (i.e. striking 'magnetic east-west') are considered first. In these cases, the effective inclination, I', equals the actual inclination, I (see Section 9.3).

Restating all the simplifying assumptions, we now consider the anomaly along a south-to-north traverse (north is on the right in all figures) over an east-west striking vertical dyke extending to infinite depth and magnetised solely by induction (Figure 8.10).

(a). At the north magnetic pole (I = 90°) the angle term *only* need be considered since cos (2I-90) equals zero for the log term. The anomaly is positive and symmetrical.

(b). At inclinations less than 90°, increasing contributions from the log term take effect and a negative lobe to the anomaly grows on the north side of the body. At I = *45°, only* the log term contributes since sin (2I-90) equals zero; the positive and negative lobes of the anomaly are of equal amplitude.

(c). At the magnetic equator (I = 0°), the effect of the log term has decayed to zero again (cos (2I-90) equals zero) and the anomaly is purely symmetrical. However, sin (2I - 90) equals -1 so the anomaly is entirely negative.

(d). Entering the southern magnetic hemisphere, the negative lobe moves towards the south of the body and increasingly large contributions of the log term cause a positive lobe to grow on the north side until, at I = -45°, positive and negative lobes are equal in amplitude once again and only the log term contributes. Note here that, as in the northern hemisphere, the negative lobe lies on the side nearest the magnetic pole - the north side in the northern hemisphere, the south side in the southern.

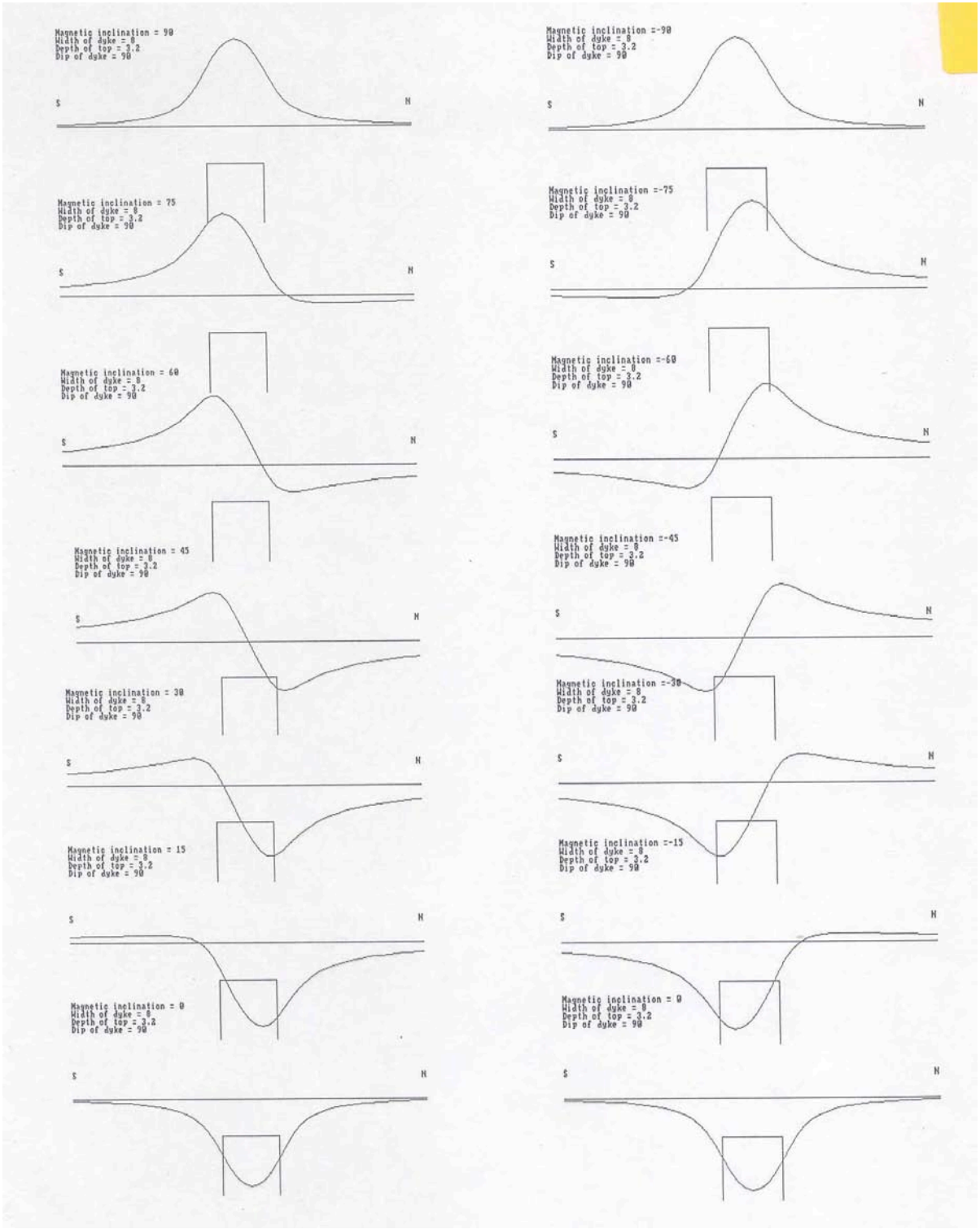

Figure 8.10 *Magnetic anomalies over a thick vertical dyke at all magnetic inclinations.*

(e). Finally, at the south magnetic pole, a positive symmetrical anomaly is achieved once again, identical to that at the north magnetic pole, since cos (2I-90) = cos -270° = zero and no contribution from the log term is expected.

Mathematically, the range of I (-90° $\leq$ I $\leq$ 90°) can be extended, but already the family of curves is complete; no new anomaly shapes can be expected for I values outside the range occurring over the surface of the earth. This family of curves is shown in Figure

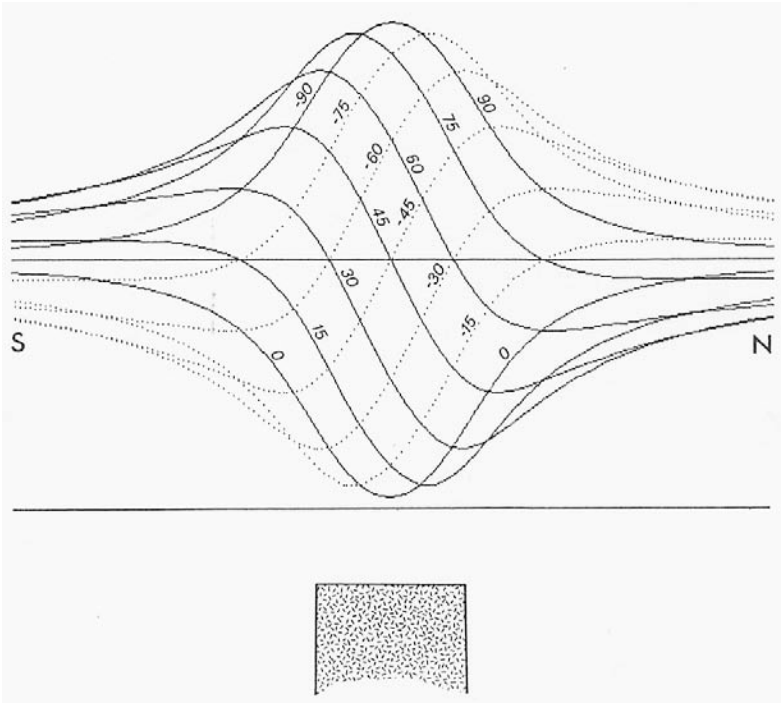

Figure 8.11 *The family of magnetic anomaly curves over a vertical dyke as I goes from +90° to 0° (solid lines) and from 0° to -90° (dotted lines). In this range, H (= 2I - d) goes from +90° to -270°. Only induced magnetisation is considered [from Reeves, 1989].*

8.11 and is the basis of the considerations in the remainder of this section and Section 9. Familiarity with the curve family provides a solid base for understanding magnetic anomaly shapes and is therefore essential for effective magnetic interpretation.

Some of the conclusions deduced above may be confirmed from physical principles by extending the methods of sketching anomalies as shown in figure 8.2 to the dyke model (Figure 8.12).

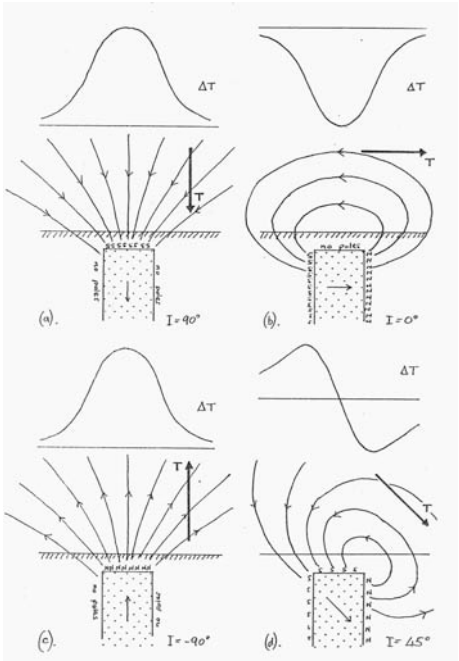

Figure 8.12 *Sketching dyke anomalies from*

8.5 The dyke model: Effect of dip

The foregoing discussion on the dyke curve family started with a number of simplifying assumptions about the geometry of the dyke and the circumstances surrounding it. In the following sections these will be progressively removed and it will demonstrated that the curve family is applicable to virtually all situations that might need to be modelled. Initially, for example, it was stated that the dyke was vertical. This section investigates what happens when this is not the case.

From the equation (Figure 8.8):

$$\delta T = (\text{amplitude factor}) [\theta \sin(2I-d) + \ln(R2/R1) \cos(2I-d)]$$

it is seen that (apart from some effect on the amplitude term which we can discount for the moment) d, the dip of the dyke, contributes to the angle whose sine and cosine are multiplied by the angle and log terms respectively. In other words, if d changes from 90° (vertical, as was assumed in Section 8.4) the value of (21-d) changes, but the resulting anomaly curve still falls within the curve family of Figure 8.11 since other factors are (virtually) unchanged. This is illustrated in Figure 8.13 for the case of I = 45° and dips of 60°, 90° and 120°. It is clear that a change in dip of φ produces the same effect on the shape of the anomaly as a change in effective magnetic inclination of $-\varphi/2$.

Note that dip values are confined to the range $0° \leq d \leq 180°$ for bodies below the ground

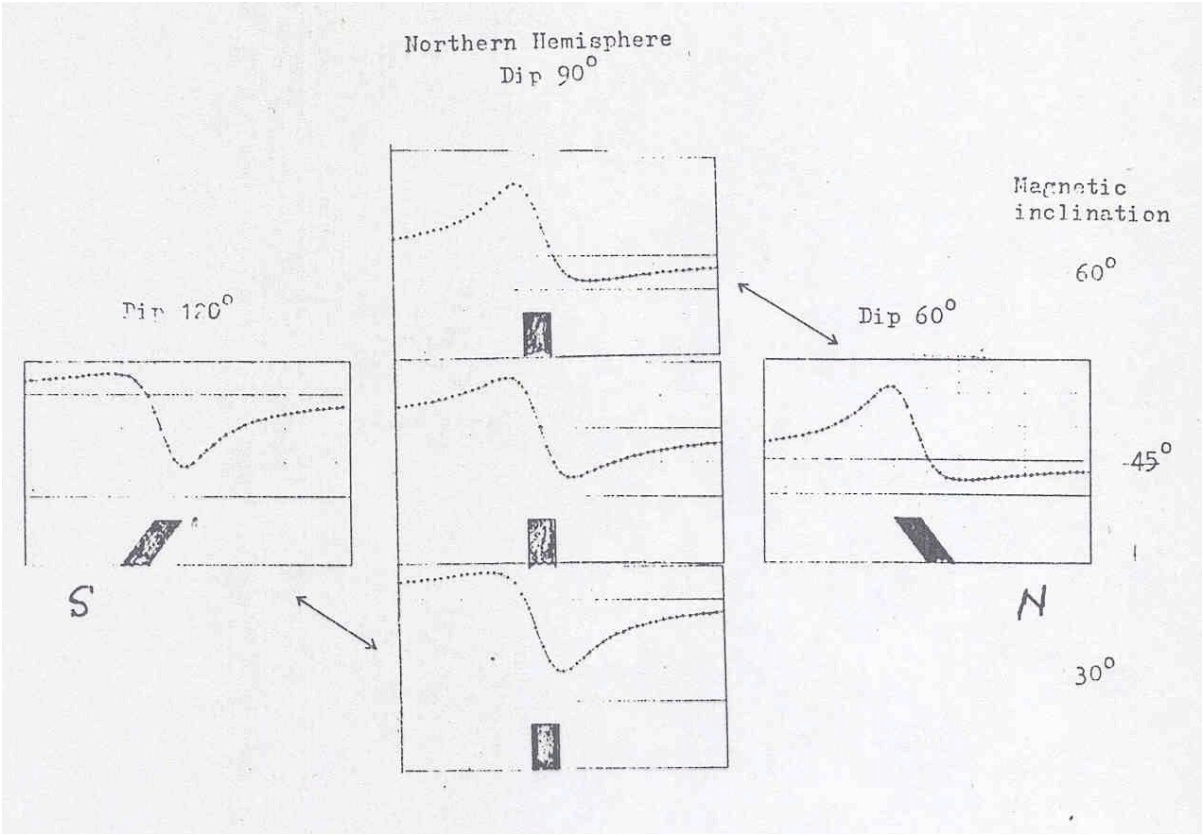

Figure 8.13 *The effect of dip on the shape of the dyke anomaly. A change in dip of φ produces the same shange in anomaly as a change in magnetic inclination of $-\varphi/2$.*

surface. It follows that, at any one locality, anomalies due to induced magnetisation may

only be expected in the range I ± 45° and so, for east-west striking bodies in a given survey area, only one half of the total curve family is needed.

8.6 The dyke model: the effect of remanent magnetisation

If the magnetisation of the dyke is *remanent* (rather than induced, as in the initial assumptions) the direction of remanence may be *any* direction. For a 2D body (infinite strike length), only the component of the remanent magnetisation vector in the plane perpendicular to the strike is important. (The component along strike only produces magnetic poles at ±∞). The inclination of the component in the normal plane is given the symbol J (Figure 8.8) and has the natural range $0° \leq I \leq 360°$. (Note that this is *twice* the range of I which is confined to $-90° \leq I \leq +90°$ since the *inducing field* never points south).

The equation for the curve family

$$\delta T = (\text{amplitude factor})[\theta \sin(2I-d) + \ln(R2/R1) \cos(2I-d)]$$

must now be amended as follows for remanent magnetisation:

$$\delta T = (\text{amplitude factor})[\theta \sin(I+J-d) + \ln(R2/R1) \cos(I+J-d)]$$

However, the family of curves is still valid, and it can be seen that for a difference (I - J) of +Ω° then the anomaly changes within the curve family from that expected for the local magnetic inclination by an amount equivalent to a change in I of -Ω/2°. This is illustrated in Figure 8.14.

By comparing any anomaly with the curve family it is possible to estimate the value of (I + J - d) but, without independent information, we cannot determine these three parameters independently. Since I is always known for a given locality, it follows that we can *either* know (or assume) d and determine the value of J, *or* we can assume no remanence and calculate a dip for the dyke. If we adopt the latter approach in the first place - which is normal interpretation practice - the calculation of an impossible dip (i.e. 180° < d < 360°) is usually the first signal that remanent magnetisation is present in the source of the anomaly. Stated another way, if the anomaly we observe falls outside the range of that half of the curve family identified at the end of Section 8.5, then probably remanent magnetisation is present.

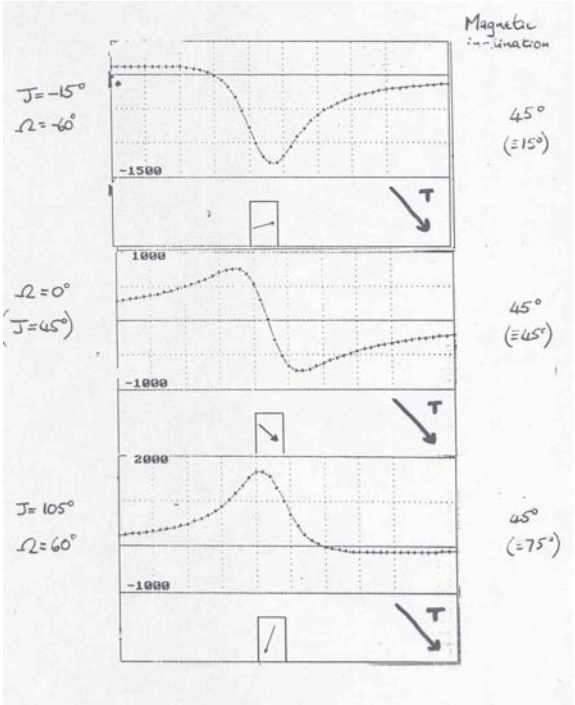

Figure 8.14 *The effect of remanent magnetisation on the shape of the dyke anomaly. A change in J of Ω produces the same change in anomaly as a change in magnetic inclination of -Ω/2.*

Note that induced ***and*** remanent magnetisation might be in play, further complicating the situation since the value of J is now the angle of the vector sum of the induced and remanent components in the plane perpendicular to strike.

* * * *

9.

The Dipping Dyke Extended to Other Models

9.1 Extending the dyke model to other bodies

The initial assumptions made in calculating the simple curve family are listed in Figure 9.1. In the present section these will be eliminated progressively to show that the lessons learned through familiarity with the curve family pay dividends when dealing with the anomalies over bodies of shapes that represent most situations likely to be encountered in geology at all magnetic inclinations. The effects of non-vertical dip and remanent magnetisation were dealt with already in Sections 8.5 and 8.6.

Initial assumptions...	...after elimination we can deal with..
1). Vertical dyke	Dipping dyke
2). Magnetised only by induction	Effects of remanent magnetisation
3). Half-width ≈ depth	Step model of semi-infinite width
4). Infinite depth-extent	Thin slabs, vertical gradient anomalies
5). East-west striking	'Effective' magnetic inclination
6). Infinite strike length (2D)	pipe-like anomalies (3D).

Figure 9.1 *The initial assumptions made in dealing with the anomaly family over dykes, and the extension to bodies of other shapes and properties.*

9.2 The dyke model: The effect of dyke shape.

(a). Width

The curves of the family shown in Figure 8.11 are calculated for a dyke with a defined width. Width is usually defined dimensionlessly by the parameter alpha (α) = w/h where 2w is the width of the top surface of the dyke and h the distance between the top surface and the plane of observation. In the examples of Figure 8.11, α = 1.25, chosen arbitrarily. Angle and log terms for a range of α values are shown in Figure 9.2. From this figure it is seen that as long as the dyke is relatively narrow (α < ~2.0) the shape of the anomaly is rather insensitive to the width of the dyke. The *amplitude* of an anomaly, meanwhile, is largely dependent on the magnetisation of the dyke material and magnetisations of rocks are known to cover a wide range of values. Taking these facts together, there is a problem of equivalence not unlike that found in other areas of geophysics where the anomaly due to a thin, highly magnetic dyke can be very similar to that of a much broader, less magnetic one. The width of a 'narrow' dyke is therefore difficult to estimate quantitatively from its anomaly alone.

As the dyke becomes *very* wide, the anomaly shape becomes somewhat more complicated. Figure 9.3 illustrates the curve family for a dyke with α = 5.0. It should be noted now that the bell-shaped angle term curve has regions of greatest slope directly above the sides (or 'contacts') of the dyke, while the log term has a maximum over one side and a minimum over the other. Note also that, for an anomaly that is largely asymmetrical, a long, almost straight, slope above the (sub-)outcrop of the body should be expected, but note also that the length of this slope has no relation to the depth of the source. Care must be taken with this possibility when using any slope-length depth estimators. A further point is that this slope only approaches its theoretical smoothness in practice when the source body is magnetically homogeneous. Commonly, local anomalies are encountered along such slopes due to concentrations or deficiencies of (e.g.) magnetite in certain parts of the wide body.

As the sides separate further, their anomalies become distinct from each other and are, in fact, the anomalies due to north-facing and south-facing contacts, faults or steps respectively. Notice that fault or contact anomalies are in general quite different depending on whether the more magnetic body lies to the south or to the north of the contact, whereas the dyke anomaly is unchanged by a change in strike of 180°.

These situations are certainly amongst those that should be modelled prior to starting a qualitative interpretation in an area in order that the interpreter may know how to recognise anomalies over fault or contact features that are quite common in the real world. The families of curves over north-facing and south-facing contacts follow a pattern rather similar to that shown in Figure 8.11 for the dyke but with a shift in phase. The fault or contact curve families are shown in Figure 9.4.

In the case of the contact, of the three sheets of poles present on the surface of the magnetic body, two are horizontal and one vertical (though the algebra can easily be extended to a non-vertical contact surface). In the case of the contact, the 'width' - as used in the case of the dyke - is no longer meaningful; it is replaced by the 'throw' of the fault and the parameter 'eta' (η) is defined as the ratio of the depth-to-the-bottom of the fault (H) to the depth-to-the-top (h), η = H/h. When η is close to 1.0, the vertical surface is of limited depth-extent, while faults with a large throw have much larger η values.

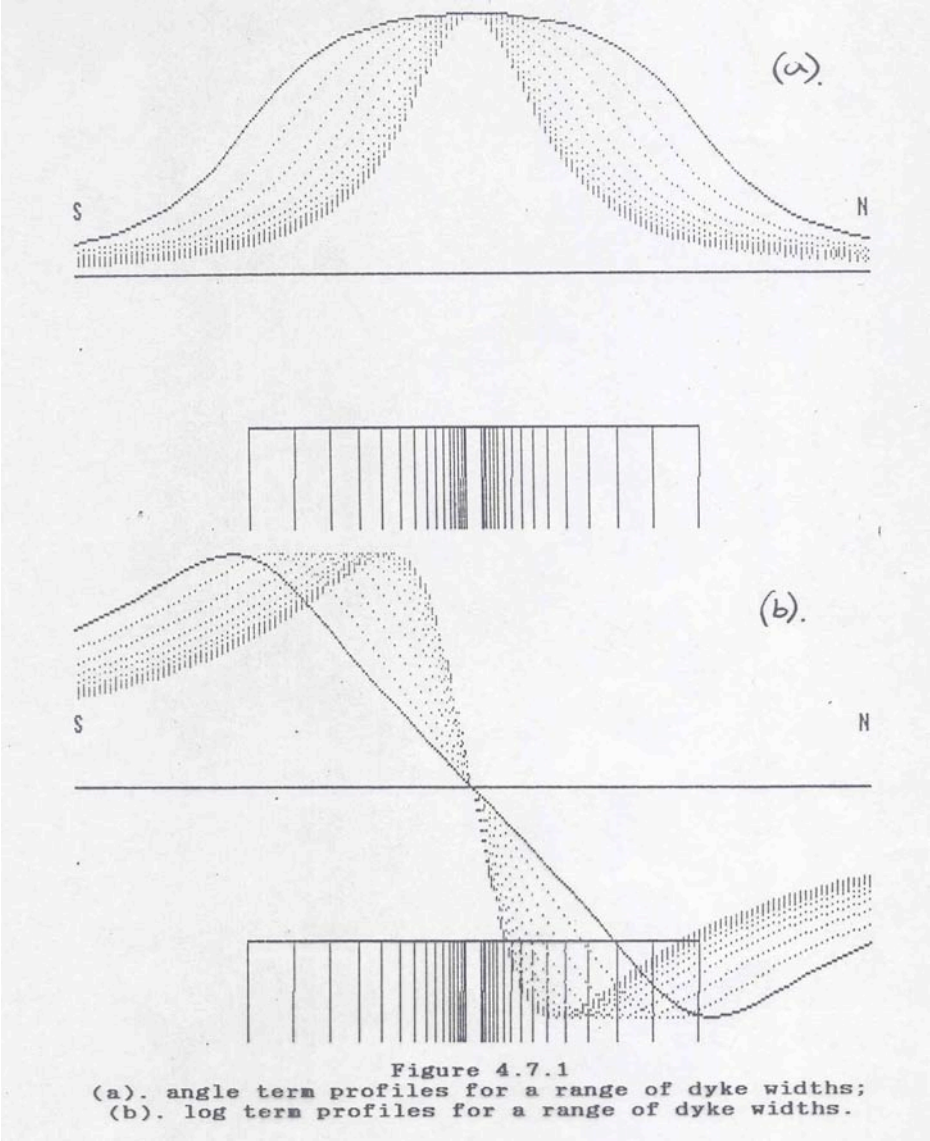

Figure 9.2 *(a) Angle term profiles for a range of dyke widths; (b) log term profiles for a range of dyke widths.*

Note, from Figure 9.4, that the anomaly over a broad body tends to have a negative anomaly over the edge closer to the pole and a positive anomaly over the edge closer to the equator.

(b). Depth extent

In all the dyke models considered so far, the sides of the dyke have extended to infinite depth. Clearly this is not the case in nature. We can, however, calculate the anomalies over dykes with limited depth extent without any more computing capability than has been used until now simply by subtracting the effect of the dyke *below* the bottom surface from that of the whole dyke from infinite depth to the top surface. This is done for the angle and log terms separately in Figure 9.5. It is seen here that, as long as the depth to the bottom of the dyke is at least several times greater than the depth to the

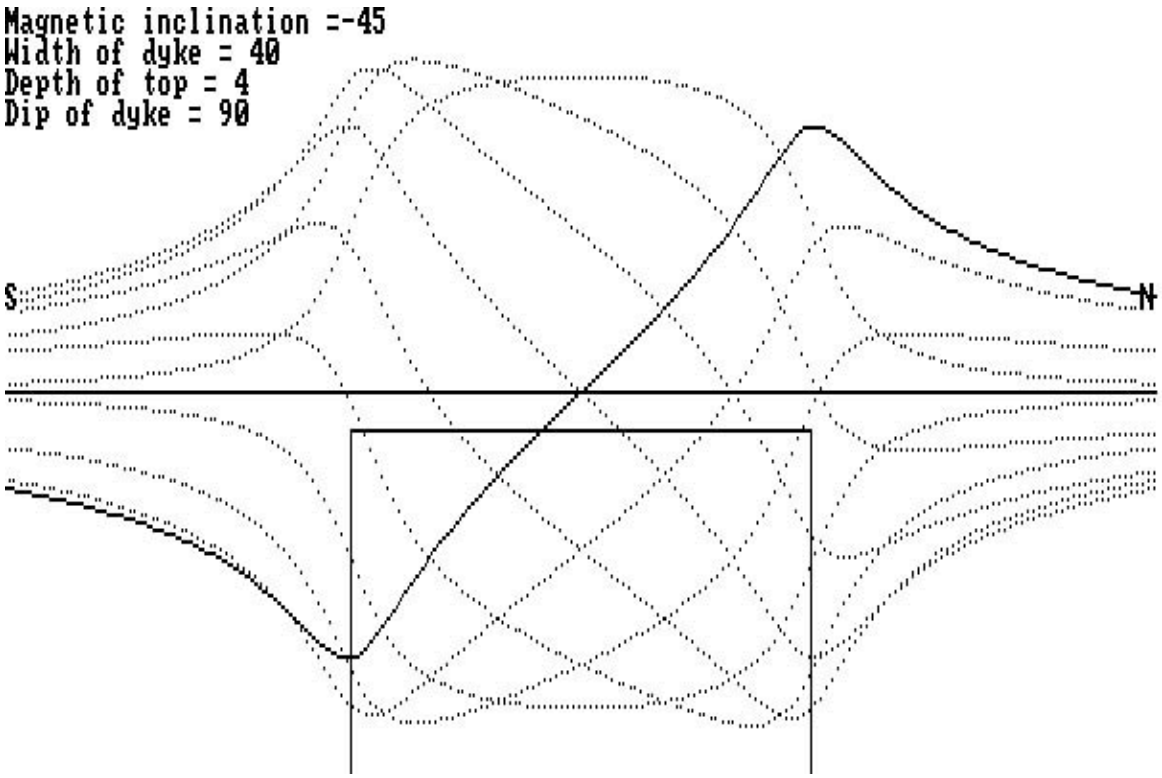

Figure 9.3 *Curve family for a thick dyke, α = 5.0.*

top, the effect of the depth of the bottom on the shape of the anomaly as a whole is minimal. As a consequence, the infinite-depth-extent dyke model is quite useful for modelling situations where this simple assumption is in fact far from true. For the same reason, to get a reliable estimate of the depth of the *bottom* of a body is seldom possible with confidence from interpretation of its magnetic anomaly.

As the bottom of the dyke approaches the top more closely, the main effect on the anomaly is to increase the *rate* with which the anomaly decays with distance from the body. In other words, the length of the profile over which the body has significant effect becomes much shorter for a vertically-thin body than over a body of large depth-extent. As seen in Figure 9.5, the total angle term (i.e. the difference between the angle subtended by the top surface and the bottom surface) easily becomes negative on *both* sides of a thin body. As a consequence of this, any anomaly having three lobes (e.g. negative, positive, negative) is likely to be due to a body of limited depth extent.

In the limit when, say, the body is only one metre thick (unit thickness), its anomaly has the same form as the ***vertical gradient*** anomaly over the original dyke of infinite depth extent, since the difference between the effects of the top and bottom surfaces is mathematically the same as the difference between the readings of the top and bottom sensors of a vertical gradient magnetometer. [The *vertical gradient* anomaly over a thin body has the same form as the *second* vertical derivative of the anomaly over a body of infinite depth extent, and so on.]

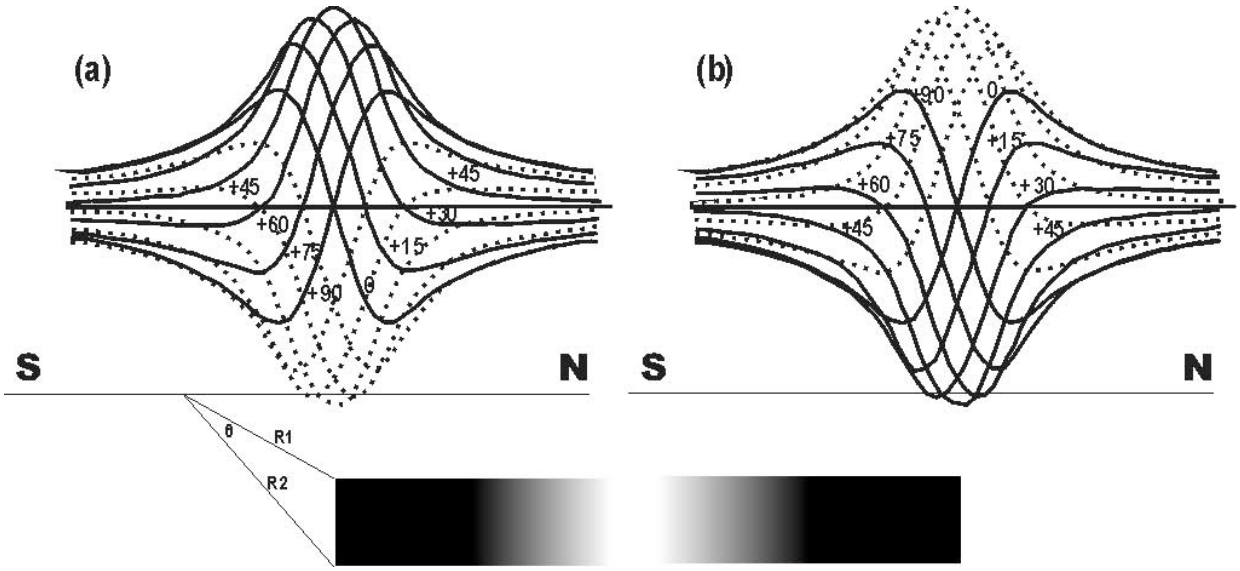

Figure 9.4 *Magnetic anomaly curve family (induced magnetisation) over a vertical edge or step (a) step facing south and (b) step facing north. Solid lines are given for the northern hemisphere for the inclinations indicated, dashed lines for the southern. Note that, for almost all inclinations, the anomalies are predominantly negative over the edge of the body nearer the pole and positive over the edge nearer the equator for* both *hemispheres.*

9.3 All 2D bodies: Effect of strike direction

So far we have been careful to simplify matters by discussing only bodies whose strike direction is at right angles to magnetic north. Nature, of course, provides bodies with ***all*** strike directions, so we must be prepared to interpret other situations.

The angle A is defined as the angle between the strike of a body and 90° east of magnetic north. For the bodies discussed so far (striking perpendicular to the magnetic north direction), A = 0°.

It was already explained that, for 2D bodies, only the component of magnetisation in the plane at right angles to the strike direction need be considered; the component of the magnetic field along-strike produces poles only at ± ∞. In the case of induced magnetisation, therefore, only the component of the inducing field in the plane at right angles to strike need be considered. Since the total field *strength* affects only the amplitude term of the anomaly, it is further only the *angle* of the component of the inducing field in the plane at right angles to strike that is important in determining the shape of the anomaly. This quantity is known as the ***effective inclination*** (I') of the inducing field and it can be shown quite easily that it may be calculated as follows:

$$I' = \tan^{-1}(\tan I / \cos A)$$

where I' is the *effective* inclination and I the *true* inclination of the geomagnetic field. Clearly for the (magnetic) east-west striking bodies discussed so far A = 0 and I'= I.

As strike direction departs from E-W, I' is always greater than I, as is illustrated for all A and I values in Figure 9.6. The effect is not large where A < 30° but grows steadily larger such that, for example, when A = 50°, and I = 60°, then I'= 70°. Note that when A = 90°, then I' = 90° regardless of I and the anomaly will be symmetrical about the north-south direction for any vertical body.

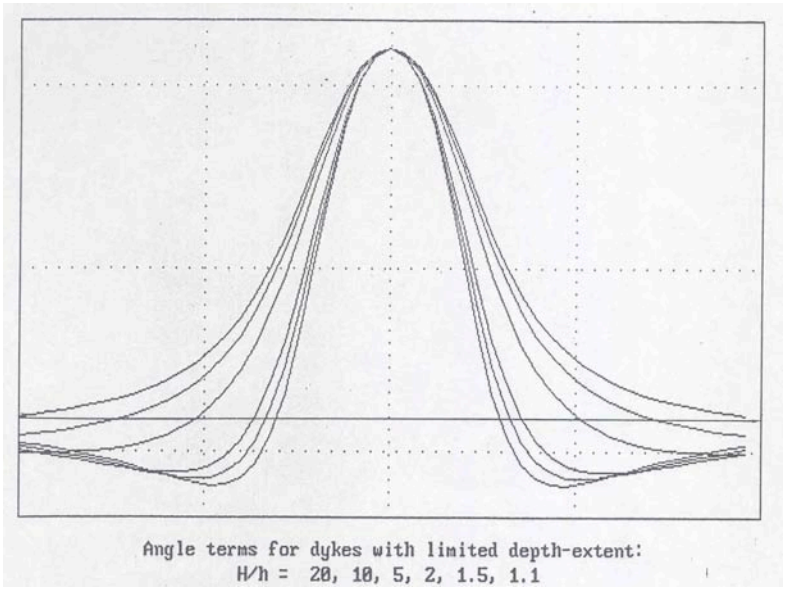

(a).

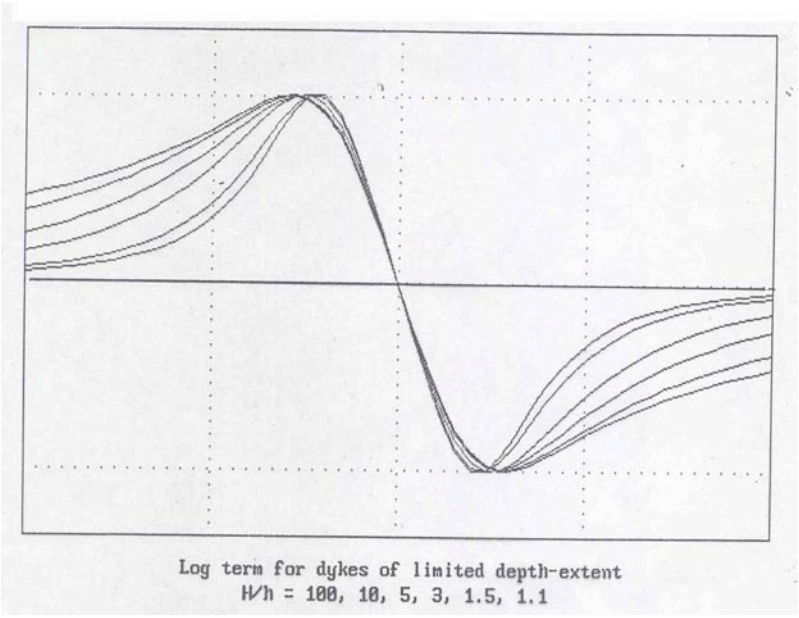

(b).

Figure 9.5 *(a) Angle terms for dykes with limited depth-extent: H/h = 20, 10, 5, 2, 1.5, 1.1; (b) Log terms for dykes of limited depth extent: H/h = 100, 10, 5, 3, 1.5, 1.1.*

It follows that, in any given survey area, we should expect to encounter magnetic anomalies that will be predominantly typical of the value of I within the curve family of Figure 8.11. But, with bodies that strike more closely north-south, the shapes of their anomalies can be expected to resemble those typical for *higher* I values. Nevertheless, the curve family still covers all the possibilities.

One very special case should not be overlooked, however. The amplitude term in the equation of Figure 8.8 cannot be ignored. Clearly, as a body strikes towards north-south, the component of the inducing field in the plane at right angles to the body becomes much weaker until it becomes zero for a truly north-south body. As long as the inducing field is not horizontal, magnetic poles will still be induced on the horizontal top surface of the dyke, which accounts for the symmetrical anomalies observed. However, at the magnetic equator where the inducing field is horizontal, neither the *sides nor the*

I

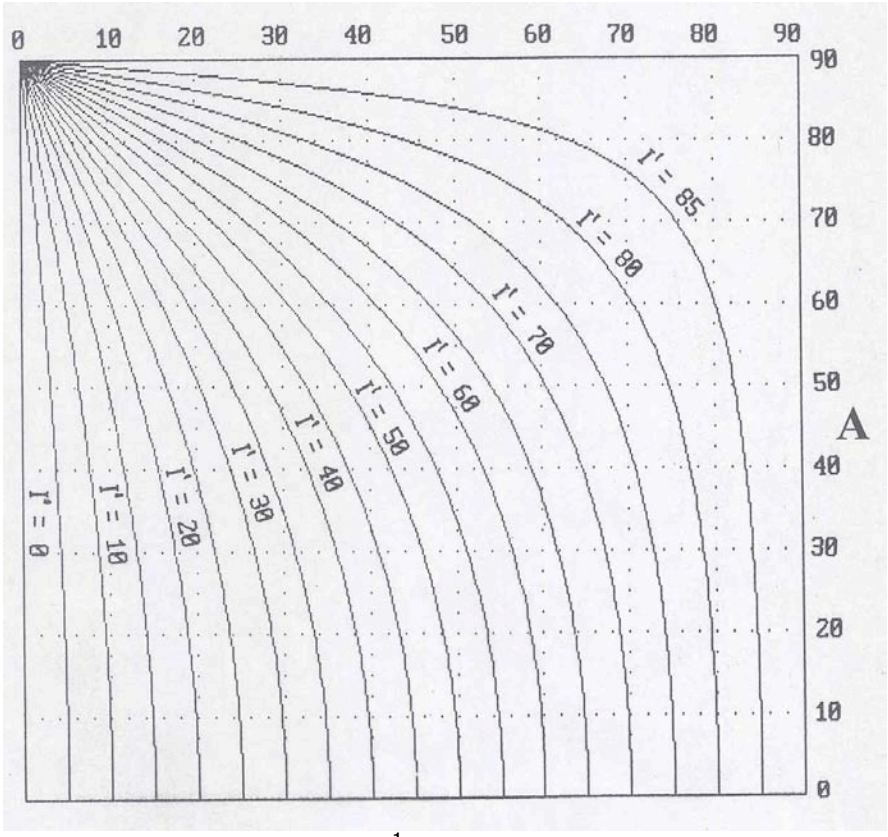

$I' = \tan^{-1} (\tan I / \cos A)$

where

I = inclination of the Earth's magnetic field

A = angle between the strike of magnetic body and east

I' = Effective inclination component of true inclination in direction perpendicular to strike

Figure 9.6 *Effective magnetic inclination, I': the effect of strike direction on 2D magnetic anomalies.*

top surface of the dyke will carry induced poles; these will occur only on the ends of the dyke at ±∞. It is thus clear that a north-south striking dyke at the earth's magnetic equator will - in theory - have an anomaly of ***zero*** amplitude. This is a 'blind spot' in the magnetic method of which the interpreter should be aware.

It follows that the process of 'reduction to the pole' for data acquired at low magnetic latitudes is doomed to failure since theory requires anomalies of zero amplitude to be transformed into anomalies of finite amplitude. Clearly anomalies of zero amplitude cannot be recognised since their amplitude is less than that of any noise present, while it is the noise, particularly poor levelling of north-south flight lines, which will acquire the amplification.

The invisibility of north-south features on anomaly maps at the magnetic equator is usually not complete, however. The foregoing discussion assumes that the magnetic properties of the body are constant along strike. This is seldom strictly true. Neither is it strictly true that the width of a dyke is exactly constant. Both these factors tend to create local anomalies along the length of a north-south striking body that betray its presence as a 'row of bubbles' on a contour map or image. See Figure 9.7 for an example.

9.4 Effect of non-infinite strike: vertical pipes.

So far the discussion has been confined to 2D bodies, i.e. to bodies of assumed infinite strike length. While the geological nature of many areas shows a tendency towards linear structures, this is by no means universal and many naturally occurring bodies are more or less circular in plan (3D). Examples are granitic plutons and kimberlite diatremes.

In fact, it can be shown that there is often no great loss of accuracy when single magnetic profiles over 3D bodies are interpreted as though they were over 2D structures. In terms of depth estimates, for example, the error from so doing is usually less than 30%.

To illustrate this similarity, Figure 9.8 shows the curve family for anomalies over vertical pipes. The first impression is that it resembles the curve family for dykes quite clearly, through some differences in detail are instructive:

(a). A circular body has no strike direction; rotation of the body about a vertical axis has no effect on the anomaly when magnetisation is solely by induction.

(b). The profiles in Figure 9.8 are for a traverse crossing the *centre* of the body. Other profiles may look different in detail and may lead to incorrect estimates of body parameters. For a 2D body, of course, all traverses are identical.

(c). The amplitude of the pipe anomaly at the magnetic equator is *half* the amplitude of the anomaly over the same pipe at the magnetic poles. This should be compared with the case of the dyke where, when striking east-west, these two amplitudes were the same, and when striking north-south at the magnetic equator the dyke anomaly became zero. (For the pipe there is obviously no effect of strike!)

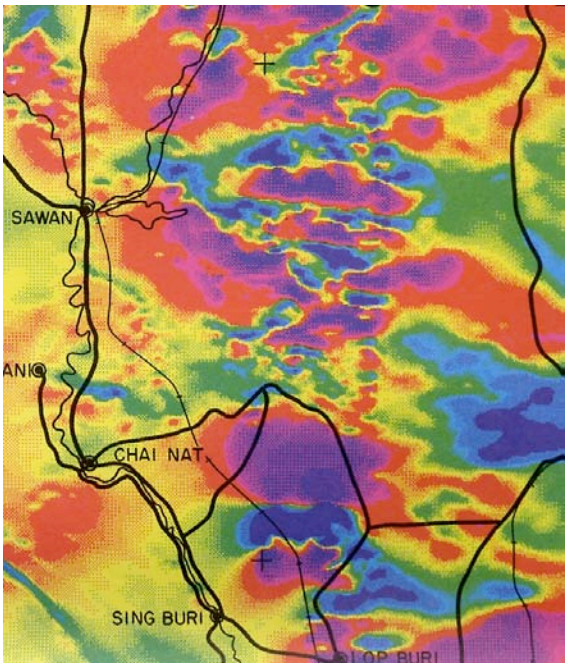

Figure 9.7 *Magnetic expression typical of north-south striking units at the magnetic equator - Thailand (courtesy of Department of Mineral Resources, Bangkok, 1989).*

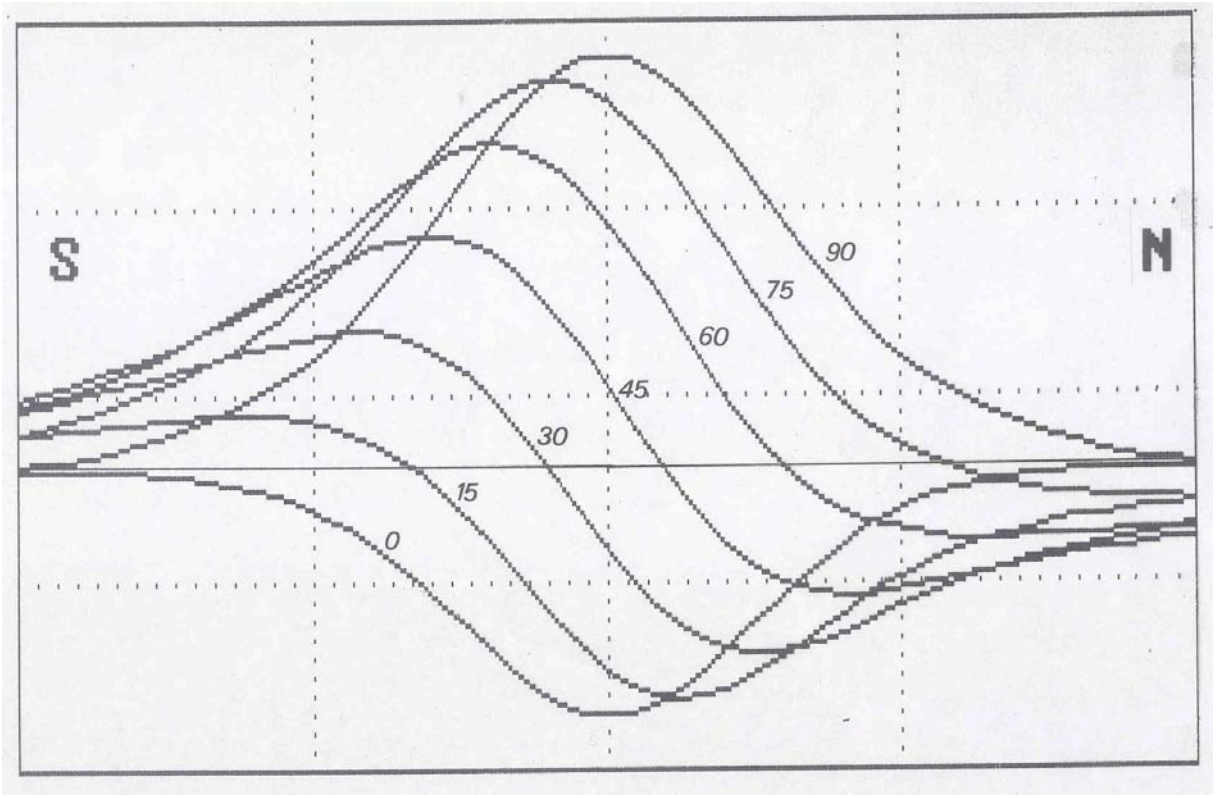

Figure 9.8 *Curve family for the anomaly over a vertical pipe as I goes from 90° to 0°.*

(d). Anomalies with equal positive and negative lobes occur in the vertical pipe case when the magnetic inclination in somewhat less than 45°, about 33° in fact. Hence, over the whole earth, circular features with induced magnetisation tend to be more often represented by anomalies with positive lobes that are larger than the negative ones, though there are many exceptions.

9.5 Interpretation of single anomalies - forward modelling and inversion

The foregoing account of magnetic anomaly shapes over common geological bodies is the background knowledge with which an interpreter should be equipped if he or she is to tackle the interpretation of a magnetic anomaly map. On such a map, usually some anomalies stand out quite clearly from the background (and the 'noise' of lesser anomalies) and may be recognised immediately as suitable cases where the theoretical anomaly of a simple body might be found to approximate closely the observed anomaly. These anomalies should be tackled first; the more difficult cases which remain often pose problems with regard to (a) identification of a sensible background level and (b) separation from adjacent anomalies. These factors test the experience and the perseverance of even the skilled interpreter!

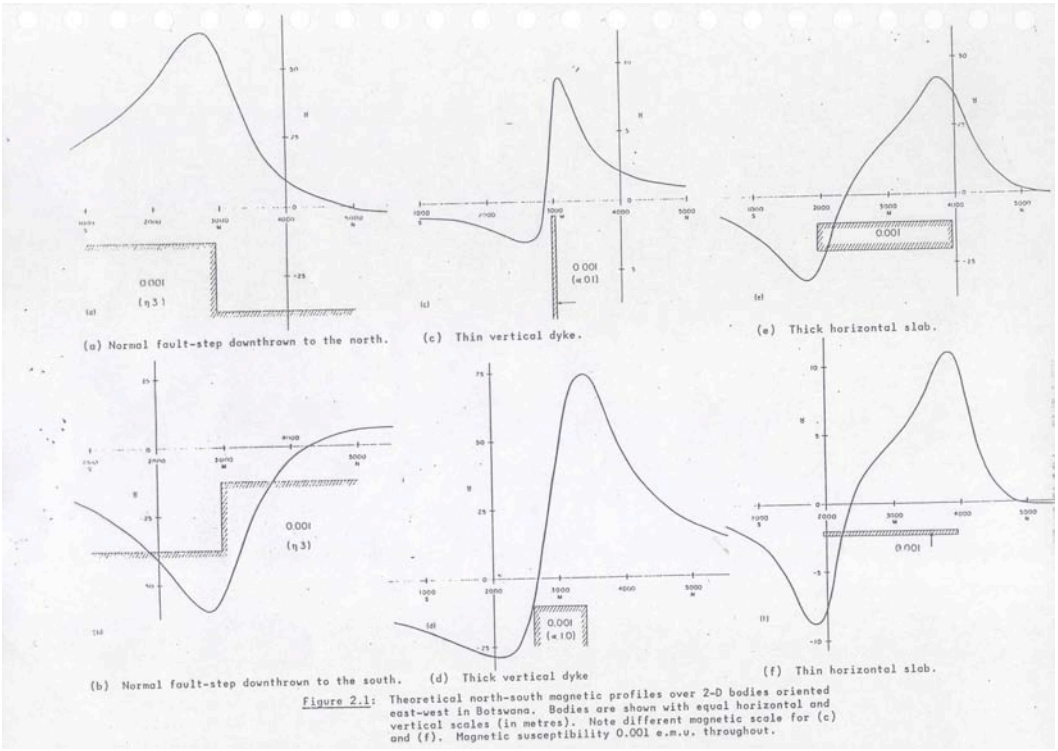

Figure 9.9 *Forward solutions for the magnetic anomalies to be expected over some typical geological bodies magnetized by induction at a given magnetic inclincation, declination and total field strength.*

The anomaly is best studied, at least in the first instance, in profile form. The profile used may be first extracted from an individual flight line, edited to cover the distance over which the anomaly exceeds, say, 10 or 20% of its peak amplitude. (The flanks are seldom so well defined that a greater distance may be usefully examined without interference from neighbouring anomalies). Alternatively, a profile may be constructed by carefully marking intersections with contour lines along the edge of a piece of paper laid on a contour map or digitally using appropriate software on a grid file. Most often the body is first assumed to be 2D and the selected traverse is more-or-less across strike. [For a truly 2D body, a traverse at any angle other than 90° to strike is simply shortened by multiplying all distances by the cosine of the angle between the traverse and the normal to the body. In many practical cases, since all distances are scaled relative to horizontal profile distances, depth estimates and all horizontal distances made from non-normal traverses may be simply multiplied by such a 'cosine correction' when necessary.]

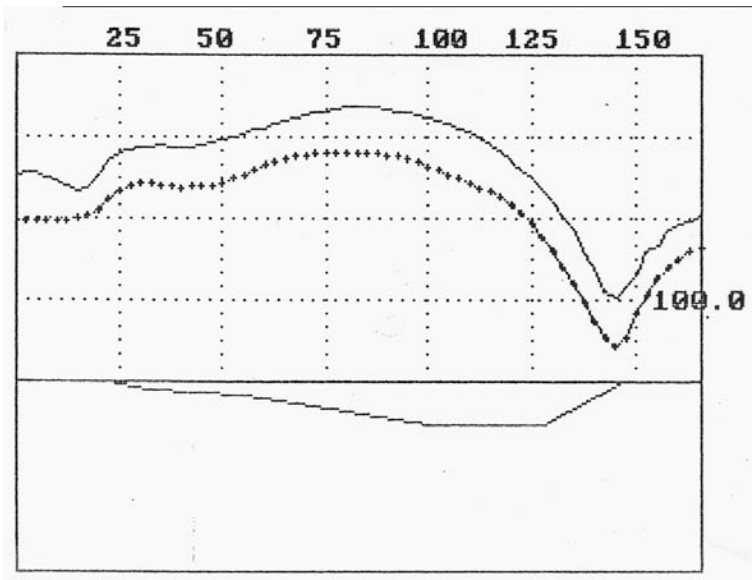

Figure 9.10 *Example of MAGPOLY interpretation. Observed anomaly as continuous line, calulcated anomaly as the crossed line. Horizontal scale in kilometers.*

The interpretation then proceeds by examining

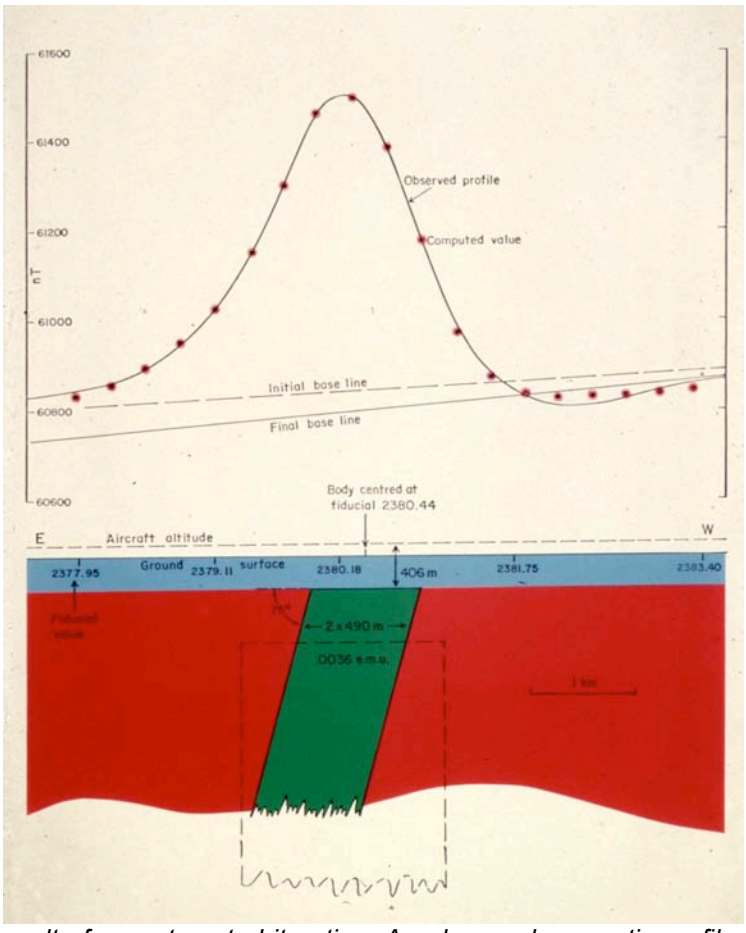

Figure 9.11 *The result of an automated iteration. An observed magnetic profile (continuous line) is matched by a number of calculated points (red dots) for a 2D body with the indicated cross section. The dashed outline indicates the initial body outline, prior to iteration. Program MAGMOD.*

the profile and deciding (from the foregoing discussion) which type of body is likely to be the source of the anomaly. This decision also requires some geological reasoning; e.g. an anomaly which is nearly circular in plan view is unlikely to be due to a fault! Given T, I and D for the survey location, forward calculations can then be made of the anomalies of likely source bodies and compared with the observed profiles. A set of such anomalies should be calculated as a starting point for working on any new area (**MTYPE** – Figure 9.9). Good forward modelling software (e.g. **MAGPOLY**) allows both observed and calculated profiles to be shown on the screen simultaneously and for changes in the body to be made readily to minimise obvious differences between observed and calculated profiles. An example of an acceptable **MAGPOLY** solution is shown in Figure 9.10.

The iteration can often be achieved automatically using more sophisticated software (such as **MAGMOD**) that displays each stage of the iterative process and allows the user to interact and fix or limit body parameters that reach unacceptable values (Figure 9.11). However, **MAGMOD** is limited to bodies of simple geometry. Sources of more complex nature may require the more intricate models offered by many-sided polygons and forward modelling under user-control.

In aeromagnetic surveys, 2D bodies are always crossed by a (considerable) number of flight lines, and the anomaly as represented on each flight line may be interpreted independently from other flight-lines. Similarity between source models on adjacent

lines gives added confidence to the robustness of the solution. Where strike-limitedness is considered important, profiles on several flight-lines may be considered to control the solution using a 3D model, such as the strike-limited and depth-limited dipping dyke formulated by Hjelt (1972).

* * * *

10.

Qualitative Interpretation and the Interpretation Map

10.1 Interpreting large numbers of anomalies

In an aeromagnetic survey it is often necessary to obtain depth (or sometimes dip or other parameters) for all the anomalies recorded on every flight line. This may involve working with many thousands of anomalies. While the principles introduced in the previous section remain valid, expediency requires that the practical task be carried out by recourse to automated (often proprietary) inversion processes, several of which have been discussed (but not always fully published) in the literature. Plotting all depth estimates on a map enables contours of the depth of the so-called 'magnetic basement' (igneous and metamorphic rocks lying below sediments and surficial cover) to be contoured. Mapping dip values may also enable the geological structure of (e.g.) a greenstone belt to be worked out in more detail (e.g. Figure 10.1).

Historically, many techniques of anomaly modelling have been applied almost exclusively to profile data from flight lines. A typical output from the so-called ‘Naudy’ method from the 1970s is shown in Figure 10.2. It should be remembered that the ‘depths’ are really source-sensor distances until the terrain clearance of the aircraft has been subtracted from each result. The errors in depth estimates obtained by methods of these types are usually quoted as ±15-20% and reflect mostly the uncertainty in the choice of model type. For example, a body forced to fit an observed anomaly may be a broad, shallow dyke, while its natural counterpart may be narrower and deeper but with very little difference in its theoretical anomaly. Where the terrain clearance is a large part of the vertical distance estimated (e.g. where the anomaly sources are (sub-) outcropping) the errors may then appear quite large and may even indicate negative depths. (E.g. 100 m ± 20 m ‘depth’ estimate less 100 m terrain clearance gives 0 ± 20 m for the depth of burial).

Two methods applicable to gridded data have become popular in recent years, largely on account of their implementation within user-friendly software packages.

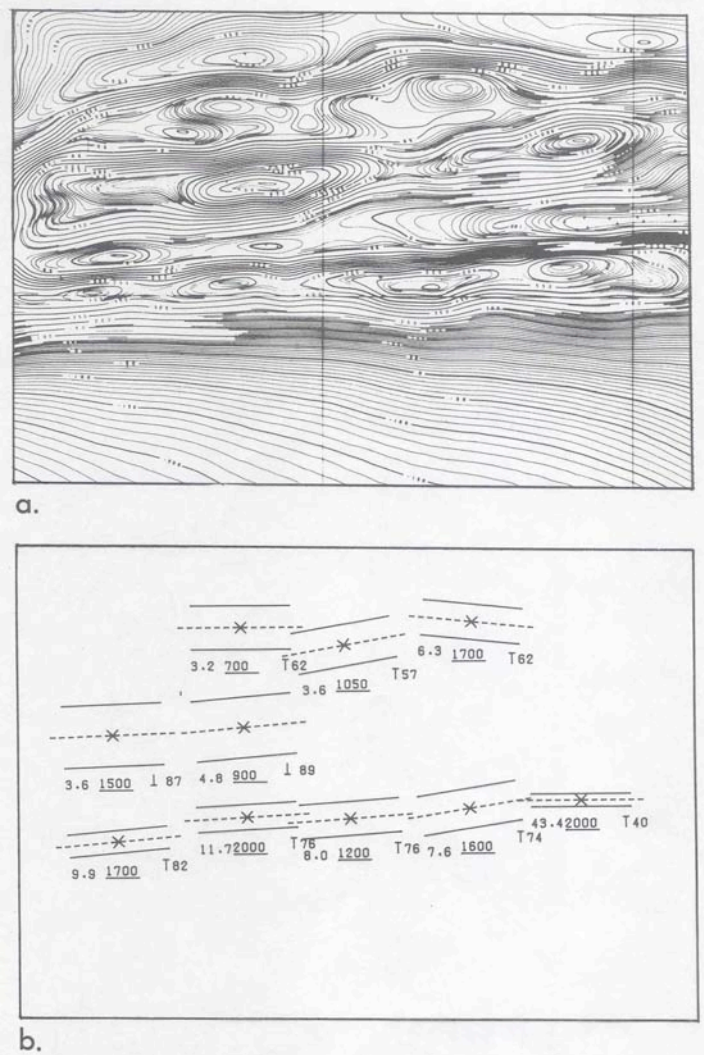

Figure 10.1 *(a) Magnetic anomaly contours. (b). Results of modelling anomalies, plotted in plan with dips, depths and magnetic susceptibilities.*

The first of these is known as ***Euler deconvolution*** (Reid et al, 1990) and exploits Euler's inhomogeniety relation to estimate source depths and positions from the maximum curvature of anomalies present in an aeromagnetic survey grid. A plethora of solutions can cause confusion to the unskilled or uncritical user, but the ability of the method to give mathematically reliable results for the positions of features in plan by a simple process is an important step in the progress from the continuously varying potential field anomaly pattern to the essentially ***dis***continuous geology that we seek to understand and map. The linearity of fracture patterns that emerges in many areas when Euler deconvolution is applied gives quantitative support to the 'lineaments' that any observer will recognise in a magnetic anomaly map, but that will almost certainly court disagreement from a second, critical observer if there is no objective substantiation. An example of Euler deconvolution in map format is given in Figure 10.2.

A second approach is called the ***analytic signal***. The idea (Roest et al, 1992) is to present magnetic anomaly information stripped of the dependence on the inclination of the earth's inducing field so that anomalies are positive and sit directly above their sources. This can be achieved also through reduction to the pole (MacLeod *et al.*, 1993). While this latter approach suffers difficulties of directional noise amplification in surveys flown at low magnetic inclinations, the analytic signal approach offers some independence from the effect of strike direction. In terms of the family of dyke anomaly curves dealt with in Sections 8 and 9, it may be noted that the analytic signal is the positive envelope to the curve family (Figure 10.3). The user must take care to note that not only magnetic bodies but also magnetic (geological) contacts produce positive analytic signal anomalies and that - unlike the anomalies we are more familiar with in potential fields - analytic signal anomalies are not simply additive.

It should be kept firmly in mind in using magnetic anomalies to map basement depth that the basic assumption is that anomalies arise mostly from magnetic inhomogeneities in the crystalline rocks and that these inhomogeneities reach the surface of the magnetic basement (see Figure 10.5). Inevitably, some bodies will lie entirely below the basement surface, while intrusions of more recent age may penetrate into the overlying

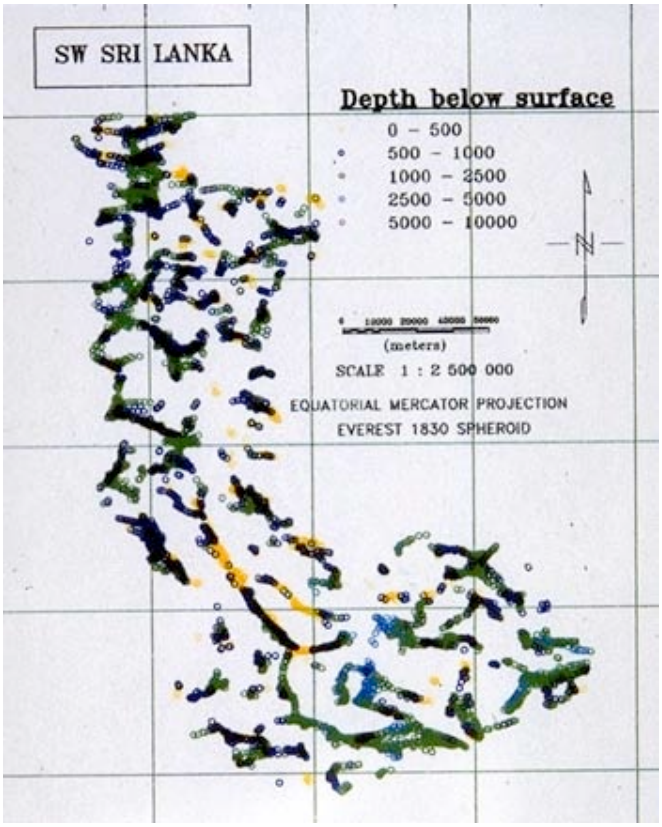

Figure 10.2 *3D Euler solutions from analysis of aeromagnetic data over SW Sri Lanka (Perera, 1997).*

sediments. Thus a certain amount of geological thought, caution and knowledge must be worked into the drawing of depth contours. Being truly an 'interpretation', the results of any one worker will include a certain amount of creative thinking which may differ from that of another. This is not a criticism. The objective is to produce a simple earth model that is consistent with all known data (including, for example, drilling results). As with all scientific models, the result should satisfy two criteria: (1) be an adequate explanation of all known data and (2) be capable of being tested by future experiment. In practice, in exploration, models are proved, disproved or refined as new information (drilling, for example) becomes available over time.

A frequent misconception in depth-contouring from magnetic survey data is that it is the *topography* of the magnetic basement surface that gives rise to the anomalies in much the same way as in the gravity case. Usually the topography of this surface is so subdued and the *average* magnetic susceptibility of the basement is so low that results based on this model are physically impossible. Much more important in fact are the local magnetic inhomogeneities (i.e. isolated, highly magnetic bodies in the basement) which give rise to the major anomalies of an area.

The current success of both analytic signal and Euler deconvolution techniques in the user community is due largely to their ability to contribute to interpretation in a qualitative sense; they have become new, semi-quantitative aids to visualisation. But visualisation is ***not*** interpretation - unless we resign ourselves to the idea that interpretation, like beauty, lies only in the eye of the beholder. Such a stance denies the value of the detailed thought processes and experience from other terranes that the professional interpreter brings to a serious interpretation project.

10.2 Concluding remarks on quantitative magnetic interpretation.

Finally, it may be observed that all quantitative interpretation methods give good, reliable results on well-defined, well separated anomalies, as may be shown by testing their performance on independently calculated theoretical profiles rather than field curves.

A practical limitation to accuracy is that the choice of model may be incorrect. Excellent fit of observed and calculated profiles is no guarantee that the model choice is correct; other models may provide equally good or better fits. The best support for interpretation

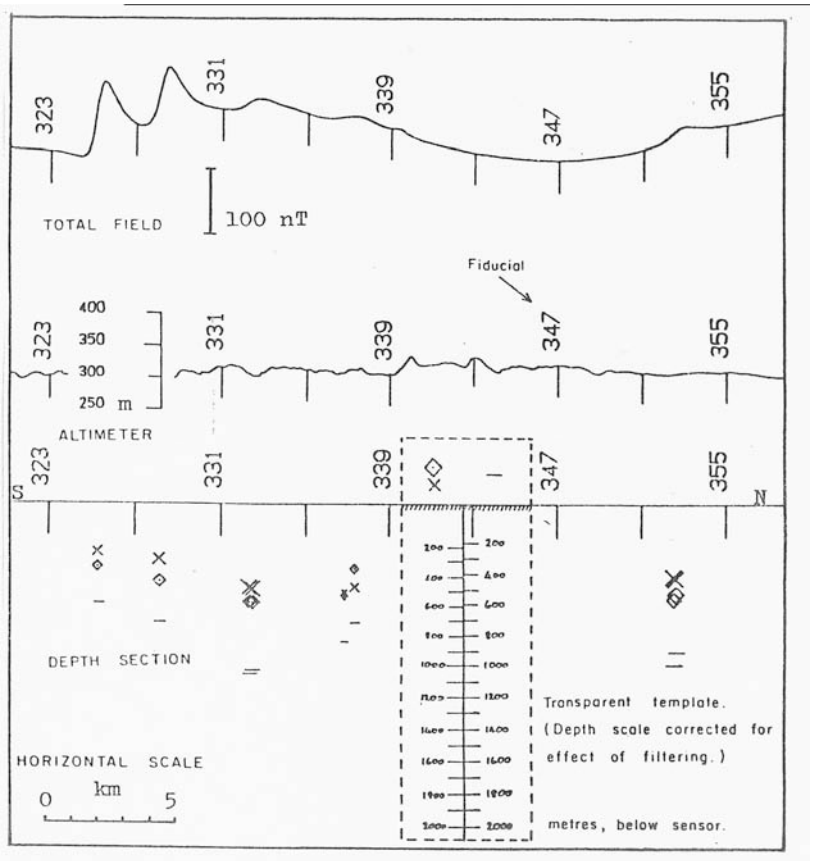

Figure 10.3 *The Naudy 'automatic' depth interpretation method employed on a single magnetic profile.*

comes from independent sources. For example, where a fault is interpreted to be nearly outcropping from a magnetic survey, a coincident ill-defined lineament on a satellite image gains new significance.

In practice, the quality of each interpretation is usually limited by the certainty which may be placed in the regional or base level of a chosen profile section and the degree to which each anomaly is free from interference from its neighbours. These practical problems place a real restriction on the number of anomalies in any one survey that are well-enough defined to merit detailed quantitative interpretation. The dedicated interpreter struggles on to reach this limit. Though the process may be time-consuming and tedious, the full value of the data should be realised in the interpretation.

10.3 Qualitative interpretation.

What is called 'qualitative interpretation' of aeromagnetic surveys is usually undertaken as an aid to geological mapping, often using the property of magnetic surveys to reveal the magnetic signature of the crystalline bedrock, even where it is covered by superficial deposits and thus invisible to the conventional field or photogeologist.

The first stage of this process is simply to prepare the geophysical data and the best available geological data at the same scale and projection (one of them preferably on a transparent overlay or both of them in a GIS platform) so that they may be directly compared. Usually there are some obvious correlations between the two data sets in the outcrop areas that allow geological deductions to be made from the geophysical data in the areas lacking in outcrop. This leads naturally into the process known as 'zoning' of the aeromagnetic map that is an important part of the qualitative interpretation process.

Zoning involves the outlining of those areas of well-defined physical expression on the aeromagnetic map that appear to the interpreter as distinct geological units. Note that one zone typically may contain many hundred individual anomalies that often have a

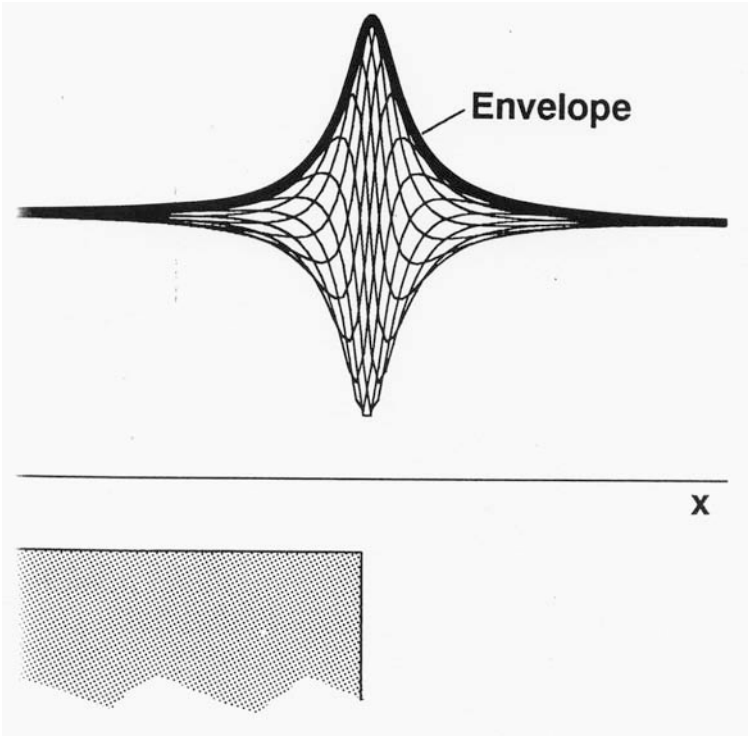

Figure 10.4 *The absolute value of the analytic signal is known as the energy envelope. (From Roest et al., 1992).*

common pattern, such as shape or amplitude of anomaly. The techniques of recognition of these zones are often similar to the criteria used by the photogeologist working with air photographs or satellite images. Figure 10.6 shows an area of an aeromagnetic map displaying several different types of magnetic signature associated with different rock types and its interpretation.

An example of the success of this process in improving detail on the geological map in a poorly-exposed area is Ivory Coast where a survey of 400 000 line km was carried out in 1974-76 and interpreted 1976-80 (Grant *et al.*, 1981). The geological map of the area suffers from the lack of exposure that inhibits geological mapping in the thickly forested and deeply weathered terrain. The aeromagnetic map of the same area shows intense detail, the qualitative interpretation of which provides a great deal of extra information (Figure 10.6), such as the location and extent of greenstone belts which might, for example, be explored for massive sulphides using airborne EM.

To assist in the zoning process - and in the delineation of structural features such as faults - considerable use has been made of equivalent earth susceptibility maps (see Section 7.3). The magnetic basement is assumed to be made up of semi-infinite vertical prisms with square tops centred on the nodes of the gridded magnetic data. By an inversion process, a magnetic susceptibility is ascribed to each prism. Commonly, the depth to the top of all the prisms has been a constant value below the survey flying height, either the ground surface or some deeper level. More recently, methods have been devised which allow the prism tops to constitute an irregular surface, such as may be determined from magnetic depth estimates or drilling information in the study area. This allows the susceptibility boundaries, as revealed by contours of the individual prism susceptibility values, to be brought more sharply into focus in the susceptibility map, and hence to facilitate the zoning process for a metamorphic basement below nonmagnetic cover of varying thickness (see, for example, Pilkington 1989).

The zoning process is, of course, subjective. To ensure rigour it is best thought of in two phases:

1) dividing a map into geophysically similar units based on the physical description of anomaly patterns;

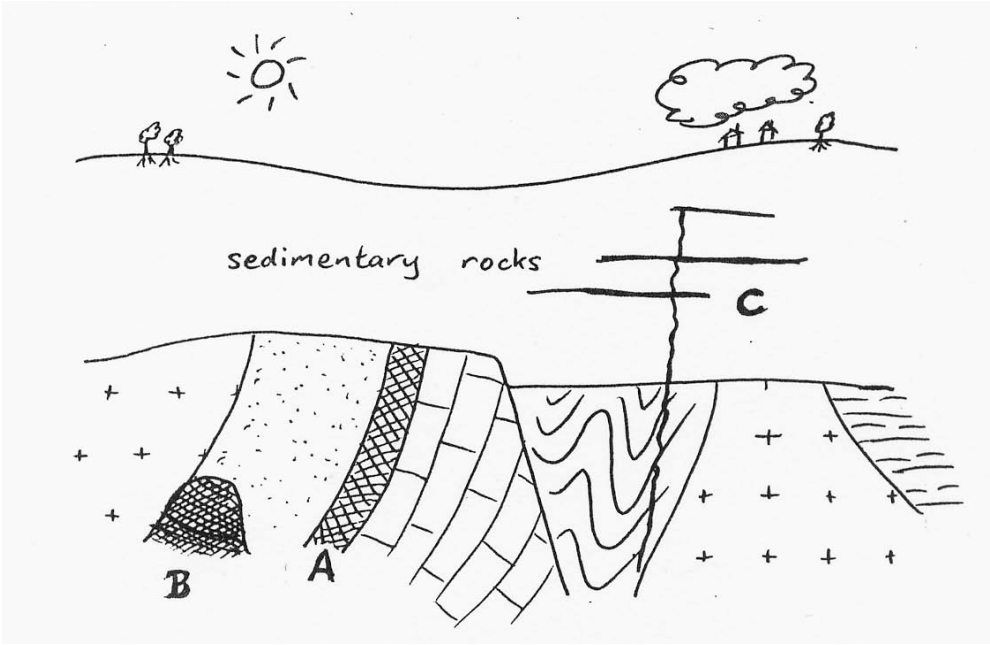

Figure 10.5 *The concept of the 'magnetic basement' and its flaws. Magnetic anomalies often arise from rock units reaching the interface between the igneous and metamorphic rocks and the overlying (non-magnetic) sediments (e.g. unit A). Other units used as depth indicators, such as B, may not reach this surface, while others still, such as C, may reach a higher level giving erroneous indications of the basement depth.*

2) ascribing geological names to the geophysical units with due reference to the information on any available geological map.

In principle, the geophysical map could be divided into an infinite number of geophysical units, each closely defined in terms of anomaly amplitudes, shapes of body outlines, spacing of magnetic lineations, and so on. In practice, the number of pigeon-holes into which identifiable zones may be placed has to be kept to a manageably small number, perhaps 20-30. We are concerned with an essentially descriptive process and description also implies simplification; description of every single anomaly is eventually less helpful than a few well-considered generalisations about anomaly pattern types. By the same token, a geological map is a generalisation and a simplification of field observations, designed to convey a general impression of the geology, and the geological legend usually contains only a few tens of entries.

The generalised geophysical units (or zones) can be defined in type areas (e.g. where geological exposure - or the quality of the geological mapping - is good), but outside the type area, other zones can show (e.g.) a majority of the same physical features, but also fail to show all of them. Is this a new or a different geophysical zone, or can it be categorized along with an existing type? Answering this question requires the establishment of thresholds of similarity - subjectivity is inevitable, but attempting to reduce it requires perseverance.

Experience seems to indicate, however, that any purely geophysical classification of rock units leads to the situation where, upon comparison with the geological map, a geophysical entity contains several distinctly different rock types and, conversely, that a single geological rock unit can contain several geophysically distinct units.

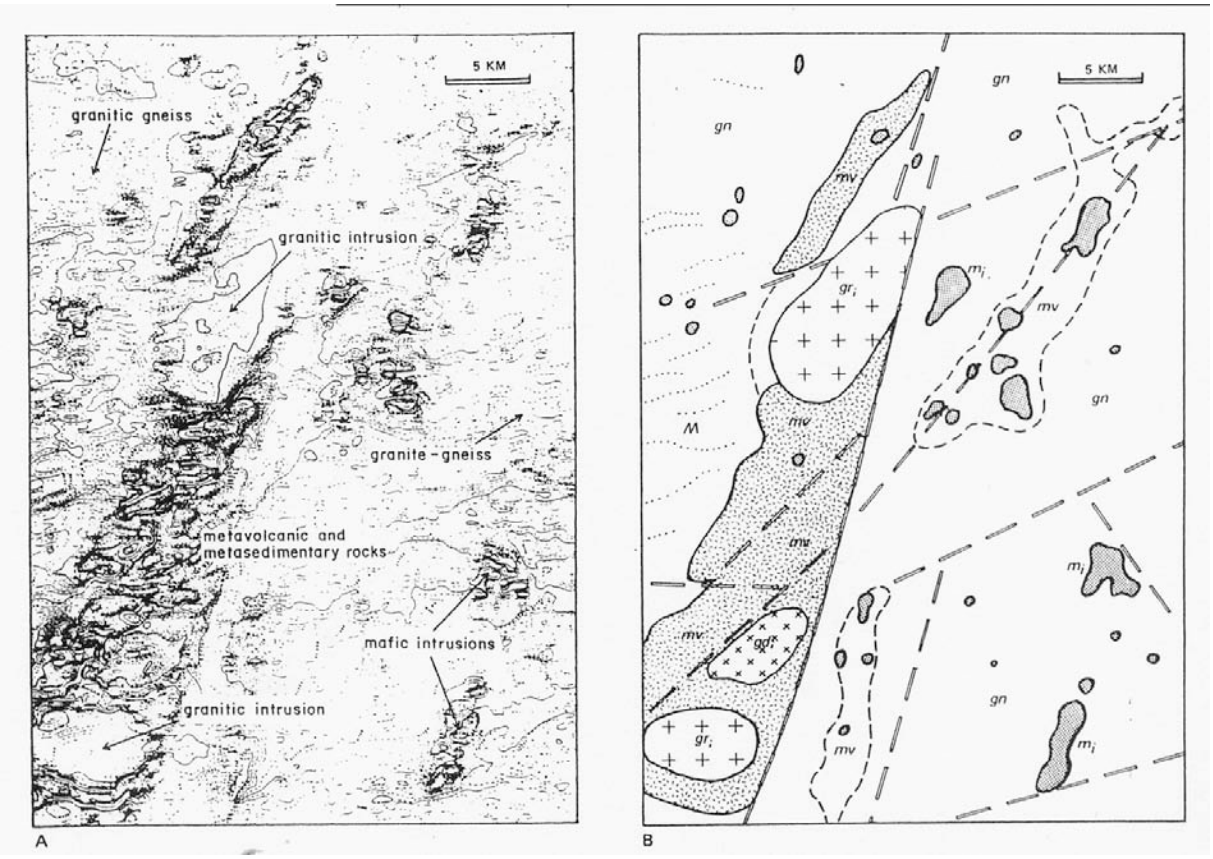

Figure 10.6 *(a). Examples of magnetic signatures. On a magnetic total field contour map from a survey over various igneous and metamorphic rock types. (b). A qualitative interpretation of the same area. Large dashed lines represent faults; solid lines - geological boundaries; broken lines - gradational geological boundaries; dotted lines - magnetic axes. Gn = gneiss; gri = intrusive granite; mi = mafic intrusion; mv = metavolvanic and metasedimentary rocks; M = migmatites; gdi = intrusive grandiorite.*

10.4 Integration with the geology.

To what extent, then, can any geophysical zoning be reconciled with the geology? The objective, after all, is to improve knowledge of the geology, and the geophysicist will quickly lose the confidence of the geologist if he or she re-draws the geological map at a stroke. At the other extreme, a lot of progress in the earth sciences would never have occurred if the geophysicist had blindly accepted current geological ideas as unchangeable. Clearly we are normally faced with a compromise. What are some of the factors to consider?

(1). Geological maps are imperfect. Where outcrop information is shown, it must be honoured in the geophysical interpretation. Where extrapolation of geological units between outcrops across large unexposed areas is shown - particularly in areas of complex metamorphic terrain - the geophysical interpreter should assert his freedom and use it wisely.

(2). Geophysical information (except for spectrometer surveys) comes from rock units at depth, as well from those at or near the surface. This is a strength of geophysical methods, making them more powerful than any other remote sensing method which only relies on information from reflections at the earth's surface. The results of quantitative

interpretation, taken together with the digitally processed map products, will help the geophysicist decide which units may outcrop, and which occur only at depth. Clearly there may be a disagreement between rocks seen to outcrop at the surface and those interpreted geophysically to occur at depth. The outcropping rocks (e.g.) may be simply non-magnetic sediments overlying the magnetic basement.

(3). Aeromagnetic surveys reflect almost exclusively the distribution of magnetite and pyrrhotite in rocks. This is fundamental - but often overlooked! Magnetic minerals are only accessory minerals and the geological descriptions of rocks seldom pay much attention to them. But they are almost the only mineral 'seen' in an aeromagnetic survey. On the positive side, we are fortunate that magnetic mineral distribution can tell us as much as it does about the geology; we should not be too surprised when it fails in detail. It is surprising, however, that for a method as widely used as magnetic survey, the magnetic rock property that gives rise to the method has been so little studied from the point of view of assisting survey interpretation. Consider, for example, the problem of the distribution of magnetite in areas where metamorphism and deformation have re-worked the bedrock repeatedly. In such circumstances the resulting distribution of magnetite may reflect only a paleo-lithology derived from the ancestral rock. In Ivory Coast (Grant *et al.*, 1980), it was repeatedly found that areas having magnetic characteristics typical of volcano-sedimentary rocks or greenstones turned out to be indisputably mapped as granitic. As such they would be expected to have the low magnetic relief typical of rather homogeneous, weakly magnetic rocks. In some areas of Ivory Coast the rocks have been mapped by geologists as 'heterogeneous granites'. Their geophysical character, however, suggests alternating tholeiites, greywackes and banded-iron formations. A photogeological study described them as 'migmatised volcano-sediments'. In one instance they cover an area roughly 200 km by 50 km - typical of some of the larger greenstone belts of the Canadian Shield. Now granitised, they may yet have possibilities for mineralisation which have been overlooked until now.

10.5 Concluding remarks on aeromagnetic interpretation

There already exists a large body of regional geophysical data - mostly aeromagnetic data, but often with some supplementary spectrometer results - and it seems unlikely that the rate of acquisition of new data will decrease in the years ahead. Meanwhile; surveys, even of a reconnaissance nature, remain to be carried out in many countries. It would appear that too little use is being made of the data that are presently available and the thorough integration of airborne geophysical results into geological mapping and regional exploration projects receives scant attention, both in the geophysical literature and from the earth science community at large.

The interpretative and deductive processes involved demand a judicious balance between the mathematical rigour of the geophysicist and the descriptive skills of the geologist. Together they form a legitimate intellectual exercise that should contribute both to the basic geological knowledge of an area and to reducing the risk factor in an exploration venture. Individuals will have different ideas as to where the process should stop. Mathematical rigour alone is unlikely to contribute much to geological understanding. On the other hand, any interpretation that abuses the principle of 'economy of hypothesis' is unlikely to gain much support either from the geophysicist or the geologist.

Probably a larger number of individuals should attempt their own interpretations. At a minimum level this requires only preparing transparencies of the geophysical data at the same scale and projection as the geological map, observing the 'thumbprints' of the known geological units and extending these to depth or to unexposed areas with the geophysical guidance and simple deductive reasoning. If gravity data are available - as they often are - this is a further contribution of information, and the value of both gravity and magnetic data together is almost invariably greater than that of the two taken separately, even if the gravity stations are comparatively widely spaced. Regional geochemical data and drilling results (from groundwater development, mineral and petroleum exploration) are also invaluable; they help give controlled feedback from geological reality to the quantitative and qualitative parts of the interpretation exercise. New results, particularly drilling results subsequent to an initial interpretation, signal the need to review and, perhaps, revise an old interpretation. Perhaps the greatest value of regional geophysical data ultimately is that it places physical constraints on the possible geology - especially in the depth dimension - and must therefore be referred to repeatedly over time as understanding of the geology of an area evolves. This theme is taken up by Riddihough in Figure 10.7.

For the explorationist, it must be said that regional geophysics is unlikely to lead directly to an ore body or an oil field but should give excellent guidance in a logically planned exploration programme. In frontier petroleum exploration, for example, if it gives some idea of gross structure and guides expensive seismic surveys away from areas with little or no thickness of sedimentary section or from planning seismic lines parallel to geological structures, then investment of time and effort in aeromagnetic data acquisition and interpretation is clearly worthwhile. Turning to mineral exploration in metamorphic terranes, regional magnetic and gravity data may be sufficient to direct work towards the greenstone belts and away from the relatively barren granites and gneisses. In the case of massive sulphide exploration, this may already be a sufficient contribution to enable the geophysicist to plan airborne EM surveys so that the expenditure involved is concentrated in those areas most likely to be rewarding.

Compilations of aeromagnetic data on continent-wide scales will almost certainly lead to new insights into the tectonic processes which shaped the continental crust and controlled mineralisation during Precambrian times. The results, however, are unlikely to be as spectacularly simple as the pattern of magnetic stripes that have already given a vital clue to the history of development of the earth's oceanic crust.

Clearly, much remains to be done if the maximum benefit from the existing regional airborne geophysical surveys around the world is to be obtained and if they are to be used to make well-considered recommendations for future phases of exploration. This is certainly an area where a close liaison between geologist and geophysicist can be expected to pay dividends, and the lessons learned will be invaluable in interpreting not only other existing surveys, but also those certain to be flown in the years ahead.

10.6 Some examples of aeromagnetic interpretation maps

By way of illustration, these notes conclude with a number of examples of aeromagnetic interpretation maps. The figure captions summarise something of what is to learned in each case, but the maps themselves should also serve as examples of what may be achieved in any interpretation exercise.

WHAT GRAVITY AND MAGNETIC DATA CAN DO FOR YOU

Ten Commandments

by Robin Riddihough, Senior Scientific Executive Officer,
Geological Survey of Canada

1. Gravity and magnetic surveys are both methods of REMOTE SENSING. They can detect the properties of rocks at a distance - from the air, on the ground or at the sea surface.
2. Anomalies and changes in the value of gravity (after allowance for varying elevation and topography) reflect changes in DENSITY.
3. Anomalies and changes in the value of the earth's magnetic field (after allowing for changes with time) reflect changes in MAGNETISATION.
4. These two properties of rocks are often diagnostic. Taken together they can eliminate many possible geological alternatives and provide fundamental constraints on a geological model.
5. Both gravity and magnetic anomalies are a function of the distance between the detector and the sources (rocks). Amplitudes decrease faster with distance for magnetic anomalies therefore they tend to 'see' shallower structures. Both methods however, provide an INTEGRATED depth spectrum of the sources they are seeing - they see much more than just the surface rocks.
6. There are two principal approached to interpretation - PATTERN and SHAPE.
7. The PATTERN of a gravity or a magnetic anomaly map is a powerful indicator of how subsurface rocks and formations are distributed. It can provide rapid indications of TRENDS, GRAIN and DISCONTINUITIES. The style of the pattern may be diagnostic of a particular rock sequence or assemblage (for example: sea-floor magnetic anomalies).
8. The SHAPE of individual anomalies can be used to determine the shape and position of density of magnetic contrasts (rock units). In theory, there are a number of geometries that will 'fit' a particular anomaly. IN PRACTICE, by using realistic geological or other geophysical controls, anomaly 'fits' will provide REAL NUMERICAL CONSTRAINTS on the anomaly sources.
9. However, always understand and appreciate the weaknesses and inaccuracies of the data. Never waste time trying to 'fit' anomalies with greater precision that they were measured at.
10. Any final interpretation must satisfy ALL the available geophysical and geological data. Gravity and magnetic anomaly information cannot be ignored. It will not go away. It is real and it is telling us something even if we do not always understand it and even if it appears to be contradicting the surface geology.

Figure 10.7 *The Ten Commandments of potential field interpretation (Riddihough, 1986)*

Figure 3

Figure 2

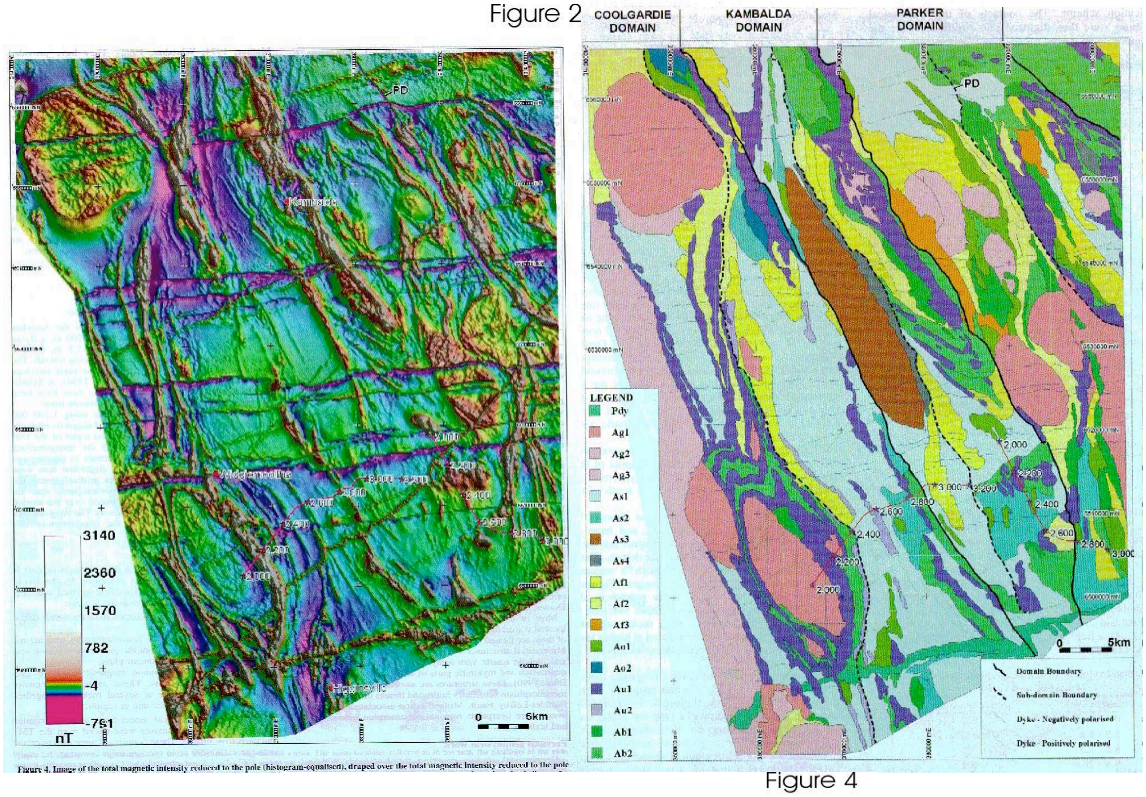

Figure 4

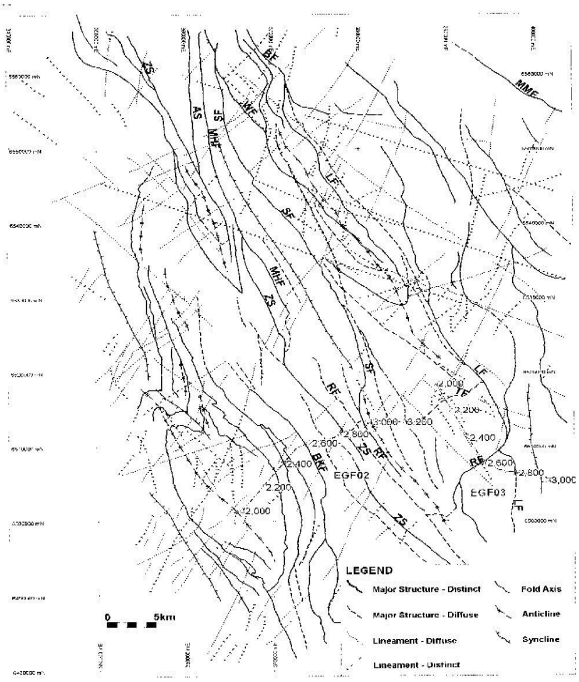

Figure 10.8 *(a) Aeromagnetic anomaly image of an area in Western Australia. (b) Lithological interpretation of the data – an area of poorly-exposed Archean basement terrane. (c) Structural interpretation. The area is clearly cut (on the aeromagnetic anomaly image) by a number of east-west striking dykes. These are not shown on the interpretation maps. (from House et al., 1999).*

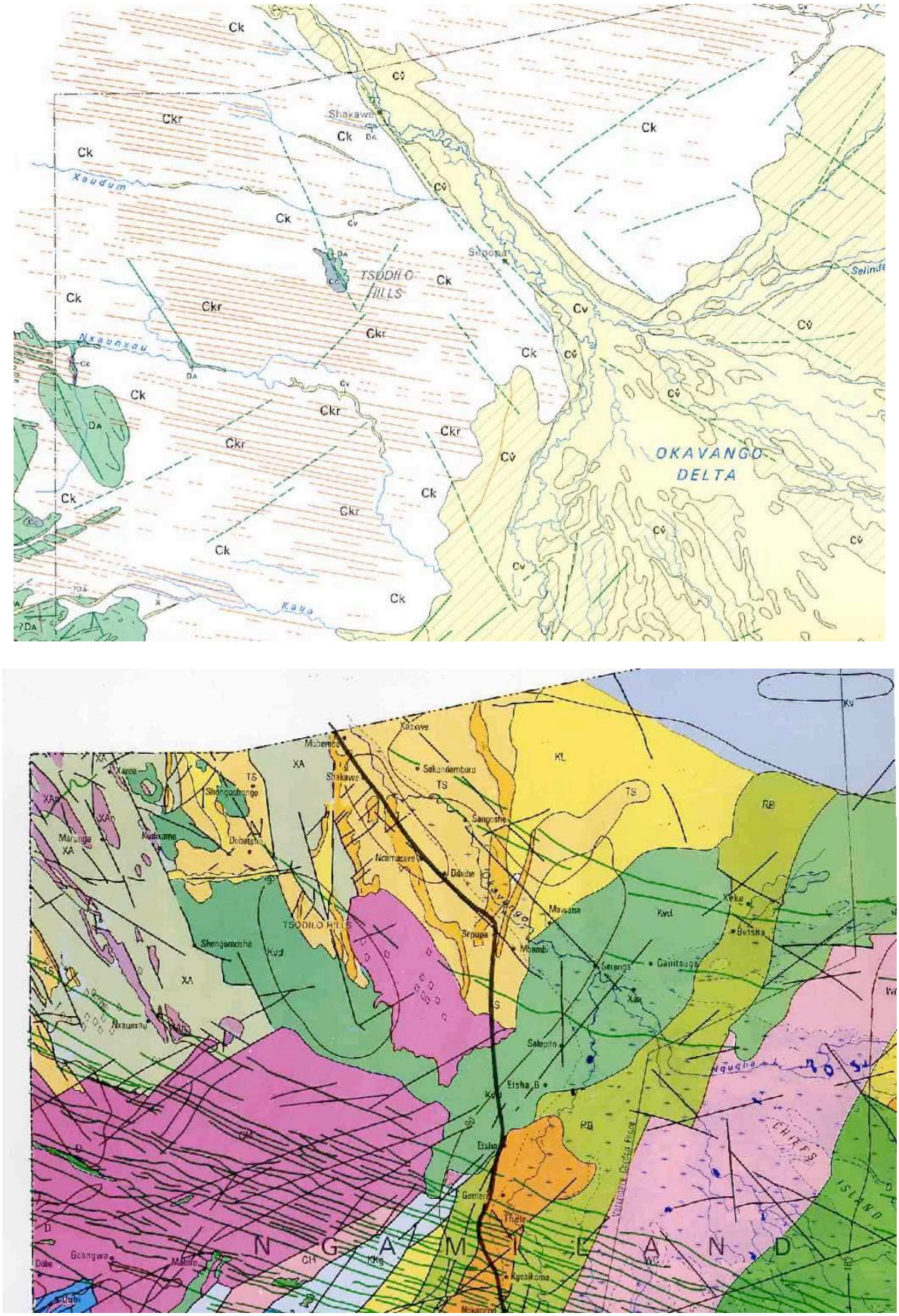

Figure 10.9 *(a) Landsat interpretation of the NW corner of Botswana (from BGS report). (b) Aeromagnetic interpretation map from a detailed survey conducted in 1999 (from BRGM report).*

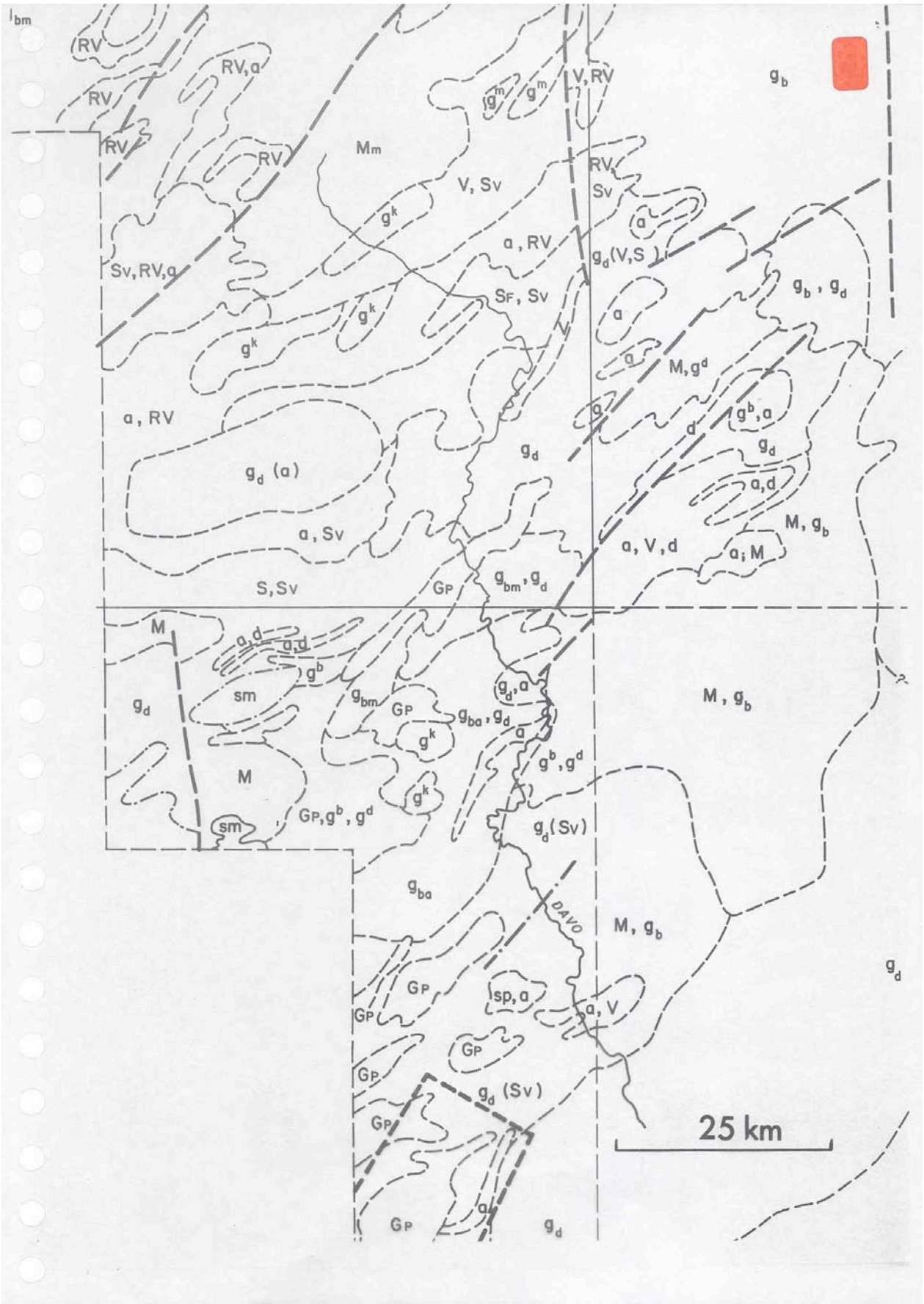

Figure 10.10 *A small area of the national aeromagnetic interpretation of Ivory Coast, 1980.*

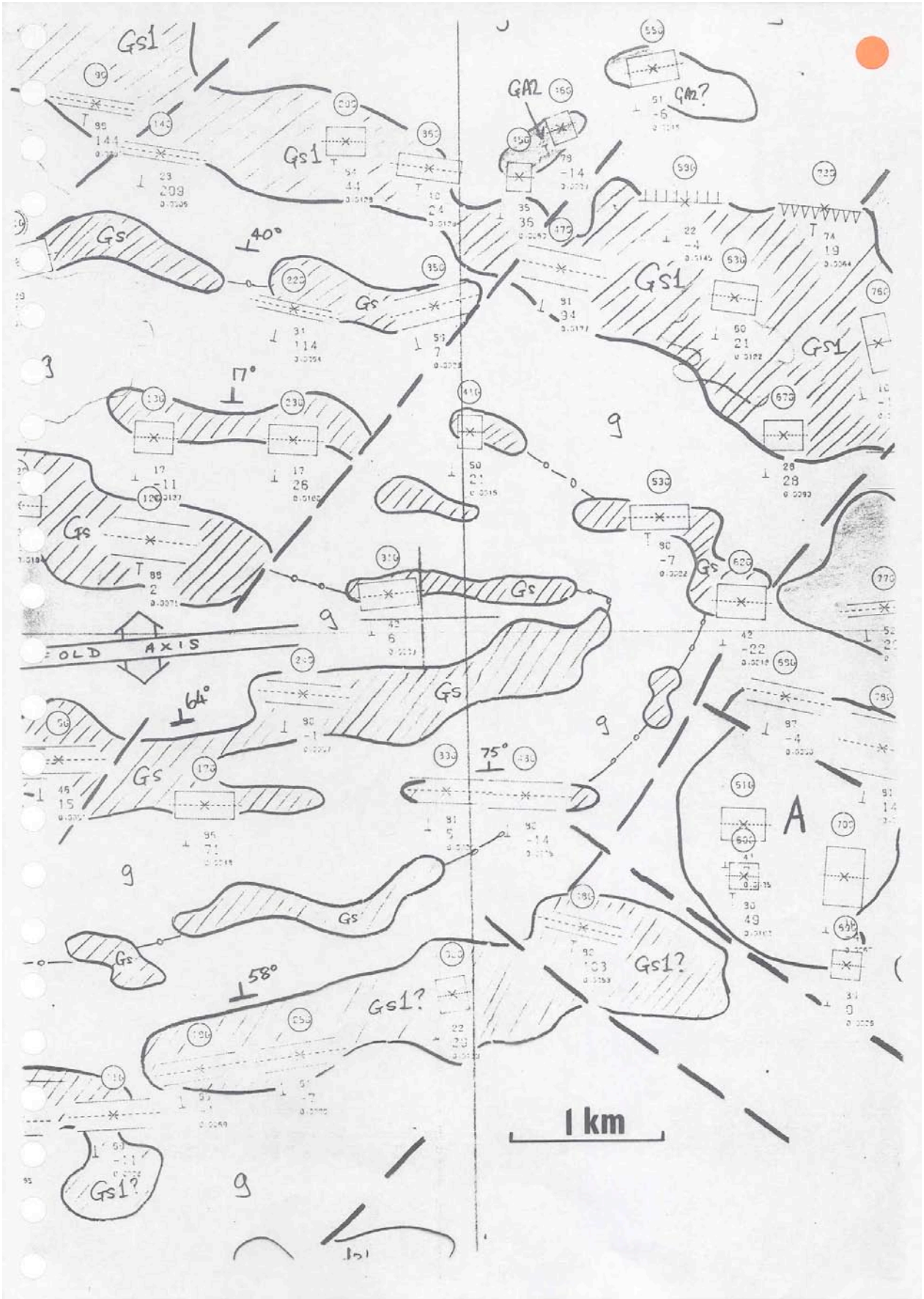

Figure 10.11 *Detailed interpretation map of a small area of the Canadian shield. The qualitative interpretation is supported by a number of quantitative models, the outlines of which are indicated on the map at true scale.*

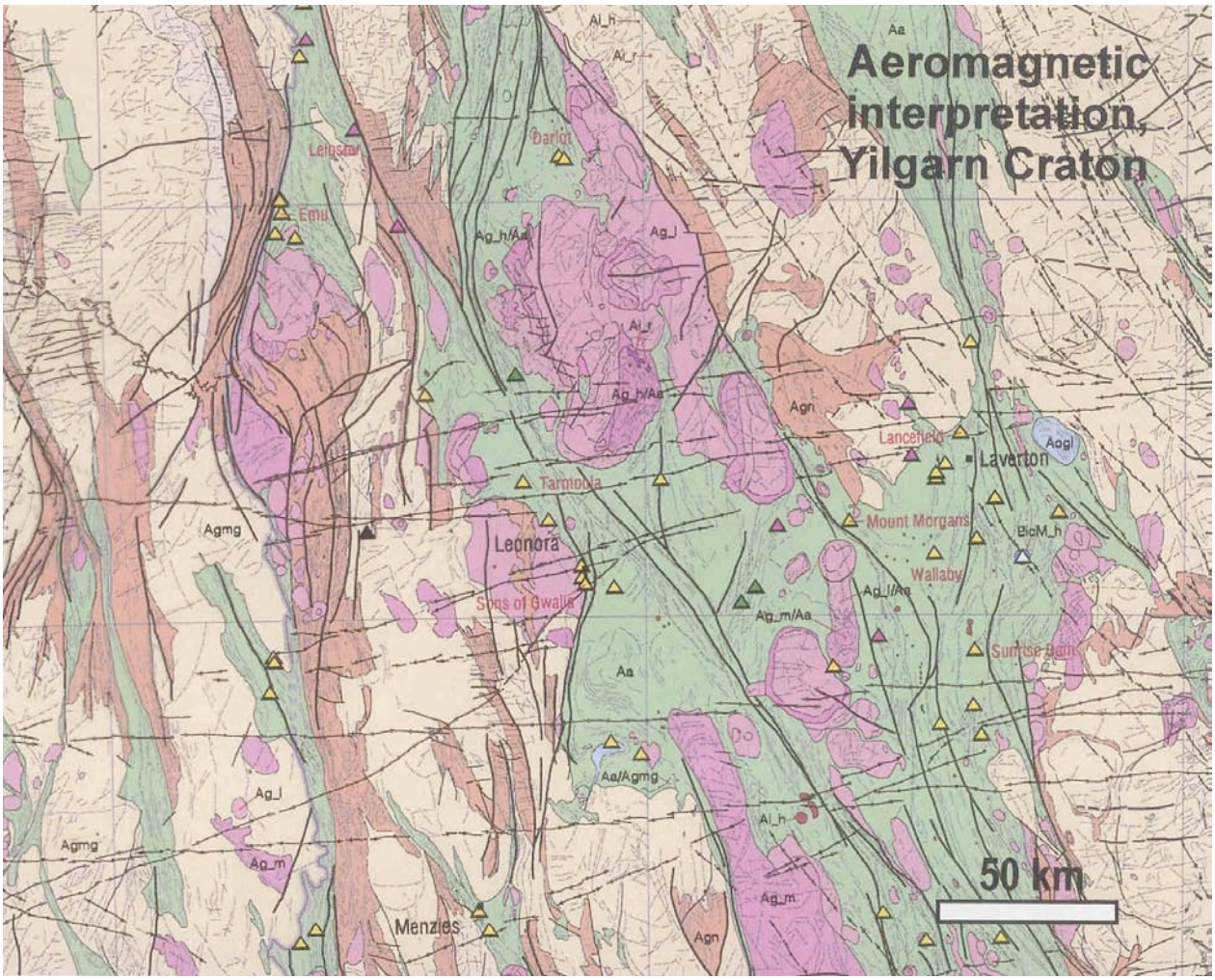

Figure 10.12 *An area of the aeromagnetic interpretation map of Western Australia (courtesy of Geoscience Australia and the Geological Survey of Western Australia). This is an area of Archean granite-greenstone terrane that is a significant gold producer (yellow triangles). Proterozoic dykes are in evidence, cutting the older rocks.*

*** *** ***

REFERENCES

A

Akima, H., 1970. 'A new method of interpolation and smooth curve fitting based on local procedures', Journal of the Association for Computing Machinery, Vol. 17, No. 4, pp 589-602.

Astier, J-L, and Paterson, N.R., 1989. Paper 59: Hydrogeological interest of aeromagnetic maps in crystalline and metamorphic areas *in* Proceedings of Exploration '87: third decennial international conference on Geophysical and Geochemical Exploration for Minerals and Groundwater, edited by G.D. Garland, Ontario Geological Survey, Special Volume 3, pp 732-745.

B

Barritt, S.D., 1993. The African Magnetic Mapping Project, ITC Journal 1993-2, pp 122- 131.

Batterham, P.M., Bullock, S.J. and Hopgood, D.N., 1983. Tanzania: integrated interpretation of aeromagnetic and radiometric maps for mineral exploration. Transactions of the Institution of Mining and Metallurgy (Sect. B, Applied Earth Sciences) vol. 92, pp B83-92.

Beldi, Z., 1993. Instrumentation for airborne magnetic surveys, Australian Geological Survey Record 1993/19, pp 21-23.

Bhattacharyya, B.K., 1965. Two-dimensional harmonic analysis as a tool for magnetic interpretation. Geophysics vol 30, pp 829-857.

Bhattacharrya, B.K., 1966: Continuous spectrum of the total magnetic field anomaly due to a rectangular prismatic body. Geophysics vol 31 pp 97-121.

Boyd, T.J, 1992. An annotated outline of GPS, ASEG Preview, October 1992 pp 15-26.

Breiner, S., 1973. Applications manual for portable magnetometers, Geometries, Palo Alto, California, 58 pp.

Briggs, I.C., 1974. Machine contouring using minimum curvature. Geophysics vol 39 pp 39-48.

Bullock, S.J., and Barritt, S.D., 1989. Real-time navigation and flight path recovery of aerial geophysical surveys: a review, *in* Proceedings of Exploration '87: Third Decennial International Conference on Geophysical and Geochemical Exploration for minerals and Groundwater, edited by G.D. Garland, Ontario Geological Survey, Special volume 3, 960 pp.

C

Clark, D.A., and Emerson D.W.,1991. Notes on rock magnetisation characteristics in applied geophysical studies. Exploration Geophysics vol. 22, pp. 547-555.

CSIR report MAG.C6, 1976: Geomagnetic secular variation observations in southern Africa, 1975, 19 pp.

D

Dobrin, M.B., 1960. Introduction to Geophysical Prospecting', 2nd Edition, p. 313.

Drury, S.A., 1987. Image interpretation in Geology, Alien & Unwin 243 pp.

E

F

Featherstone, W.E., 1995. The global positioning system (GPS) and its use in geophysical exploration. Exploration Geophysics, vol 26 pp 1-18.

G

Gibson, R.I., and Millegan, P.S., 1998. Geologic applications of gravity and magnetics: case histories. SEG Geophysical Reference Series No. 8, AAPG Studies in Geology No. 43., 162 pp.

Gonzalez-Casnova, P. and Alvarez, R., 1985. Splines in Geophysics, Geophysics Vol. 50, pp 2831-2848.

Grant, F.S., 1973: The magnetic susceptibility mapping method for interpreting aeromagnetic surveys'. Presented at the 43rd Annual International Meeting of the Society of Exploration Geophysicists, Mexico City, November 1973.

Grant, F.S., 1985a. Aeromagnetics, Geology and ore environments, I. magnetite in igneous, sedimentary and metamorphic rocks: an overview. Geoexploration vol 23, pp 303-333.

Grant, F.S., 1985b. Aeromagnetics, Geology and ore environments, II. magnetite and ore environments. Geoexploration vol 23, pp 335-362.

Grant, F.S., and Reeves, C.V., 1981. Regional geophysical interpretation of an airborne

magnetometer and gamma-ray spectrometer survey of Ivory Coast, West Africa', AGU Spring Meeting, Toronto, May 1980.

Grant, F.S., and West, G.F., 1965. Interpretation theory in applied geophysics. McGraw-Hill, New York.

Griffiths, D.H., and King, R.F., 1981. Applied geophysics for geologists and engineers, Pergamon Press, 230 pp.

Gunn, P., 1997. Airborne magnetic and radiometric surveys. Thematic issue, AGSO Journal of Australian Geology and Geophysics, vol 17 No. 2, 216 pp.

Gupta, V.K., and Grant, F.S., 1985. Mineral exploration aspects of gravity and aeromagnetic surveys in the Sudbury-Cobalt area, Ontario', pp 392-412 of Hinze (1985) - below.

H

Hadipandoyo, S., 1986. A comparison of several methods of gridding and contouring geophysical anomaly fields. MSc thesis, ITC, 133 pp + appendices.

Haggerty, S.E., 1979. The aeromagnetic mineralogy of igneous rocks. Canadian Journal of Earth Sciences, vol 16 1281-1293.

Heirtzler, J., Le Pichon, X and Baron, 1966. Deep-Sea Research vol 13, p 428.

Henkel, H., 1991. Petrophysical properties (density and magnetisation) of rocks from the northern part of the Baltic Shield, Tectonophysics, vol 192, pp 1-19.

Hinze, W.J., 1985. The utility of regional gravity and magnetic anomaly maps. Society of Exploration Geophysicists, 454 pp.

Hjelt, S., 1972. Magnetostatistic anomalies of dipping prisms. Geoexploration 10, pp 239-254.

Hofmann-Wellenhof, B., Lichtenegger, H., and Collins, J., 1992. GPS Theory and Practice, Springer-Verlag, 326 pp.

Hood, P.J., and Teskey, D.J. Aeromagnetic gradiometer program of the Geological Survey of Canada, Geophysics vol 54, pp 1012-1022, 1989.

Horsfall, K., 1999. AGSO's airborne survey operations grounded after 48 years. AusGeo News, August 1991, pp 6-8.

I

J

K

Kearey, P. and Brooks, V., 1984. Introduction to Geophysical Exploration, Chapter 2, pp 10-26.

Kearey, P., and Vine, F.J., 1990. Global Tectonics, Blackwell Scientific Publications, 302 pp.

Kilty, K.T., 1983. Werner deconvolution of profile potential field data. Geophysics, vol 48, pp 234-237.

Korhonen, J.V. and others, 2002. Magnetic anomaly map of the Fennoscandian Shield. Scale 1:2 000 000. Geological Survey of Finland (and others).

Kowalik, W.S., and Glenn, W.E., 1987. Image processing of aeromagnetic data and integration with Landsat images for improved structural interpretation. Geophysics vol 52 pp 875-885, 1987.

L

Lewis, M., 1993. United Nations airborne geophysical activities in developing countries, ITC Journal 1993-2, pp 132-139.

M

MacLeod, I.N., Jones, K., and Fan Dai, T., 1993. 3-D analytic signal in the interpretation of total magnetic field data at low magnetic latitudes. Exploration Geophysics vol 24, pp 679-688.

MacLeod, I.N., Vierra, S., Chaves, A.C., 1993. Analytic signal and reduction-to-the-pole in the interpretation of total magnetic field at low magnetic latitudes. Proc of the 3rd International Congress of the Brazilian Geophysical Society, Rio de Janiero, November 1993.

McElhinny, M.W., and McFadden, P.L., 2000. Paleomagnetism – continents and oceans. Academic Press, 386 pp.

Milligan, P.R., Morse, M.P., and Rajagopalan, S., 1992. Pixel map preparation using the HSV colour model. Exploration Geophysics vol 23, pp 219-224.

Minty, B.R.S., Simple micro-levelling for aeromagnetic data, Exploration Geophysics vol 22, pp 591-592, 1991.

N

Naudy, H., c.1976. Automatic determination of

depth on aeromagnetic profiles. CGG publication.

Naudy, H. and Dreyer, H., 1968. Essai de filtrage non-lineaire aux profiles aeromagnetiques. Geophysical Prospecting vol. 16, pp 171-178.

O

O'Sullivan, K.N., 1991. A map for all reasons: the role of image processing in mineral exploration. Minerals Industry International, Jan 1991, p 8-14.

P

Paterson, N.R., and Reeves, C.V., 1985. Applications of gravity and magnetic surveys : the-state-of-the-art in 1985. Geophysics vol 50 pp 2558-2594.

Parasnis, D.S., 1997. Principles of Applied Geophysics (5e). 429 pp.

Pederson, L.B., Rasmussen, T.M., and Dyrelius, D., 1990. Construction of component maps from aeromagnetic total field maps. Geophysical Prospecting, vol 38, pp 795-804.

Peirce, J, and Lipkov, L., 1988. Structural interpretation of the Rukwa rift, Tanzania. Geophysics, vol 53, pp 824-836.

Peters, 1949. Geophysics, vol 14, pp 290-320.

Pilkington, M., and Keating, P., 2006. The relationship between local wavenumber and analytic signal in magnetic interpretation. Geophysics, vol 71, pp L-1 to L-3

Proubasta, D., 1985. Airborne surveying: the view from the cockpit. Leading Edge, April 1985 pp 20-25.

Q

Quinn, J.M., Coleman, R.J., Peck, M.R. and Lauber, S.E., 1991. The joint US/UK 1990 epoch world magnetic model, US Naval Oceanographic Office, Technical Report TR 304.

R

Reeves, C.V., 1985. The Kalahari Desert, central southern Africa - a case history of regional gravity and magnetic exploration in W.J. Hinze (ed), The utility of gravity and magnetic surveys, Society of Exploration Geophysicists, special volume, pp 144-156.

Reeves, C. V., 1989. Aeromagnetic interpretation and rock magnetism, First Break, vol 7 pp 275-286.

Reeves, C.V., 1989. Paper 23: Geophysical mapping of Precambrian granite-greenstone terranes as an aid to Exploration *in* Proceedings of Exploration '87: third decennial International conference on Geophysical and Geochemical Exploration for Minerals and Groundwater, edited by G.D. Garland, Ontario Geological Survey, Special Volume 3, pp 254-266.

Reeves, C.V., 1992. New horizons in airborne geophysical mapping, Exploration Geophysics, vol 23, pp 273-280.

Reeves C V 2001 The role of airborne geophysical reconnaissance in exploration geoscience. First Break, vol 19.9, pp. 501-508.

Reeves C V and Bullock S J 2006 Airborne exploration. Fugro Airborne Surveys Limited (in press).

Reeves C V Macnab R and Maschenkov S 1998. Compiling all the world's magnetic anomalies. EOS American Geophysical Union, July 14, p 338.

Reeves C.. Reford S.W. and Milligan P.R., 1997. Airborne Geophysics: Old Methods, New Images. *In* Gubbins AG Proceedings of Exploration 97, Fourth Decennial International Conference on Mineral Exploration, p 13-30. GEO F/X, 1068 pp.

Reeves, C. V., and Zeil, P. A., 1990. Airborne Geophysics and remote sensing some common ground in presentation techniques and interpretation. IMM Remote Sensing volume, pp 75-88.

Reford, M.S. and Sumner, J.S. 1964. Aeromagnetics. Geophysics 29 pp 482-516.

Reid, A.B., 1980. Aeromagnetic survey design. Geophysics vol 45, pp 973-6.

Reid, A.B. , Allsop, J.M., Granser, H., Millett, A.J., and Somerton, I.W., 1990. Magnetic interpretation in three dimensions using Euler deconvolution. Geophysics vol 55, pp 80-91.

Riddihough, R., 1986. *In:* Interpretation of gravity and magnetic anomalies for non specialists, Canadian Geophysical Union short course, organized by A. K. Goodacre. 361 pp.

Roest W R Verhoef J and Pilkington M 1992 Magnetic interpretation using the 3-D analytic signal. Geophysics vol. 57 pp. 116-125.

S

Smith, W.H.F., and Wessel, P., 1990. Gridding with continuous curvature splines in tension.

Geophysics vol 55 pp pp 293-305.

Sowerbutts, W.T.C., 1987. Magnetic mapping of the Butterton dyke: an example of detailed geophysical surveying. Journal of the Geological Society, vol 144, pp 29-33.

Spector, A., and Grant, F.S., 1970. Statistical models for interpreting aeromagnetic data. Geophysics, vol 35 pp 293-302.

T

Talwani, M., and Heirtzler, J.R., 1964. Computation of magnetic anomalies caused by two dimensional structures of arbitrary shape. Contribution No. 621. *in* Computers in the Minerals Industries, part 1 vol 9 pp 464-480. Stanford University Publications, Geological Sciences.

Talwani, M., Worzel, J.L, and Landisman, M., 1959. Rapid gravity computation for two-dimensional bodies with application to the Mendocino submarine fracture zone. Journal of Geophysical Research, vol 64, pp 49-59.

Tarlowski, C, McEwin, A.J., Reeves, C.V., and Barton, C.E., 1996. Dewarping the composite aeromagnetic anomaly map of Australia using control traverses and base stations. Geophysics vol 61, pp 696-705.

Tarlowski, C., Simonis, F., Whitaker, A. and Milligan, P., 1992. The magnetic anomaly map of Australia. Exploration Geophysics, vol 23 pp 339-342.

Telford, W.M, Geldart, L.P, Sheriff, R.E, and Keys, D.A., 1976. Applied Geophysics, Chapters 2 and 3.

Teskey et al, 1991. Guide to aeromagnetic specifications and contracts. GSC Open File 2349.

Teskey, D., and Broome, J., 1984. Computer programs for the production of shaded relief and stereo shaded relief maps. Geological Survey of Canada, Current Research, Part B, Paper 84-1 B, pp 375-389.

Teskey, D.J., and Hood, P.J., 1991. The Canadian aeromagnetic database: evolution and applications to the definition of major crustal boundaries. Tectonophysics vol 192, pp 41-56.

Thompson, D.T., 1982. EULDPH: a new technique for making computer-assisted depth estimates from magnetic data. Geophysics vol 47, pp 31-37.

Tucker, D.H., Hone, I.G., Downie, D., Luyendyk, A., Horsfall, K., Anfiloff, V., 1988. Aeromagnetic regional survey of onshore Australia. Geophysics, vol 53 pp 254-265.

U

V

W

Wang Qinge, ?year? A helium (He4) optically pumped magnetometer suitable for airborne measurements. An Overview of Exploration, pp 231-243.

Wasilewski, P., and Hood, P., 1991. Magnetic anomalies – land and sea. Special Issue. Tectonophysics, vol 192 No. ½.

Wellman, P. 1991. Block structure of continental crust derived from gravity and magnetic maps with Australian examples, pp 102-108 *in* The Utitility of Regional Gravity and Magnetic Anomaly Maps, ed W.J. Hinze, Society of Exploration Geophysicist, 454pp.

Whitaker, A., Wellman, P., Reith, H., 1987. The use of magnetic surveys in mapping greenstone terrane near Kalgoorlie, Western Australia. Exploration Geophysics, vol 18, pp 371-380.

Wonik, T., 1990. Experience with the use of global reference fields for compilation of aeromagnetic data for Europe. Journal of Geomagnetism and Geoelectricity, vol 42, pp 1087-1097.

Wu Chaojun, 1989 : Adequate sampling in magnetic survey. MSc thesis, ITC, 67 pp.

X

Y

Z

Zonenshain, L.P., Verhoef, J., Macnab, R. and Meyers, H., 1991. Magnetic imprints of continental accretion in the USSR. Eos, Tranactions of the American Geophysical Union, vol 72, No. 29,pages 305 – 310.

Last update: 2006 February 3.